



**A & M Engineering and  
Environmental Services, Inc.**  
Consulting - Design - Construction - Remediation

May 24, 2026

Ms. Hillary Young, P.E.  
Chief Engineer  
Land Protection Division  
Oklahoma Department of Environmental Quality  
P. O. Box 1677,  
Oklahoma City, Oklahoma 73101-1677

**RE: Response to Notice of Deficiency (NOD) Letter Dated March 5, 2026  
Class I Non-Hazardous Injection Well Operating Permit Renewal Application  
Well ID: MES #1  
Mid-Way Environmental Services, Inc.  
Lincoln County, Oklahoma  
Operating Permit No. IW-NH-41001-OP**

Dear Ms. Young:

On behalf of Mid-Way Environmental Services, Inc. (MES), A & M Engineering and Environmental Services, Inc. (A & M) respectfully submits this letter and attachments in response to the Notice of Deficiency (NOD) letter dated March 5, 2026, regarding MES's Class I Non-Hazardous Injection Well Operating Permit Renewal Application.

The format utilized in responding to the NODs includes a citation of the individual NOD and the prepared response. For convenience of review and where applicable, revised figures and tables are included with the individual NOD response.

In order to provide a re-assessment of certain calculations and interpretations previously submitted to DEQ, Mid-Way contracted the services of Evren M. Ozbayoglu, PhD, a Professor of Petroleum Engineering and the Director of Drilling Research Project at the University of Tulsa (TU).

The deficiencies cited in the March 5, 2026-letter have been addressed in sufficient detail with respect to the general conditions and operation of the Mid-Way Class I Non-Hazardous Injection Well and believe approval of the renewal of Operating Permit is appropriate.

If you have any questions on this matter, or if you require any additional information, please do not hesitate to call me on (918) 665-6575 or email me at omohammad@aandmengineering.com.

Sincerely,  
A & M Engineering and Environmental Services, Inc.

A handwritten signature in blue ink, appearing to read "Orphius Mohammad".

Orphius Mohammad, PhD., P.E.  
Senior Environmental Engineer

cc: Tolga Ertugrul, P.E., President, MES  
Evren M. Ozbayoglu, PhD, TU

Enclosed: NOD Response

**MID-WAY ENVIRONMENTAL SERVICES, INC.**  
**CLASS I NON-HAZARDOUS WASTE INJECTION WELL**  
**MES #1**  
**PERMIT NO. IW-NH-41001-OP**

**RESPONSE TO NOTICE OF DEFICIENCY LETTER**  
**DATED MARCH 5, 2026**



**PREPARED FOR:**  
**MID-WAY ENVIRONMENTAL SERVICES, INC.**  
**120 NORTH 8<sup>TH</sup> AVENUE**  
**STROUD, OKLAHOMA 74079**

**MAY 24, 2026**

**PREPARED BY:**  
**A & M ENGINEERING AND ENVIRONMENTAL SERVICES, INC.**  
**10010 EAST 16TH STREET**  
**TULSA, OKLAHOMA 74128-4813**  
**PHONE (918)-665-6575 & FAX (918)-665-6576**  
**EMAIL: [aandm@aandmengineering.com](mailto:aandm@aandmengineering.com)**

**CERTIFICATE OF AUTHORIZATION NUMBER 1326**



**A & M Engineering and  
Environmental Services, Inc.**  
Consulting - Design - Construction - Remediation

**MID-WAY ENVIRONMENTAL SERVICES, INC.**  
**PERMIT RENEWAL APPLICATION**  
**OPERATING Permit No. IW-NH-41001-OP**  
**FOR MES #1**

**TABLE OF CONTENTS**

| <b>SECTION</b>                 | <b>PAGE</b> |
|--------------------------------|-------------|
| COVER LETTER                   |             |
| <b>1 DEFICIENCY NO 1</b> ..... | 4           |
| <b>2 DEFICIENCY NO 2</b> ..... | 9           |
| <b>3 DEFICIENCY NO 3</b> ..... | 12          |
| <b>4 DEFICIENCY NO 4</b> ..... | 41          |
| <b>5 DEFICIENCY NO 5</b> ..... | 48          |



## FIGURES

| <u>FIGURE</u>   | <u>PAGE</u> |
|---|-------------|
| <b>FIGURE 3-1:</b> Pressure increase as a function of radial distance from the wellbore .....   | 26          |
| <b>FIGURE 3-2:</b> Pressure increase at ZEI (r=4904 ft) as a function of time, with flow rate data.....   | 27          |
| <b>FIGURE 4-1:</b> Hall Plot for Mid-Way Class I Injection Well [(a) Hall Integral (Primary Vertical Axis) (b) Analytical Hall Derivative (Secondary Vertical Axis)] .....  | 42          |
| <b>FIGURE 4-2:</b> Hall Plot for Mid-Way Class I Injection Well [(a) Hall Integral (Primary Vertical Axis) (b) Revised Hall Derivative using the graphical calculation for the slope of the Hall integral (Secondary Vertical Axis)] .....    | 43          |
| <b>FIGURE 4-3:</b> Hall Plot for Mid-Way Class I Injection Well (a) Hall Integral (Primary Vertical Axis) (b) Analytical Hall Derivative (Primary Vertical Axis) (c) Seismic Activity within 10 miles radius (Secondary Vertical Axis)] ..... | 44          |



## APPENDICES

|              |   |
|--------------|---|
| APPENDIX - A | Wyoming Department of Environmental Quality Guidance Document Number 1 – Permitting of Class I Injection Wells  |
| APPENDIX - B | Schlumberger Transient Analysis Report October 15, 2010   |
| APPENDIX - C | Response to Notice of Deficiency Letter Dated October 9, 2013 - Response to Deficiency Number 6   |
| APPENDIX - D | Well Completion Report for Twin Cities Saltwater Disposal Well – Oklahoma Corporation Commission  |
| APPENDIX - E | MES-1 2024 and 2025 PFT Report  |
| APPENDIX - F | Response to Notice of Deficiency Letter Dated October 9, 2013 - Response to Deficiency Number 7   |
| APPENDIX - G | Analysis on Hydraulics during Injection Process, and, Pressure Distribution within the Formation by Evren M. Ozbayoglu, December 2013                             |
| APPENDIX - H | Schlumberger Re-evaluation of MES October 2010 PFT by Yosmar Gonzalez, January, 2014  |
| APPENDIX - I | MES’ Response to NOD Letter Dated May 19, 2025, Table 8: A Summary of the Bottomhole Pressures measured at the end of Shut-In period, recorded during annual PFTs |
| APPENDIX - J | Table 5: Existing MES-1 UIC Permit - maximum allowable injection pressures for various specific gravities of injectate  |



## DEFICIENCY NO 1

**In Deficiency No. 2 of DEQ's May 19, 2025 NOD, DEQ asked Mid-Way to provide evaluations and methods used to determine the fixed Area of Review ("AOR"), including calculations for the zone of endangering influence ("ZEI"). In response, Mid-Way provided the injectant front calculation by volumetric calculations. Please include dispersion into the volumetric calculations in order to evaluate its effect. Please also provide a calculation of the ZEI, as previously requested, using the Modified Theis equations in 40 C.F.R. § 146.6(a)(2).**

### RESPONSE:

The Zone of Endangering Influence (ZEI) using the Modified Theis equation in 40 C.F.R. § 146.6(a)(2) as adapted in the “Underground Injection Control (UIC) Program Water Quality Division – Guidance Document Number 1, Permitting of Class I Injection Wells”, developed by the Wyoming Department of Environmental Quality (see **Appendix A**) is calculated as shown:

$$r = \sqrt{\frac{2.25 K H t}{S 10^x}}$$

$$x = \frac{4\pi K H \left(\frac{W}{G} - B\right)}{2.3 Q}$$

$r$  = Radius of endangering influence from injection well (length)

$K$  = Hydraulic conductivity of the injection zone (length/time) =  $k \left(\frac{\rho g}{\mu}\right)$

$k$  = formation permeability

$\rho$  = Density of the fluid in the injection zone

$\mu$  = Viscosity of the fluid in the injection zone

$H$  = Thickness of the injection zone (length)

$t$  = Time of injection (time)

$S$  = Storage coefficient (dimensionless) =  $\phi C_t H$

$\phi$  = Porosity

$C_t$  = Compressibility



$Q$  = Injection rate (volume/time)

$B$  = Observed original hydrostatic head of injection zone (length)

$W$  = Hydrostatic head of underground source of drinking water (length)

$G$  = Specific gravity of fluid in the injection zone (dimensionless)

The Modified Theis equation assumes a constant injection rate over the evaluated period. In this case, the projected future injection rates are substantially higher than the historical injection rates. Consequently, applying the projected future injection rate retroactively from the onset of injection activities in 2015 would produce an unrealistically large Area of Review (AoR) and would not be valid since over a decade of operational data exists. To address this limitation, one must first estimate the recent average formation pressure in the vicinity of the well using static pressure measurements. The Pressure Falloff Test (PFT) conducted at the end of 2024 was selected for this purpose since the pressure gauge was set at depth of 5,340 ft, which is consistent with historical events. Please note, material obstruction was encountered above a depth of 5,340 ft during the 2025 PFT event so the pressure gauge was set to a depth of 5,228 ft. Maintenance was conducted following the 2025 PFT event and this obstruction was cleared.

The formation pressure reported from the November 2024 PFT (provided in **Appendix E**) was 2,518.6 pound per square-inch (psi) at a depth of 5,340 feet (ft.). This value was independently validated through the calculations presented below, which yielded a formation pressure of 2,518.2 psi at the same depth.

As shown in the Schlumberger Transient Analysis Report for the October 2010 PFT event (**Appendix B**), the reservoir pressure at a depth of 5,300 ft was 2,495 psi. As thoroughly explained (and accepted by DEQ) in Midway Environmental Services' (MES) Deficiency Number 6 answer in Response to Notice of Deficiency Letter Dated October 9, 2013 (**Appendix C**), the average of the static pressure gradient measurements taken on May 7, 2010 and October 11, 2010 between a depth of 5,000 and 7,000 ft, corresponding to the Arbuckle injection zone of MES-1, was 0.486 psi/ft. It should be noted that this gradient is not the average pressure gradient for the entire well length but corresponds specifically to the injection formation fluid pressure gradient. Applying this gradient between a depth of 5,340 ft and 5,300 ft and then adding a reservoir pressure of 2,495



psi measured at 5,300 ft, the initial formation pressure at a depth of 5,340 ft from the October 2010 “virgin” well condition is calculated to be 2,514.4 psi.

The static formation pressure obtained immediately prior to injection during the December 2024 PFT indicated a bottomhole pressure of 2,522.3 psi at 5,340 ft. Because the well had been injecting wastewater for an extended period, the pressure in the vicinity of the wellbore was elevated above the original reservoir pressure. Therefore, to estimate the average formation pressure, a representative pressure profile within the formation was developed and averaged. The pressure distribution within the formation is dependent on both reservoir and fluid properties; accordingly, superposition-based pressure modeling was utilized to estimate the pressure profile.

From the PFT data, the pressure increases at the wellbore relative to the initial formation pressure was determined as follows:

$$\Delta P = 2522.3 - 2514.4 = 7.8 \text{ psi}$$

At the wellbore radius ( $r_w = 0.5 \text{ ft}$ ), the pressure profile was assumed to follow the exponential relationship:

$$\Delta P(r) = A e^{b r}$$

where  $r$  represents the radial distance from the well. Assuming line-source behavior, the coefficient  $A$  was taken as 7.8 psi. Based on the superposition pressure profile calculations, the exponential decay coefficient was determined to be  $b = -0.0002316$ . The resulting superposition calculations estimated a pressure increase of 17.3 psi at  $r = 10 \text{ ft}$  and 5.3 psi at  $r = 5,000 \text{ ft}$ .

To estimate the average reservoir pressure within a radial distance of  $r < 5,000 \text{ ft}$ , the pressure profile was integrated over the region of interest. The average pressure increase was calculated as

$$\Delta \bar{P} = \frac{\int_0^{5000} r \Delta P(r) dr}{\int_0^{5000} r dr} = \frac{\int_0^{5000} r (7.8 e^{(-0.0002316 r)}) dr}{\int_0^{5000} r dr} = 3.8 \text{ psi}$$

The resulting average pressure increase within the 5,000-ft radius was determined to be approximately 3.8 psi. It should be noted that selecting an outer radius greater than 5,000 ft would yield a smaller average pressure increase because the pressure distribution decreases with radial distance from the wellbore. Accordingly, the average formation pressure at a depth of 5,340 ft was

estimated as  $2,514.4 + 3.8 = 2,518.2$  psi. This is only 0.4 psi less than the 2,518.6 psi reservoir pressure reported in the November 2024 PFT analysis, which validates the PFT value.

Using this validated formation pressure, the reservoir pressure at the end of 2024 was adopted as the average formation pressure for determination of the parameter  $B$  in the Modified Theis equation used to estimate the ZEI.

For the ZEI analysis, the base of the Underground Source of Drinking Water (USDW) was approximated to occur at a depth of 50 ft based on actual monitoring well observations at the site. Accordingly, the value of  $W$  was taken as 50 ft. To estimate the value of  $B$ , the formation pressure at 50 ft was calculated by referencing the validated formation pressure of 2,518.6 psi at 5,340 ft and adjusting it to the shallower datum using the measured formation pressure gradient. The resulting calculation is shown below:

$$B = \frac{2518.6 + (50 - 5340)(0.486)}{(0.433)} = -121 \text{ ft}$$

Because both hydraulic heads,  $B$  and  $W$ , are defined relative to freshwater conditions, the parameter  $G$ , representing the specific gravity of the fluid within the injection zone, was also referenced to freshwater conditions. Using the measured “virgin” formation fluid pressure gradient prior to injection in 2010, the equivalent specific gravity, unadjusted for temperature, was estimated as  $0.486/0.433 = 1.122$ . As previously mentioned, the analysis for the evaluation of the specific gravity of the Arbuckle formation fluid, prior to initiating commercial activities at MES-1, was performed in MES’ Deficiency Number 6 answer in Response to Notice of Deficiency Letter Dated October 9, 2013 and can be found in **Appendix C**.

The injection rate ( $Q$ ) of injectate has been taken as 462 gallon per minute (gpm) (slightly above the 450 gpm maximum injection rate in the existing UIC permit) prior to being normalized to the specific gravity of freshwater. Substitution of the remaining parameters into the Modified Theis equation yielded the calculated radius of the ZEI as 4,904 ft at the end of 2035, corresponding to 11 years after the end of 2024. Therefore, the ZEI calculated in accordance with the requirements of 40 C.F.R. § 146.6(a)(2) is 4,904 ft at the end of 2035. Since the calculated radius is less than 1



mile (5,280 ft) for timeframe being considered, the previously considered 1-mile AoR fixed radius was conservative.

The ZEI calculation using the Modified Theis Equation in 40 C.F.R. § 146.6(a)(2) is not a volumetric analysis. In MES' Deficiency No. 2 response to DEQ from the Response to Notice of Deficiency Letter Dated May 19, 2025 (submitted December 7, 2025), volumetric calculations accounting for dispersion were provided. This is because effective sweep efficiency was accounted for in the analysis, which considers both macroscopic (percentage of reservoir rock volume), and microscopic (percentage of pore volume) sweep efficiencies. In a homogeneous reservoir, sweep efficiency captures the macroscopic displacement behavior, and dispersion effects are negligible at the field scale because the flow is convection-dominated since the Peclet Number,  $N_{Pe}$  is relatively high. To elaborate on this, consider the definition of  $N_{Pe}$ :

$$N_{Pe} = \frac{v_r L}{D}$$

where  $v_r$  is the radial velocity at radial distance of interest,  $L$  is the longitudinal distance (can be assumed similar to radial distance),  $D$  is the dispersion coefficient.  $D$  can be expressed as the combination of mechanical dispersion,  $D_{mechanical}$ , and molecular diffusion,  $D_{molecular}$ , such that:

$$D = D_{mechanical} + D_{molecular} = \alpha_L v_r + D_{molecular}$$

Here,  $D_{molecular}$  will be very small for field scale systems. Thus,  $D$  can be approximated as:

$$D \approx \alpha_L v_r$$

where  $\alpha_L$  is the longitudinal dispersivity (in length units), and for field scale, it can be assumed between 1 and 10 ft. Inserting  $D$  into  $N_{Pe}$  yields:

$$N_{Pe} = \frac{v_r L}{D} = \frac{v_r L}{\alpha_L v_r} = \frac{L}{\alpha_L}$$

Considering  $L$  is approximated as the radial distance of interest,  $N_{Pe}$  can be approximated as a function of  $L$  and  $\alpha_L$  only. Assuming  $\alpha_L$  is 5 ft and  $L$  is 4,904 ft (radius of the ZEI),  $N_{Pe}$  is approximately equal to 1,000. If  $N_{Pe}$  is much larger than 1, this indicates a convection dominated system, and dispersion is small compared to advective transport. Thus, dispersion effects can be neglected, and a piston-type Bulkley-Leverett front-end can be safely assumed. Please refer to the aforementioned previously submitted response for more specific details concerning this analysis.

## DEFICIENCY NO 2

In response to Deficiency No. 3 regarding an evaluation of wells within 1 mile of the Mid-Way injection well ("MES-1"), Mid-Way provided updated information on wells within the 1-mile AOR and indicated the Twin Cities saltwater disposal well was the only well penetrating the Arbuckle injection zone. Mid-Way also provided an estimate of the pressure increase at this well due to MES-1 injections and monitoring of reservoir pressures at MESA for the period of 2013 to December 2025, and concluded the potential for fluid movement into underground sources of drinking water is negligible. However, the evaluation did not include potential effects of injection at the maximum allowable rate for 24 hours / day, 7 days / week, and 365 days / year for 10 years and assumed the Twin Cities injection was zero, discounting the potential interference effects from the Twin Cities injection well on pressure increase. Please update, as necessary, the previous assessment of the pressure calculations addressing the potential interference by the Twin Cities injection well conducted as part of Mid -Way's January 10, 2014 NOD Response #7. Please include a citation and the reference for that assessment.

### RESPONSE:

MES recently discovered that the Twin Cities Saltwater Disposal Well (TCSDW) located within 0.85 miles of MES-1 was altered. As shown in **Appendix D**, in November 2024, the TCSDW was plugged back above the Arbuckle Formation and now terminates in the Wilcox Formation preventing all communication with the Arbuckle Formation. More specifically, at 5,003 ft bgs, a Cast Iron Bridge Plug was installed over the Arbuckle formation and 10 ft of concrete was installed. The well passed a MIT on November 27, 2024.

In light of the plugback of the TCSDW, interference effects from this well on future injection activities at MES-1 will not exist. The latest, 2025, PFT results at MES-1 take into account any pressure or other system impacts from TCSDW at MES-1. This is inherent to the PFT analysis. Since injection into the Arbuckle formation at TCSDW has occurred since at least 2004 and ended in November of 2024, any pressure interference from TCSDW on MES-1 would have been observed by now and if it did exist, it certainly wouldn't increase in the future since TCSDW is



not longer in communication with the Arbuckle Formation. During the initial UIC permitting process of MES-1, only one PFT was conducted following the acidizing of MES-1. Therefore, due to the existence of a singular PFT dataset, MES, as a conservative precaution, conducted a superposition radial pressure analysis accounting for possible interference effects from TCSDW assuming continuous injection at TCSDW and using the maximum injection rate available in Oklahoma Corporation Commission records for this well of 13 BBL/minute. The necessity for this analysis was questionable at the time especially given the fact that, as stated in MES' response to NOD #7 of the Response to NOD Dated October 9, 2013:

*To date, no increase in pressure has been observed at MES #1 since 2010 thereby indicating that either the injector is located on the other side of a possible no-flow boundary and therefore not impacting MES #1, or that the effect of the injector is very limited due to the high permeability of the reservoir. Despite the possibility that the Twin Cities injector may not be hydraulically connected to MES #1, Dr. Ozbayoglu does consider the possible interference of the injector in his hydraulic calculations.*

This type of conservative analysis is no longer justified because MES has 11 years of annual PFT data to rely on that would have any interference from TCSDW on MES-1 built-into the modeling. From a pressure transient analysis perspective, any sustained interference from the Twin Cities SWD well would be expected to manifest in the fall-off test response as late-time deviations from infinite-acting radial flow, such as boundary-dominated behavior or pressure derivative anomalies. However, none of the pressure fall-off tests conducted since 2017, including the most recent tests, show evidence of boundary effects or external interference. Instead, the reservoir behavior is consistently interpreted as infinite-acting within the radius of investigation (on the order of several thousand feet), which is comparable to the distance between the two wells. Furthermore, the absence of a long-term increase in reservoir pressure, despite years of concurrent injection operations, indicates that any potential pressure contribution from the Twin Cities well has been either negligible or effectively dissipated within the permeable Arbuckle formation.

Furthermore, the existence of interference on MES-1 from TCSDW is negligible not only due to the observations quoted above between 2010 and 2014 but also because the bottomhole reservoir



pressures and bottomhole pressures at the end of shut-in in MES-1 have not steadily increased during the past decade that measurements have been recorded during PFT events. In fact, if anything, the static reservoir pressures have decreased. Please refer to **Table 8** of MES' Response to NOD Letter Dated May 19, 2025 (**Appendix I**) for a summary of the bottomhole pressures measured at the end of shut-in and bottomhole reservoir pressures recorded during annual PFT. When considering static bottomhole reservoir pressures at the same depth, this table shows that the reservoir pressure tended to decrease each year and has certainly decreased between the present time and the commencement of commercial activities at MES-1 over a decade ago. This is strong evidence that the interference on MES-1 from TCSDW has been negligible.

As it relates to the pressure increase analysis DEQ references in this question, all future year reservoir pressure analysis and injectant front analysis by volumetric calculations submitted in MES' Response to NOD Letter Dated May 19, 2025 and MES' response presented in this submittal (Response to NOD Letter Dated March 5, 2026) consider continuous injection for 24 hours/day, 7 days/week, and 365 days /year for at least 10 years at 11 BBL/minute (or 462 gpm), which is slightly higher than the 450 gpm maximum allowable injection rate in MES' current UIC permit. Actual injection rate and volume data exists through present so this information was naturally used for all prior year analysis, especially since these "operating conditions" are reflected in PFT analysis.



### DEFICIENCY NO 3

#### **In response to Deficiency No. 4:**

- a. **Regarding pressure buildup over time within the Arbuckle injection zone, please also show an example calculation for one of the reservoir pressure profiles provided in Figure 1 of Mid Way's NOD response, at the ZEI calculated radius identified in Item 1 above, after ten (10) years of injection at the requested maximum allowable injection rate and at 24 hours/day and 7 days/week. Please also provide a summary explanation of how the increases in reservoir pressures around MES-1 due to injection supports the use of a 1-mile AOR.**
- b. **Please provide an evaluation of the maximum allowable injection pressure ("MAIP") for injectate with a specific gravity of 0.95, similar to what Mid-Way provided for fluids with specific gravities of 1.0 and 1.2. Also, please provide the calculations of the MAIP for injectates with specific gravities of 0.95, 1.0 and 1.2 using the procedure in OAC 252:652-9-1(1).**
- c. **Regarding the formation pressure and fracture pressure gradient noted in Tables 6A and 7A, please provide a citation and the reference for the values 0.472 psi/ft and 0.639 psi/ft, respectively. For Table 6B, please show example calculations for Row 1 with citations and references for the parameters used, along with an explanation of why the calculated maximum allowable pressure is greater with increased injection time (see Column 16).**
- d. **On page 14 of Mid-Way's response, it is stated that "When a wellhead pressure is observed when injection is not occurring at MES-1, this is due to the formation pressure being greater than the hydrostatic pressure of the fluid inside the well (not artesian conditions)." Please provide a summary explanation of why this situation is not considered artesian (both within the well bore and adjacent to the well); and include a citation and the assessment referenced in Mid -Way's January 10, 2014 NOD Response #6. That assessment provides the details and includes the corrected estimate of the specific gravity of the Arbuckle reservoir fluid (S.G. 1.135). Also, please ensure this value is used in any calculations utilizing the Arbuckle reservoir fluid specific gravity.**



**RESPONSE 3(a):**

As provided in Response 1, the ZEI calculated using the Modified Theis equation is 4,904 ft at the end of 2035, corresponding to 11 years after the end of 2024.

The pressure response of an injection well in a cylindrical reservoir can be described using the radial diffusivity equation, which relates pressure change to both time and radial distance from the well. The following equations describe the Diffusivity approach:

$$\Delta P(r, t) = \sum_{j=1}^N \left( \frac{141.2 q \mu}{k h} P_D(r_D, t_D) \right)_j$$

$$P_D(r_D, t_D) = -\frac{1}{2} Ei \left( -\frac{r_D^2}{4 t_D} \right)$$

$$r_D = \frac{r}{r_w}$$

$$t_D = \frac{0.000267 k t}{\phi \mu C_t r_w^2}$$

Here,

$$Ei(x) = \sum_{j=1}^{\infty} \frac{x^j}{j j!} + \ln(x) + \gamma$$

where  $\gamma = 0.5772156649$

$q$  = Injection rate (volume/time)

$\mu$  = Viscosity of the fluid

$k$  = formation permeability

$\phi$  = Porosity

$C_t$  = Total compressibility



$h$  = Formation thickness

$r_w$  = Wellbore radius

$r$  = Radial distance from the wellbore

The governing equation assumes that pressure propagates outward through the reservoir as fluid is injected, with the rate of propagation controlled by reservoir properties such as permeability, porosity, fluid viscosity, compressibility, and formation thickness. For a constant injection rate, the pressure increase is largest near the wellbore and decreases with distance as the pressure disturbance spreads radially through the formation. Because average injection rates may vary from year to year, the total pressure increase can be estimated using the superposition principle; each yearly injection rate is treated as a separate constant rate pressure contribution that begins at its corresponding time, and the total pressure increase at any radial distance is calculated by summing the individual pressure responses from all prior injection periods. Diffusivity equation combined with superposition provides a time-dependent pressure profile that accounts for changing injection history while preserving the radial nature of flow in a cylindrical reservoir.

**Table 3-0:** Waste volume injection at MES Class I Injection Well

| Year Number | Year (end) | Total Volume, in bbl, Injected in that Year ( $V_{inj}$ ) |
|-------------|------------|---|
| Year-1      | 2015       | 128,983   |
| Year-2      | 2016       | 135,979   |
| Year-3      | 2017       | 143,635   |
| Year-4      | 2018       | 535,095   |
| Year-5      | 2019       | 362,545   |
| Year-6      | 2020       | 134,984   |
| Year-7      | 2021       | 298,225   |
| Year-8      | 2022       | 180,744   |
| Year-9      | 2023       | 245,330   |
| Year-10     | 2024       | 376,610   |
| Year-11     | 2025       | 742,032   |
| Year-12     | 2026       | 5,781,600   |

|         |      |           |
|---------|------|-----------|
| Year-13 | 2027 | 5,781,600 |
| Year-14 | 2028 | 5,781,600 |
| Year-15 | 2029 | 5,781,600 |
| Year-16 | 2030 | 5,781,600 |
| Year-17 | 2031 | 5,781,600 |
| Year-18 | 2032 | 5,781,600 |
| Year-19 | 2033 | 5,781,600 |
| Year-20 | 2034 | 5,781,600 |
| Year-21 | 2035 | 5,781,600 |
| Year-22 | 2036 | 5,781,600 |

Input:

$$k = 250 \text{ md}$$

$$h = 300 \text{ ft}$$

$$r_w = 0.329 \text{ ft}$$

$$\mu = 1 \text{ cp}$$

$$C_t = 7.3 \times 10^{-6} \text{ psi}^{-1}$$

$$\phi = 0.14$$

$$q = \frac{V_{inj}}{(1 \text{ year}) \left( \frac{365 \text{ day}}{1 \text{ year}} \right)} = \frac{V_{inj}}{365}$$

$$t_D = \frac{0.000267 k t}{\phi \mu C_t r_w^2} = \frac{0.000267 (250) t \left( \frac{365 \text{ day}}{1 \text{ year}} \right) \left( \frac{24 \text{ hr}}{1 \text{ day}} \right)}{(0.14) (1) (7.3 \times 10^{-6}) (0.329)^2} = 5.286 \times 10^9 t$$

$$r_D = \frac{r}{0.329}$$

Thus;

$$\Delta P(r, t) = \sum_{j=1}^N \left( \frac{141.2 q (1)}{(250) (300)} \left[ -\frac{1}{2} Ei \left( -\frac{r_D^2}{4 t_D} \right) \right] \right)_j$$



1) Sample calculations for Row-1 at the ZEI ( $r = 4,904$  ft):

$$r_D = \frac{4904}{0.329} = 14905.8$$

Year-1 (end of 2015);

Flow rate (for  $V_{inj} = 128,983$  bbl):

$$q = \frac{V_{inj}}{365} = \frac{128,983}{365} = 353.38 \text{ bbl/d}$$

$t = 1$  (for end of 2015):

$$t_D = 5.286 \times 10^9 t = 5.286 \times 10^9 (1) = 5.286 \times 10^9$$

$$-\frac{r_D^2}{4 t_D} = -\frac{(14905.8)^2}{4 (5.286 \times 10^9)} = -0.01051$$

$$\Delta P(4904,1) = \frac{141.2 (353.38) (1)}{(250) (300)} \left[ -\frac{1}{2} Ei(0.01051) \right] = 1.853 \text{ psi}$$

$t = 2$  (for end of 2016):

$$t_D = 5.286 \times 10^9 t = 5.286 \times 10^9 (2) = 1.057 \times 10^{10}$$

$$-\frac{r_D^2}{4 t_D} = -\frac{(14905.8)^2}{4 (1.057 \times 10^{10})} = -5.255 \times 10^{-3}$$

$$\begin{aligned} \Delta P(4904,2) &= \frac{141.2 (353.38) (1)}{(250) (300)} \left[ -\frac{1}{2} Ei(-5.255 \times 10^{-3}) + \frac{1}{2} Ei(-0.01051) \right] \\ &= 0.2302 \text{ psi} \end{aligned}$$

$t = 3$  (for end of 2017):

$$t_D = 5.286 \times 10^9 t = 5.286 \times 10^9 (3) = 1.586 \times 10^{10}$$



$$-\frac{r_D^2}{4 t_D} = -\frac{(14905.8)^2}{4 (1.586 \times 10^{10})} = -3.502 \times 10^{-3}$$

$$\begin{aligned} \Delta P(4904,3) &= \frac{141.2 (353.38) (1)}{(250) (300)} \left[ -\frac{1}{2} Ei(-3.502 \times 10^{-3}) + \frac{1}{2} Ei(-5.255 \times 10^{-3}) \right] \\ &= 0.1348 \text{ psi} \end{aligned}$$

$t = 4$  (for end of 2018):

$$t_D = 5.286 \times 10^9 t = 5.286 \times 10^9 (4) = 2.114 \times 10^{10}$$

$$-\frac{r_D^2}{4 t_D} = -\frac{(14905.8)^2}{4 (2.114 \times 10^{10})} = -2.628 \times 10^{-3}$$

$$\begin{aligned} \Delta P(4904,4) &= \frac{141.2 (353.38) (1)}{(250) (300)} \left[ -\frac{1}{2} Ei(-2.628 \times 10^{-3}) + \frac{1}{2} Ei(-3.502 \times 10^{-3}) \right] \\ &= 0.0956 \text{ psi} \end{aligned}$$

Similar calculations are conducted until  $t = 22$  (end of 2036).

Year-2 (end of 2016);

Flow rate (for  $V_{inj} = 135,979$  bbl):

$$q = \frac{V_{inj}}{365} = \frac{135,979}{365} = 372.54 \text{ bbl/d}$$

$t = 1$  (for end of 2016):

$$t_D = 5.286 \times 10^9 t = 5.286 \times 10^9 (1) = 5.286 \times 10^9$$

$$-\frac{r_D^2}{4 t_D} = -\frac{(14905.8)^2}{4 (5.286 \times 10^9)} = -0.01051$$

$$\Delta P(4904,1) = \frac{141.2 (372.54) (1)}{(250) (300)} \left[ -\frac{1}{2} Ei(0.01051) \right] = 1.3945 \text{ psi}$$



$t = 2$  (for end of 2017):

$$t_D = 5.286 \times 10^9 t = 5.286 \times 10^9 (2) = 1.057 \times 10^{10}$$

$$-\frac{r_D^2}{4 t_D} = -\frac{(14905.8)^2}{4 (1.057 \times 10^{10})} = -5.255 \times 10^{-3}$$

$$\begin{aligned} \Delta P(4904,2) &= \frac{141.2 (372.54) (1)}{(250) (300)} \left[ -\frac{1}{2} Ei(-5.255 \times 10^{-3}) + \frac{1}{2} Ei(-0.01051) \right] \\ &= 0.2412 \text{ psi} \end{aligned}$$

$t = 3$  (for end of 2018):

$$t_D = 5.286 \times 10^9 t = 5.286 \times 10^9 (3) = 1.586 \times 10^{10}$$

$$-\frac{r_D^2}{4 t_D} = -\frac{(14905.8)^2}{4 (1.586 \times 10^{10})} = -3.502 \times 10^{-3}$$

$$\begin{aligned} \Delta P(4904,3) &= \frac{141.2 (372.54) (1)}{(250) (300)} \left[ -\frac{1}{2} Ei(-3.502 \times 10^{-3}) + \frac{1}{2} Ei(-5.255 \times 10^{-3}) \right] \\ &= 0.1416 \text{ psi} \end{aligned}$$

$t = 4$  (for end of 2019):

$$t_D = 5.286 \times 10^9 t = 5.286 \times 10^9 (4) = 2.114 \times 10^{10}$$

$$-\frac{r_D^2}{4 t_D} = -\frac{(14905.8)^2}{4 (2.114 \times 10^{10})} = -2.628 \times 10^{-3}$$

$$\begin{aligned} \Delta P(4904,4) &= \frac{141.2 (372.54) (1)}{(250) (300)} \left[ -\frac{1}{2} Ei(-2.628 \times 10^{-3}) + \frac{1}{2} Ei(-3.502 \times 10^{-3}) \right] \\ &= 0.1006 \text{ psi} \end{aligned}$$



Similar calculations are conducted until  $t = 21$  (end of 2036).

Year-3 (end of 2017);

Flow rate (for  $V_{inj} = 135,979$  bbl):

$$q = \frac{V_{inj}}{365} = \frac{143,635}{365} = 393.52 \text{ bbl/d}$$

$t = 1$  (for end of 2016):

$$t_D = 5.286 \times 10^9 t = 5.286 \times 10^9 (1) = 5.286 \times 10^9$$

$$-\frac{r_D^2}{4 t_D} = -\frac{(14905.8)^2}{4 (5.286 \times 10^9)} = -0.01051$$

$$\Delta P(4904,1) = \frac{141.2 (393.52) (1)}{(250) (300)} \left[ -\frac{1}{2} Ei(0.01051) \right] = 1.4730 \text{ psi}$$

$t = 2$  (for end of 2018):

$$t_D = 5.286 \times 10^9 t = 5.286 \times 10^9 (2) = 1.057 \times 10^{10}$$

$$-\frac{r_D^2}{4 t_D} = -\frac{(14905.8)^2}{4 (1.057 \times 10^{10})} = -5.255 \times 10^{-3}$$

$$\begin{aligned} \Delta P(4904,2) &= \frac{141.2 (372.54) (1)}{(250) (300)} \left[ -\frac{1}{2} Ei(-5.255 \times 10^{-3}) + \frac{1}{2} Ei(-0.01051) \right] \\ &= 0.2548 \text{ psi} \end{aligned}$$

$t = 3$  (for end of 2019):

$$t_D = 5.286 \times 10^9 t = 5.286 \times 10^9 (3) = 1.586 \times 10^{10}$$

$$-\frac{r_D^2}{4 t_D} = -\frac{(14905.8)^2}{4 (1.586 \times 10^{10})} = -3.502 \times 10^{-3}$$



$$\Delta P(4904,3) = \frac{141.2 (372.54) (1)}{(250) (300)} \left[ -\frac{1}{2} Ei(-3.502 \times 10^{-3}) + \frac{1}{2} Ei(-5.255 \times 10^{-3}) \right]$$

$$= 0.1495 \text{ psi}$$

$t = 4$  (for end of 2020):

$$t_D = 5.286 \times 10^9 \quad t = 5.286 \times 10^9 (4) = 2.114 \times 10^{10}$$

$$-\frac{r_D^2}{4 t_D} = -\frac{(14905.8)^2}{4 (2.114 \times 10^{10})} = -2.628 \times 10^{-3}$$

$$\Delta P(4904,4) = \frac{141.2 (372.54) (1)}{(250) (300)} \left[ -\frac{1}{2} Ei(-2.628 \times 10^{-3}) + \frac{1}{2} Ei(-3.502 \times 10^{-3}) \right]$$

$$= 0.1062 \text{ psi}$$

Similar calculations are conducted until  $t = 20$  (end of 2036).

This process continues until Year-22 (end of 2036). Then, superposition principle is applied such that for a particular year are summed up. For example, for Year-3 (2017), the differential pressures for  $t = 1$  (1.47 psi),  $t = 2$  (0.24 psi) and  $t = 3$  (0.13 psi) are added, and 1.84 psi is calculated. The results of such calculations for all years are tabulated in **Table 3-1**. Similar calculations have been conducted at the wellbore wall (considering the skin), 0.5 mile from the wellbore, 1 mile from the wellbore, and 2 miles from the wellbore. Results are tabulated in **Tables 3-2, 3-3, 3-4** and **3-5**, respectively.

**Table 3-1** Pressure calculation summary for Row-1 ( $r = 4904$  ft). Units are in psi.

|               | Year-1     | Year-2     | Year-3     | Year-4     | Year-5     | Year-6 | Year-7 | Year-8 | Year-9 | Year-10 | Year-11 | Year-12 | Year-13 | Year-14 | Year-15 | Year-16 | Year-17 | Year-18 | Year-19 | Year-20 | Year-21 | Year-22 |
|---------------|------------|------------|------------|------------|------------|--------|--------|--------|--------|---------|---------|---------|---------|---------|---------|---------|---------|---------|---------|---------|---------|---------|
|               | 2015       | 2016       | 2017       | 2018       | 2019       | 2020   | 2021   | 2022   | 2023   | 2024    | 2025    | 2026    | 2027    | 2028    | 2029    | 2030    | 2031    | 2032    | 2033    | 2034    | 2035    | 2036    |
| 2015          | 1.32 (t=1) | 0.23 (t=2) | 0.13 (t=3) | 0.10 (t=4) | 0.07 (t=4) | 0.06   | 0.05   | 0.04   | 0.04   | 0.04    | 0.03    | 0.03    | 0.03    | 0.02    | 0.02    | 0.02    | 0.02    | 0.02    | 0.02    | 0.02    | 0.02    | 0.02    |
| 2016          |            | 1.39 (t=1) | 0.24 (t=2) | 0.14 (t=3) | 0.10 (t=3) | 0.08   | 0.06   | 0.05   | 0.05   | 0.04    | 0.04    | 0.03    | 0.03    | 0.03    | 0.03    | 0.02    | 0.02    | 0.02    | 0.02    | 0.02    | 0.02    | 0.02    |
| 2017          |            |            | 1.47 (t=1) | 0.25 (t=2) | 0.15 (t=3) | 0.11   | 0.08   | 0.07   | 0.06   | 0.05    | 0.04    | 0.04    | 0.04    | 0.03    | 0.03    | 0.03    | 0.03    | 0.02    | 0.02    | 0.02    | 0.02    | 0.02    |
| 2018          |            |            |            | 5.49 (t=1) | 0.95 (t=2) | 0.56   | 0.40   | 0.31   | 0.25   | 0.21    | 0.18    | 0.16    | 0.15    | 0.13    | 0.12    | 0.11    | 0.10    | 0.10    | 0.09    | 0.08    | 0.08    | 0.07    |
| 2019          |            |            |            |            | 3.72 (t=1) | 0.64   | 0.38   | 0.27   | 0.21   | 0.17    | 0.14    | 0.12    | 0.11    | 0.10    | 0.09    | 0.08    | 0.07    | 0.07    | 0.06    | 0.06    | 0.06    | 0.05    |
| 2020          |            |            |            |            |            | 1.38   | 0.24   | 0.14   | 0.10   | 0.08    | 0.06    | 0.05    | 0.05    | 0.04    | 0.04    | 0.03    | 0.03    | 0.03    | 0.03    | 0.02    | 0.02    | 0.02    |
| 2021          |            |            |            |            |            |        | 3.06   | 0.53   | 0.31   | 0.22    | 0.17    | 0.14    | 0.12    | 0.10    | 0.09    | 0.08    | 0.07    | 0.07    | 0.06    | 0.06    | 0.05    | 0.05    |
| 2022          |            |            |            |            |            |        |        | 1.85   | 0.32   | 0.19    | 0.13    | 0.10    | 0.08    | 0.07    | 0.06    | 0.05    | 0.05    | 0.04    | 0.04    | 0.04    | 0.03    | 0.03    |
| 2023          |            |            |            |            |            |        |        |        | 2.52   | 0.44    | 0.26    | 0.18    | 0.14    | 0.12    | 0.10    | 0.08    | 0.07    | 0.07    | 0.06    | 0.06    | 0.05    | 0.05    |
| 2024          |            |            |            |            |            |        |        |        |        | 3.86    | 0.67    | 0.39    | 0.28    | 0.22    | 0.18    | 0.15    | 0.13    | 0.11    | 0.10    | 0.09    | 0.08    | 0.08    |
| 2025          |            |            |            |            |            |        |        |        |        |         | 7.61    | 1.32    | 0.77    | 0.55    | 0.43    | 0.35    | 0.29    | 0.26    | 0.23    | 0.20    | 0.18    | 0.17    |
| 2026          |            |            |            |            |            |        |        |        |        |         |         | 59.29   | 10.26   | 6.02    | 4.28    | 3.32    | 2.71    | 2.29    | 1.99    | 1.75    | 1.57    | 1.42    |
| 2027          |            |            |            |            |            |        |        |        |        |         |         |         | 59.29   | 10.26   | 6.02    | 4.28    | 3.32    | 2.71    | 2.29    | 1.99    | 1.75    | 1.57    |
| 2028          |            |            |            |            |            |        |        |        |        |         |         |         |         | 59.29   | 10.26   | 6.02    | 4.28    | 3.32    | 2.71    | 2.29    | 1.99    | 1.75    |
| 2029          |            |            |            |            |            |        |        |        |        |         |         |         |         |         | 59.29   | 10.26   | 6.02    | 4.28    | 3.32    | 2.71    | 2.29    | 1.99    |
| 2030          |            |            |            |            |            |        |        |        |        |         |         |         |         |         |         | 59.29   | 10.26   | 6.02    | 4.28    | 3.32    | 2.71    | 2.29    |
| 2031          |            |            |            |            |            |        |        |        |        |         |         |         |         |         |         |         | 59.29   | 10.26   | 6.02    | 4.28    | 3.32    | 2.71    |
| 2032          |            |            |            |            |            |        |        |        |        |         |         |         |         |         |         |         |         | 59.29   | 10.26   | 6.02    | 4.28    | 3.32    |
| 2033          |            |            |            |            |            |        |        |        |        |         |         |         |         |         |         |         |         |         | 59.29   | 10.26   | 6.02    | 4.28    |
| 2034          |            |            |            |            |            |        |        |        |        |         |         |         |         |         |         |         |         |         |         | 59.29   | 10.26   | 6.02    |
| 2035          |            |            |            |            |            |        |        |        |        |         |         |         |         |         |         |         |         |         |         |         | 59.29   | 10.26   |
| 2036          |            |            |            |            |            |        |        |        |        |         |         |         |         |         |         |         |         |         |         |         |         | 59.29   |
| Superposition | 1.32       | 1.62       | 1.84       | 5.98       | 4.99       | 2.83   | 4.27   | 3.26   | 3.85   | 5.29    | 9.34    | 61.87   | 71.34   | 76.98   | 81.02   | 84.18   | 86.77   | 88.98   | 90.89   | 92.58   | 94.10   | 95.48   |



**Table 3-2** Pressure calculation summary for Row-1 ( $r = 10$  ft), which represents wellbore wall. Units are in psi.

|               | Year-1     | Year-2     | Year-3     | Year-4      | Year-5      | Year-6 | Year-7 | Year-8 | Year-9 | Year-10 | Year-11 | Year-12 | Year-13 | Year-14 | Year-15 | Year-16 | Year-17 | Year-18 | Year-19 | Year-20 | Year-21 | Year-22 |
|---------------|------------|------------|------------|-------------|-------------|--------|--------|--------|--------|---------|---------|---------|---------|---------|---------|---------|---------|---------|---------|---------|---------|---------|
|               | 2015       | 2016       | 2017       | 2018        | 2019        | 2020   | 2021   | 2022   | 2023   | 2024    | 2025    | 2026    | 2027    | 2028    | 2029    | 2030    | 2031    | 2032    | 2033    | 2034    | 2035    | 2036    |
| 2015          | 5.44 (t=1) | 0.23 (t=2) | 0.13 (t=3) | 0.10 (t=4)  | 0.07 (t=4)  | 0.06   | 0.05   | 0.04   | 0.04   | 0.04    | 0.03    | 0.03    | 0.03    | 0.02    | 0.02    | 0.02    | 0.02    | 0.02    | 0.02    | 0.02    | 0.02    | 0.02    |
| 2016          |            | 5.74 (t=1) | 0.24 (t=2) | 0.14 (t=3)  | 0.10 (t=3)  | 0.08   | 0.06   | 0.05   | 0.05   | 0.04    | 0.04    | 0.03    | 0.03    | 0.03    | 0.03    | 0.02    | 0.02    | 0.02    | 0.02    | 0.02    | 0.02    | 0.02    |
| 2017          |            |            | 6.06 (t=1) | 0.26 (t=2)  | 0.15 (t=3)  | 0.11   | 0.08   | 0.07   | 0.06   | 0.05    | 0.04    | 0.04    | 0.04    | 0.03    | 0.03    | 0.03    | 0.03    | 0.02    | 0.02    | 0.02    | 0.02    | 0.02    |
| 2018          |            |            |            | 22.57 (t=1) | 0.96 (t=2)  | 0.56   | 0.40   | 0.31   | 0.25   | 0.21    | 0.18    | 0.16    | 0.15    | 0.13    | 0.12    | 0.11    | 0.10    | 0.10    | 0.09    | 0.08    | 0.08    | 0.07    |
| 2019          |            |            |            |             | 15.29 (t=1) | 0.65   | 0.38   | 0.27   | 0.21   | 0.17    | 0.14    | 0.12    | 0.11    | 0.10    | 0.09    | 0.08    | 0.07    | 0.07    | 0.06    | 0.06    | 0.06    | 0.05    |
| 2020          |            |            |            |             |             | 5.69   | 0.24   | 0.14   | 0.10   | 0.08    | 0.06    | 0.05    | 0.05    | 0.04    | 0.04    | 0.03    | 0.03    | 0.03    | 0.03    | 0.02    | 0.02    | 0.02    |
| 2021          |            |            |            |             |             |        | 12.58  | 0.53   | 0.31   | 0.22    | 0.17    | 0.14    | 0.12    | 0.10    | 0.09    | 0.08    | 0.07    | 0.07    | 0.06    | 0.06    | 0.05    | 0.05    |
| 2022          |            |            |            |             |             |        |        | 7.62   | 0.32   | 0.19    | 0.13    | 0.10    | 0.08    | 0.07    | 0.06    | 0.05    | 0.05    | 0.04    | 0.04    | 0.04    | 0.03    | 0.03    |
| 2023          |            |            |            |             |             |        |        |        | 10.35  | 0.44    | 0.26    | 0.18    | 0.14    | 0.12    | 0.10    | 0.08    | 0.07    | 0.07    | 0.06    | 0.06    | 0.05    | 0.05    |
| 2024          |            |            |            |             |             |        |        |        |        | 15.89   | 0.67    | 0.39    | 0.28    | 0.22    | 0.18    | 0.15    | 0.13    | 0.11    | 0.10    | 0.09    | 0.08    | 0.08    |
| 2025          |            |            |            |             |             |        |        |        |        |         | 31.30   | 1.33    | 0.78    | 0.55    | 0.43    | 0.35    | 0.29    | 0.26    | 0.23    | 0.20    | 0.18    | 0.17    |
| 2026          |            |            |            |             |             |        |        |        |        |         |         | 243.89  | 10.34   | 6.05    | 4.29    | 3.33    | 2.72    | 2.30    | 1.99    | 1.76    | 1.57    | 1.42    |
| 2027          |            |            |            |             |             |        |        |        |        |         |         |         | 243.89  | 10.34   | 6.05    | 4.29    | 3.33    | 2.72    | 2.30    | 1.99    | 1.76    | 1.57    |
| 2028          |            |            |            |             |             |        |        |        |        |         |         |         |         | 243.89  | 10.34   | 6.05    | 4.29    | 3.33    | 2.72    | 2.30    | 1.99    | 1.76    |
| 2029          |            |            |            |             |             |        |        |        |        |         |         |         |         |         | 243.89  | 10.34   | 6.05    | 4.29    | 3.33    | 2.72    | 2.30    | 1.99    |
| 2030          |            |            |            |             |             |        |        |        |        |         |         |         |         |         |         | 243.89  | 10.34   | 6.05    | 4.29    | 3.33    | 2.72    | 2.30    |
| 2031          |            |            |            |             |             |        |        |        |        |         |         |         |         |         |         |         | 243.89  | 10.34   | 6.05    | 4.29    | 3.33    | 2.72    |
| 2032          |            |            |            |             |             |        |        |        |        |         |         |         |         |         |         |         |         | 243.89  | 10.34   | 6.05    | 4.29    | 3.33    |
| 2033          |            |            |            |             |             |        |        |        |        |         |         |         |         |         |         |         |         |         | 243.89  | 10.34   | 6.05    | 4.29    |
| 2034          |            |            |            |             |             |        |        |        |        |         |         |         |         |         |         |         |         |         |         | 243.89  | 10.34   | 6.05    |
| 2035          |            |            |            |             |             |        |        |        |        |         |         |         |         |         |         |         |         |         |         |         | 243.89  | 10.34   |
| 2036          |            |            |            |             |             |        |        |        |        |         |         |         |         |         |         |         |         |         |         |         |         | 243.89  |
| Superposition | 5.44       | 5.97       | 6.44       | 23.07       | 16.58       | 7.15   | 13.80  | 9.04   | 11.69  | 17.32   | 33.04   | 246.47  | 256.02  | 261.68  | 265.73  | 268.90  | 271.50  | 273.70  | 275.62  | 277.32  | 278.84  | 280.21  |



**Table 3-3** Pressure calculation summary for Row-1 ( $r = 2,640$  ft = 0.5 mile). Units are in psi.

|               | Year-1     | Year-2     | Year-3     | Year-4     | Year-5     | Year-6 | Year-7 | Year-8 | Year-9 | Year-10 | Year-11 | Year-12 | Year-13 | Year-14 | Year-15 | Year-16 | Year-17 | Year-18 | Year-19 | Year-20 | Year-21 | Year-22 |       |
|---------------|------------|------------|------------|------------|------------|--------|--------|--------|--------|---------|---------|---------|---------|---------|---------|---------|---------|---------|---------|---------|---------|---------|-------|
|               | 2015       | 2016       | 2017       | 2018       | 2019       | 2020   | 2021   | 2022   | 2023   | 2024    | 2025    | 2026    | 2027    | 2028    | 2029    | 2030    | 2031    | 2032    | 2033    | 2034    | 2035    | 2036    |       |
| 2015          | 1.73 (t=1) | 0.23 (t=2) | 0.13 (t=3) | 0.10 (t=4) | 0.07 (t=4) | 0.06   | 0.05   | 0.04   | 0.04   | 0.04    | 0.03    | 0.03    | 0.03    | 0.02    | 0.02    | 0.02    | 0.02    | 0.02    | 0.02    | 0.02    | 0.02    | 0.02    |       |
| 2016          |            | 1.83 (t=1) | 0.24 (t=2) | 0.14 (t=3) | 0.10 (t=3) | 0.08   | 0.06   | 0.05   | 0.05   | 0.04    | 0.04    | 0.03    | 0.03    | 0.03    | 0.03    | 0.02    | 0.02    | 0.02    | 0.02    | 0.02    | 0.02    | 0.02    |       |
| 2017          |            |            | 1.93 (t=1) | 0.26 (t=2) | 0.15 (t=3) | 0.11   | 0.08   | 0.07   | 0.06   | 0.05    | 0.04    | 0.04    | 0.04    | 0.03    | 0.03    | 0.03    | 0.03    | 0.02    | 0.02    | 0.02    | 0.02    | 0.02    |       |
| 2018          |            |            |            | 7.19 (t=1) | 0.96 (t=2) | 0.56   | 0.40   | 0.31   | 0.25   | 0.21    | 0.18    | 0.16    | 0.15    | 0.13    | 0.12    | 0.11    | 0.10    | 0.10    | 0.09    | 0.08    | 0.08    | 0.07    |       |
| 2019          |            |            |            |            | 4.87 (t=1) | 0.65   | 0.38   | 0.27   | 0.21   | 0.17    | 0.14    | 0.12    | 0.11    | 0.10    | 0.09    | 0.08    | 0.07    | 0.07    | 0.06    | 0.06    | 0.06    | 0.05    |       |
| 2020          |            |            |            |            |            | 1.81   | 0.24   | 0.14   | 0.10   | 0.08    | 0.06    | 0.05    | 0.05    | 0.04    | 0.04    | 0.03    | 0.03    | 0.03    | 0.03    | 0.02    | 0.02    | 0.02    |       |
| 2021          |            |            |            |            |            |        | 4.01   | 0.53   | 0.31   | 0.22    | 0.17    | 0.14    | 0.12    | 0.10    | 0.09    | 0.08    | 0.07    | 0.07    | 0.06    | 0.06    | 0.05    | 0.05    |       |
| 2022          |            |            |            |            |            |        |        | 2.43   | 0.32   | 0.19    | 0.13    | 0.10    | 0.08    | 0.07    | 0.06    | 0.05    | 0.05    | 0.04    | 0.04    | 0.04    | 0.03    | 0.03    |       |
| 2023          |            |            |            |            |            |        |        |        | 3.29   | 0.44    | 0.26    | 0.18    | 0.14    | 0.12    | 0.10    | 0.08    | 0.07    | 0.07    | 0.06    | 0.06    | 0.05    | 0.05    |       |
| 2024          |            |            |            |            |            |        |        |        |        | 5.06    | 0.67    | 0.39    | 0.28    | 0.22    | 0.18    | 0.15    | 0.13    | 0.11    | 0.10    | 0.09    | 0.08    | 0.08    |       |
| 2025          |            |            |            |            |            |        |        |        |        |         | 9.97    | 1.32    | 0.77    | 0.55    | 0.43    | 0.35    | 0.29    | 0.26    | 0.23    | 0.20    | 0.18    | 0.17    |       |
| 2026          |            |            |            |            |            |        |        |        |        |         |         | 77.65   | 10.31   | 6.04    | 4.29    | 3.32    | 2.72    | 2.30    | 1.99    | 1.76    | 1.57    | 1.42    |       |
| 2027          |            |            |            |            |            |        |        |        |        |         |         |         | 77.65   | 10.31   | 6.04    | 4.29    | 3.32    | 2.72    | 2.30    | 1.99    | 1.76    | 1.57    |       |
| 2028          |            |            |            |            |            |        |        |        |        |         |         |         |         | 77.65   | 10.31   | 6.04    | 4.29    | 3.32    | 2.72    | 2.30    | 1.99    | 1.76    |       |
| 2029          |            |            |            |            |            |        |        |        |        |         |         |         |         |         | 77.65   | 10.31   | 6.04    | 4.29    | 3.32    | 2.72    | 2.30    | 1.99    |       |
| 2030          |            |            |            |            |            |        |        |        |        |         |         |         |         |         |         | 77.65   | 10.31   | 6.04    | 4.29    | 3.32    | 2.72    | 2.30    |       |
| 2031          |            |            |            |            |            |        |        |        |        |         |         |         |         |         |         |         | 77.65   | 10.31   | 6.04    | 4.29    | 3.32    | 2.72    |       |
| 2032          |            |            |            |            |            |        |        |        |        |         |         |         |         |         |         |         |         | 77.65   | 10.31   | 6.04    | 4.29    | 3.32    |       |
| 2033          |            |            |            |            |            |        |        |        |        |         |         |         |         |         |         |         |         |         | 77.65   | 10.31   | 6.04    | 4.29    |       |
| 2034          |            |            |            |            |            |        |        |        |        |         |         |         |         |         |         |         |         |         |         | 77.65   | 10.31   | 6.04    |       |
| 2035          |            |            |            |            |            |        |        |        |        |         |         |         |         |         |         |         |         |         |         |         |         | 77.65   |       |
| 2036          |            |            |            |            |            |        |        |        |        |         |         |         |         |         |         |         |         |         |         |         |         |         | 77.65 |
| Superposition | 1.73       | 2.06       | 2.31       | 7.68       | 6.15       | 3.26   | 5.22   | 3.84   | 4.63   | 6.49    | 11.70   | 80.23   | 89.75   | 95.41   | 99.46   | 102.63  | 105.22  | 107.43  | 109.34  | 111.04  | 112.56  | 113.93  |       |



**Table 3-4** Pressure calculation summary for Row-1 ( $r = 5,280 \text{ ft} = 1 \text{ mile}$ ). Units are in psi.

|               | Year-1     | Year-2     | Year-3     | Year-4     | Year-5     | Year-6 | Year-7 | Year-8 | Year-9 | Year-10 | Year-11 | Year-12 | Year-13 | Year-14 | Year-15 | Year-16 | Year-17 | Year-18 | Year-19 | Year-20 | Year-21 | Year-22 |       |
|---------------|------------|------------|------------|------------|------------|--------|--------|--------|--------|---------|---------|---------|---------|---------|---------|---------|---------|---------|---------|---------|---------|---------|-------|
| 2015          | 1.27 (t=1) | 0.23 (t=2) | 0.13 (t=3) | 0.10 (t=4) | 0.07 (t=4) | 0.06   | 0.05   | 0.04   | 0.04   | 0.04    | 0.03    | 0.03    | 0.03    | 0.02    | 0.02    | 0.02    | 0.02    | 0.02    | 0.02    | 0.02    | 0.02    | 0.02    | 0.02  |
| 2016          |            | 1.34 (t=1) | 0.24 (t=2) | 0.14 (t=3) | 0.10 (t=3) | 0.08   | 0.06   | 0.05   | 0.05   | 0.04    | 0.04    | 0.03    | 0.03    | 0.03    | 0.03    | 0.02    | 0.02    | 0.02    | 0.02    | 0.02    | 0.02    | 0.02    | 0.02  |
| 2017          |            |            | 1.42 (t=1) | 0.25 (t=2) | 0.15 (t=3) | 0.11   | 0.08   | 0.07   | 0.06   | 0.05    | 0.04    | 0.04    | 0.04    | 0.03    | 0.03    | 0.03    | 0.03    | 0.02    | 0.02    | 0.02    | 0.02    | 0.02    | 0.02  |
| 2018          |            |            |            | 5.29 (t=1) | 0.95 (t=2) | 0.56   | 0.40   | 0.31   | 0.25   | 0.21    | 0.18    | 0.16    | 0.15    | 0.13    | 0.12    | 0.11    | 0.10    | 0.10    | 0.09    | 0.08    | 0.08    | 0.08    | 0.07  |
| 2019          |            |            |            |            | 3.58 (t=1) | 0.64   | 0.38   | 0.27   | 0.21   | 0.17    | 0.14    | 0.12    | 0.11    | 0.10    | 0.09    | 0.08    | 0.07    | 0.07    | 0.06    | 0.06    | 0.06    | 0.06    | 0.05  |
| 2020          |            |            |            |            |            | 1.33   | 0.24   | 0.14   | 0.10   | 0.08    | 0.06    | 0.05    | 0.05    | 0.04    | 0.04    | 0.03    | 0.03    | 0.03    | 0.03    | 0.02    | 0.02    | 0.02    | 0.02  |
| 2021          |            |            |            |            |            |        | 2.95   | 0.53   | 0.31   | 0.22    | 0.17    | 0.14    | 0.12    | 0.10    | 0.09    | 0.08    | 0.07    | 0.07    | 0.06    | 0.06    | 0.05    | 0.05    | 0.05  |
| 2022          |            |            |            |            |            |        |        | 1.79   | 0.32   | 0.19    | 0.13    | 0.10    | 0.08    | 0.07    | 0.06    | 0.05    | 0.05    | 0.04    | 0.04    | 0.04    | 0.03    | 0.03    | 0.03  |
| 2023          |            |            |            |            |            |        |        |        | 2.42   | 0.43    | 0.26    | 0.18    | 0.14    | 0.12    | 0.10    | 0.08    | 0.07    | 0.07    | 0.06    | 0.05    | 0.05    | 0.05    | 0.05  |
| 2024          |            |            |            |            |            |        |        |        |        | 3.72    | 0.67    | 0.39    | 0.28    | 0.22    | 0.18    | 0.15    | 0.13    | 0.11    | 0.10    | 0.09    | 0.08    | 0.08    | 0.08  |
| 2025          |            |            |            |            |            |        |        |        |        |         | 7.33    | 1.31    | 0.77    | 0.55    | 0.43    | 0.35    | 0.29    | 0.26    | 0.23    | 0.20    | 0.18    | 0.17    | 0.17  |
| 2026          |            |            |            |            |            |        |        |        |        |         |         |         |         |         |         |         |         |         |         |         |         |         |       |
| 2027          |            |            |            |            |            |        |        |        |        |         |         | 57.12   | 10.24   | 6.02    | 4.27    | 3.32    | 2.71    | 2.29    | 1.99    | 1.75    | 1.57    | 1.42    | 1.42  |
| 2028          |            |            |            |            |            |        |        |        |        |         |         |         | 57.12   | 10.24   | 6.02    | 4.27    | 3.32    | 2.71    | 2.29    | 1.99    | 1.75    | 1.57    | 1.57  |
| 2029          |            |            |            |            |            |        |        |        |        |         |         |         |         |         | 57.12   | 10.24   | 6.02    | 4.27    | 3.32    | 2.71    | 2.29    | 1.99    | 1.99  |
| 2030          |            |            |            |            |            |        |        |        |        |         |         |         |         |         |         | 57.12   | 10.24   | 6.02    | 4.27    | 3.32    | 2.71    | 2.29    | 2.29  |
| 2031          |            |            |            |            |            |        |        |        |        |         |         |         |         |         |         |         | 57.12   | 10.24   | 6.02    | 4.27    | 3.32    | 2.71    | 2.71  |
| 2032          |            |            |            |            |            |        |        |        |        |         |         |         |         |         |         |         |         | 57.12   | 10.24   | 6.02    | 4.27    | 3.32    | 3.32  |
| 2033          |            |            |            |            |            |        |        |        |        |         |         |         |         |         |         |         |         |         | 57.12   | 10.24   | 6.02    | 4.27    | 4.27  |
| 2034          |            |            |            |            |            |        |        |        |        |         |         |         |         |         |         |         |         |         |         | 57.12   | 10.24   | 6.02    | 6.02  |
| 2035          |            |            |            |            |            |        |        |        |        |         |         |         |         |         |         |         |         |         |         |         |         | 57.12   | 10.24 |
| 2036          |            |            |            |            |            |        |        |        |        |         |         |         |         |         |         |         |         |         |         |         |         |         | 57.12 |
| Superposition | 1.27       | 1.57       | 1.79       | 5.78       | 4.85       | 2.78   | 4.16   | 3.20   | 3.76   | 5.15    | 9.06    | 59.69   | 69.15   | 74.78   | 78.82   | 81.98   | 84.57   | 86.78   | 88.69   | 90.38   | 91.90   | 93.28   | 93.28 |



**Table 3-5** Pressure calculation summary for Row-1 ( $r = 10,560 \text{ ft} = 2 \text{ miles}$ ). Units are in psi.

|               | Year-1     | Year-2     | Year-3     | Year-4     | Year-5     | Year-6 | Year-7 | Year-8 | Year-9 | Year-10 | Year-11 | Year-12 | Year-13 | Year-14 | Year-15 | Year-16 | Year-17 | Year-18 | Year-19 | Year-20 | Year-21 | Year-22 |       |
|---------------|------------|------------|------------|------------|------------|--------|--------|--------|--------|---------|---------|---------|---------|---------|---------|---------|---------|---------|---------|---------|---------|---------|-------|
|               | 2015       | 2016       | 2017       | 2018       | 2019       | 2020   | 2021   | 2022   | 2023   | 2024    | 2025    | 2026    | 2027    | 2028    | 2029    | 2030    | 2031    | 2032    | 2033    | 2034    | 2035    | 2036    |       |
| 2015          | 0.83 (t=1) | 0.22 (t=2) | 0.13 (t=3) | 0.09 (t=4) | 0.07 (t=4) | 0.06   | 0.05   | 0.04   | 0.04   | 0.03    | 0.03    | 0.03    | 0.03    | 0.03    | 0.02    | 0.02    | 0.02    | 0.02    | 0.02    | 0.02    | 0.02    | 0.02    | 0.02  |
| 2016          |            | 0.87 (t=1) | 0.23 (t=2) | 0.14 (t=3) | 0.10 (t=3) | 0.08   | 0.06   | 0.05   | 0.05   | 0.04    | 0.04    | 0.03    | 0.03    | 0.03    | 0.03    | 0.02    | 0.02    | 0.02    | 0.02    | 0.02    | 0.02    | 0.02    | 0.02  |
| 2017          |            |            | 0.92 (t=1) | 0.25 (t=2) | 0.15 (t=3) | 0.11   | 0.08   | 0.07   | 0.06   | 0.05    | 0.04    | 0.04    | 0.04    | 0.03    | 0.03    | 0.03    | 0.03    | 0.02    | 0.02    | 0.02    | 0.02    | 0.02    | 0.02  |
| 2018          |            |            |            | 3.42 (t=1) | 0.92 (t=2) | 0.55   | 0.39   | 0.30   | 0.25   | 0.21    | 0.18    | 0.16    | 0.14    | 0.13    | 0.12    | 0.11    | 0.10    | 0.09    | 0.09    | 0.08    | 0.08    | 0.07    | 0.07  |
| 2019          |            |            |            |            | 2.32 (t=1) | 0.63   | 0.37   | 0.27   | 0.21   | 0.17    | 0.14    | 0.12    | 0.11    | 0.10    | 0.09    | 0.08    | 0.07    | 0.07    | 0.06    | 0.06    | 0.06    | 0.06    | 0.05  |
| 2020          |            |            |            |            |            | 0.86   | 0.23   | 0.14   | 0.10   | 0.08    | 0.06    | 0.05    | 0.05    | 0.04    | 0.04    | 0.03    | 0.03    | 0.03    | 0.03    | 0.02    | 0.02    | 0.02    | 0.02  |
| 2021          |            |            |            |            |            |        | 1.91   | 0.51   | 0.31   | 0.22    | 0.17    | 0.14    | 0.12    | 0.10    | 0.09    | 0.08    | 0.07    | 0.07    | 0.06    | 0.06    | 0.05    | 0.05    | 0.05  |
| 2022          |            |            |            |            |            |        |        | 1.16   | 0.31   | 0.19    | 0.13    | 0.10    | 0.08    | 0.07    | 0.06    | 0.05    | 0.05    | 0.04    | 0.04    | 0.04    | 0.03    | 0.03    | 0.03  |
| 2023          |            |            |            |            |            |        |        |        | 1.57   | 0.42    | 0.25    | 0.18    | 0.14    | 0.11    | 0.10    | 0.08    | 0.07    | 0.07    | 0.06    | 0.05    | 0.05    | 0.05    | 0.05  |
| 2024          |            |            |            |            |            |        |        |        |        | 2.41    | 0.65    | 0.39    | 0.28    | 0.21    | 0.18    | 0.15    | 0.13    | 0.11    | 0.10    | 0.09    | 0.08    | 0.08    | 0.08  |
| 2025          |            |            |            |            |            |        |        |        |        |         | 4.75    | 1.28    | 0.76    | 0.54    | 0.42    | 0.35    | 0.29    | 0.25    | 0.22    | 0.20    | 0.18    | 0.17    | 0.17  |
| 2026          |            |            |            |            |            |        |        |        |        |         |         | 36.99   | 9.97    | 5.92    | 4.23    | 3.29    | 2.69    | 2.28    | 1.98    | 1.75    | 1.56    | 1.41    | 1.41  |
| 2027          |            |            |            |            |            |        |        |        |        |         |         |         | 36.99   | 9.97    | 5.92    | 4.23    | 3.29    | 2.69    | 2.28    | 1.98    | 1.75    | 1.56    | 1.41  |
| 2028          |            |            |            |            |            |        |        |        |        |         |         |         |         | 36.99   | 9.97    | 5.92    | 4.23    | 3.29    | 2.69    | 2.28    | 1.98    | 1.75    | 1.56  |
| 2029          |            |            |            |            |            |        |        |        |        |         |         |         |         |         | 36.99   | 9.97    | 5.92    | 4.23    | 3.29    | 2.69    | 2.28    | 1.98    | 1.75  |
| 2030          |            |            |            |            |            |        |        |        |        |         |         |         |         |         |         | 36.99   | 9.97    | 5.92    | 4.23    | 3.29    | 2.69    | 2.28    | 1.98  |
| 2031          |            |            |            |            |            |        |        |        |        |         |         |         |         |         |         |         | 36.99   | 9.97    | 5.92    | 4.23    | 3.29    | 2.69    | 2.28  |
| 2032          |            |            |            |            |            |        |        |        |        |         |         |         |         |         |         |         |         | 36.99   | 9.97    | 5.92    | 4.23    | 3.29    | 2.69  |
| 2033          |            |            |            |            |            |        |        |        |        |         |         |         |         |         |         |         |         |         | 36.99   | 9.97    | 5.92    | 4.23    | 3.29  |
| 2034          |            |            |            |            |            |        |        |        |        |         |         |         |         |         |         |         |         |         |         | 36.99   | 9.97    | 5.92    | 4.23  |
| 2035          |            |            |            |            |            |        |        |        |        |         |         |         |         |         |         |         |         |         |         |         | 36.99   | 9.97    | 5.92  |
| 2036          |            |            |            |            |            |        |        |        |        |         |         |         |         |         |         |         |         |         |         |         |         | 36.99   | 9.97  |
| Superposition | 0.83       | 1.09       | 1.29       | 3.90       | 3.56       | 2.28   | 3.10   | 2.54   | 2.88   | 3.82    | 6.45    | 39.51   | 48.73   | 54.29   | 58.28   | 61.42   | 63.99   | 66.18   | 68.09   | 69.77   | 71.28   | 72.65   | 72.65 |



The pressure distribution as a function of radial distance from the wellbore at the end of year 2035 (i.e., 10 years of continuous injection with the maximum allowable injection rate) is shown in **Figure 3-1**. Considering ZEI ( $r=4,904$  ft), the expected pressure at this point is 94.1 psi. ZEI calculation methodology reveals a head difference of 185.79 ft for the formation fluid density of  $1.122 \text{ g/cm}^3$ , which states 90.3 psi. Thus, ZEI and diffusion calculation methodology reveals a similar pressure increase for the considered conditions at the end of year 2035, which is a conservative case, since the injection rates and durations will not reach such levels during the operation period.

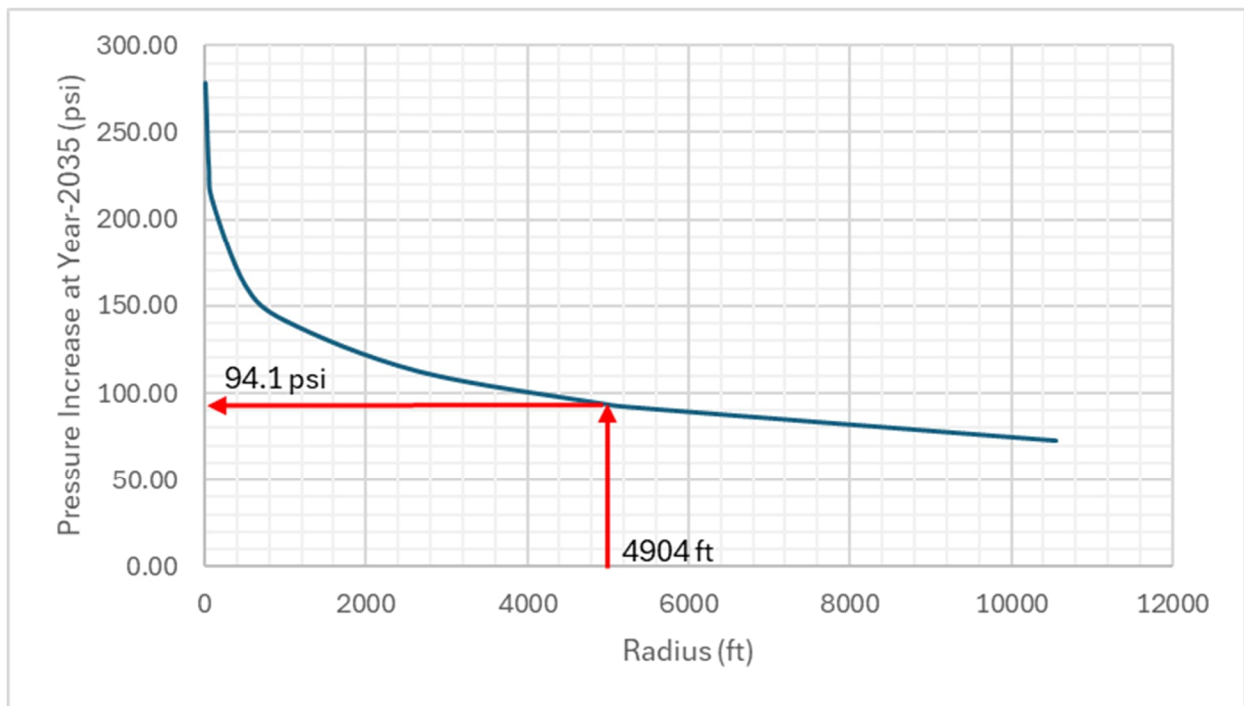


**Figure 3-1** Pressure increase as a function of radial distance from the wellbore

In **Figure 3-2**, the pressure increase at ZEI,  $r = 4,904$  ft, is presented as a function of time. In this plot, the injection rates are also shown for 2025 and earlier, and the maximum allowed injection rate is considered after 2025. The pressure increase estimations using both diffusivity approach and Theis model are compared. The differences for pressure increase are reasonably low, and indicates a good agreement (at the end of year 2035, pressure increase estimations are 94.1 psi and

80.45 for diffusivity approach with superposition and Theis model, respectively). More conservative conditions are used in diffusivity approach, which leads to higher values.

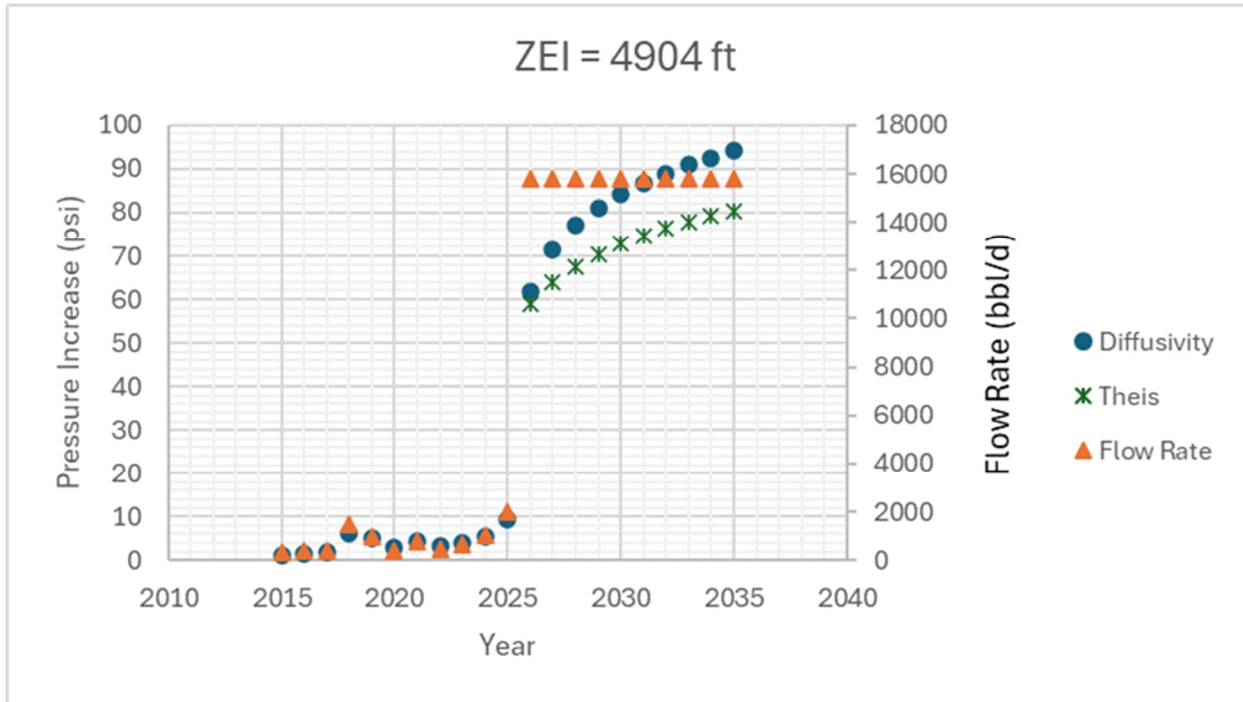


**Figure 3-2** Pressure increase at ZEI ( $r=4,904$  ft) as a function of time, with flow rate data

### **RESPONSE 3(b):**

Equations and Nomenclature:

Fluid velocity in the tubing,  $v$ :

$$v = \frac{Q}{2.448 d^2}$$

$v$  in ft/s, injection flow rate,  $Q$ , in gpm, tubing ID,  $d$ , in inches

Reynolds number:

$$N_{Re} = \frac{928 v \rho d}{\mu}$$

Density,  $r$ , in lb/gal, viscosity,  $\mu$ , in cp

Critical Reynolds number for the decision of laminar or turbulent flow (simplified approach):

$$N_{Re_c} = 2100$$

Fanning friction factors for laminar and turbulent flow conditions, respectively:

$$f_f = \frac{16}{N_{Re}}$$

$$\frac{1}{\sqrt{f_f}} = -3.6 \log\left(\frac{6.9}{N_{Re}}\right)$$

Frictional pressure loss,  $\Delta P_f$ , inside the tubing:

$$\Delta P_f = \frac{f_f \rho v^2}{25.5 d} L_t$$

$\Delta P_f$  in psi, tubing length,  $L_t$ , is in ft

Hydrostatic pressure,  $P_{hyd}$ :

$$P_{hyd} = 0.052 \rho L_t$$

$P_{hyd}$  in psi

Pressure loss in the reservoir is estimated by the transient pressure distribution estimation methodology.

Expected bottomhole pressure,  $P_{bh_{expected}}$ :

$$P_{bh_{expected}} = \Delta P + g_p L_t$$

$P_{bh_{expected}}$  in psi, formation pressure gradient,  $g_p$ , in psi/ft

Estimated wellhead injection pressure,  $P_{wh_{estimated}}$ :



$$P_{wh_{estimated}} = P_{bh_{expected}} - P_{hyd} + \Delta P_f$$

$P_{wh_{estimated}}$  in psi

Maximum allowable bottomhole pressure at top of the injection zone,  $P_{bh_{max}}$ :

$$P_{bh_{max}} = g_{ff} L_{t_{inj}}$$

$P_{bh_{max}}$  in psi, formation fracture pressure gradient,  $g_{ff}$ , in psi/ft, depth of the top of the injection zone,  $L_{t_{inj}}$ , in ft

Maximum possible injection pressure at surface,  $P_{wh_{max}}$ :

$$P_{wh_{max}} = P_{bh_{max}} - P_{hyd} + \Delta P_f$$

$P_{wh_{max}}$  in psi

Design factor for injection pressure based on fracture pressure,  $SF_{P_{ff}}$ :

$$SF_{P_{ff}} = \frac{P_{wh_{max}}}{P_{wh_{estimated}}}$$

Design factor for injection pressure based on **Table 5** (Existing MES-1 UIC Permit - maximum allowable injection pressures for various specific gravities of injectate) (**Appendix J**),  $SF_{P_{inj_{max}}}$ :

$$SF_{P_{inj}} = \frac{P_{inj_{max}}}{P_{wh_{estimated}}}$$

Design factor for maximum bottomhole pressure,  $SF_{P_{bh_{max}}}$ :

$$SF_{P_{bh}} = \frac{P_{bh_{max}}}{P_{bh_{expected}}}$$

Sample Calculations:

Input data Used:

|                         |            |
|-------------------------|------------|
| Fluid injection rate:   | 11 bbl/min |
| Fluid density:          | 1.0 sp.gr  |
| Tubing ID:              | 3.958"     |
| Tubing length:          | 5,203 ft   |
| Top of injection zone:  | 5,175 ft   |
| Fluid viscosity:        | 1 cp       |
| Formation permeability: | 250 md     |



|                              |                           |
|------------------------------|---------------------------|
| Formation porosity:          | 14%                       |
| Formation thickness:         | 300 ft                    |
| Effective wellbore diameter: | 21.8 ft                   |
| Total compressibility:       | $5.46 \times 10^{-6}$ psi |
| Formation pressure gradient: | 0.472 psi/ft              |
| Fracture pressure gradient:  | 0.639 psi/ft              |

(Effective wellbore diameter is determined based on the 2025 PTA report, indicating a -3.5 skin factor.)

Fluid velocity in the tubing:

$$v = \frac{(11)(42)}{2.448 (3.958)^2} = 12 \text{ ft/s}$$

Reynolds number:

$$N_{Re} = \frac{928 (12) (1.0 \times 8.34) (3.958)}{(1)} = 369,036$$

Critical Reynolds:

$$N_{Re_c} = 2100$$

Flow is “turbulent”. Fanning friction factor for turbulent flow conditions:

$$f_f = \left[ \frac{1}{-3.6 \log \left( \frac{6.9}{246,024} \right)} \right]^2 = 0.00345$$

Frictional pressure loss inside the tubing:

$$\Delta P_f = \frac{(0.00345) (8.34) (12)^2}{25.5 (3.958)} (5203) = 215.4 \text{ psi}$$

Hydrostatic pressure:

$$P_{hyd} = 0.052 (8.34) (5203) = 2256.4 \text{ psi}$$

For injection of 1 year, 5 years and 10 years, pressure loss in the reservoir are calculated using the transient pressure distribution methodology as 251 psi, 275 psi, and 286 psi, respectively.

Expected bottomhole pressures for 1 year, 5 years and 10 years of injection period:

$$P_{bh_{expected-1\text{ year}}} = (251) + (0.472) (5203) = 2707 \text{ psi}$$

$$P_{bh_{expected-5\text{ years}}} = (275) + (0.472) (5203) = 2731 \text{ psi}$$



$$P_{bh_{expected-10\ years}} = (286) + (0.472) (5203) = 2741 \text{ psi}$$

Estimated wellhead injection pressures for 1 year, 5 years and 10 years of injection period:

$$P_{wh_{estimated-1\ year}} = (2707) - (2256) + (215) = 666 \text{ psi}$$

$$P_{wh_{estimated-5\ years}} = (2731) - (2256) + (215) = 690 \text{ psi}$$

$$P_{wh_{estimated-10\ years}} = (2741) - (2256) + (215) = 700 \text{ psi}$$

Maximum allowable bottomhole pressure at top of the injection zone:

$$P_{bh_{max}} = (0.639) (5175) = 3307 \text{ psi}$$

Maximum possible injection pressure at surface:

$$P_{wh_{max}} = (3307) - (2256) + (215) = 1265 \text{ psi}$$

In the previous report, a typo was detected on the equation for maximum possible injection pressure, and it is corrected in this version.

Design factors for injection pressure based on fracture pressure for 1 year, 5 years and 10 years of injection period:

$$SF_{P_{ff-1\ year}} = \frac{(1265)}{(666)} = 1.90$$

$$SF_{P_{ff-5\ years}} = \frac{(1265)}{(690)} = 1.83$$

$$SF_{P_{ff-10\ years}} = \frac{(1265)}{(700)} = 1.81$$

Design factor for injection pressure for 1 year, 5 years and 10 years of injection period based on **Table 5** (maximum allowable injection pressures for various specific gravities of injectate) (**Appendix J**); for 1.0 sp.gr fluid, it is 1260 psi:

$$SF_{P_{inj-1\ year}} = \frac{(1260)}{(666)} = 1.89$$

$$SF_{P_{inj-5\ years}} = \frac{(1260)}{(690)} = 1.83$$

$$SF_{P_{inj-10\ years}} = \frac{(1260)}{(700)} = 1.80$$

Design factor for maximum bottomhole pressure for 1 year, 5 years and 10 years of injection period:

$$SF_{P_{bh-1\text{ year}}} = \frac{(3307)}{(2707)} = 1.22$$

$$SF_{P_{bh-5\text{ years}}} = \frac{(3307)}{(2731)} = 1.21$$

$$SF_{P_{bh-1\text{ year}}} = \frac{(3307)}{(2741)} = 1.21$$

Considering Okla. Admin. Code § 252:652-9-1 with the assumption that overburden pressure is known (i.e., calculated as 0.979 psi/ft), the document states “The maximum total pressure gradient (applied injection pressure plus fluid pressure) shall not exceed sixty-five percent (65%) of the established overburden pressure gradient, expressed in pounds per square inch per foot (psi/ft) of depth from ground surface to the top of the disposal zone.” Considering the top of the injection zone, 65% of the overburden pressure is

$$\sigma_{ob-65\%_{5175\text{ ft}}} = (0.65)(0.979)(5175) = 3293\text{ psi}$$

Design factor for 65% of the overburden pressure at the top of the injection zone for 1 year, 5 years and 10 years of injection period:

$$SF_{\sigma_{ob-1\text{ year}}} = \frac{(3293)}{(2707)} = 1.22$$

$$SF_{\sigma_{ob-5\text{ year}}} = \frac{(3293)}{(2731)} = 1.21$$

$$SF_{\sigma_{ob-10\text{ year}}} = \frac{(3393)}{(2741)} = 1.20$$

Considering Okla. Admin. Code § 252:652-9-1 with the assumption that overburden pressure is not known, the document states “If the effective overburden pressure gradient is not established, the maximum total pressure gradient shall not exceed 0.65 psi/ft of depth from ground surface to the top of the disposal zone.” Considering the top of the injection zone, 0.65 psi/ft pressure gradient corresponds to

$$P_{0.65\text{ psi/ft}_{5175\text{ ft}}} = (0.65)(5175) = 3,364\text{ psi}$$

Design factor for 65% of the overburden pressure at the top of the injection zone for 1 year, 5 years and 10 years of injection period:

$$SF_{\sigma_{ob-1\ year}} = \frac{(3364)}{(2707)} = 1.24$$

$$SF_{\sigma_{ob-5\ year}} = \frac{(3364)}{(2731)} = 1.23$$

$$SF_{\sigma_{ob-10\ year}} = \frac{(3364)}{(2741)} = 1.23$$

These results are summarized in **Table 3-7** in the first 3 rows, just to provide an example how the calculations are conducted.

**Table 3-6** Specific gravity = 0.95

| Injection Rate (bb/min) | Velocity Inside Tubing (ft/s) | Viscosity (cp) | Reynolds Number | Critical Reynolds Number | Fanning Friction Factor | Frictional Pressure Loss Gradient (psi/ft) | Frictional Pressure Loss Inside Tubing (psi) | Hydrostatic Pressure (psi) | Formation Permeability (md) | Injection Time (year) | Bottomhole Injection Pressure Minus Reservoir Pressure (psi) | Expected Bottomhole Injection Pressure (psi) | Estimated Wellhead Injection Pressure (psi) | Fracture Pressure at Casing Shoe (psi) | Maximum Possible Surface Injection Pressure (psi) | Injection Pressure Design Factor (for P_frac) | Injection Pressure Design Factor (for P_inj_max Table-5) | Bottomhole Pressure Design Factor (P_frac/P_bh) | Okla. Admin. Code § 252:652-9-1 Overburden Pressure Gradient Known (0.979 psi/ft), <65% of it at injection zone (5175 ft) = 3293 psi, Design Factor | Okla. Admin. Code § 252:652-9-1 Overburden Pressure Gradient not known, <0.65 psi/ft, Design Factor |
|-------------------------|-------------------------------|----------------|-----------------|--------------------------|-------------------------|--|--|----------------------------|-----------------------------|-----------------------|--|--|---|--|---|---|--|---|---|---|
| 11                      | 12.0                          | 1              | 350584.3        | 2100                     | 0.00348                 | 0.040                                      | 206.5  | 2143.6                     | 250                         | 1                     | 251  | 2707   | 770   | 3307                                   | 1369  | 1.78  | 1.75   | 1.22  | 1.22  | 1.24  |
|                         |                               |                |                 |                          |                         |  |  |                            |                             | 5                     | 275  | 2731   | 794   | 3307                                   | 1369  | 1.72  | 1.70   | 1.21  | 1.21  | 1.23  |
|                         |                               |                |                 |                          |                         |  |  |                            |                             | 10                    | 286  | 2741   | 804   | 3307                                   | 1369  | 1.70  | 1.68   | 1.21  | 1.20  | 1.23  |
| 11                      | 12.0                          | 1.5            | 233722.8        | 2100                     | 0.00376                 | 0.043                                      | 222.9  | 2143.6                     | 250                         | 1                     | 368  | 2824   | 903   | 3307                                   | 1386  | 1.54  | 1.50   | 1.17  | 1.17  | 1.19  |
|                         |                               |                |                 |                          |                         |  |  |                            |                             | 5                     | 404  | 2860   | 939   | 3307                                   | 1386  | 1.48  | 1.44   | 1.16  | 1.15  | 1.18  |
|                         |                               |                |                 |                          |                         |  |  |                            |                             | 10                    | 419  | 2875   | 954   | 3307                                   | 1386  | 1.45  | 1.41   | 1.15  | 1.15  | 1.17  |
| 11                      | 12.0                          | 1              | 350584.3        | 2100                     | 0.00348                 | 0.040                                      | 206.5  | 2143.6                     | 200                         | 1                     | 310  | 2766   | 829   | 3307                                   | 1369  | 1.65  | 1.63   | 1.20  | 1.19  | 1.22  |
|                         |                               |                |                 |                          |                         |  |  |                            |                             | 5                     | 340  | 2796   | 859   | 3307                                   | 1369  | 1.60  | 1.57   | 1.18  | 1.18  | 1.20  |
|                         |                               |                |                 |                          |                         |  |  |                            |                             | 10                    | 353  | 2809   | 871   | 3307                                   | 1369  | 1.57  | 1.55   | 1.18  | 1.17  | 1.20  |
| 11                      | 12.0                          | 1.5            | 233722.8        | 2100                     | 0.00376                 | 0.043                                      | 222.9  | 2143.6                     | 200                         | 1                     | 453  | 2909   | 988   | 3307                                   | 1386  | 1.40  | 1.37   | 1.14  | 1.13  | 1.16  |
|                         |                               |                |                 |                          |                         |  |  |                            |                             | 5                     | 498  | 2954   | 1033  | 3307                                   | 1386  | 1.34  | 1.31   | 1.12  | 1.11  | 1.14  |
|                         |                               |                |                 |                          |                         |  |  |                            |                             | 10                    | 518  | 2974   | 1053  | 3307                                   | 1386  | 1.32  | 1.28   | 1.11  | 1.11  | 1.13  |
| 18.8                    | 20.6                          | 1              | 599180.4        | 2100                     | 0.00316                 | 0.105                                      | 547.8  | 2143.6                     | 250                         | 1                     | 429  | 2885   | 1289  | 3307                                   | 1711  | 1.33  | 1.05   | 1.15  | 1.14  | 1.17  |
|                         |                               |                |                 |                          |                         |  |  |                            |                             | 5                     | 470  | 2926   | 1330  | 3307                                   | 1711  | 1.29  | 1.01   | 1.13  | 1.13  | 1.15  |
|                         |                               |                |                 |                          |                         |  |  |                            |                             | 10                    | 488  | 2944   | 1348  | 3307                                   | 1711  | 1.27  | 1.00   | 1.12  | 1.12  | 1.14  |
| 15.85                   | 17.4                          | 1.5            | 336773.4        | 2100                     | 0.00351                 | 0.063                                      | 432.0  | 2143.6                     | 250                         | 1                     | 530  | 2986   | 1274  | 3307                                   | 1595  | 1.25  | 1.06   | 1.11  | 1.10  | 1.13  |
|                         |                               |                |                 |                          |                         |  |  |                            |                             | 5                     | 582  | 3037   | 1326  | 3307                                   | 1595  | 1.20  | 1.02   | 1.09  | 1.08  | 1.11  |
|                         |                               |                |                 |                          |                         |  |  |                            |                             | 10                    | 604  | 3060   | 1348  | 3307                                   | 1595  | 1.18  | 1.00   | 1.08  | 1.08  | 1.10  |
| 17.45                   | 19.1                          | 1              | 556154.1        | 2100                     | 0.00321                 | 0.092                                      | 478.2  | 2143.6                     | 200                         | 1                     | 491  | 2947   | 1282  | 3307                                   | 1641  | 1.28  | 1.05   | 1.12  | 1.12  | 1.14  |
|                         |                               |                |                 |                          |                         |  |  |                            |                             | 5                     | 539  | 2995   | 1329  | 3307                                   | 1641  | 1.23  | 1.02   | 1.10  | 1.10  | 1.12  |
|                         |                               |                |                 |                          |                         |  |  |                            |                             | 10                    | 560  | 3015   | 1350  | 3307                                   | 1641  | 1.22  | 1.00   | 1.10  | 1.09  | 1.12  |
| 14.35                   | 15.7                          | 1.5            | 304902.1        | 2100                     | 0.00358                 | 0.069                                      | 360.7  | 2143.6                     | 200                         | 1                     | 591  | 3047   | 1264  | 3307                                   | 1524  | 1.21  | 1.07   | 1.09  | 1.08  | 1.10  |
|                         |                               |                |                 |                          |                         |  |  |                            |                             | 5                     | 650  | 3106   | 1323  | 3307                                   | 1524  | 1.15  | 1.02   | 1.06  | 1.06  | 1.08  |
|                         |                               |                |                 |                          |                         |  |  |                            |                             | 10                    | 675  | 3131   | 1348  | 3307                                   | 1524  | 1.13  | 1.00   | 1.06  | 1.05  | 1.07  |



**Table 3-7** Specific gravity = 1.0

| Injection Rate (bbl/min) | Velocity Inside Tubing (ft/s) | Viscosity (cp) | Reynolds Number | Critical Reynolds Number | Fanning Friction Factor | Frictional Pressure Loss Gradient (psi/ft) | Frictional Pressure Loss Inside Tubing (psi) | Hydrostatic Pressure (psi) | Formation Permeability (md) | Injection Time (year) | Bottomhole Injection Pressure Minus Reservoir Pressure (psi) | Expected Bottomhole Injection Pressure (psi) | Estimated Wellhead Injection Pressure (psi) | Fracture Pressure at Casing Shoe (psi) | Maximum Possible Surface Injection Pressure (psi) | Injection Pressure Design Factor (for P_frac) | Injection Pressure Design Factor (for P_inj_max Table-5) | Bottomhole Pressure Design Factor (P_frac/P_bh) | Okla. Admin. Code §252:652-9-1 Overburden Pressure Gradient Known (0.979 psi/ft), <65% of it at injection zone (5175 ft) = 3293 psi, Design Factor | Okla. Admin. Code §252:652-9-1 Overburden Pressure Gradient not known, <0.65 psi/ft, Design Factor |
|--------------------------|-------------------------------|----------------|-----------------|--------------------------|-------------------------|--|--|----------------------------|-----------------------------|-----------------------|--|--|---|--|---|---|--|---|--|--|
| 11                       | 12.0                          | 1              | 369036.1        | 2100                     | 0.00345                 | 0.041                                      | 215.4  | 2256.4                     | 250                         | 1                     | 251  | 2707   | 666   | 3307                                   | 1265  | 1.90  | 1.89   | 1.22  | 1.22   | 1.24   |
|                          |                               |                |                 |                          |                         |  |  |                            |                             | 5                     | 275  | 2731   | 690   | 3307                                   | 1265  | 1.83  | 1.83   | 1.21  | 1.21   | 1.23   |
|                          |                               |                |                 |                          |                         |  |  |                            |                             | 10                    | 286  | 2741   | 700   | 3307                                   | 1265  | 1.81  | 1.80   | 1.21  | 1.20   | 1.23   |
| 11                       | 12.0                          | 1.5            | 246024          | 2100                     | 0.00372                 | 0.045                                      | 232.3  | 2256.4                     | 250                         | 1                     | 368  | 2824   | 799   | 3307                                   | 1282  | 1.60  | 1.58   | 1.17  | 1.17   | 1.19   |
|                          |                               |                |                 |                          |                         |  |  |                            |                             | 5                     | 404  | 2860   | 835   | 3307                                   | 1282  | 1.54  | 1.51   | 1.16  | 1.15   | 1.18   |
|                          |                               |                |                 |                          |                         |  |  |                            |                             | 10                    | 419  | 2875   | 851   | 3307                                   | 1282  | 1.51  | 1.48   | 1.15  | 1.15   | 1.17   |
| 11                       | 12.0                          | 1              | 369036.1        | 2100                     | 0.00345                 | 0.041                                      | 215.4  | 2256.4                     | 200                         | 1                     | 310  | 2766   | 725   | 3307                                   | 1265  | 1.75  | 1.74   | 1.20  | 1.19   | 1.22   |
|                          |                               |                |                 |                          |                         |  |  |                            |                             | 5                     | 340  | 2796   | 755   | 3307                                   | 1265  | 1.68  | 1.67   | 1.18  | 1.18   | 1.20   |
|                          |                               |                |                 |                          |                         |  |  |                            |                             | 10                    | 353  | 2809   | 767   | 3307                                   | 1265  | 1.65  | 1.64   | 1.18  | 1.17   | 1.20   |
| 11                       | 12.0                          | 1.5            | 246024          | 2100                     | 0.00372                 | 0.045                                      | 232.3  | 2256.4                     | 200                         | 1                     | 453  | 2909   | 885   | 3307                                   | 1282  | 1.45  | 1.42   | 1.14  | 1.13   | 1.16   |
|                          |                               |                |                 |                          |                         |  |  |                            |                             | 5                     | 498  | 2954   | 930   | 3307                                   | 1282  | 1.38  | 1.35   | 1.12  | 1.11   | 1.14   |
|                          |                               |                |                 |                          |                         |  |  |                            |                             | 10                    | 518  | 2974   | 949   | 3307                                   | 1282  | 1.35  | 1.33   | 1.11  | 1.11   | 1.13   |
| 18.8                     | 20.6                          | 1              | 630716.2        | 2100                     | 0.00314                 | 0.110                                      | 571.4  | 2256.4                     | 250                         | 1                     | 429  | 2885   | 1200  | 3307                                   | 1622  | 1.35  | 1.05   | 1.15  | 1.14   | 1.17   |
|                          |                               |                |                 |                          |                         |  |  |                            |                             | 5                     | 470  | 2926   | 1241  | 3307                                   | 1622  | 1.31  | 1.02   | 1.13  | 1.13   | 1.15   |
|                          |                               |                |                 |                          |                         |  |  |                            |                             | 10                    | 488  | 2944   | 1259  | 3307                                   | 1622  | 1.29  | 1.00   | 1.12  | 1.12   | 1.14   |
| 15.87                    | 17.4                          | 1.5            | 354945.6        | 2100                     | 0.00348                 | 0.087                                      | 451.5  | 2256.4                     | 250                         | 1                     | 530  | 2986   | 1181  | 3307                                   | 1502  | 1.27  | 1.07   | 1.11  | 1.10   | 1.13   |
|                          |                               |                |                 |                          |                         |  |  |                            |                             | 5                     | 582  | 3038   | 1233  | 3307                                   | 1502  | 1.22  | 1.02   | 1.09  | 1.08   | 1.11   |
|                          |                               |                |                 |                          |                         |  |  |                            |                             | 10                    | 605  | 3061   | 1256  | 3307                                   | 1502  | 1.20  | 1.00   | 1.08  | 1.08   | 1.10   |
| 17.48                    | 19.1                          | 1              | 586431.8        | 2100                     | 0.00318                 | 0.096                                      | 500.3  | 2256.4                     | 200                         | 1                     | 492  | 2948   | 1192  | 3307                                   | 1550  | 1.30  | 1.06   | 1.12  | 1.12   | 1.14   |
|                          |                               |                |                 |                          |                         |  |  |                            |                             | 5                     | 540  | 2996   | 1240  | 3307                                   | 1550  | 1.25  | 1.02   | 1.10  | 1.10   | 1.12   |
|                          |                               |                |                 |                          |                         |  |  |                            |                             | 10                    | 561  | 3016   | 1260  | 3307                                   | 1550  | 1.23  | 1.00   | 1.10  | 1.09   | 1.12   |
| 14.44                    | 15.8                          | 1.5            | 322962.5        | 2100                     | 0.00354                 | 0.073                                      | 380.4  | 2256.4                     | 200                         | 1                     | 595  | 3051   | 1175  | 3307                                   | 1430  | 1.22  | 1.07   | 1.08  | 1.08   | 1.10   |
|                          |                               |                |                 |                          |                         |  |  |                            |                             | 5                     | 654  | 3110   | 1234  | 3307                                   | 1430  | 1.16  | 1.02   | 1.06  | 1.06   | 1.08   |
|                          |                               |                |                 |                          |                         |  |  |                            |                             | 10                    | 680  | 3135   | 1259  | 3307                                   | 1430  | 1.14  | 1.00   | 1.05  | 1.05   | 1.07   |



**Table 3-8** Specific gravity = 1.05

| Injection Rate (bbL/min) | Velocity Inside Tubing (ft/s) | Viscosity (cp) | Reynolds Number | Critical Reynolds Number | Fanning Friction Factor | Frictional Pressure Loss Gradient (psi/ft) | Frictional Pressure Loss Inside Tubing (psi) | Hydrostatic Pressure (psi) | Formation Permeability (md) | Injection Time (year) | Bottomhole Injection Pressure Minus Reservoir Pressure (psi) | Expected Bottomhole Injection Pressure (psi) | Estimated Wellhead Injection Pressure (psi) | Fracture Pressure at Casing Shoe (psi) | Maximum Possible Surface Injection Pressure (psi) | Injection Pressure Design Factor (for P_frac) | Injection Pressure Design Factor (for P_inj_max Table-5) | Bottomhole Pressure Design Factor (P_frac/P_bh) | Okla. Admin. Code § 252:652-9-1 Overburden Pressure Gradient Known (0.979 psi/ft), <65% of it at injection zone (5175 ft) = 3293 psi, Design Factor | Okla. Admin. Code § 252:652-9-1 Overburden Pressure Gradient not known, <0.65 psi/ft, Design Factor |
|--------------------------|-------------------------------|----------------|-----------------|--------------------------|-------------------------|--|--|----------------------------|-----------------------------|-----------------------|--|--|---|--|---|---|--|---|---|---|
| 11                       | 12.05                         | 1              | 387488          | 2100                     | 0.00342                 | 0.0431                                     | 224  | 2369                       | 250                         | 1                     | 251  | 2706   | 561   | 3307                                   | 1161  | 2.07  | 2.05   | 1.22  | 1.22  | 1.24  |
|                          |                               |                |                 |                          |                         |  |  |                            |                             | 5                     | 275  | 2730   | 585   | 3307                                   | 1161  | 1.98  | 1.96   | 1.21  | 1.21  | 1.23  |
|                          |                               |                |                 |                          |                         |  |  |                            |                             | 10                    | 285  | 2741   | 596   | 3307                                   | 1161  | 1.95  | 1.93   | 1.21  | 1.20  | 1.23  |
| 11                       | 12.05                         | 1.5            | 258325          | 2100                     | 0.00369                 | 0.0465                                     | 242  | 2369                       | 250                         | 1                     | 367  | 2823   | 695   | 3307                                   | 1179  | 1.69  | 1.65   | 1.17  | 1.17  | 1.19  |
|                          |                               |                |                 |                          |                         |  |  |                            |                             | 5                     | 403  | 2859   | 731   | 3307                                   | 1179  | 1.61  | 1.57   | 1.16  | 1.15  | 1.18  |
|                          |                               |                |                 |                          |                         |  |  |                            |                             | 10                    | 418  | 2874   | 747   | 3307                                   | 1179  | 1.58  | 1.54   | 1.15  | 1.15  | 1.17  |
| 11                       | 12.05                         | 1              | 387488          | 2100                     | 0.00342                 | 0.0431                                     | 224  | 2369                       | 200                         | 1                     | 309  | 2765   | 620   | 3307                                   | 1161  | 1.87  | 1.85   | 1.20  | 1.19  | 1.22  |
|                          |                               |                |                 |                          |                         |  |  |                            |                             | 5                     | 339  | 2795   | 650   | 3307                                   | 1161  | 1.79  | 1.77   | 1.18  | 1.18  | 1.20  |
|                          |                               |                |                 |                          |                         |  |  |                            |                             | 10                    | 352  | 2808   | 663   | 3307                                   | 1161  | 1.75  | 1.73   | 1.18  | 1.17  | 1.20  |
| 11                       | 12.05                         | 1.5            | 258325          | 2100                     | 0.00369                 | 0.0465                                     | 242  | 2369                       | 200                         | 1                     | 452  | 2908   | 780   | 3307                                   | 1179  | 1.51  | 1.47   | 1.14  | 1.13  | 1.16  |
|                          |                               |                |                 |                          |                         |  |  |                            |                             | 5                     | 497  | 2953   | 825   | 3307                                   | 1179  | 1.43  | 1.39   | 1.12  | 1.12  | 1.14  |
|                          |                               |                |                 |                          |                         |  |  |                            |                             | 10                    | 517  | 2972   | 845   | 3307                                   | 1179  | 1.39  | 1.36   | 1.11  | 1.11  | 1.13  |
| 18.55                    | 19.2                          | 1              | 587102.8        | 2100                     | 0.00317                 | 0.096                                      | 580.5  | 2369.3                     | 250                         | 1                     | 424  | 2879   | 1091  | 3307                                   | 1518  | 1.39  | 1.05   | 1.15  | 1.14  | 1.17  |
|                          |                               |                |                 |                          |                         |  |  |                            |                             | 5                     | 464  | 2920   | 1131  | 3307                                   | 1518  | 1.34  | 1.02   | 1.13  | 1.13  | 1.15  |
|                          |                               |                |                 |                          |                         |  |  |                            |                             | 10                    | 481  | 2937   | 1149  | 3307                                   | 1518  | 1.32  | 1.00   | 1.13  | 1.12  | 1.15  |
| 15.74                    | 17.2                          | 1.5            | 369639.9        | 2100                     | 0.00345                 | 0.089                                      | 462.9  | 2369.3                     | 250                         | 1                     | 526  | 2982   | 1076  | 3307                                   | 1400  | 1.30  | 1.07   | 1.11  | 1.10  | 1.13  |
|                          |                               |                |                 |                          |                         |  |  |                            |                             | 5                     | 578  | 3033   | 1127  | 3307                                   | 1400  | 1.24  | 1.02   | 1.09  | 1.09  | 1.11  |
|                          |                               |                |                 |                          |                         |  |  |                            |                             | 10                    | 600  | 3056   | 1149  | 3307                                   | 1400  | 1.22  | 1.00   | 1.08  | 1.08  | 1.10  |
| 17.27                    | 18.9                          | 1              | 608355.9        | 2100                     | 0.00316                 | 0.098                                      | 509.5  | 2369.3                     | 200                         | 1                     | 486  | 2942   | 1082  | 3307                                   | 1447  | 1.34  | 1.06   | 1.12  | 1.12  | 1.14  |
|                          |                               |                |                 |                          |                         |  |  |                            |                             | 5                     | 534  | 2989   | 1130  | 3307                                   | 1447  | 1.28  | 1.02   | 1.11  | 1.10  | 1.13  |
|                          |                               |                |                 |                          |                         |  |  |                            |                             | 10                    | 554  | 3010   | 1150  | 3307                                   | 1447  | 1.26  | 1.00   | 1.10  | 1.09  | 1.12  |
| 14.31                    | 15.7                          | 1.5            | 336057.7        | 2100                     | 0.00351                 | 0.075                                      | 389.4  | 2369.3                     | 200                         | 1                     | 590  | 3046   | 1066  | 3307                                   | 1327  | 1.24  | 1.08   | 1.09  | 1.08  | 1.10  |
|                          |                               |                |                 |                          |                         |  |  |                            |                             | 5                     | 648  | 3104   | 1124  | 3307                                   | 1327  | 1.18  | 1.02   | 1.07  | 1.06  | 1.08  |
|                          |                               |                |                 |                          |                         |  |  |                            |                             | 10                    | 674  | 3129   | 1149  | 3307                                   | 1327  | 1.15  | 1.00   | 1.06  | 1.05  | 1.07  |



**Table 3-9** Specific gravity = 1.2

| Injection Rate (bbU/min) | Velocity Inside Tubing (ft/s) | Viscosity (cp) | Reynolds Number | Critical Reynolds Number | Fanning Friction Factor | Frictional Pressure Loss Gradient (psi/ft) | Frictional Pressure Loss Inside Tubing (psi) | Hydrostatic Pressure (psi) | Formation Permeability (md) | Injection Time (year) | Bottomhole Injection Pressure Minus Reservoir Pressure (psi) | Expected Bottomhole Injection Pressure (psi) | Estimated Wellhead Injection Pressure (psi) | Fracture Pressure at Casing Shoe (psi) | Maximum Possible Surface Injection Pressure (psi) | Injection Pressure Design Factor (for P <sub>frac</sub> ) | Injection Pressure Design Factor (for P <sub>inj_max</sub> Table-5) | Bottomhole Pressure Design Factor (P <sub>frac</sub> /P <sub>bh</sub> ) | Okla. Admin. Code § 252:652-9-1 Overburden Pressure Gradient Known (0.979 psi/ft), <65% of it at injection zone (5175 ft) = 3293 psi, Design Factor | Okla. Admin. Code § 252:652-9-1 Overburden Pressure Gradient not known, <0.65 psi/ft, Design Factor |
|--------------------------|-------------------------------|----------------|-----------------|--------------------------|-------------------------|--|--|----------------------------|-----------------------------|-----------------------|--|--|---|--|---|---|---|---|---|---|
| 11                       | 12.0                          | 1              | 442843.3        | 2100                     | 0.00334                 | 0.048                                      | 250.0  | 2707.7                     | 250                         | 1                     | 251  | 2707   | 249   | 3307                                   | 849   | 3.41  | 3.29  | 1.22  | 1.22  | 1.24  |
|                          |                               |                |                 |                          |                         |  |  |                            |                             | 5                     | 275  | 2731   | 273   | 3307                                   | 849   | 3.11  | 3.00  | 1.21  | 1.21  | 1.23  |
|                          |                               |                |                 |                          |                         |  |  |                            |                             | 10                    | 286  | 2741   | 284   | 3307                                   | 849   | 2.99  | 2.89  | 1.21  | 1.20  | 1.23  |
| 11                       | 12.0                          | 1.5            | 295228.8        | 2100                     | 0.00360                 | 0.052                                      | 269.4  | 2707.7                     | 250                         | 1                     | 368  | 2824   | 385   | 3307                                   | 868   | 2.25  | 2.13  | 1.17  | 1.17  | 1.19  |
|                          |                               |                |                 |                          |                         |  |  |                            |                             | 5                     | 404  | 2860   | 421   | 3307                                   | 868   | 2.06  | 1.95  | 1.16  | 1.15  | 1.18  |
|                          |                               |                |                 |                          |                         |  |  |                            |                             | 10                    | 419  | 2875   | 437   | 3307                                   | 868   | 1.99  | 1.88  | 1.15  | 1.15  | 1.17  |
| 11                       | 12.0                          | 1              | 442843.3        | 2100                     | 0.00334                 | 0.048                                      | 250.0  | 2707.7                     | 200                         | 1                     | 310  | 2766   | 308   | 3307                                   | 849   | 2.76  | 2.66  | 1.20  | 1.19  | 1.22  |
|                          |                               |                |                 |                          |                         |  |  |                            |                             | 5                     | 340  | 2796   | 338   | 3307                                   | 849   | 2.51  | 2.43  | 1.18  | 1.18  | 1.20  |
|                          |                               |                |                 |                          |                         |  |  |                            |                             | 10                    | 353  | 2809   | 351   | 3307                                   | 849   | 2.42  | 2.34  | 1.18  | 1.17  | 1.20  |
| 11                       | 12.0                          | 1.5            | 295228.8        | 2100                     | 0.00360                 | 0.052                                      | 269.4  | 2707.7                     | 200                         | 1                     | 453  | 2909   | 471   | 3307                                   | 868   | 1.84  | 1.74  | 1.14  | 1.13  | 1.16  |
|                          |                               |                |                 |                          |                         |  |  |                            |                             | 5                     | 498  | 2954   | 516   | 3307                                   | 868   | 1.68  | 1.59  | 1.12  | 1.11  | 1.14  |
|                          |                               |                |                 |                          |                         |  |  |                            |                             | 10                    | 518  | 2974   | 535   | 3307                                   | 868   | 1.62  | 1.53  | 1.11  | 1.11  | 1.13  |
| 17.86                    | 19.6                          | 1              | 719016.4        | 2100                     | 0.00306                 | 0.116                                      | 604.9  | 2707.7                     | 250                         | 1                     | 408  | 2864   | 761   | 3307                                   | 1204  | 1.58  | 1.08  | 1.15  | 1.15  | 1.17  |
|                          |                               |                |                 |                          |                         |  |  |                            |                             | 5                     | 447  | 2903   | 800   | 3307                                   | 1204  | 1.51  | 1.03  | 1.14  | 1.13  | 1.16  |
|                          |                               |                |                 |                          |                         |  |  |                            |                             | 10                    | 464  | 2919   | 817   | 3307                                   | 1204  | 1.47  | 1.00  | 1.13  | 1.13  | 1.15  |
| 15.27                    | 16.7                          | 1.5            | 409831.3        | 2100                     | 0.00339                 | 0.094                                      | 488.6  | 2707.7                     | 250                         | 1                     | 510  | 2966   | 747   | 3307                                   | 1087  | 1.46  | 1.10  | 1.11  | 1.11  | 1.13  |
|                          |                               |                |                 |                          |                         |  |  |                            |                             | 5                     | 560  | 3016   | 797   | 3307                                   | 1087  | 1.36  | 1.03  | 1.10  | 1.09  | 1.12  |
|                          |                               |                |                 |                          |                         |  |  |                            |                             | 10                    | 582  | 3038   | 819   | 3307                                   | 1087  | 1.33  | 1.00  | 1.09  | 1.08  | 1.11  |
| 16.7                     | 18.3                          | 1              | 672316.6        | 2100                     | 0.00310                 | 0.103                                      | 535.1  | 2707.7                     | 200                         | 1                     | 470  | 2926   | 753   | 3307                                   | 1134  | 1.50  | 1.09  | 1.13  | 1.13  | 1.15  |
|                          |                               |                |                 |                          |                         |  |  |                            |                             | 5                     | 516  | 2972   | 799   | 3307                                   | 1134  | 1.42  | 1.03  | 1.11  | 1.11  | 1.13  |
|                          |                               |                |                 |                          |                         |  |  |                            |                             | 10                    | 536  | 2991   | 819   | 3307                                   | 1134  | 1.39  | 1.00  | 1.11  | 1.10  | 1.12  |
| 13.94                    | 15.3                          | 1.5            | 374135.5        | 2100                     | 0.00344                 | 0.080                                      | 414.0  | 2707.7                     | 200                         | 1                     | 575  | 3030   | 737   | 3307                                   | 1013  | 1.37  | 1.11  | 1.09  | 1.09  | 1.11  |
|                          |                               |                |                 |                          |                         |  |  |                            |                             | 5                     | 632  | 3087   | 794   | 3307                                   | 1013  | 1.28  | 1.03  | 1.07  | 1.07  | 1.09  |
|                          |                               |                |                 |                          |                         |  |  |                            |                             | 10                    | 656  | 3112   | 818   | 3307                                   | 1013  | 1.24  | 1.00  | 1.06  | 1.06  | 1.08  |



**RESPONSE 3(c):**

Surface porosity,  $\phi_o$ , decline constant,  $k$ , average brine density,  $\rho_f$ , formation grain and injection depth,  $D$ , are considered by using the historic data available as:

$$\begin{aligned}\phi_o &= 16.265 \% \\ k &= 0.000177 \text{ ft}^{-1} \\ \rho_f &= 1.09 \text{ sp. gr} \\ \rho_g &= 2.4 \text{ sp. gr} \\ D &= 5200 \text{ ft}\end{aligned}$$

Overburden pressure,  $\sigma_{ob}$ , is calculated by:

$$\begin{aligned}\sigma_{ob} &= \rho_g g D - \frac{(\rho_g - \rho_f) g \phi_o}{k} [1 - e^{-k D}] \\ &= 0.052 (2.4) (8.33) (5200) \\ &\quad - \frac{0.052(2.4 - 1.09)(8.33)(0.163)}{(0.000177)} [1 - e^{-(0.000177)(5200)}] = 5092 \text{ psi}\end{aligned}$$

Overburden pressure gradient,  $g_{ob}$ , at injection zone estimated:

$$g_{ob} = \frac{(5092)}{(5200)} = 0.979 \text{ psi/ft}$$

Using Biot's Model, effective matrix stress gradient in vertical direction,  $g_z$ :

$$g_z = 0.979 - 0.472 \approx 0.5 \text{ psi/ft}$$

Formation pressure gradient,  $g_p$ , from PFT data:

$$g_p = 0.472 \text{ psi/ft}$$

Using Bottomhole Reservoir Pressures from the 2024 and 2025 PFT analysis presented in Table 8 of MES' Response to NOD Letter Dated May 19, 2025 (**Appendix I**), which were taken directly from the PFT reports, the formation pressure gradient in 2024 was 0.47165 psi/ft and the formation pressure gradient in 2025 was 0.4733 psi/ft. Therefore, the formation pressure gradient considered for this analysis as 0.472 psi/ft is reasonable, since it is the approximate average of these two numbers as well.

Fracture pressure gradient,  $g_{ff}$ , using Hubbert & Willis method at injection zone:

$$g_{ff} = g_p + \frac{g_z}{3} = (0.472) + \frac{(0.5)}{3} = 0.639 \text{ psi/ft}$$



**RESPONSE 3(d):**

The observed wellhead pressure at MES-1 under non-injection conditions should not be considered artesian flow because it results from the difference between the formation pressure and the hydrostatic pressure of the fluid column inside the well, rather than from the formation naturally flowing to the surface. The formation pressure at 5,203 ft is estimated to be 2,456 psi using a pressure gradient of 0.472 psi/ft (using 2024 and 2025 PFT data as explained in the previous paragraph), while the hydrostatic pressure depends entirely on the specific gravity of the fluid present in the wellbore. A fluid with a specific gravity of 1.09 or greater is sufficient to balance the formation pressure, resulting in 0 psi wellhead pressure under static conditions. Therefore, any positive wellhead pressure observed is simply due to the well containing a lighter fluid column with insufficient hydrostatic head, not because the formation itself is artesian. As mentioned and supported in the response to Deficiency Number 1, the fluid in the Arbuckle formation has specific gravity greater than 1.09.



## DEFICIENCY NO 4

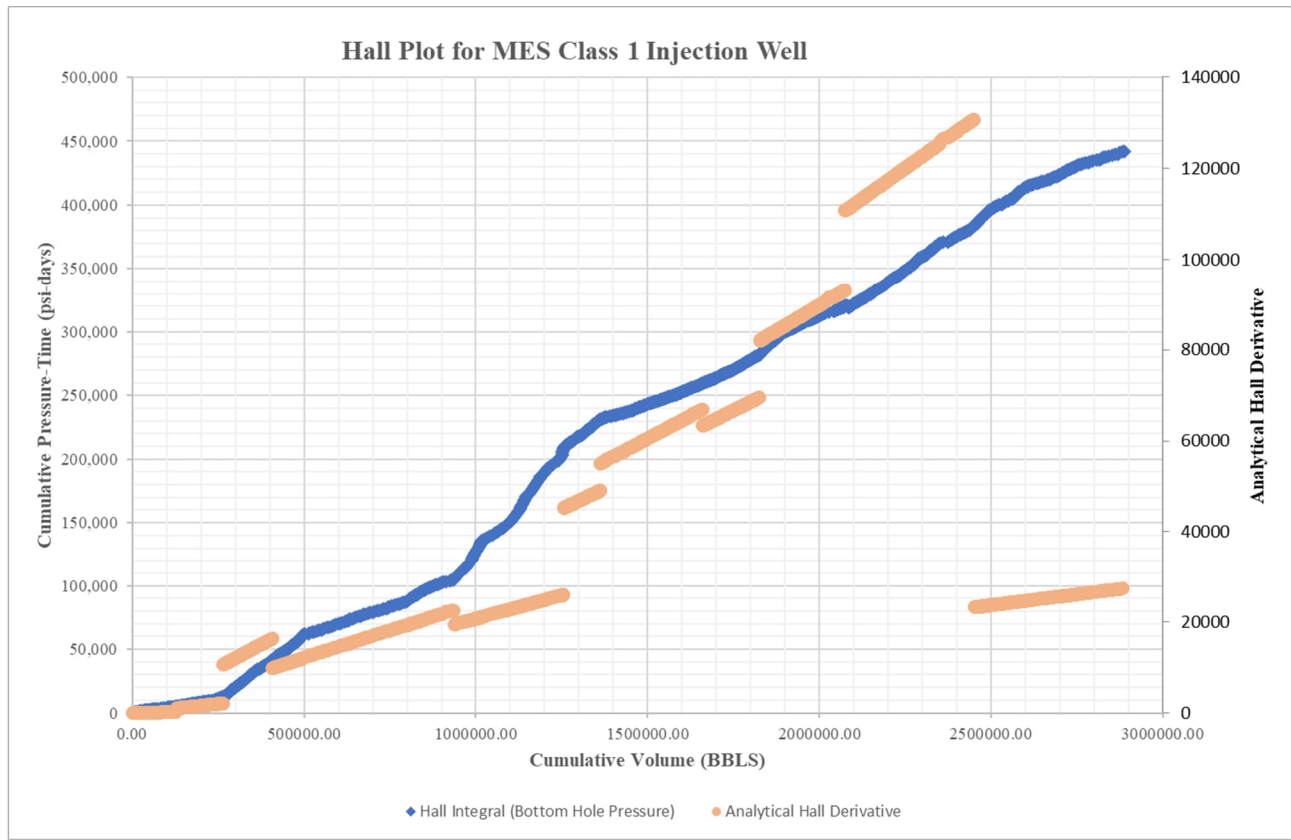
**In response to Deficiency No. 6 regarding updates to Mid-Way's Seismic Contingency Plan:**

- a. Mid-Way provided an updated revised Hall Plot inclusive of the Hall derivative to account for recent injection data. On the Hall Plot Figures provided in Appendix D, it appears the full range of the X-axes are not shown on the graphs (Figures 1-1, 1-2, and 2-1); please provide graphs showing the complete range of values.**
- b. For Figure 1-1, please provide a sample calculation for rows before and after the discontinuity occurring on the Analytical Hall Derivative around January 3, 2025. Please also provide a more detailed explanation for the several discontinuities appearing on Figures 1-1 and 2-1, most notably the extreme difference in Analytical Hall Derivative values between 2024 and 2025.**
- c. The secondary vertical axis scales are compressed on the graphs and reduce the utility of the graphs. Scales should be consistent with the range of the data being presented.**

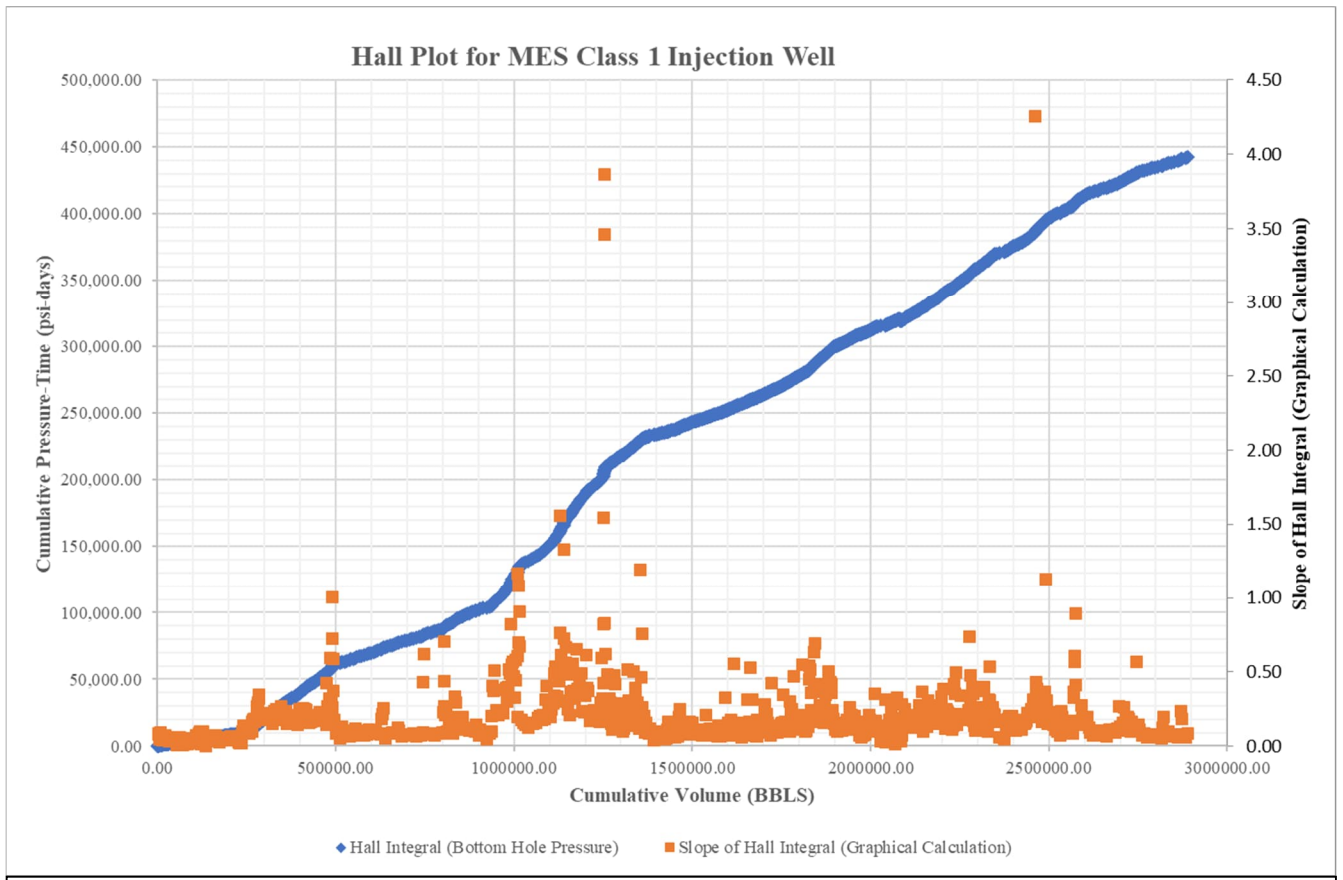
### **RESPONSE 4(a):**

Figure 1-1, 1-2, and 2-1 as provided in Appendix D in December 2025 NOD response has been updated showing complete range of values as follows. Figure 1-1, 1-2, and 2-1 have been re-numbered to **Figure 4-1, 4-2 and 4-3** to match the current document.

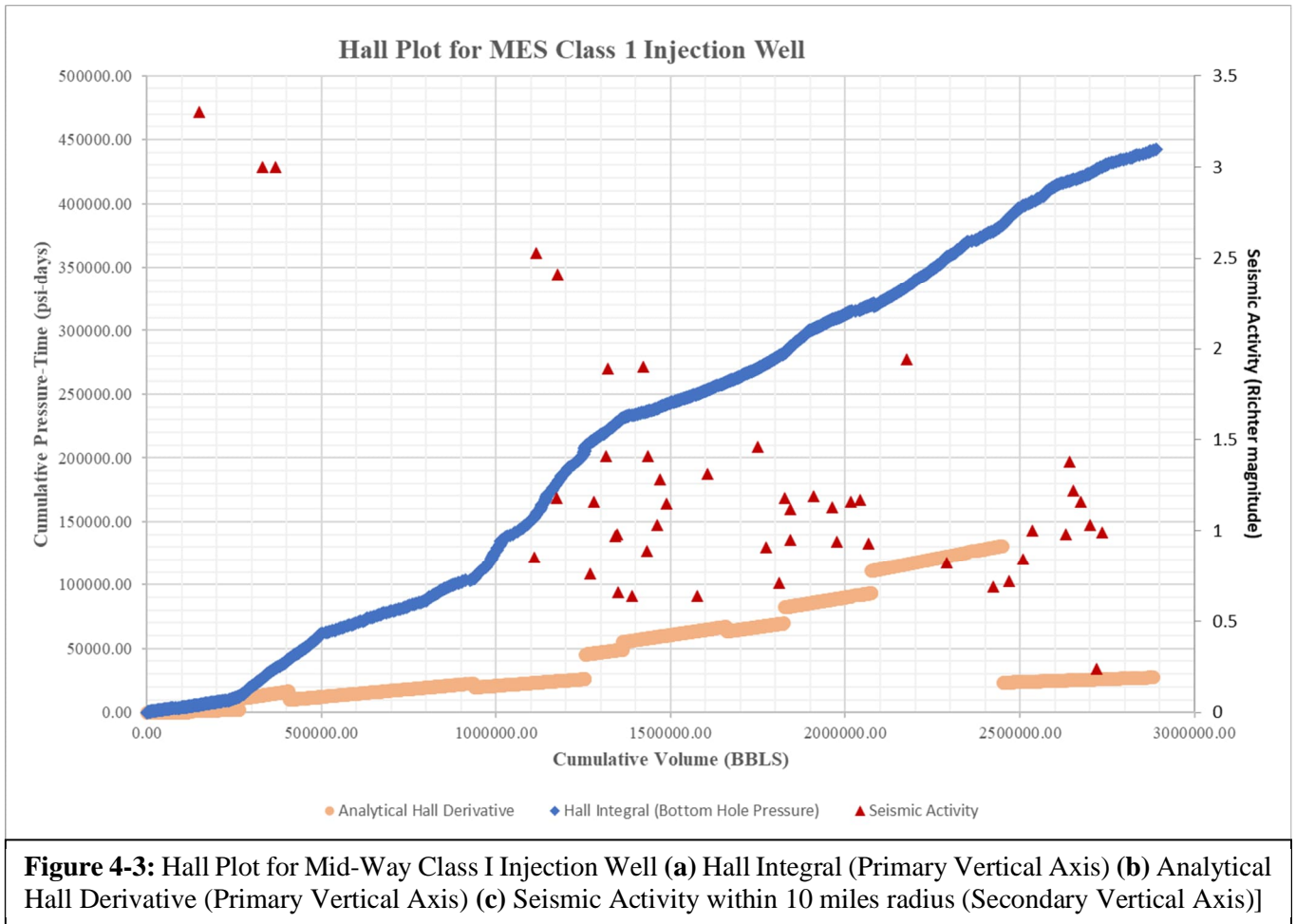




**Figure 4-1:** Hall Plot for Mid-Way Class I Injection Well [(a) Hall Integral (Primary Vertical Axis) (b) Analytical Hall Derivative (Secondary Vertical Axis)]



**Figure 4-2:** Hall Plot for Mid-Way Class I Injection Well [(a) Hall Integral (Primary Vertical Axis) (b) Revised Hall Derivative using the graphical calculation for the slope of the Hall integral (Secondary Vertical Axis)]



**RESPONSE 4(b):**

Sample Calculation for rows before and after the discontinuity occurring on the Analytical Hall Derivative around January 3, 2025 are as follows.

Hall Derivative is calculated using the following Hall Derivative equations (1, 2).

$$D_{hi} = \alpha_1 W_i [\ln(r_e/r_w) - 0.5 + s^*] \dots\dots\dots (1)$$

Where,

$\alpha_1$  : Reservoir Factors

$$\alpha_1 = 141.2 B \mu / (kh) \dots\dots\dots (2)$$

B : Formation Volume Factor [Generally 1 for Water]

Parameters,  $\mu$ , kh,  $r_e$ ,  $P_e$  and  $s^*$  were used from the 2015 to 2025 Schlumberger Pressure Fall Off Test (PFT) Reports [Submitted annually to DEQ with the PFT Reports as an attachment] and are summarized in the following table.

|                             |            |       | 2015     | 2016     | 2017     | 2018     | 2019     | 2020     | 2021     | 2022     | 2023     | 2024     | 2025     |
|-----------------------------|------------|-------|----------|----------|----------|----------|----------|----------|----------|----------|----------|----------|----------|
| Skin                        | $S^*$      |       | -4.56    | 4.98     | 1.53     | 24.1     | 9.82     | 0.93     | 5.5      | 23       | 16.6     | 19.8     | -4.47    |
| Radial Distance to $P_e$    | $r_e$      | ft    | 6810     | 7980     | 6810     | 9640     | 8380     | 3200     | 3400     | 5760     | 3000     | 4269     | 3743     |
| Permeable Thickness         | kh         | md-ft | 540000   | 263000   | 38800    | 199000   | 133000   | 37740.0  | 49965    | 119700   | 79330.1  | 76210.3  | 65198    |
| Reservoir Factors           | $\alpha_1$ |       | 0.000261 | 0.000537 | 0.003639 | 0.000710 | 0.001062 | 0.003741 | 0.002826 | 0.001180 | 0.001780 | 0.001853 | 0.002166 |
| Reservoir Pressure          | $P_e$      | psig  | 2516.3   | 2556.3   | 2509.3   | 2490.3   | 1852.3   | 2649.3   | 2518     | 2522     | 2514.57  | 2503.93  | 2460     |
| Depth                       |            | ft    | 5300     | 5300     | 5300     | 5300     | 5300     | 5650     | 5340     | 5340     | 5340     | 5340     | 5228     |
| Reservoir Pressure @5127 ft | $P_e$      | psig  | 2434     | 2473     | 2427     | 2409     | 1792     | 2404     | 2418     | 2421     | 2414     | 2404     | 2412     |

$W_i$  : Cumulative Injection [from daily injection historical data in barrels]

$r_w$  : Wellbore radius [0.328 ft]

Hall Derivative calculation for row, 12/30/2024:

$$D_{hi} = 0.001853 \times 2452088.67 \times [\ln\left(\frac{4269}{0.328}\right) - 0.5 + 19.8]$$

$$=130722.34$$



Hall Derivative calculation for row, 1/3/2025:

$$D_{hi} = 0.002166 \times 2451422.88 \times \left[ \ln\left(\frac{3743}{0.328}\right) - 0.5 + (-4.47) \right]$$

$$= 23236.85$$

Apparently, the Hall Derivative exhibits different segments corresponding to each year of data from 2015 to 2025 and this is consistent as previously provided analysis (approved by DEQ in 2021). The segmentations are due to differences between datasets from each year PFT model (most notably the Radial Distance to  $P_e$  and Skin data).

In the above example calculation, the data variation between 12/30/2024 and 1/3/2025 are summarized in the following table:

|   |            | 2024       | 2025       |
|---|------------|------------|------------|
| <b>Skin</b>                                       | $S^*$      | 19.8       | -4.47      |
| <b>Radial Distance to <math>P_e</math></b>        | $r_e$      | 4269       | 3743       |
| <b>Permeable Thickness</b>                        | $kh$       | 76210.3    | 65198      |
| <b>Reservoir Factors</b>                          | $\alpha_1$ | 0.001853   | 0.002166   |
| <b>Reservoir Pressure</b>                         | $P_e$      | 2503.93    | 2460       |
| <b>Depth, ft</b>                                  |            | 5340       | 5228       |
| <b>Reservoir Pressure @5127 ft</b>                | $P_e$      | 2404       | 2412       |
|   |            |            |            |
|   |            | 12/30/2024 | 1/3/2025   |
| <b>Cumulative Volume, <math>W_i</math> (BBLs)</b> |            | 2452088.67 | 2454122.88 |

The difference in data set used from PFT analysis contributes to a different starting point of Hall Derivatives in the plot (**Figure 4-1**). Although the Hall Derivative plot is segmented, the slope of all the segments is quite consistent.



**RESPONSE 4(c):**

The secondary axis scale in **Figure 4-1** (previously Figure 1-1) has been updated (see **Response 4(a)**).



## **DEFICIENCY NO 5**

**In response to Deficiency No. 8 regarding pressure fall-off tests ("PFTs"):**

- a. Please include the 2024 and 2025 PFT full reports.**
- b. Please provide a brief summary of the assessments in Mid -Way's previous January 10, 2014 NOD Response #7 addressing no-flow boundaries observed in the initial PFTs for the MES-1 injection well (see Item 2 above). Please include a citation and the reference.**
- c. Please indicate if features of no-flow boundaries (and / or interferences from the Twin Cities saltwater disposal well) are reflected in the current PFT data. If not, what changes 1 conditions have occurred since the initial tests such that no-flow boundary features are no longer present.**
- d. Please also address any changes in injection conditions that would explain the drop in permeability between the first and second PFTs (in 2015 and 2016, respectively) as shown on Table 8.**

### **RESPONSE 5(a):**

2024 and 2025 PFT Reports are attached in the **Appendix E**



## **RESPONSE 5(b):**

The following is a summary of the assessments in Mid -Way's previous January 10, 2014, NOD Response #7 addressing no-flow boundaries observed in the initial PFTs for the MES-1 injection well:

The second pressure fall-off test conducted for MES #1 has been subject to multiple professional interpretations, each of which is technically supportable based on the available data. Dr. Ozbayoglu, consistent with EPA's assessment, originally applied a finite homogeneous reservoir model with two possible perpendicular no-flow boundaries and used that framework to evaluate reservoir response, fracture pressure, anticipated pressure buildup, and wastewater front migration. Schlumberger, on the other hand, interpreted the data as supporting a dual porosity reservoir model characterized by a transition between two radial flow regimes. Schlumberger's re-evaluation further noted that the later-time pressure derivative response may reflect either the limited injection duration or the presence of reservoir boundaries but nonetheless continued to support the dual porosity interpretation based on the observed radial flow behavior.

Mid-Way has also identified additional factors that may have influenced the pressure fall-off test results and their interpretation, including the use of large volumes of fresh water during testing. Differences in density and viscosity between the injected fresh water and native formation fluids may have affected the observed pressure response. In addition, published literature has shown that injection of fresh water into saltwater-bearing fractured dolomite formations similar to the Arbuckle may establish convection currents driven by salinity-related density gradients. While the specific effect of such processes on the MES #1 short-term test cannot be quantified with certainty, they represent reasonable considerations in evaluating the variability in reservoir model interpretations.

Notwithstanding these differing interpretations, the available analyses consistently indicate that conservative, worst-case assumptions were used to assess anticipated operating conditions at MES #1. Under the proposed injection scenario, projected formation pressure increase, pressure



distribution, and wastewater front advancement remain within acceptable limits and do not indicate exceedance of formation fracture pressure or initiation of fractures. Accordingly, the results support the conclusion that the Arbuckle Group is suitable for the safe injection of wastewater at MES #1, consistent with its long-standing and widespread use as a disposal interval for fluids associated with oil and gas exploration and production activities.

**Citation/Reference (Appendix F, G, and H)**

1. Ozbayoglu, E.M., “*Analysis on Hydraulics during Injection Process, and, Pressure Distribution within the Formation*”, Report, Mid-Way MES#1, December, 2013.
2. Gonzalez, Y., “*A & M Engineering and Environmental Services, Inc., Well: MES#1 (October 2010) Pressure Fall Off Review*”, Report, January, 2014.
3. Response to Notice of Deficiency Letter Dated October 9, 2013 - Response to Deficiency Number 7



**RESPONSE 5(C):**

The 2010 PFT identified a reservoir system influenced by two perpendicular no-flow boundaries located approximately 1,200 ft from the well, along with possible interference from the nearby Twin Cities disposal well. These features were inferred from late-time deviations in the pressure derivative response, which is typical when a pressure transient reaches a boundary or interacts with external disturbances. The 2010 interpretation also relied on a dual-porosity conceptual model with strong fracture contribution and stimulation effects, which enhanced the detectability of such structural or external influences.

The October 2025 PFT shows no diagnostic signature of boundaries or interference. The pressure transient behavior is well matched using a radial composite reservoir model with infinite boundary conditions, explicitly indicating that the reservoir is behaving as a system that is effectively unbounded within the time and spatial scale of the test. The interpretation identifies wellbore storage, a short duration near wellbore response, and a clear infinite acting radial flow (IARF) regime between approximately 59 and 68 hours, from which permeability and reservoir pressure are reliably estimated. There is no reported late-time derivative upturn or stabilization characteristic of boundary effects, which would normally indicate the presence of impermeable barriers or pressure interference.

The radius of investigation is approximately 3,743 ft for the 2025 test. This radius extends well beyond the ~1,200 ft boundary distances inferred in the 2010 analysis. If those boundaries were still hydraulically significant, they would be expected to be observed in the late-time pressure derivative. Their absence indicates that either the originally inferred boundaries are no longer acting as effective no-flow barriers, or their influence has been overwhelmed by broader pressure equilibration within the reservoir system.

PFT interpretation since at least 2017, including 2025 PFT, consistently supports the assumption of “infinite boundary” conditions and the explicit exclusion of other wells from the model,



meaning that no measurable interference from the Twin Cities well is required to match the data. This shows that any pressure effects are either negligible within the timeframe of the test or have become sufficiently uniform that they no longer produce a distinct transient signature.

From a pressure transient analysis perspective, any sustained interference from the Twin Cities disposal well would be observed as late-time deviations in the pressure derivative, such as boundary effects or non-radial flow behavior. No such features are observed in the 2025 PFT or other recent tests. Additionally, the radius of investigation for the 2025 test extends beyond the distance to the previously inferred boundaries and is comparable to the distance to the Twin Cities well, yet no interference signature is detected. This indicates that any interaction between the wells is negligible. Since 2010, long-term injection has expanded and stabilized the reservoir pressure field and introduced radial composite behavior, resulting in a more uniform pressure distribution that further reduces the detectability and significance of boundary and interference effects.

The absence of no-flow boundary signatures in the 2025 PFT indicates that the previously interpreted boundaries are no longer hydraulically effective, or were not true impermeable boundaries. The 2010 interpretation relied on a dual-porosity/fractured model and late-time derivative behavior that may have reflected transient heterogeneity or limited test duration rather than true sealing boundaries. Also, sustained injection since 2015 has likely increased reservoir connectivity through fracture dilation or reactivation, reducing the effectiveness of any semi-sealing features. Long-term pressure buildup has led to a more uniform pressure field, diminishing localized gradient effects and the detectability of boundaries in pressure derivatives.



**RESPONSE 5(d):**

Permeability estimation in a cylindrical reservoir from a pressure fall-off test is based on the interpretation of pressure decline following an injection period, typically analyzed using radial flow theory and superposition principles. During injection, fluid is introduced at a known rate, and upon shut-in, the pressure response is recorded as the reservoir equilibrates. For a homogeneous, isotropic reservoir with radial flow geometry, the late-time pressure behavior during the fall-off period exhibits a semilog straight-line trend when plotted against Horner time. The slope of this straight line is directly related to the formation permeability–thickness product ( $kh$ ), as derived from solutions to the diffusivity equation under radial flow conditions. By identifying the appropriate infinite-acting radial flow regime and applying the Horner method, permeability can be calculated using the measured pressure change per logarithmic cycle, fluid properties (viscosity and formation volume factor), and test conditions (flow rate and thickness of the producing interval). In cases where reservoir boundaries or heterogeneities exist, deviations from ideal radial flow behavior may occur, requiring more advanced interpretation methods such as type-curve matching or numerical modeling. In all cases, the reliability of the permeability estimate depends on correctly identifying the dominant flow regime and accounting for near-wellbore effects such as skin, which can significantly influence the pressure response.

The pressure fall-off tests conducted in 2015 and 2016 for the MES #1 injection well exhibit a clear and substantial reduction in interpreted permeability, accompanied by a fundamental shift in near-wellbore behavior. In 2015, the interpreted permeability ranged approximately from 1140 to 1800 md depending on the selected analytical model, while the 2016 results indicate a lower permeability range of approximately 620 to 877 md. At the same time, the skin factor transitioned from negative values in 2015 (approximately  $-2.9$  to  $-5.2$ ) to positive values in 2016 (approximately  $+5$  to  $+10$ ), indicating a shift from enhanced injectivity conditions to near-wellbore flow restriction.

The 2015 test exhibited an early-time linear flow regime, which is characteristic of high-conductivity channel flow and suggests that injectivity was enhanced by near wellbore existing



high conductivity pathways that were active during the test. The 2016 test did not show any evidence of linear flow, indicating that high conductivity channel dominated flow was no longer present or no longer contributing significantly to the pressure response. The disappearance of this flow regime would lead to a significant reduction in the apparent permeability derived from the test, as pathway conductivity can dominate the pressure response in permeable systems.

The 2015 analysis indicates the absence of near-wellbore flow restriction, while the 2016 analysis identifies the presence of near-wellbore flow restriction with a positive skin factor. In permeable carbonate systems such as the Arbuckle Formation, relatively minor pore plugging or mobility reduction in the near-wellbore region may produce increase in pressure drop and corresponding decreases in interpreted permeability. Such damage may arise from several mechanisms, including fines migration, precipitation of scale or other solids, or similar. The injection of fluids with differing densities and salinities relative to the native formation fluids can lead to mixing, mobility contrasts, and complex flow behavior, including convective processes within the reservoir. These effects can enhance the potential for particle transport, chemical reactions, and localized plugging, all of which contribute to a reduction in effective permeability near the wellbore.

The 2015 PFT was conducted after a prolonged period of minimal or no injection activity, and the report notes that the pressure response may have been affected by this limited injection history. The 2016 report further confirms that the late-time behavior observed in the 2015 test was influenced by the relatively short injection history preceding that test. Under such conditions, the 2015 results may reflect transient cleanup effects or temporarily enhanced injectivity associated with initial injection into a relatively undisturbed formation. As injection operations continued, the system would be expected to evolve toward a more representative long-term condition, which is more likely captured in the 2016 test.

The available evidence indicates that the apparent reduction in permeability between the 2015 and 2016 PFTs is primarily the result of changes in near-wellbore conditions and injection dynamics rather than a fundamental degradation of the bulk reservoir properties. The 2015 test reflects a



condition in which injectivity was enhanced by high conductivity channel-dominated flow and the absence of flow restriction, whereas the 2016 test reflects a system in which pathway effects are no longer evident and the near-wellbore region has been impaired by restriction mechanisms. This transition is manifested quantitatively in the increase in required injection pressure, the shift from negative to positive skin, and the reduction in interpreted permeability.

The observed reduction in permeability between the 2015 and 2016 pressure fall-off tests reflects a change in permeability rather than a fundamental deterioration of the reservoir. The 2015 results were influenced by high conductivity channel-dominated flow and limited prior injection history, which enhanced the measured response, whereas the 2016 results reflect a more stabilized system with increased near-wellbore resistance and the absence of conductive pathway contribution. As a result, the lower permeability estimated in 2016 is primarily attributable to near-wellbore flow restriction and changes in flow regime, rather than a change in the intrinsic properties of the formation.



# APPENDIX A

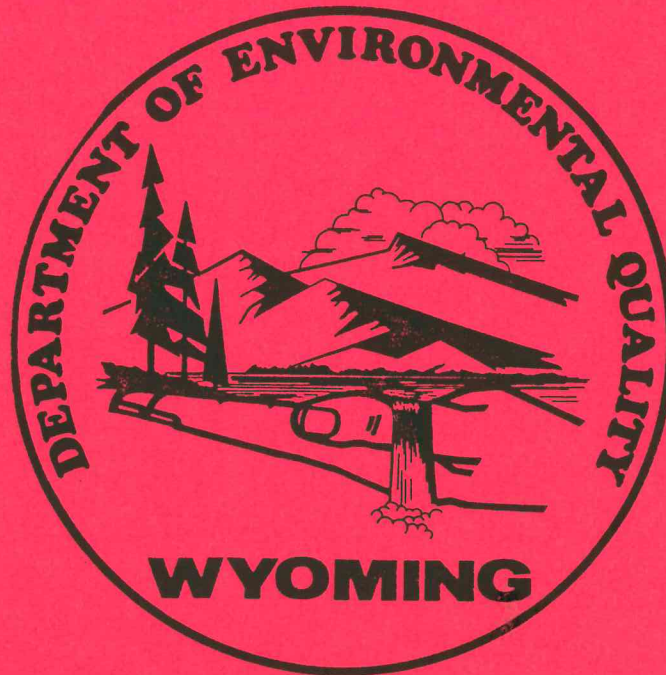
**WYOMING DEPARTMENT OF ENVIRONMENTAL QUALITY  
GUIDANCE DOCUMENT NUMBER 1  
PERMITTING OF CLASS I INJECTION WELLS**



UNDERGROUND INJECTION CONTROL PROGRAM  
WATER QUALITY DIVISION  
WYOMING DEPARTMENT OF ENVIRONMENTAL QUALITY

GUIDANCE DOCUMENT NUMBER 1

PERMITTING OF CLASS I INJECTION WELLS



May 11, 1994

THIS GUIDANCE DOCUMENT WAS PREPARED BY THE WATER QUALITY DIVISION OF THE WYOMING DEPARTMENT OF ENVIRONMENTAL QUALITY TO PROVIDE GUIDANCE IN THE PREPARATION OF PERMIT APPLICATIONS FOR CLASS I INJECTION WELLS. THIS DOCUMENT IS MEANT TO EXPLAIN THE TECHNICAL ASPECTS OF THE PERMITTING PROCESS BUT THIS DOCUMENT SHOULD NOT BE QUOTED IN APPLICATIONS. IF THERE ARE ANY CONFLICTS BETWEEN THIS DOCUMENT AND THE REGULATIONS, THE REGULATIONS WILL PREVAIL.

Section 1.0 The Area Of Review Calculation

Chapter XIII, Section 5(b)(iv) states that:

"(b) A complete application for a Class I well shall include:

(iv) A calculation of the area of review, which requires the calculation of the cone of influence and the area of the ultimate limit of emplaced waste."

Determining the area of review is important and should be done as soon as information can be gathered about the site of the injection. It is recommended that this calculation be done before land work is done and before extensive effort is made to accumulate information about adjacent wells. The area of review will determine how much work is required in both of these areas.

1.1 The Cone of Influence.

There are three separate calculations required. The first of these calculations is called the cone of influence. Section 5(b)(iv)(A) states that the cone of influence is calculated as:

"(A) The formula for determining the cone of influence is:

$$r = \left( \frac{2.25 K H t}{S 10^x} \right)^{1/2} \quad (\text{EQUATION 1})$$

$$\text{where: } x = \left( \frac{W}{G} \cdot B \right) \left( \frac{4\pi K H}{2.3Q} \right) \quad (\text{EQUATION 2})$$

r = Radius of the cone of influence of an injection well (feet)

K = Hydraulic conductivity of the injection zone (feet/day)

H = Thickness of the injection zone (feet)

t = Time of injection (days)

S = Storage coefficient (dimensionless)

Q = Injection rate (cubic feet/day)

B = Original hydrostatic head of injection zone (feet) measured from the base of the injection zone

W = Hydrostatic head of underground source of drinking water (feet) measured from the base of the injection zone

G = Specific gravity of fluid in the injection zone (dimensionless)

$\pi$  = 3.142 (dimensionless)"

The above calculation would be easily done, except that most of the information available is likely to be in different units. The first conversion that usually has to be done is to convert intrinsic permeability in millidarcies to the permeability in ft/day which is required by the above formula. The formula for this conversion is as follows:

$$K = K_i (\rho g / \mu) \quad (\text{EQUATION 3})$$

where:  $K$  = Permeability in cm/sec  
 $K_i$  = Intrinsic Permeability in millidarcies  
 $\rho$  = .999099 gm/cm<sup>3</sup> - the density of water  
 $g$  = 980 cm/sec<sup>2</sup> - the acceleration of gravity  
 $\mu$  = .011404 gm/(sec cm)

and: there are  $9.87 \times 10^{-9}$  cm<sup>2</sup>/darcy  
and: there are 2835 ft/day per cm/sec

EXAMPLE: An applicant finds that the receiver has a reported intrinsic permeability of 107 millidarcies.

$$\begin{aligned} K_i &= 107 \text{ millidarcies} = .107 \text{ darcies} \\ K_i &= (.107 \text{ darcies}) (9.87 \times 10^{-9} \text{ cm}^2/\text{darcy}) \\ K_i &= 1.056 \times 10^{-9} \text{ cm}^2 \\ K &= \frac{(1.056 \times 10^{-9} \text{ cm}^2) (.999099 \text{ gm/cm}^3) (980 \text{ cm/sec}^2)}{.011404 \text{ gm/(sec cm)}} \\ K &= 90.665 \times 10^{-6} \text{ cm/sec} \\ K &= (90.665 \times 10^{-6} \text{ cm/sec}) (2835 \text{ ft/day} / \text{cm/sec}) \\ K &= .2570 \text{ ft/day} \end{aligned}$$

The thickness of the injection zone is the entire thickness of the zone being injected into which is hydrologically continuous. This is regardless of the interval actually perforated.

EXAMPLE: An applicant wishes to inject into the Minnelusa Formation at a depth of 8596 feet. The perforated interval is 8586 to 8596. The Minnelusa Formation itself extends from 8586 to 8603. The thickness of the injection zone is therefore, 8603 - 8586 = 17 feet.

The pumping time is the duration of the permit being sought, usually 10 years or 3650 days. This value is entered in days. The

pumping time used should be the total planned duration of the project. If you intend to inject for 25 years, then that should be what is used. The permit itself must be reissued every 10 years, but the duration used should be the project duration, not the permit duration. These permits allow for injection continuously, there is no provision for limiting injection to working days. For this reason, the pumping time should be based on 365 day years.

EXAMPLE: The applicant wishes to inject for only 10 years and then plans to shut in the well. 10 years X 365 days = 3650 days.

The Coefficient of Storage is the thickness of the injection zone multiplied by 10<sup>-6</sup>/ft. This is per the EPA Guidance Document on Area of Review calculations on page V-14. The coefficient of storage is a dimensionless number.

EXAMPLE: The Minnelusa Formation is 17 feet thick at this location. The coefficient of storage is therefore  $17 \times 10^{-6}$ .

There are two terms in equation 1 which now must be determined. B, the original hydrostatic head of injection zone (feet), and W, the hydrostatic head of underground source of drinking water (USDW) (feet). The important point in determining these values is that they must both be measured from the same datum. In the regulations, it states that they should both be measured from the base of the injection zone. By measuring them from the base of the injection zone, one is always subtracting one positive number from another positive number. The most troublesome number to determine may be the static head in the overlying USDW. Some assumption is usually necessary. The applicant can look to USGS water supply papers, for estimates of water levels in wells, or one can make the assumption that the USDW is under artesian head at the location, or one can make the assumption that the deepest USDW is a water table aquifer with no artesian head. The most conservative assumption that can be made is to assume that the head on the USDW exactly equals the head in the receiver. If this assumption is made, the entire equation reduces to the radius within which there will be any increase in reservoir pressure.

EXAMPLE: The reservoir pressure in the Minnelusa Formation at this location is 2000 psi. Converting this to a static pressure will yield a pressure in feet of water as measured from the base of the injection zone.  
 $2000 \text{ psi} / .433 \text{ psi/ft} = 4615 \text{ feet}$

The pressure in the overlying USDW in this case has been approximated by the land surface. At this location, well within the boundaries of the Powder River Basin, most aquifers are under artesian head, but not a great deal of artesian head. Assuming that the head is just great enough to bring the water to the surface from the deepest USDW means that the depth to the base of the receiver becomes the head in the USDW. In this example the head is 8603 feet.

$$W - B = 8603 - 4615 = 3988 \text{ feet}$$

The next step in the example is to convert the Q or discharge rate into the units required by the equation. If you are using barrels per day (bbl/day) or gallons per day (gal/day), which are the normal units, you must convert to cubic feet per day. There are 42 gallons per barrel and 7.48 gallons per cubic foot.

EXAMPLE: The applicant wishes to inject 2000 bbl/day.  
 $Q = 2000 \text{ bbl/day} = (2000 \text{ bbl/day}) (42 \text{ gal/bbl}) / 7.48 \text{ gal/ft}^3$   
 $Q = 11,229 \text{ cubic feet per day}$

The next step is to determine the specific gravity of the fluid in the injection zone. Fresh water has a specific gravity of 1.00. The most concentrated brine, with a TDS of 280,000 mg/l has a specific gravity of 1.1. It may be possible to find measured specific gravity numbers. The so called API standard water analyses for produced water many times has the specific gravity determined. If these numbers are not available, one can assume a straight line relationship exists between specific gravity and TDS. The following example shows how this calculation would be done.

EXAMPLE: The fluid in the injection zone has been shown to contain 200,000 mg/l in Total Dissolved Solids.

$$\frac{G - 1}{200,000} = \frac{1.1 - 1}{280,000} \quad (\text{EQUATION 4})$$

$$G - 1 = .0714$$

$$G = 1.0714$$

At this point in the example, we are ready to calculate the exponential term (EQUATION 2) which goes in the denominator under the radical. The equation for this exponential term is, in itself, quite complex. The equation is:

$$x = \left( \frac{W - B}{G} \right) \left( \frac{4\pi KH}{2.3Q} \right) \quad (\text{EQUATION 2})$$

EXAMPLE:

$$x = \left( \frac{8603 \text{ ft} - 4615 \text{ ft}}{1.0714} \right) \left( \frac{4(3.14)(.257\text{ft/day})(17 \text{ ft})}{(2.3)(11,229 \text{ ft}^3/\text{day})} \right)$$

$$x = (3414)(.0021) = 7.2589$$

The final calculation is then made into equation 1 as follows:

$$r = \left( \frac{2.25 K H t}{S 10^x} \right)^{1/2} \quad (\text{EQUATION 1})$$

$$r = \left( \frac{(2.25)(.257\text{ft/day})(17\text{ft})(3650 \text{ days})}{(17 \times 10^{-6})(10^{7.2589})} \right)^{1/2}$$

$$r = 32 \text{ feet}$$

The above equation will generally yield a larger number as the difference between W and B becomes smaller. For example, in the above calculation, if the difference had been 2500 feet instead of the 3,414 which was calculated, then r would have been 78 feet instead of 32 feet. This should not be surprising. From an environmental point of view, the best receiver will be one which has a very low initial reservoir pressure, especially compared to any overlying USDW. Applicants will find that played out oil producing zones, particularly those zones which have had large volumes of fluid removed and not replaced.

The regulations do not preclude injecting into a zone which may be overpressurized prior to injection. However, this department will look at these applications very carefully in terms of plugging of existing wells, and the quality of construction. In the event that the zone to be injected into is already at a pressure higher than the USDW, the above equation would yield infinity. Applicants should use the assumption that the pressure in the USDW exactly equals the pressure in the receiver. This will yield the total radius of any increased pressure in the receiver as a result of the injection. This assumption is likely to yield an area of review of several miles.

## **APPENDIX B**

**SCHLUMBERGER TRANSIENT ANALYSIS REPORT OCTOBER 15, 2010**



*A & M Engineering and  
Environmental Services, Inc.*

*Mid-Way Environmental Services, Inc.  
Stroud, Oklahoma*

REPORT NO.  
AZIN00016

**S T A R**

**Schlumberger**

PAGE NO. 1

**Schlumberger Transient Analysis Report**

TEST DATE:  
15-Oct-10

**Based on Model Verified Interpretation  
Of Well Test Data**

|   |  |
|---|--|
| <b>COMPANY : A &amp; M ENGINEERING</b>  | <b>WELL: MES WD #1</b>   |
| <b>TEST IDENTIFICATION</b><br>Test Type ..... INJECTION / FALLOFF<br>Test No. .... ONE<br>Formation ..... ARBUCKLE<br>Test Interval (ft) ..... 5,170 - 6,900  | <b>WELL LOCATION</b><br>Field .....<br>County ..... LINCOLN<br>State ..... OK<br>Location ..... SEC 9-14N-5E   |
| <b>COMPLETION CONFIGURATION</b><br>Casing / Liner Size (in) ..... 8 5/8<br>Perforated Interval (ft) ..... OPEN HOLE<br>Perforated Interval (ft) .....<br>Perforated Interval (ft) .....<br>Perforated Interval (ft) .....<br>Perforated Interval (ft) .....<br>Perforated Interval (ft) .....<br>Net Pay (ft) ..... 180 (5,100 - 5,518)   | <b>TEST STRING CONFIGURATION</b><br>Tubing Length O.D. (in) ..... 4 1/2<br>Packer Depth (ft) ..... 5,115<br>Gauge Depth (ft) / Type ..... 5300 / SLSR<br>Downhole Valve (Y/N) / Type ..... N/A                         |
| <b>INTERPRETATION RESULTS</b><br>Model of Behavior ..... TWO POROSITY<br>Fluid Type Used for Analysis ..... WATER<br>Ext. Reservoir Pressure (psi) ..... 2,495 @ GAUGE<br>Transmissibility (md.ft/cp) ..... 96,600<br>Effective Permeability (md) ..... 537<br>Skin ..... -7.8<br>Radius of Investigation (ft) ..... 10,373<br>P @ Delta t = 0 (psi)..... 2,527<br>Storativity Ratio..... 0.088<br>Interporosity Coefficient ..... 9.30E-08 | <b>TEST CONDITIONS</b><br>Tbg / Wellhead Pressure (psi) .....  |
|   | <b>ROCK / FLUID / WELLBORE PROPERTIES</b><br>Gas Gravity (API) ..... N/A<br>Viscosity (cp) ..... 1<br>Total Compressibility (1/psi) ..... 3.E-06<br>Porosity (%) ..... 13.5<br>Reservoir Temperature (deg F) ..... 130 |

**INJECTION RATE DURING TEST: 11,520 STB/D**

**SUMMARY:**

This report contains the analysis of the data acquired during an injection - fall-off test conducted on the A & M Engineering MES WD #1 well in Lincoln County, Oklahoma. This test was performed by Schlumberger's Oklahoma City Testing District (405 745 2796). The data was taken using slickline conveyed, electronic pressure gauges. The gauges were run in the wellbore and fluid was injected at step rates according to the pumping schedule. Once the final step rate injection was completed, the well was shut in and a pressure fall-off test was conducted.

The data was modeled using a two porosity reservoir model with changing wellbore storage and skin. The radial flow regime was reached after approximately 20 hours of fall-off and continued until test termination. Both the log-log (diagnostic plot) and semi-log analysis techniques were used to interpret this data with an excellent agreement from both result sets. The permeability was calculated to be 537 md, using a thickness of 180 feet at a gauge depth of 5,300 feet (last gauge station). The skin was calculated to be negative 7.8. The reservoir pressure was extrapolated from the reservoir model to be 2,495 psi at gauge depth.

For further discussion of this analysis, please refer to the interpretation discussion on page two of this report. If you have any questions, please call Victor Abu at 405 840 1621.

## ANALYSIS DISCUSSION

### A & M Engineering MES WD #1 BHP Analysis and Interpretation Discussion:

This report contains the analysis of the data acquired during an injection - falloff test conducted on the A & M Engineering MES WD # 1 well in Lincoln County, Oklahoma. This test was performed by Schlumberger's Oklahoma City Testing District (405 745 2796) and the data was provided to Schlumberger's Data and Consulting Services, Oklahoma City (405 840 1621) for interpretation.

The data was taken using slickline conveyed electronic pressure gauges. The gauges were run in the wellbore and fluid was injected at step rates according to the pumping schedule. Once the final step rate injection was completed, the well was shut in and a pressure fall-off test was conducted. Static gradient stops were taken as the gauges were retrieved from the wellbore.

The data was modeled using a two porosity reservoir model with changing wellbore storage and skin. A two porosity model assumes the reservoir consists of two permeability systems, one with a much greater permeability than the other. The fluid is stored in the lower permeability matrix system and flows through the higher permeability to the wellbore.

The radial flow regime was reached after approximately 20 hours of fall-off time and continued till the end of the fall-off test. The radial flow regime is indicated by the constant pressure derivative on the plot of log-log pressure and pressure derivative versus shut in time (using the pseudopressure function). Both log log type curve matching techniques and semi log analysis techniques were used to interpret this data. Agreement between the two methods was excellent. A comparison of the results of the two techniques is presented in the table below.

|          | Permeability | Skin  | Res. Pressure |
|----------|--------------|-------|---------------|
| Semi Log | 537 md       | -7.76 | 2,494 psi     |
| Log Log  | 537 md       | -7.84 | 2,495 psi     |

Based on the log-log diagnostic plot, the total system permeability was calculated to be approximately 537 md, using a thickness of 180 feet and a gauge reference depth of 5,300 feet. This permeability calculated from a two porosity model is a measure of how easily the reservoir fluid moves from the lower permeability system (matrix) to the higher permeability (fracture) system and then to the wellbore. The skin was calculated to be negative 7.8. Due to the higher permeability system being the primary conduit to the wellbore, a two porosity reservoir in it's natural state, has a skin of negative 3.5. The additional (negative) skin calculated on this test would then indicate a stimulated wellbore due to the matrix acidizing job conducted prior to this test. The reservoir pressure was extrapolated from the type curve to be 2,495 psi at the gauge depth of 5,300 feet.

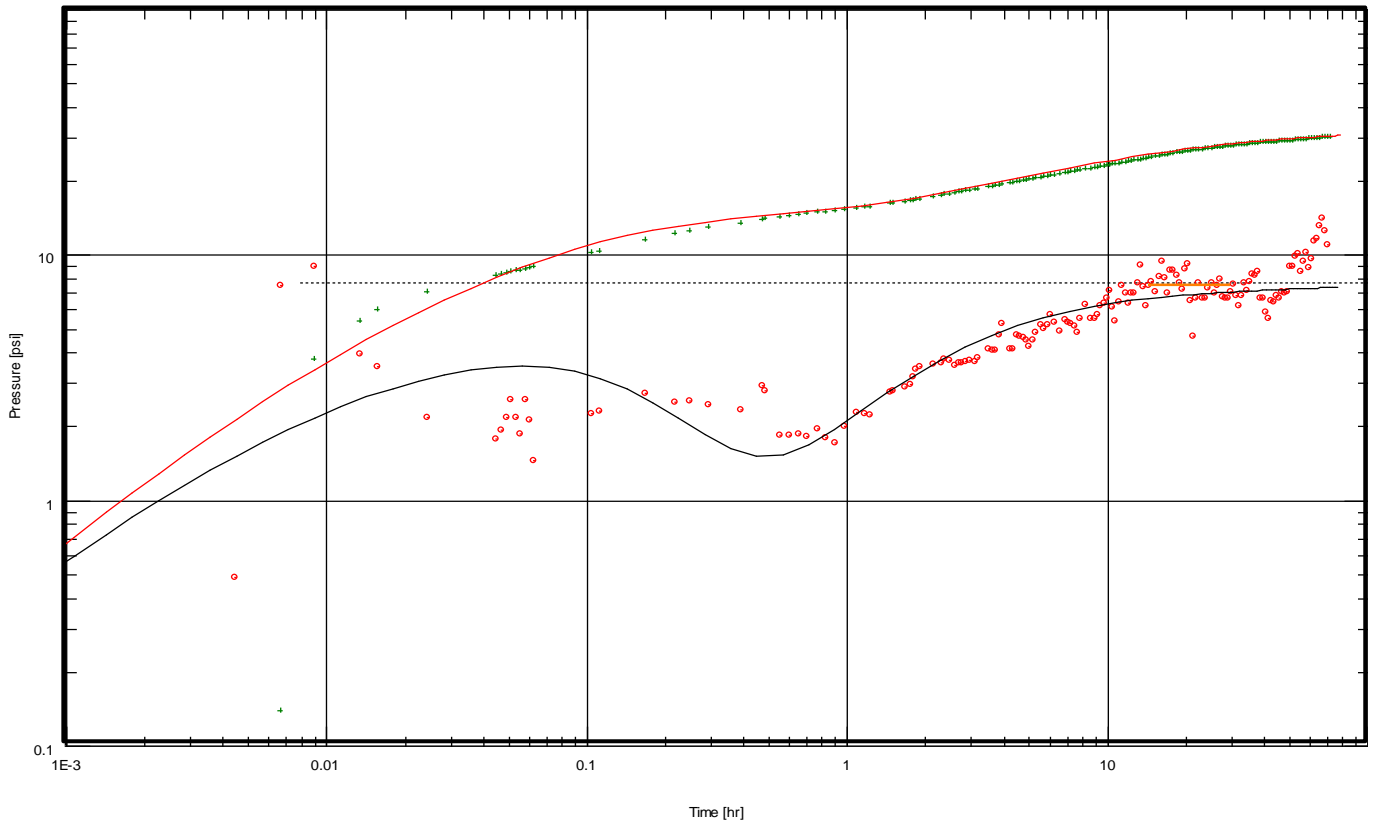
In order to validate the results of this analysis, a simulation of the test sequence was made using the model constructed from this interpretation. The measured data was then plotted on the same scale as the simulated data. Agreement between the measured data and simulated data is excellent. This plot is presented in the body of this report.

If you have any questions, please call Victor Abu at 405 840 1621.

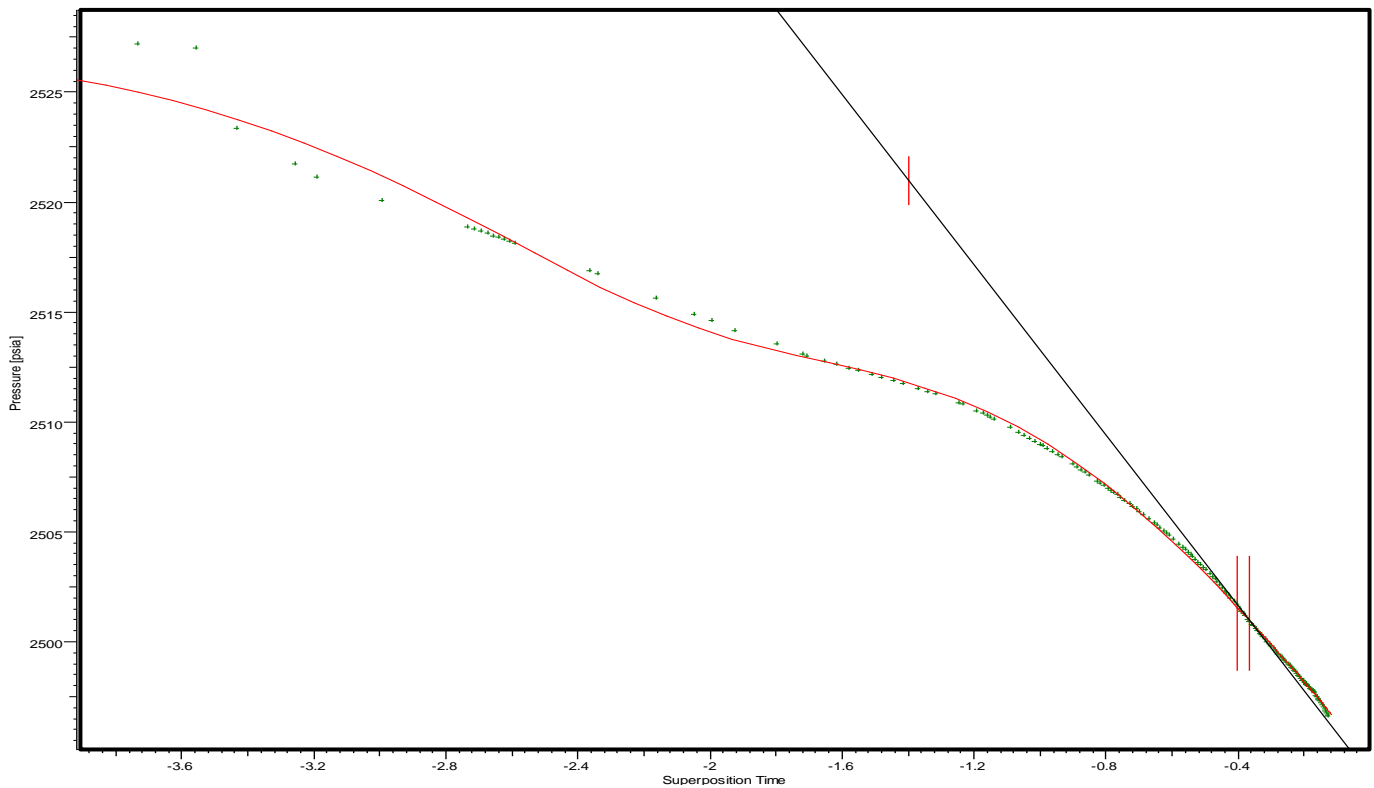
# INTERPRETATION PLOTS



## LOG LOG DIAGNOSTIC PLOT



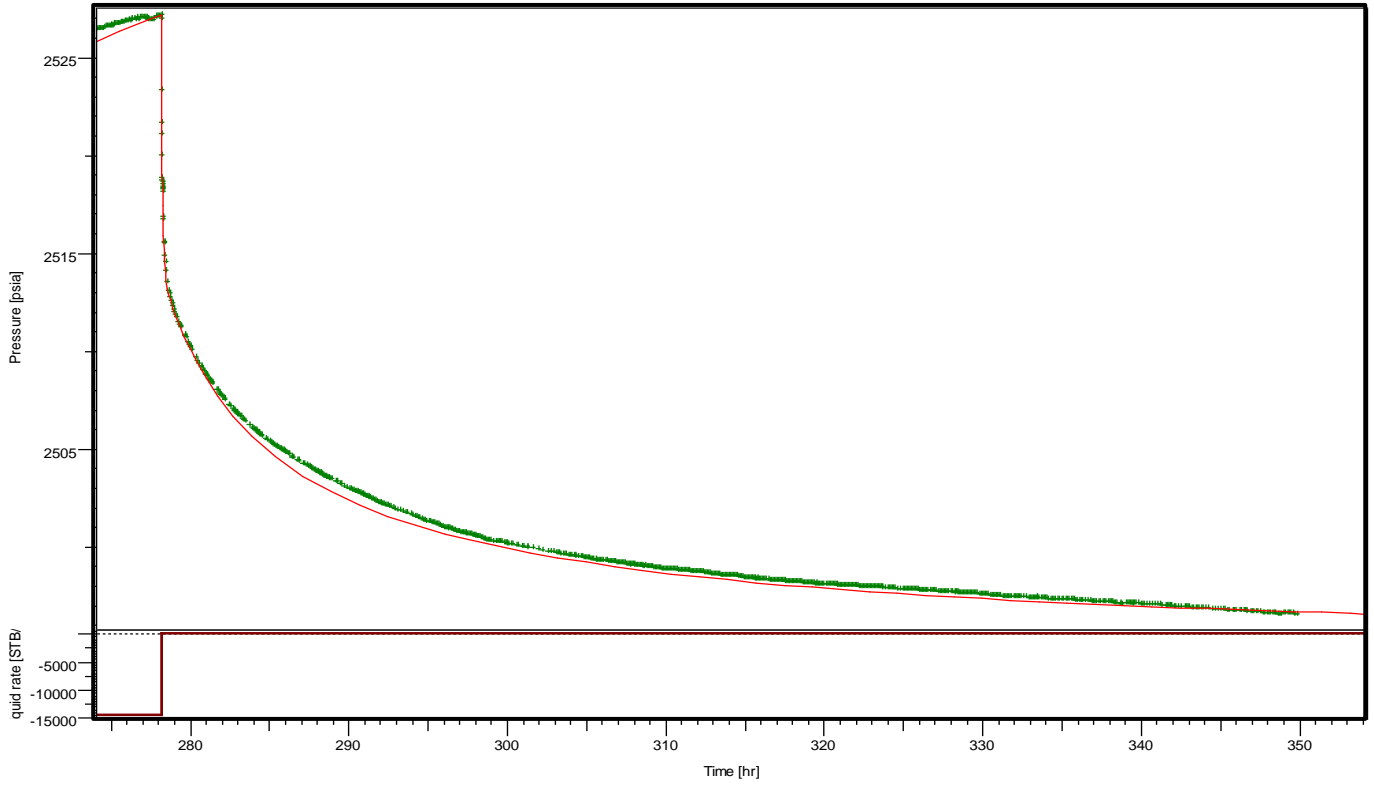
## SEMI LOG PLOT



INTERPRETATION PLOTS

CONTINUED

PRESSURE SIMULATION



|                         |
|-------------------------|
| <b>FLOWRATE HISTORY</b> |
|-------------------------|



| <b>Flow Period<br/>Duration (hrs)</b> | <b>Flow Period<br/>Injection Rate (STB/D)</b> |
|---------------------------------------|---|
| 24                                    | 11520   |
| 72*                                   | 0   |

*\* shut-in / fall-off period*

|  |
|--|
| <p>All interpretations are opinions based on inferences from electrical or other measurements and Schlumberger does not guarantee the accuracy or correctness. Schlumberger shall not, except in the case of gross or willful negligence, be liable or responsible for any loss, costs, damages or expenses incurred or sustained resulting from any interpretations made by any Schlumberger officer, agent or employee. This interpretation is subject to all of the General Terms and Conditions as presented in Schlumberger's current price schedule.</p> |
|--|

## **APPENDIX C**

### **RESPONSE TO NOTICE OF DEFICIENCY LETTER DATED OCTOBER 9, 2013 - RESPONSE TO DEFICIENCY NUMBER 6**



## **DEFICIENCY NUMBER 6**

**Static Arbuckle reservoir pressure is identified as 200 psi at the surface in the Mid – Way report document titled “Analysis Reports for Injection Well MES #1.” This data indicates that the reservoir is essentially “artesian”, already capable of flowing at the surface, without considering any additional injection from the proposed Mid – Way disposal well. Additional injection into the interval would result in an increase in the “artesian” pressure conditions, providing a potential pathway through area wells not properly plugged or constructed into underground sources of drinking water (USDW). The current area of review (AOR) radius of one mile is likely insufficient to address the infinite radius of pressure influence concern. Mid – Way should reassess the appropriate size AOR needed to protect the USDW.**

### **Response:**

The natural surface pressure attributed to the static Arbuckle reservoir pressure at MES #1 is not 200 psi and the fluid in the Arbuckle Group in the area of MES #1 is not capable of flowing to the surface. The pressure at the surface of MES #1 is 0 psig (gauge) or about 16 psia (absolute), which is approximately one U.S. Standard Atmosphere. It is true that approximately 200 psia has been observed at the wellhead of MES #1 at times (implying an artesian condition), but the observed pressure occurs only after a significant amount of fresh water has been injected into the formation through the well.

During each of the injection and pressure fall-off testing events conducted in May and October of 2010, Mid-Way injected an average of about 11,000 barrels of freshwater through MES #1, essentially causing the entire length of the injection tubing to be filled with fresh water having a density less than that of fluid within the Arbuckle Group. Although not preferable, fresh water was utilized in the injection testing due to regulatory limitations on using locally available salt water from oil production and the availability of large volumes of fresh water from local surface water impoundments. The difference in density between the natural formation fluids and the fresh water in the tubing results in the observed surface pressure.

Downhole measured pressure data indicates that the static “formation pressure” near the end of the injection tubing at 5,203 ft below ground surface (bgs) remained essentially unchanged before and after injection fall-off testing. The pressure observed at the surface of MES #1 is the static “formation pressure” minus the hydrostatic pressure of the column of fluid in the tubing. The pressure observed at the wellhead of MES #1 is dictated by the density of the column of fluid in the injection tubing.

## **Timeline of Freshwater Injection and Back Flow at MES #1**

To prove that the “artesian” condition observed at the surface of MES #1 is not due to the natural static Arbuckle reservoir pressure but rather is a result of injecting freshwater into the system, a general timeline of when fresh water was pumped into MES #1 (causing pressure buildup) and when it was allowed to back flow (cessation of “artesian” condition) is a necessary reference. Following is a timeline of such events and is entirely based on information presented in the April 2012 MES *Construction Completion Report and Application for Operating Permit*.

- Drilling of MES #1 was completed on April 18, 2010. After drilling was completed, a work over rig was mobilized to the site on May 4, 2010. Utilizing rented tubing, the well was cleaned out by reverse circulating (pumping down the casing to evacuate drilling mud through the tubing) 550 barrels of freshwater and evacuating drilling mud and fluids. After the drilling mud was evacuated, the well started back-flowing. The well stopped back-flowing after approximately 2 hours. The tail-pipe of the temporary injection tubing was set at 5,108 ft bgs during this process.
- The first injection and pressure fall-off test was conducted on May 7 – 10, 2010. Neither pressure buildup nor flow was observed at the wellhead between the well cleanout activities and the start of this testing event. Prior to injection on May 7, 2010, the static pressure at MES #1 was atmospheric pressure because the well was allowed to back flow in May 2010. During this testing event roughly 10,000 barrels of freshwater was injected into MES #1.
- Based on the pressure and temperature log data collected during the first injection and pressure fall-off test, a decision was made to stimulate (acidize) the injection zone with the intention of opening the lower portion of the injection zone. Mid-Way developed a three-stage Stimulation Procedure that called for the injection of a dilute hydrochloric acid (HCl) solution into targeted portions of the injection zone followed by the injection of freshwater to flush the tubing. Mid-Way submitted the procedure to DEQ for review. After receiving DEQ’s approval, the well Stimulation Procedure was executed on July 6-7, 2010. Following testing, the well was shut in overnight and a pressure of 50 – 100 psig was observed at the wellhead the following day. The pressure was relieved by allowing the well to back flow. Flow ceased after approximately 30 to 40 minutes. All of the discharged back flow consisted of fresh water. After the pressure was relieved, the rental tubing and packers were pulled out and laid down. MES #1 was then completed with the permanent 4-1/2” injection tubing and packer on July 12, 2010. The tail-pipe of the permanent injection tubing extends to 5,203 ft bgs.
- The second injection and pressure fall-off test was conducted on October 11 – 15, 2010. Pressure buildup was not observed at the wellhead between July 12, 2010 and the start of this testing event. Prior to injection on October 11, 2010, the static pressure at MES #1 was atmospheric pressure because the well was allowed to back flow in July 2010.

During this testing event more than 12,000 barrels of freshwater was again injected into MES #1.

- In response to the seismic events in Lincoln County in late 2011, a series of tests were performed in February of 2012 to verify the integrity of MES #1. It is estimated that an additional 330 barrels of freshwater was injected into MES #1 during these testing procedures.

**Evaluation of Static Pressure and Temperature Measurements Prior to Injection and Pressure Fall-Off Tests at MES #1**

**Table 6-1**, shown below, contains the static pressure and temperature readings in MES #1 before conducting the injection and pressure fall-off tests on May 7, 2010 and October 11, 2010 as measured by Schlumberger Testing Services. This table is identical to **Table 2-1** on page 30 of Mid-Way’s April 2012 *Construction Completion Report and Application for Operating Permit*.

**TABLE 6-1: MES #1 Injection Well Static Pressure Measurements Prior to Injection and Pressure Fall-Off Testing**

|       | May 7, 2010 Measurements |                    |                  | October 11, 2010 Measurements |                    |                  |
|-------|--------------------------|--------------------|------------------|-------------------------------|--------------------|------------------|
| Depth | Pressure (psia)          | Gradient (psia/ft) | Temperature (°F) | Pressure (psia)               | Gradient (psia/ft) | Temperature (°F) |
| 0     | 15.37                    | -                  | 68.1             | 16.97                         | -                  | 60.75            |
| 100   | 55.91                    | 0.405              | 68.75            | 53.30                         | 0.363              | 60.85            |
| 500   | 228.56                   | 0.432              | 71.02            | 224.52                        | 0.428              | 62.10            |
| 1,000 | 444.84                   | 0.433              | 73.9             | 439.38                        | 0.430              | 64.53            |
| 1,500 | 661.02                   | 0.432              | 76.87            | 656.29                        | 0.434              | 67.60            |
| 2,000 | 885.14                   | 0.448              | 80.13            | 884.34                        | 0.456              | 71.89            |
| 2,500 | 1,129.40                 | 0.489              | 84.59            | 1,129.78                      | 0.491              | 77.20            |
| 3,000 | 1,373.60                 | 0.488              | 89.22            | 1,372.90                      | 0.486              | 83.64            |
| 3,500 | 1,617.99                 | 0.489              | 94.35            | 1,616.68                      | 0.488              | 88.77            |
| 4,000 | 1,862.32                 | 0.489              | 100.27           | 1,860.57                      | 0.488              | 97.23            |
| 4,500 | 2,106.40                 | 0.488              | 106.26           | 2,105.68                      | 0.490              | 104.50           |

|              |          |       |        |          |       |        |
|--------------|----------|-------|--------|----------|-------|--------|
| <b>5,000</b> | 2,350.31 | 0.488 | 111.56 | 2,347.22 | 0.483 | 112.96 |
| <b>5,500</b> | 2,593.77 | 0.487 | 117.08 | 2,589.17 | 0.484 | 119.39 |
| <b>6,000</b> | 2,836.94 | 0.486 | 120.92 | 2,833.29 | 0.488 | 123.84 |
| <b>6,500</b> | 3,080.06 | 0.486 | 124.05 | 3,077.85 | 0.489 | 125.62 |
| <b>7,000</b> | 3,322.81 | 0.486 | 132.80 | 3,319.61 | 0.484 | 130.80 |

Considering the measurements taken on both May 7, 2010 and October 11, 2010, the data in **Table 6-1** indicates that the average static pressure gradient between a depth of 5,000 and 7,000 ft, which is Mid-Way’s targeted injection zone, is 0.486 psia/ft and that the average temperature for the same interval is approximately 125° F. It should be noted that the pressure gradients shown in the table are not cumulative; they report the change in gradient based on each 500 ft interval.

For example, consider the October 11, 2010 pressure gradient shown for a depth of 5,500 ft. The reported pressure gradient of 0.484 psia/ft is actually the change in pressure gradient between the depth of 5,000ft and 5,500 ft or  $\frac{2,589.19 \text{ psi} - 2,347.22 \text{ psi}}{5,500 \text{ ft} - 5,000 \text{ ft}}$ . Therefore, pressure gradients shown for depths of 5,500 ft, 6,000 ft, 6,500 ft and 7,000 ft in **Table 6-1** correspond to the pressure gradients between a depth of 5,000 ft and 7,000 ft.

Water at 125° F has a specific weight of 61.63 lb/ft<sup>3</sup> and a density of 1.9155 slugs/ft<sup>3</sup>, which corresponds to a freshwater hydrostatic pressure gradient of 0.428 psia/ft. Using this information, the specific gravity of the formation fluid in the targeted injection zone can be calculated by taking the average of the static pressure gradient measurements taken on May 7, 2010 and October 11, 2010 between a depth of 5,000 and 7,000 ft (0.486 psia/ft) and dividing it by the freshwater hydrostatic pressure gradient of 0.428 psia/ft. Consequently, the calculated specific gravity of the formation fluid between a depth of 5,000 ft and 7,000 ft is 1.135.

As indicated in the timeline of when freshwater was pumped into MES #1 and when it was allowed to back flow, the static pressure measurements in **Table 6-1** were taken after fresh water was allowed to back flow and naturally cease. This process has never taken more than approximately 2 hours. Significantly, the static pressure readings in **Table 6-1** reveal that following the back flow of fresh water, the static pressure at the surface of MES #1 was 0 psig or about 16 psia. Furthermore, the static pressure gradients between a depth of 100 ft and the ground surface on May 7, 2010 and October 11, 2010 were calculated to be 0.405 psia/ft and 0.363 psia/ft respectively. Freshwater between 60° F and 70°F should have a pressure gradient of 0.433 psia/ft. The fact that the static pressure gradients based on measured data between a depth of 100 ft and the ground surface on May 7, 2010 and October 11, 2010 were calculated to be less than the pressure gradient of fresh water, indicates that the column of fluid in the tubing was less than 100 feet in thickness and did not reach to the ground surface. This means that after freshwater is allowed to back flow and naturally cease in MES #1, the wellhead

pressure is 0 psig and an artesian condition does not exist. If a naturally occurring artesian condition existed at MES #1, back flow would not cease in a relatively short period of time.

It should also be noted that the static pressure gradients in **Table 6-1** are not representative of the natural potentiometric conditions in MES #1, despite the fact that these measurements were taken after the well was allowed to back flow. As previously mentioned, freshwater between 60°F and 70°F should have a pressure gradient of 0.433 psia/ft. Consequently, the 500 ft interval static pressure gradients in **Table 6-1** clearly reveal that approximately the upper 2,000 ft of the column of fluid in the injection tubing did not consist of natural formation water but was freshwater. This conclusion is significant for the following reasons:

- As discussed, since the specific gravity of the formation fluid is 1.135, the natural potentiometric surface of the Arbuckle Group at MES #1 is far below the ground surface. This assessment is consistent with the findings of Oklahoma State University Professor James O. Puckette’s dissertation for his doctorate degree, dated December 1996. The findings presented in this document, entitled *Evaluation of Underpressured Reservoirs as Potential Repositories for Liquid Waste*, indicates that the potentiometric surface of the Arbuckle referenced to a Mean Sea Level (msl) datum (NGVD 1929) in the vicinity of MES #1 is at an elevation of 500 to 600 ft msl or 274.5 to 374.5 ft below the ground surface.
- September 29, 2010 analytical testing of fluid back flowing from the MES #1 well yielded a specific gravity of 1.05. The analyzed fluid was collected after the well had back flowed for approximately 2 hours on May 5, 2010 and, based on visual criteria, was initially believed to be formation water. However, the tested fluid is now believed to have been a mixture of fresh water and formation water. This is supported by the fact that the chloride levels in the sampled fluid were approximately 45,000 ppm, while available information on the chloride levels in the Arbuckle Group within the area of MES#1 shows concentrations to be in the range of 120,000 to 140,000 ppm (see **Figure 1-12** in **Attachment 1**). Testing of a mixture of freshwater and formation water results in the discrepancy between the 1.05 specific gravity from the September 29, 2010 analytical testing and the 1.135 specific gravity calculated from the pressure gradients in **Table 6-1**.

### **Evaluation of Static Pressure and Temperature Measurements After Injection and Pressure Fall-Off Tests at MES #1**

**Table 6-2**, shown below, contains static pressure readings and pressure gradients based on measured data collected by Schlumberger Testing Services in MES #1 on May 10, 2010 after the injection and pressure fall-off testing event was completed. This data is significant because it provides static pressures at uniform depths below the ground surface during the observed “artesian” condition caused by injection of fresh water and indicated by a pressure of 204 psi at

the surface of MES #1. The original data used to create **Table 6-2** is taken directly from page 11 of Schlumberger’s Testing Services Report, dated May 10, 2010, and is available in **Appendix O** of Mid-Way’s April 2012 *Construction Completion Report and Application for Operating Permit*. **Table 6-2** does not include static pressures measurements following injection and pressure fall-off testing on October 15, 2010 because Schlumberger did not record any such measurements above a depth of 5,700 ft during this test.

**TABLE 6- 2: MES #1 Injection Well Static Pressure Measurements from May 10, 2010 Following Injection and Pressure Fall-Off Testing**

| Depth (ft) | Pressure (psia) | Gradient (psia/ft) | Depth Interval Used to Calculate Gradient (ft) |
|------------|-----------------|--------------------|--|
| 6,100      | 2,880.917       | -                  | -  |
| 7,000      | 3,303.073       | 0.469              | 6,100 - 7,000                                  |
| 6,000      | 2,821.274       | 0.482              | 6,000 - 7,000                                  |
| 5,000      | 2,358.848       | 0.462              | 5,000 - 6,000                                  |
| 4,000      | 1,928.010       | 0.431              | 4,000 - 5,000                                  |
| 3,000      | 1,495.989       | 0.432              | 3,000 - 4,000                                  |
| 2,000      | 1,063.524       | 0.432              | 2,000 - 3,000                                  |
| 1,000      | 631.169         | 0.432              | 1,000 - 2,000                                  |
| 500        | 415.252         | 0.432              | 500 - 1,000                                    |
| 100        | 242.441         | 0.432              | 100 - 500                                      |
| 0          | 204.064         | 0.384              | 0 - 100  |

The pressure gradients in **Table 6-2** show a clear distinction between freshwater and formation fluid. The pressure gradients between the surface and a depth of 5,000 ft are almost uniformly 0.432 psia/ft. This pressure gradient corresponds to freshwater with a specific weight of about 62.165 lb/ft<sup>3</sup>, which is the specific weight of freshwater at 85° F. Coincidentally, the weighted average of all of the actual static temperature data in **Table 6-1** between the surface and a depth of 5,000 ft is 84.0° F.

In **Table 6-2**, the static pressure gradient of 0.462 psia/ft between a depth of 5,000 and 6,000 ft indicates that there was a transition from fresh water to a mixture of fresh water and denser formation fluid below a depth 5,000 ft. Using an average gradient of 0.475 psia/ft for the mixture between freshwater and formation fluid based on the gradients measured between a depth of 6,000 ft and 7,000 ft in **Table 6-2**, and the pressure gradient of 0.431 psia/ft measured between a depth of 4,000 ft and 5,000 in the same table, simple weighted averaging reveals that there was transition from freshwater to a mixture of freshwater and denser formation water below a depth of 5,100 ft. Consequently, the measured data indicates that the entire

column of temporary injection tubing (5,108 ft) contained freshwater following the May 10, 2010 injection and pressure fall-off tests. Based on the data presented in **Table 6-1**, this clearly was not the case before injection began.

The data provided conclusively proves that the “artesian” condition observed at MES #1 is a direct result of injecting a significant amount of freshwater into the well and the density differences between the freshwater and natural formation water. It is also noteworthy that there are marginal differences in the static pressures near the end of the injection tubing (5,203 ft bgs) in **Tables 6-1** and **6-2** despite the fact that the surface pressure at MES #1 was 0 psig on May 7, 2010 and October 11, 2010 and 204 psia following injection and pressure fall-off testing on May 10, 2010.

### **Additional Testing Conducted by Mid-Way on October 25, 2013**

After receipt of the October 9, 2013 Notice of Deficiency letter, a Testing Plan designed to collect sufficient information to prepare a response to Deficiency No. 6 was submitted to DEQ . The Testing Plan called for opening the valve located at the top of the injection well, allowing the water to drain into a frac tank; sampling of the back flowing water, as well as collection of the following information:

1. The duration of the back flow drainage into the frac tank.
2. Pressure, temperature, and the volume of the backflow.
3. The Specific Gravity and Chloride levels of back flow water collected at regular intervals.
4. Observe the system to identify any pressure buildup at the surface of the well following the cessation of the backflow.

On October 25, 2013 Mid-Way implemented the approved Testing Plan and collected samples and data in accordance with the Testing Plan. The field and laboratory sampling results are summarized in **Tables 6-3A** and **6-3B** below. The project Field Sampling and Analysis Data Sheet, Chain of Custody Form, and Laboratory Report are provided in **Attachment 3** of these responses.

**TABLE 6- 3A: MES #1 Injection Well – Summary of Field Sampling and Laboratory Results from October 25, 2013 Testing Event**

| Sample ID | Time  | Flow Meter Reading (gallons) | Pressure at Wellhead (psig) | Specific Gravity (g/cc @ 4 ° C) | Chloride in Water (mg/L) | Comments   |
|-----------|-------|------------------------------|-----------------------------|---------------------------------|--------------------------|--|
| -         | 0     | 226,168                      | 204                         | -                               | -                        | Prior to Opening Valve   |
| MES 1     | 12:31 | 226,168                      | 204                         | 1.002                           | 29.0                     | Initial Sample Before Opening Valve  |
| -         | 12:36 | 226,168                      | -                           | -                               | -                        | Opened Valve   |
| MES 2     | 12:41 | 226,753                      | 22                          | 1.002                           | 34.9                     | Clear-Slight Odor  |
| MES 3     | 12:46 | 227,428                      | 11                          | 1.002                           | 108                      | Grayish - Slight Odor  |
| MES 4     | 12:51 | 227,990                      | 6                           | 1.002                           | 412                      | Clear  |
| MES 5     | 12:56 | 228,080                      | 4                           | 1.002                           | 237                      | Clear  |
| -         | 12:58 | 228,083                      | 4                           | -                               | -                        | Flow Stopped. Pressure at Wellhead Attributed to Head From Discharge Line. |
| -         | 1:00  | 228,083                      |                             | -                               | -                        | Left Valve Open and Went to Lunch  |
| -         | 2:09  | 228,083                      | 0                           | -                               | -                        | After Lunch  |
| MES 6     | 2:30  | 228,138                      | 0                           | 1.002                           | 182                      | After Suction of 55 Gallons Using Vacuum Truck                             |

**TABLE 6-3B: SUMMARY OF FIELD DATA COLLECTED OCTOBER 25, 2013**

| Sample ID | Temp (° C) | pH (std units) | Sp. Cond. (units as noted) | Salinity (pNa)* |
|-----------|------------|----------------|----------------------------|-----------------|
| MES 1     | 15.1       | 8.9            | 396 µS                     | > 1             |
| MES 2     | 22.5       | 8.8            | 404 µS                     | > 1             |
| MES 3     | 26.2       | 9.0            | 2.32 mS                    | > 1             |
| MES 4     | 26.7       | 9.0            | 873 µS                     | > 1             |
| MES 5     | 26.5       | 9.4            | 424 µS                     | > 1             |
| MES 6     | 19.5       | 9.4            | 242 µS                     | > 1             |

\*pNa = measure of Na ion activity. >1 pNa=<5.85g/L NaCl

As shown in **Table 6-3A**, after the valve at the top of the injection well was opened, 1,915 gallons of water, equivalent to approximately a 3,000 LF column of fluid in the injection tubing, back flowed during a 22 minute period before naturally stopping. Laboratory results for samples MES 1 – MES 5, reveal that all of this fluid was fresh water with a specific gravity of 1.002.

After flow ceased, the sampling crew left the valve open and went to lunch. During this period, no additional flow was recorded by the flow meter; which again supports the fact that the MES #1 well is not a naturally occurring artesian well.

Following lunch, the crew removed 55 gallons from MES #1 using a vacuum truck and a final sample, MES 6, was collected. The laboratory results of sample MES 6 reveal that it was also fresh water with a specific gravity of 1.002. This result supports the measurements in **Table 6-1**, which as previously discussed, clearly indicate that after the well was allowed to back flow, the upper 2,000 ft of the column of fluid in the injection tubing still consisted of freshwater.

Since completing the October 25, 2013 sampling and testing event, there has not been a pressure buildup at the wellhead of MES #1. This is due to the fact that denser formation fluid has replaced all of the fresh water in the injection tubing that was allowed to flow out of the well and equilibrium with the natural formation pressure has been achieved. No additional flow has been observed at the surface from MES #1.

## **Conclusion**

It is believed that the information and discussion presented above, conclusively shows that there is not a natural “artesian” condition present at MES #1. The static pressure at the surface of MES #1 is 0 psig. The observed “artesian” conditions at MES #1 were a direct result of fresh water injection through the well, and the density differences between the fresh water and denser natural formation fluid with a specific gravity of 1.135.

Ultimately, the static pressure at the wellhead of MES #1 can be calculated by subtracting the hydrostatic pressure of the column of fluid in the injection tubing from the static “formation pressure” at the top of the injection zone. Assuming that the static “formation pressure” is approximately constant within the injection zone, which the measurements in **Tables 6-1** and **6-2** support, then the pressure to be observed at the wellhead of MES #1 is dictated by the density of the column of fluid in the injection tubing. The density differences between the formation and tubing fluids results in the pressures observed at the surface.

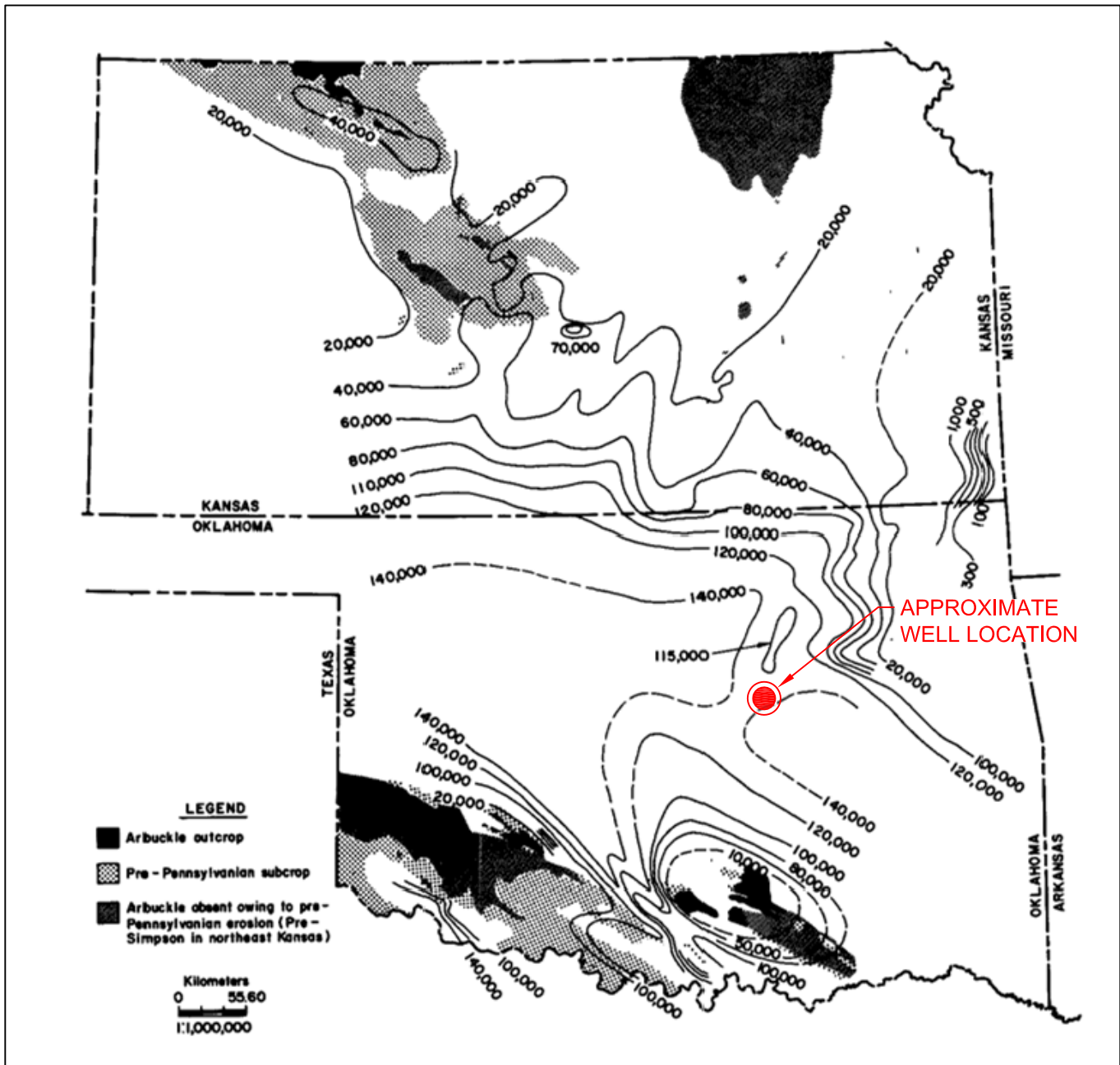
Pressure increases resulting from injection of fresh water into formations containing brine has been observed and documented previously. In fact, EPA Region 5 has a formally approved test to determine the mechanical integrity of Class III injection wells called the Water-Brine Interface Test (W-BIT) that is based on the same principles of classical mechanics discussed in this response. In the EPA Region 5 internet publication entitled, *Underground Injection Control (UIC) Section Regional Guidance #5 - Determination of the Mechanical Integrity of Injection Wells*, the strategy governing the W-BIT test is described, in part, as follows:

*a decrease in wellhead pressure will be observed in the event of loss of a fluid of lower density filling a standpipe open to a reservoir filled with a fluid of higher density . . . Because the cavern is pressurized sufficiently to cause the heavy brine to flow to the surface, the pressure within the well filled with fresh water is greater than the hydrostatic*

*pressures in any aquifer through which the well passes. Therefore, any leak will allow fresh water to flow outward, to be replaced by dense brine flowing into the well from the cavern. Because the liquid pressure gradient of the brine from the cavern which replaces the leaked fresh water is greater than that of the freshwater, less pressure is transmitted from the cavern upward through the well to the well head.*

Finally, in accordance with 40CFR Part 146, *Underground Injection Control Program; Criteria and Standards*, a fixed radius of ¼ mile was chosen for the MES #1 Area of Review (AOR). For purposes of active oil and gas well/plugged well evaluation however, the ¼ mile AOR was expanded to a one-mile radius from the proposed injection well.

The MES#1 well is not an artesian well. Anticipated pressure increases in the formation due to injection are not anticipated to result in an artesian condition that potentially could rise to underground sources of drinking water through improperly plugged wells. Of the 38 plugged and 20 active wells within the one-mile radius of MES#1, only one well (the active Twin Cities #1 Salt Water Injection Well) penetrates into the Arbuckle Group. All other wells within one mile are completed/plugged in shallower strata not hydraulically connected to the Arbuckle Zone. The calculated water front after 50 years of normal facility injection operations is not anticipated to extend beyond one mile from MES #1. Mid-Way Environmental Services, Inc. believes the one-mile radius of review for the plugged/active wells is appropriate.



REFERENCE: A. GENE COLLINS, *GEOCHEMISTRY OF OILFIELD WATERS*, 1975.



**A & M ENGINEERING AND ENVIRONMENTAL SERVICES, INC.**

ENGINEERING – ENVIRONMENTAL – CONSTRUCTION

**CHLORIDE CONCENTRATION (MG/L) OF THE ARBUCKLE FORMATION WATERS  
MID-WAY ENVIRONMENTAL SERVICES, INC.**

|                     |                   |                           |
|---------------------|-------------------|---------------------------|
| SCALE:<br>AS SHOWN  | DATE:<br>1/6/2014 | FIGURE NO.<br>FIGURE 1-12 |
| APPROVED BY:<br>TAT | DRAWN BY:<br>DME  | PROJECT NO.<br>1706-002   |

**ATTACHMENT 3**

**FIELD SAMPLING AND ANALYSIS DATA SHEET, CHAIN OF CUSTODY FORM,**

**AND**

**LABORATORY REPORT FORM FOR THE OCTOBER 25, 2013 TEST**



Green Country Testing, Inc.  
6825 E 38th Street  
Tulsa, OK 74145  
TEL: 918-828-9977 FAX: 918-828-7756  
Website: [www.greencountrytesting.com](http://www.greencountrytesting.com)



October 30, 2013

Altay Erturgrul  
A & M Engineering  
10010 E. 16th St.  
Tulsa, OK 74128-4813  
TEL: (918) 665-6575  
FAX (918) 656-6576

RE: Mid-Way Environ Srvces 1706-003

Order No.: 1310328

Dear Altay Erturgrul:

Green Country Testing, Inc. received 6 sample(s) on 10/25/2013 for the analyses presented in the following report.

In accordance with your instructions, Green Country Testing conducted the analysis shown on the following pages on samples submitted by your company. The results relate only to the items tested. Unless otherwise noted, all analysis were conducted using EPA approved methodologies. Test reports meet all the NELAC requirements. All relevant sampling information is on the attached chain-of-custody form. The initials SUB as the analyst designate any testing sub-contracted by Green Country Testing.

Certifications/Accreditation: OK - 7604 - AR - ADEQ - KS - E-10232 - LA - 4002

A scope of Certified/Accredited parameters is available upon request. If you have any questions regarding these tests results, please feel free to call.

Sincerely,

A handwritten signature in black ink, appearing to read "Brian Duzan", with a stylized flourish at the end.

Brian Duzan  
Laboratory Director

CC:  
Gavin James

Original

Green Country Testing, Inc.  
 6825 E 38th Street  
 Tulsa, OK 74145  
 TEL: 918-828-9977 FAX: 918-828-7756  
 Website: [www.greencountrytesting.com](http://www.greencountrytesting.com)



# Analytical Report

(continuous)

WO#: 1310328

Date Reported: 10/30/2013

**CLIENT:** A & M Engineering  
**Project:** Mid-Way Environ Srvces 1706-003

**Lab Order:** 1310328

**Lab ID:** 1310328-001

**Collection Date:** 10/25/2013 12:31:00 PM

**Client Sample ID:** MES-1

**Matrix:** GROUNDWATER

| Analyses                    | Result | RL     | Qual | Units                   | DF | Date Analyzed         |
|-----------------------------|--------|--------|------|-------------------------|----|-----------------------|
| <b>CHLORIDE IN WATER</b>    |        |        |      | <b>A4500-CL-E, 1997</b> |    | Analyst: <b>KP</b>    |
| Chloride                    | 29.0   | 5.00   |      | mg/L                    | 1  | 10/30/2013 3:43:00 PM |
| <b>SPECIFIC GRAVITY - N</b> |        |        |      | <b>A2710F, 1997</b>     |    | Analyst: <b>KP</b>    |
| Specific Gravity            | 1.002  | 0.0100 |      | g/cc @ 4°C              | 1  | 10/30/2013 2:01:00 PM |

**Lab ID:** 1310328-002

**Collection Date:** 10/25/2013 12:41:00 PM

**Client Sample ID:** MES-2

**Matrix:** GROUNDWATER

| Analyses                    | Result | RL     | Qual | Units                   | DF | Date Analyzed         |
|-----------------------------|--------|--------|------|-------------------------|----|-----------------------|
| <b>CHLORIDE IN WATER</b>    |        |        |      | <b>A4500-CL-E, 1997</b> |    | Analyst: <b>KP</b>    |
| Chloride                    | 34.9   | 5.00   |      | mg/L                    | 1  | 10/30/2013 3:43:00 PM |
| <b>SPECIFIC GRAVITY - N</b> |        |        |      | <b>A2710F, 1997</b>     |    | Analyst: <b>KP</b>    |
| Specific Gravity            | 1.002  | 0.0100 |      | g/cc @ 4°C              | 1  | 10/30/2013 2:01:00 PM |

**Qualifiers:**

- |  |  |
|--|--|
| * Value exceeds Maximum Contaminant Level.   | C Value is below Minimum Compound Limit.             |
| E Value above quantitation range             | H Holding times for preparation or analysis exceeded |
| J Analyte detected below quantitation limits | M Manual Integration used to determine area response |
| N Non-NELAC Accredited Parameter             | ND Not Detected at the Reporting Limit               |
| P Second column confirmation exceeds         | PL Permit Limit                                      |
| R RPD outside accepted recovery limits       | RL Reporting Detection Limit                         |

Green Country Testing, Inc.  
 6825 E 38th Street  
 Tulsa, OK 74145  
 TEL: 918-828-9977 FAX: 918-828-7756  
 Website: [www.greencountrytesting.com](http://www.greencountrytesting.com)



# Analytical Report

(continuous)

WO#: 1310328

Date Reported: 10/30/2013

**CLIENT:** A & M Engineering  
**Project:** Mid-Way Environ Srvces 1706-003

**Lab Order:** 1310328

**Lab ID:** 1310328-003 **Collection Date:** 10/25/2013 12:46:00 PM  
**Client Sample ID:** MES-3 **Matrix:** GROUNDWATER

| Analyses                    | Result | RL     | Qual | Units                   | DF | Date Analyzed         |
|-----------------------------|--------|--------|------|-------------------------|----|-----------------------|
| <b>CHLORIDE IN WATER</b>    |        |        |      | <b>A4500-CL-E, 1997</b> |    | Analyst: <b>KP</b>    |
| Chloride                    | 108    | 5.00   |      | mg/L                    | 1  | 10/30/2013 3:43:00 PM |
| <b>SPECIFIC GRAVITY - N</b> |        |        |      | <b>A2710F, 1997</b>     |    | Analyst: <b>KP</b>    |
| Specific Gravity            | 1.002  | 0.0100 |      | g/cc @ 4°C              | 1  | 10/30/2013 2:01:00 PM |

**Lab ID:** 1310328-004 **Collection Date:** 10/25/2013 12:51:00 PM  
**Client Sample ID:** MES-4 **Matrix:** GROUNDWATER

| Analyses                    | Result | RL     | Qual | Units                   | DF | Date Analyzed         |
|-----------------------------|--------|--------|------|-------------------------|----|-----------------------|
| <b>CHLORIDE IN WATER</b>    |        |        |      | <b>A4500-CL-E, 1997</b> |    | Analyst: <b>KP</b>    |
| Chloride                    | 412    | 50.0   |      | mg/L                    | 10 | 10/30/2013 3:43:00 PM |
| <b>SPECIFIC GRAVITY - N</b> |        |        |      | <b>A2710F, 1997</b>     |    | Analyst: <b>KP</b>    |
| Specific Gravity            | 1.002  | 0.0100 |      | g/cc @ 4°C              | 1  | 10/30/2013 2:01:00 PM |

**Qualifiers:**

- |  |  |
|--|--|
| * Value exceeds Maximum Contaminant Level.   | C Value is below Minimum Compound Limit.             |
| E Value above quantitation range             | H Holding times for preparation or analysis exceeded |
| J Analyte detected below quantitation limits | M Manual Integration used to determine area response |
| N Non-NELAC Accredited Parameter             | ND Not Detected at the Reporting Limit               |
| P Second column confirmation exceeds         | PL Permit Limit                                      |
| R RPD outside accepted recovery limits       | RL Reporting Detection Limit                         |

Green Country Testing, Inc.  
 6825 E 38th Street  
 Tulsa, OK 74145  
 TEL: 918-828-9977 FAX: 918-828-7756  
 Website: [www.greencountrytesting.com](http://www.greencountrytesting.com)



# Analytical Report

(continuous)

WO#: 1310328

Date Reported: 10/30/2013

**CLIENT:** A & M Engineering  
**Project:** Mid-Way Environ Srvces 1706-003

**Lab Order:** 1310328

**Lab ID:** 1310328-005

**Collection Date:** 10/25/2013 12:56:00 PM

**Client Sample ID:** MES-5

**Matrix:** GROUNDWATER

| Analyses                    | Result | RL     | Qual | Units                   | DF | Date Analyzed         |
|-----------------------------|--------|--------|------|-------------------------|----|-----------------------|
| <b>CHLORIDE IN WATER</b>    |        |        |      | <b>A4500-CL-E, 1997</b> |    | Analyst: <b>KP</b>    |
| Chloride                    | 237    | 5.00   |      | mg/L                    | 1  | 10/30/2013 3:43:00 PM |
| <b>SPECIFIC GRAVITY - N</b> |        |        |      | <b>A2710F, 1997</b>     |    | Analyst: <b>KP</b>    |
| Specific Gravity            | 1.002  | 0.0100 |      | g/cc @ 4°C              | 1  | 10/30/2013 2:01:00 PM |

**Lab ID:** 1310328-006

**Collection Date:** 10/25/2013 2:30:00 PM

**Client Sample ID:** MES-6

**Matrix:** GROUNDWATER

| Analyses                    | Result | RL     | Qual | Units                   | DF | Date Analyzed         |
|-----------------------------|--------|--------|------|-------------------------|----|-----------------------|
| <b>CHLORIDE IN WATER</b>    |        |        |      | <b>A4500-CL-E, 1997</b> |    | Analyst: <b>KP</b>    |
| Chloride                    | 182    | 5.00   |      | mg/L                    | 1  | 10/30/2013 3:43:00 PM |
| <b>SPECIFIC GRAVITY - N</b> |        |        |      | <b>A2710F, 1997</b>     |    | Analyst: <b>KP</b>    |
| Specific Gravity            | 1.002  | 0.0100 |      | g/cc @ 4°C              | 1  | 10/30/2013 2:01:00 PM |

**Qualifiers:**

- |  |  |
|--|--|
| * Value exceeds Maximum Contaminant Level.   | C Value is below Minimum Compound Limit.             |
| E Value above quantitation range             | H Holding times for preparation or analysis exceeded |
| J Analyte detected below quantitation limits | M Manual Integration used to determine area response |
| N Non-NELAC Accredited Parameter             | ND Not Detected at the Reporting Limit               |
| P Second column confirmation exceeds         | PL Permit Limit                                      |
| R RPD outside accepted recovery limits       | RL Reporting Detection Limit                         |



# QC SUMMARY REPORT

WO#: 1310328  
 30-Oct-13

**Client:** A & M Engineering  
**Project:** Mid-Way Environ Srvces 1706-003

**TestNo:** A2710F, 1997

|            |                 |           |       |           |              |                |            |             |        |        |      |          |  |           |  |             |  |      |  |          |  |      |
|------------|-----------------|-----------|-------|-----------|--------------|----------------|------------|-------------|--------|--------|------|----------|--|-----------|--|-------------|--|------|--|----------|--|------|
| Sample ID  | 1310328-001ADUP | SampType: | DUP   | TestCode: | SP_GR        | Units:         | g/cc @ 4°C | Prep Date:  |        | RunNo: | 9344 |          |  |           |  |             |  |      |  |          |  |      |
| Client ID: | MES-1           | Batch ID: | R9344 | TestNo:   | A2710F, 1997 | Analysis Date: | 10/30/2013 | SeqNo:      | 119654 |        |      |          |  |           |  |             |  |      |  |          |  |      |
| Analyte    |                 | Result    |       | PQL       |              | SPK value      |            | SPK Ref Val |        | %REC   |      | LowLimit |  | HighLimit |  | RPD Ref Val |  | %RPD |  | RPDLimit |  | Qual |

|                  |      |        |  |  |  |  |  |  |  |       |         |    |
|------------------|------|--------|--|--|--|--|--|--|--|-------|---------|----|
| Specific Gravity | 1.00 | 0.0100 |  |  |  |  |  |  |  | 1.002 | 0.00998 | 20 |
|------------------|------|--------|--|--|--|--|--|--|--|-------|---------|----|

- Qualifiers:**
- \* Value exceeds Maximum Contaminant Level.
  - E Value above quantitation range
  - M Manual Integration used to determine area response
  - P Second column confirmation exceeds
  - RL Reporting Detection Limit
  - B Analyte detected in the associated Method Blank
  - H Holding times for preparation or analysis exceeded
  - N Non-NELAC Accredited Parameter
  - PL Permit Limit
  - S Spike Recovery outside accepted recovery limits
  - C Value is below Minimum Compound Limit.
  - J Analyte detected below quantitation limits
  - ND Not Detected at the Reporting Limit
  - R RPD outside accepted recovery limits



# QC SUMMARY REPORT

WO#: 1310328  
 30-Oct-13

**Client:** A & M Engineering  
**Project:** Mid-Way Environ Srvces 1706-003

**TestNo:** A4500-CI-E, 1997

|            |                 |           |              |           |                      |             |             |                |                   |           |               |      |          |      |
|------------|-----------------|-----------|--------------|-----------|----------------------|-------------|-------------|----------------|-------------------|-----------|---------------|------|----------|------|
| Sample ID  | <b>MB-R9353</b> | SampType: | <b>MBLK</b>  | TestCode: | <b>CHLOR</b>         | Units:      | <b>mg/L</b> | Prep Date:     |                   | RunNo:    | <b>9353</b>   |      |          |      |
| Client ID: | <b>PBW</b>      | Batch ID: | <b>R9353</b> | TestNo:   | <b>A4500-CI-E, 1</b> |             |             | Analysis Date: | <b>10/30/2013</b> | SeqNo:    | <b>119686</b> |      |          |      |
| Analyte    |                 | Result    |              | PQL       | SPK value            | SPK Ref Val |             | %REC           | LowLimit          | HighLimit | RPD Ref Val   | %RPD | RPDLimit | Qual |
| Chloride   |                 | < 5.00    |              | 5.00      |                      |             |             |                |                   |           |               |      |          |      |

|            |                  |           |              |           |                      |             |             |                |                   |           |               |      |          |      |
|------------|------------------|-----------|--------------|-----------|----------------------|-------------|-------------|----------------|-------------------|-----------|---------------|------|----------|------|
| Sample ID  | <b>LCS-R9353</b> | SampType: | <b>LCS</b>   | TestCode: | <b>CHLOR</b>         | Units:      | <b>mg/L</b> | Prep Date:     |                   | RunNo:    | <b>9353</b>   |      |          |      |
| Client ID: | <b>LCSW</b>      | Batch ID: | <b>R9353</b> | TestNo:   | <b>A4500-CI-E, 1</b> |             |             | Analysis Date: | <b>10/30/2013</b> | SeqNo:    | <b>119687</b> |      |          |      |
| Analyte    |                  | Result    |              | PQL       | SPK value            | SPK Ref Val |             | %REC           | LowLimit          | HighLimit | RPD Ref Val   | %RPD | RPDLimit | Qual |
| Chloride   |                  | 186       |              | 5.00      | 200.0                | 0           |             | 93.2           | 80                | 120       |               |      |          |      |

|            |                       |           |              |           |                      |             |             |                |                   |           |               |      |          |      |
|------------|-----------------------|-----------|--------------|-----------|----------------------|-------------|-------------|----------------|-------------------|-----------|---------------|------|----------|------|
| Sample ID  | <b>1310328-001AMS</b> | SampType: | <b>MS</b>    | TestCode: | <b>CHLOR</b>         | Units:      | <b>mg/L</b> | Prep Date:     |                   | RunNo:    | <b>9353</b>   |      |          |      |
| Client ID: | <b>MES-1</b>          | Batch ID: | <b>R9353</b> | TestNo:   | <b>A4500-CI-E, 1</b> |             |             | Analysis Date: | <b>10/30/2013</b> | SeqNo:    | <b>119689</b> |      |          |      |
| Analyte    |                       | Result    |              | PQL       | SPK value            | SPK Ref Val |             | %REC           | LowLimit          | HighLimit | RPD Ref Val   | %RPD | RPDLimit | Qual |
| Chloride   |                       | 146       |              | 5.00      | 120.0                | 29.05       |             | 97.5           | 5                 | 178       |               |      |          |      |

|            |                        |           |              |           |                      |             |             |                |                   |           |               |      |          |      |
|------------|------------------------|-----------|--------------|-----------|----------------------|-------------|-------------|----------------|-------------------|-----------|---------------|------|----------|------|
| Sample ID  | <b>1310328-001AMSD</b> | SampType: | <b>MSD</b>   | TestCode: | <b>CHLOR</b>         | Units:      | <b>mg/L</b> | Prep Date:     |                   | RunNo:    | <b>9353</b>   |      |          |      |
| Client ID: | <b>MES-1</b>           | Batch ID: | <b>R9353</b> | TestNo:   | <b>A4500-CI-E, 1</b> |             |             | Analysis Date: | <b>10/30/2013</b> | SeqNo:    | <b>119690</b> |      |          |      |
| Analyte    |                        | Result    |              | PQL       | SPK value            | SPK Ref Val |             | %REC           | LowLimit          | HighLimit | RPD Ref Val   | %RPD | RPDLimit | Qual |
| Chloride   |                        | 143       |              | 5.00      | 120.0                | 29.05       |             | 94.6           | 5                 | 178       | 146.1         | 2.41 | 13.6     |      |

|            |                       |           |              |           |                      |             |             |                |                   |           |               |      |          |      |
|------------|-----------------------|-----------|--------------|-----------|----------------------|-------------|-------------|----------------|-------------------|-----------|---------------|------|----------|------|
| Sample ID  | <b>1310328-002AMS</b> | SampType: | <b>MS</b>    | TestCode: | <b>CHLOR</b>         | Units:      | <b>mg/L</b> | Prep Date:     |                   | RunNo:    | <b>9353</b>   |      |          |      |
| Client ID: | <b>MES-2</b>          | Batch ID: | <b>R9353</b> | TestNo:   | <b>A4500-CI-E, 1</b> |             |             | Analysis Date: | <b>10/30/2013</b> | SeqNo:    | <b>119692</b> |      |          |      |
| Analyte    |                       | Result    |              | PQL       | SPK value            | SPK Ref Val |             | %REC           | LowLimit          | HighLimit | RPD Ref Val   | %RPD | RPDLimit | Qual |
| Chloride   |                       | 151       |              | 5.00      | 120.0                | 34.86       |             | 96.9           | 5                 | 178       |               |      |          |      |

**Qualifiers:**

|  |  |  |
|--|--|--|
| * Value exceeds Maximum Contaminant Level.           | B Analyte detected in the associated Method Blank    | C Value is below Minimum Compound Limit.     |
| E Value above quantitation range                     | H Holding times for preparation or analysis exceeded | J Analyte detected below quantitation limits |
| M Manual Integration used to determine area response | N Non-NELAC Accredited Parameter                     | ND Not Detected at the Reporting Limit       |
| P Second column confirmation exceeds                 | PL Permit Limit                                      | R RPD outside accepted recovery limits       |
| RL Reporting Detection Limit                         | S Spike Recovery outside accepted recovery limits    |  |



# QC SUMMARY REPORT

WO#: 1310328  
 30-Oct-13

**Client:** A & M Engineering  
**Project:** Mid-Way Environ Srvces 1706-003

**TestNo:** A4500-CI-E, 1997

|            |                        |           |              |           |                      |             |             |                |                   |             |               |          |      |
|------------|------------------------|-----------|--------------|-----------|----------------------|-------------|-------------|----------------|-------------------|-------------|---------------|----------|------|
| Sample ID  | <b>1310328-002AMSD</b> | SampType: | <b>MSD</b>   | TestCode: | <b>CHLOR</b>         | Units:      | <b>mg/L</b> | Prep Date:     |                   | RunNo:      | <b>9353</b>   |          |      |
| Client ID: | <b>MES-2</b>           | Batch ID: | <b>R9353</b> | TestNo:   | <b>A4500-CI-E, 1</b> |             |             | Analysis Date: | <b>10/30/2013</b> | SeqNo:      | <b>119693</b> |          |      |
| Analyte    |                        | Result    |              | PQL       | SPK value            | SPK Ref Val | %REC        | LowLimit       | HighLimit         | RPD Ref Val | %RPD          | RPDLimit | Qual |
| Chloride   |                        | 149       |              | 5.00      | 120.0                | 34.86       | 95.5        | 5              | 178               | 151.1       | 1.12          | 13.6     |      |

|                    |  |  |  |
|--------------------|--|--|--|
| <b>Qualifiers:</b> | * Value exceeds Maximum Contaminant Level.           | B Analyte detected in the associated Method Blank    | C Value is below Minimum Compound Limit.     |
|                    | E Value above quantitation range                     | H Holding times for preparation or analysis exceeded | J Analyte detected below quantitation limits |
|                    | M Manual Integration used to determine area response | N Non-NELAC Accredited Parameter                     | ND Not Detected at the Reporting Limit       |
|                    | P Second column confirmation exceeds                 | PL Permit Limit                                      | R RPD outside accepted recovery limits       |
|                    | RL Reporting Detection Limit                         | S Spike Recovery outside accepted recovery limits    |  |

1310328

# A & M ENGINEERING AND ENVIRONMENTAL SERVICES, INC.

ENGINEERING - ENVIRONMENTAL - CONSTRUCTION

10010 E. 16th Street - TULSA, OKLAHOMA 74128-4813  
 TEL: (918)665-8575 FAX: (918)665-8576 E-Mail: aandm@aandmengineering.com

|                                    |  |                              |
|------------------------------------|--|------------------------------|
| SAMPLING FIRM<br>A & M Engineering | CLIENT CONTACT<br>A.M. Estepul         | PHONE NUMBER<br>918-665-6575 |
| PROJECT NUMBER<br>1706-003         | PROJECT NAME<br>MID-WAY ENVIRON. SRVES |                              |

SAMPLERS: (Signature)  
*Thomas L. Tuleau*

ANALYTICAL TESTS REQUIRED  
*Specific Gravity Total Solids*

| STA. NO | DATE     | TIME   | COMP | GRAB | STATION LOCATION | MATRIX | NO. OF CONTAINERS | RUSH ? |    | REMARKS   |
|---------|----------|--------|------|------|------------------|--------|-------------------|--------|----|---|
|         |          |        |      |      |                  |        |                   | YES    | NO |   |
| MES-1   | 10/25/13 | 12:31p |      | X    |                  | GW     | 1                 | X      | X  | * Run Specific Gravity to 3 places past the Decimal ±.001 * |
| MES-2   | 10/25/13 | 12:41p |      | X    |                  | GW     | 1                 | X      | X  |   |
| MES-3   | 10/25/13 | 12:46p |      | X    |                  | GW     | 1                 | X      | X  |   |
| MES-4   | 10/25/13 | 12:51p |      | X    |                  | GW     | 1                 | X      | X  |   |
| MES-5   | 10/25/13 | 12:56p |      | X    |                  | GW     | 1                 | X      | X  |   |
| MES-6   | 10/25/13 | 2:30p  |      | X    |                  | GW     | 1                 | X      | X  |   |

|   |                  |               |  |  |      |      |                          |
|---|------------------|---------------|--|--|------|------|--------------------------|
| RELINQUISHED BY: (Signature)<br><i>Thomas L. Tuleau</i> | DATE<br>10/25/13 | TIME<br>16:48 | RECEIVED BY: (Signature)<br><i>Becky Akers</i> | RELINQUISHED BY: (Signature)               | DATE | TIME | RECEIVED BY: (Signature) |
| RELINQUISHED BY: (Signature)                            | DATE             | TIME          | RECEIVED BY: (Signature)                       | RELINQUISHED BY: (Signature)               | DATE | TIME | RECEIVED BY: (Signature) |
| RELINQUISHED BY: (Signature)                            | DATE             | TIME          | RECEIVED BY: (Signature)                       | REMARKS:<br>Rec'd on use c 1 <sup>cc</sup> |      |      |                          |

#503-20, 21, 11, 23, 18, 25

# APPENDIX D

## WELL COMPLETION REPORT FOR TWIN CITIES SALTWATER DISPOSAL WELL OKLAHOMA CORPORATION COMMISSION



Oklahoma Corporation Commission  
 Oil & Gas Conservation Division  
 Post Office Box 52000  
 Oklahoma City, Oklahoma 73152-2000  
 Rule 165: 10-3-25

API No.: 35081235950001

**Completion Report**

Spud Date: February 27, 2001

OTC Prod. Unit No.:

Drilling Finished Date: March 19, 2001

**Amended**

1st Prod Date:

Amend Reason: PLUGGED BACK ARBUCKLE TO THE WILCOX

Completion Date: April 23, 2001

Recomplete Date: November 27, 2024

**Drill Type: STRAIGHT HOLE**

Well Name: TWIN CITIES SWD 1

Purchaser/Measurer:

Location: LINCOLN 5 14N 5E  
 C SW SW SE  
 425 FSL 225 FWL of 1/4 SEC  
 Latitude: 35.710876 Longitude: -96.794972  
 Derrick Elevation: 0 Ground Elevation: 874

First Sales Date:

Operator: FREEDOM OPERATING COMPANY LLC 24073

2250 E 73RD ST STE 500  
 TULSA, OK 74136-6834

| Completion Type |               |
|-----------------|---------------|
| X               | Single Zone   |
|                 | Multiple Zone |
|                 | Commingled    |

| Location Exception                                  |  |
|---|--|
| Order No  |  |
| There are no Location Exception records to display. |  |

| Increased Density                                  |  |
|--|--|
| Order No   |  |
| There are no Increased Density records to display. |  |

| Casing and Cement |        |        |       |      |     |     |            |
|-------------------|--------|--------|-------|------|-----|-----|------------|
| Type              | Size   | Weight | Grade | Feet | PSI | SAX | Top of CMT |
| SURFACE           | 13 5/8 |        |       | 225  |     | 260 | SURFACE    |
| PRODUCTION        | 9 5/8  |        |       | 5060 |     | 280 | 4200       |

| Liner                                  |      |        |       |        |     |     |           |              |
|--|------|--------|-------|--------|-----|-----|-----------|--------------|
| Type                                   | Size | Weight | Grade | Length | PSI | SAX | Top Depth | Bottom Depth |
| There are no Liner records to display. |      |        |       |        |     |     |           |              |

**Total Depth: 6600**

| Packer |              |
|--------|--------------|
| Depth  | Brand & Type |
| 4611   | ARROW SET 1X |

| Plug  |           |
|-------|-----------|
| Depth | Plug Type |
| 5003  | CIBP      |

| Initial Test Data |
|-------------------|
|                   |

| Test Date | Formation | Oil BL/Day | Oil-Gravity (API) | Gas MCF/Day | Gas-Oil Ratio Cu FT/BBL | Water BBL/Day | Pumpin or Flowing | Initial Shut-In Pressure | Choke Size | Flow Tubing Pressure |
|-----------|-----------|------------|-------------------|-------------|-------------------------|---------------|-------------------|--------------------------|------------|----------------------|
|-----------|-----------|------------|-------------------|-------------|-------------------------|---------------|-------------------|--------------------------|------------|----------------------|

There are no Initial Data records to display.

**Completion and Test Data by Producing Formation**

Formation Name: WILCOX

Code: 202WLCX

Class: DISP

**Spacing Orders**

| Order No                                       | Unit Size |
|--|-----------|
| There are no Spacing Order records to display. |           |

**Perforated Intervals**

| From | To   |
|------|------|
| 4674 | 4790 |

**Acid Volumes**

|  |
|--|
| There are no Acid Volume records to display. |
|--|

**Fracture Treatments**

|  |
|--|
| There are no Fracture Treatments records to display. |
|--|

**Recycled Water**

| Source  | Percentage Used | Complete Volume (Barrels) | Date Of Frac | Qualifies For Gross Production Tax |
|---|-----------------|---------------------------|--------------|------------------------------------|
| There are no Recycled Water records to display. |                 |                           |              |                                    |

| Formation | Top  |
|-----------|------|
| WILCOX    | 4674 |

Were open hole logs run? No

Date last log run:

Were unusual drilling circumstances encountered? No

Explanation:

**Other Remarks**

PLUGGED BACK THE ARBUCKLE TO WILCOX (UIC PERMIT #2400402503) WITH CIBP OVER THE ARBUCKLE AT 5,003' WITH 10'CMT. MIT PASSED ON 11-27-2024. DOFI AFTER PLUGBACK WAS 11-27-2024.

**FOR COMMISSION USE ONLY**

1153133

Status: ACCEPTED

# APPENDIX E

## MES-1 2024 AND 2025 PFT REPORT



## MES-1 2025 PFT REPORT

Raw Data is not included in this appendix. Raw data is provided to DEQ with the stand alone PFT Report Submission





**A & M Engineering and  
Environmental Services, Inc.**  
Consulting - Design - Construction - Remediation

May 23, 2026

Ms. Hillary Young, P.E.  
Chief Engineer  
Land Protection Division  
Oklahoma Department of Environmental Quality  
P.O. Box 1677  
Oklahoma City, Oklahoma 73101

**RE: Annual (2025) Pressure Fall-off Test  
Mid-Way Environmental Services, Inc.  
Davenport, Oklahoma  
Permit Number IW-NH-41001-OP**

Dear Ms. Young:

Enclosed please find the results of the 2025 Pressure Fall-off Test (PFT) conducted at the above reference Mid-Way Environmental Services, Inc. (Mid-Way) commercial Class I Non-Hazardous injection well. The 2025 PFT was conducted during the period of October 15, 2025, through October 20, 2025. The PFT was conducted in accordance with the PFT Plan submitted to the Oklahoma Department of Environmental Quality (DEQ) in June 2025. The PFT Plan outlined the procedures to be followed in conducting the test and for procedures to be followed in gathering static temperature and pressure data to generate and compare the current pressure gradients with historic data.

The 2025 PFT utilized four (4) 5 kpsi rated gauges; two (2) for surface measurement recording and two (2) for bottom hole measurement recording. As DEQ suggested in the October 12, 2020 meeting, Mid-Way chose to use both surface and bottom hole gauge for 2024 PFT so that a comparison can be done between surface and bottom hole gauge for the PFT at Mid-Way. Pressure transient data interpretation and curve matching was performed by a Senior Reservoir Engineer with Schlumberger. A copy of the Schlumberger Pressure Transient Test Interpretation Report (Report) is included for review. The bottom hole gauge Pressure Transient Analysis can be found in Table 3 and Section B of the Report. The static temperature and pressure readings and gradient calculations are also included in Appendix 2 of the Report. Attached Table 2 presents a comparison of the historical formation temperature, pressure, and gradient information.

To allow the well to stabilize and reach equilibrium, the injection well had not been operated for period of approximately 5 days (120 hours) prior to initiating the PFT. Personnel from Precision Wireline, LLC of Enid, Oklahoma calibrated and connected the surface recording gauges directly to a port on the injection well and set the bottom hole gauges at a depth of 5,228 feet. The facility's horizontally mounted centrifugal pump was used as the primary pump for injection and the average pumping rate calculated for the injection period was 200.32 gallons per minute. A total quantity of 580,327 gallons of water was injected during the test. For the PFT conducted on October 15<sup>th</sup> through 20<sup>th</sup> of 2025, the injection (pumping) period was 48 hours 17 minutes, and the monitored recovery (fall-off) period was 72 hours.

After the 72-hour recovery portion of the test, the bottom hole gauges were used to record static temperature and pressure readings at every 500 feet interval as the tool was retrieved; with a final reading at a depth of 100 feet and 0 feet from the surface.

At the completion of the test, the surface and bottom hole gauges were retrieved by Precision Wireline, LLC personnel and the data recorded during the test was forwarded to a Senior Reservoir Engineer with Schlumberger for pressure transient data interpretation and curve matching.

Parameters utilized by Schlumberger in the pressure transient analysis included:

Formation thickness (h) = 300'

Porosity ( $\Phi$ ) = 14.0%

Water Viscosity ( $\mu_w$ ) = 1 cp

Radius of the well (r) = 0.329'

Q = 9,157 Bbl/Day

Compressibility (Ct) = 3E-6

Type curve matching was utilized by Schlumberger in analysis of the pressure transient data. Based on "best fit" to type curves, the data recorded during the 2025 PFT best fits a Radial Composite Reservoir Model, indicating different flow regimes over time. The model (chosen based on the type curves) is the similar as the one used during the 2024 test interpretation.

In the Radial Composite Model, the well is at the center of a circular homogeneous zone, communicating with an infinite homogeneous reservoir. The radius of investigation based on the 2025 results is calculated to be 3,743 feet.

Calculated formation parameters based on the Radial Composite Model indicate a permeability (k) of 217 millidarcys (md) with a -4.47 skin factor. According to Schlumberger analysis and interpretation, this negative skin could be due to acid treatment or presence of possible linear flow.

The bottom hole pressure at the end of the fall off period was 2,491.563 psi, which is similar to historic pressures estimated for the well. A Cartesian plot of recorded data (pressure vs. time) is presented in Figure 1 and 2 of the attached Schlumberger Pressure Transient Test Interpretation Report. A summary of the bottom hole pressures estimated over the last several years is presented in the table below:

**Table 1:** Estimated Bottom Hole Pressure from the Measured Surface Pressure

| Calendar Year | Estimated Bottom Hole Pressure (psi) |
|---------------|--------------------------------------|
| 2010          | 2,495                                |
| 2015          | 2,537                                |
| 2016          | 2,649                                |
| 2017          | 2,574                                |
| 2018          | 2,509                                |
| 2019          | 1,869                                |
| 2020          | 2,672                                |
| 2021          | 2,529                                |
| 2022          | 2,536.7*                             |
| 2023          | 2,529.27*                            |
| 2024          | 2,507.59*                            |
| 2025          | 2,491.56**                           |

\* Bottom hole pressure estimated at depth of 5,340 ft below ground surface

\*\* Bottom hole pressure estimated at depth of 5,228 ft below ground surface

Attached Table 2 presents a comparison of the historical formation pressure, temperature, and gradient information. The data indicates no apparent changes to bottom-hole pressure or temperature because of the injection activities. Please note that the pressure reading recorded near the top of the well head was comparable to the well head pressure observed on the facility's continuous recording equipment prior to initiating the static survey.

Ms. Hillary Young, P.E.

May 23, 2026

Page -4-

If you have any questions on this matter, or if you need additional information, please do not hesitate to contact me at 918-665-6575.

Sincerely,

A & M Engineering and Environmental Services, Inc.



Orphi Muhammad, PhD, P.E.

Senior Environmental Engineer

- Enclosures:
- (i) Table 2: Historical Static formation Pressure, Temperature, and Gradient information
  - (ii) Schlumberger Pressure Transient Analysis Report
  - (iii) Precision Wireline Data Summary
  - (iv) Raw Pressure Data [Bottom Hole Gauge]
  - (v) Raw Pressure Data [Surface Gauge]

Cc: Mr. John Mitsdarfer, DEQ  
Ms. Brigette Haley, DEQ  
Mr. Tolga Ertugrul, P.E., President, Mid-Way

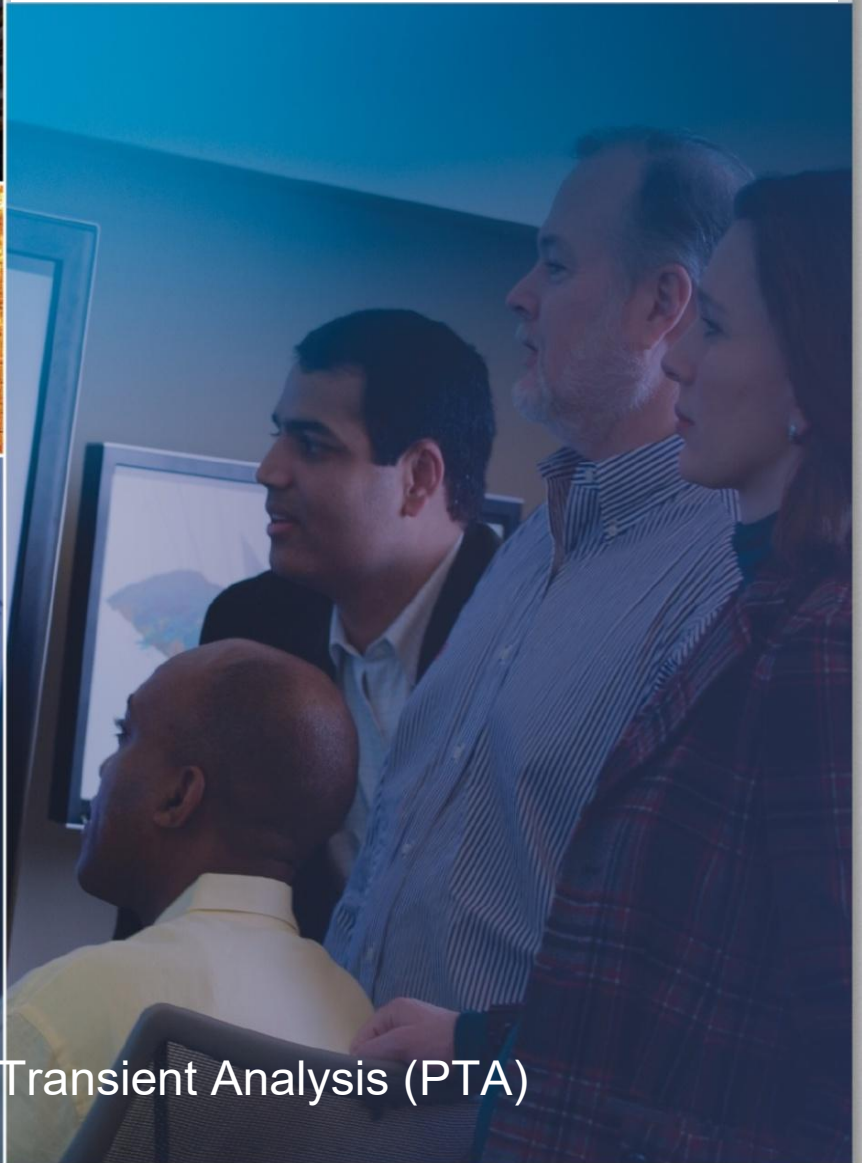
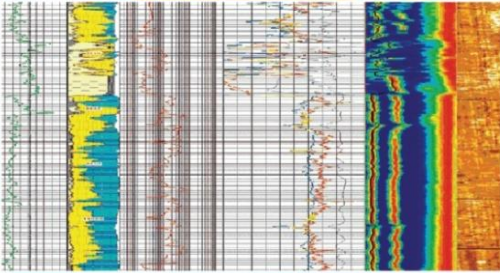
**Table 2:**  
**Historical Static formation Pressure, Temperature, and Gradient information**

TABLE 2  
FORMATION PRESSURE, TEMPERATURE, AND GRADIENT DATA

| Depth<br>(ft bgs) | May 7, 2010       |                      |                     | October 11, 2010  |                      |                     | September 14, 2015 |                      |                     | September 6, 2016 |                      |                     | September 25, 2017 <sup>1</sup> |                      |                     | January 17, 2019 <sup>2</sup> |                      |                     | December 9, 2019 <sup>3</sup> |                      |                     | November 16, 2020 <sup>3</sup> |                      |                     | November 15, 2021 <sup>3</sup> |                      |                     | November 14, 2022 <sup>3</sup> |                      |                     | November 13, 2023 <sup>3</sup> |                      |                     | November 18, 2024 <sup>3</sup> |                      |                     | October 20, 2025 <sup>3</sup> |                      |                     |   |   |   |   |   |   |   |   |
|-------------------|-------------------|----------------------|---------------------|-------------------|----------------------|---------------------|--------------------|----------------------|---------------------|-------------------|----------------------|---------------------|---------------------------------|----------------------|---------------------|-------------------------------|----------------------|---------------------|-------------------------------|----------------------|---------------------|--------------------------------|----------------------|---------------------|--------------------------------|----------------------|---------------------|--------------------------------|----------------------|---------------------|--------------------------------|----------------------|---------------------|--------------------------------|----------------------|---------------------|-------------------------------|----------------------|---------------------|---|---|---|---|---|---|---|---|
|                   | Pressure<br>(psf) | Gradient<br>(psf/ft) | Temperature<br>(°F) | Pressure<br>(psf) | Gradient<br>(psf/ft) | Temperature<br>(°F) | Pressure<br>(psf)  | Gradient<br>(psf/ft) | Temperature<br>(°F) | Pressure<br>(psf) | Gradient<br>(psf/ft) | Temperature<br>(°F) | Pressure<br>(psf)               | Gradient<br>(psf/ft) | Temperature<br>(°F) | Pressure<br>(psf)             | Gradient<br>(psf/ft) | Temperature<br>(°F) | Pressure<br>(psf)             | Gradient<br>(psf/ft) | Temperature<br>(°F) | Pressure<br>(psf)              | Gradient<br>(psf/ft) | Temperature<br>(°F) | Pressure<br>(psf)              | Gradient<br>(psf/ft) | Temperature<br>(°F) | Pressure<br>(psf)              | Gradient<br>(psf/ft) | Temperature<br>(°F) | Pressure<br>(psf)              | Gradient<br>(psf/ft) | Temperature<br>(°F) | Pressure<br>(psf)              | Gradient<br>(psf/ft) | Temperature<br>(°F) | Pressure<br>(psf)             | Gradient<br>(psf/ft) | Temperature<br>(°F) |   |   |   |   |   |   |   |   |
| 0                 | 15.37             | -                    | 68.1                | 16.97             | -                    | 60.75               | 225.90             | -                    | 75.66               | 260*              | -                    | 90                  | 270*                            | -                    | 80*                 | 217.75*                       | -                    | 214.90              | -                             | 55.22                | 194.64              | -                              | 67.89                | 192.11              | -                              | 66.36                | 212.05              | -                              | 57.50                | 184.67              | -                              | 73.10                | 147.27              | -                              | 65.36                | 187.78              | -                             | 78.19                |                     |   |   |   |   |   |   |   |   |
| 100               | 55.91             | 0.405                | 68.75               | 53.3              | 0.363                | 60.85               | 280.42             | 0.545                | 66.92               | 299.40            | 0.394                | 64.91               | 317.69                          | 0.477                | 66.71               | 267.51                        | 0.498                | 268.22              | 0.533                         | 61.9                 | 254.89              | 0.603                          | 62.76                | 236.29              | 0.442                          | 63.76                | 267.25              | 0.552                          | 65.00                | 233.02              | 0.483                          | 64.27                | 195.58              | 0.483                          | 67.08                | 243.80              | 0.560                         | 67.07                |                     |   |   |   |   |   |   |   |   |
| 500               | 228.56            | 0.432                | 71.02               | 224.52            | 0.428                | 62.1                | 454.10             | 0.434                | 69.87               | 471.00            | 0.429                | 67.49               | 491.21                          | 0.434                | 69.48               | 441.89                        | 0.436                | 64.29               | 441.05                        | 0.432                | 64.21               | 429.60                         | 0.437                | 65.15               | 411.21                         | 0.437                | 65.96               | 440.40                         | 0.433                | 67.17               | 407.09                         | 0.435                | 66.46               | 372.23                         | 0.442                | 69.38               | 418.58                        | 0.437                | 69.47               |   |   |   |   |   |   |   |   |
| 1,000             | 444.84            | 0.433                | 73.9                | 439.38            | 0.43                 | 64.53               | 671.40             | 0.435                | 72.18               | 688.59            | 0.435                | 70.76               | 708.60                          | 0.435                | 72.59               | 659.81                        | 0.436                | 68.21               | 657.66                        | 0.433                | 67.66               | 648.22                         | 0.437                | 68.77               | 630.18                         | 0.438                | 69.26               | 656.40                         | 0.432                | 70.46               | 624.35                         | 0.435                | 69.57               | 592.47                         | 0.440                | 72.40               | 636.26                        | 0.435                | 71.95               |   |   |   |   |   |   |   |   |
| 1,500             | 661.02            | 0.432                | 76.87               | 656.29            | 0.434                | 67.6                | 888.38             | 0.434                | 77.13               | 905.11            | 0.429                | 75.15               | 925.77                          | 0.434                | 76.79               | 878.01                        | 0.436                | 71.67               | 873.84                        | 0.432                | 71.56               | 867.30                         | 0.438                | 72.99               | 848.54                         | 0.437                | 73.11               | 873.15                         | 0.435                | 74.25               | 841.60                         | 0.435                | 73.39               | 812.33                         | 0.440                | 75.87               | 837.03                        | 0.442                | 75.27               |   |   |   |   |   |   |   |   |
| 2,000             | 885.14            | 0.488                | 80.13               | 884.34            | 0.456                | 71.89               | 1106.01            | 0.435                | 81.62               | 1119.93           | 0.434                | 80.03               | 1142.70                         | 0.434                | 81.07               | 1096.19                       | 0.436                | 75.7                | 1089.89                       | 0.432                | 75.67               | 1085.68                        | 0.437                | 77.93               | 1067.12                        | 0.437                | 77.28               | 1088.07                        | 0.430                | 78.32               | 1058.63                        | 0.434                | 77.35               | 1032.58                        | 0.440                | 79.68               | 1076.16                       | 0.438                | 79.31               |   |   |   |   |   |   |   |   |
| 2,500             | 1,129.40          | 0.489                | 84.59               | 1,129.78          | 0.491                | 77.2                | 1322.08            | 0.432                | 87.21               | 1335.49           | 0.431                | 85.98               | 1360.15                         | 0.435                | 86.48               | 1314.35                       | 0.436                | 80.66               | 1305.96                       | 0.432                | 80.75               | 1302.98                        | 0.435                | 83.02               | 1285.55                        | 0.437                | 82.39               | 1304.89                        | 0.434                | 83.40               | 1276.14                        | 0.435                | 82.81               | 1252.63                        | 0.440                | 84.40               | 1295.93                       | 0.440                | 83.88               |   |   |   |   |   |   |   |   |
| 3,000             | 1,373.60          | 0.488                | 89.22               | 1,372.90          | 0.486                | 83.64               | 1539.75            | 0.435                | 92.7                | 1551.58           | 0.432                | 91.68               | 1576.88                         | 0.433                | 91.59               | 1532.55                       | 0.436                | 85.54               | 1522.43                       | 0.433                | 85.94               | 1522.22                        | 0.438                | 88.47               | 1504.03                        | 0.437                | 87.57               | 1523.31                        | 0.437                | 88.59               | 1493.60                        | 0.435                | 87.69               | 1472.81                        | 0.440                | 88.99               | 1514.85                       | 0.438                | 88.38               |   |   |   |   |   |   |   |   |
| 3,500             | 1,617.99          | 0.489                | 94.35               | 1,616.68          | 0.488                | 88.77               | 1756.43            | 0.433                | 100.16              | 1766.69           | 0.430                | 99.15               | 1794.16                         | 0.435                | 98.82               | 1750.18                       | 0.435                | 93.07               | 1738.75                       | 0.433                | 93.65               | 1740.34                        | 0.436                | 96.21               | 1722.46                        | 0.437                | 95.00               | 1740.19                        | 0.434                | 95.99               | 1710.98                        | 0.435                | 94.83               | 1692.95                        | 0.440                | 95.75               | 1733.98                       | 0.438                | 94.92               |   |   |   |   |   |   |   |   |
| 4,000             | 1,862.32          | 0.489                | 100.27              | 1,860.57          | 0.488                | 97.23               | 1973.23            | 0.434                | 107.28              | 1981.86           | 0.430                | 106.92              | 2011.17                         | 0.434                | 105.89              | 1967.75                       | 0.435                | 99.11               | 1954.44                       | 0.431                | 99.84               | 1958.55                        | 0.436                | 102.95              | 1940.67                        | 0.436                | 101.56              | 1956.52                        | 0.433                | 102.32              | 1928.24                        | 0.435                | 101.31              | 1912.91                        | 0.440                | 101.61              | 1953.02                       | 0.438                | 100.67              |   |   |   |   |   |   |   |   |
| 4,500             | 2,106.40          | 0.488                | 106.26              | 2,105.68          | 0.49                 | 104.5               | 2189.40            | 0.432                | 113.81              | 2196.54           | 0.429                | 113.74              | 2228.19                         | 0.434                | 112.3               | 2184.87                       | 0.434                | 106.04              | 2170.58                       | 0.432                | 106.54              | 2176.40                        | 0.436                | 109.38              | 2158.22                        | 0.435                | 107.99              | 2172.78                        | 0.433                | 109.10              | 2145.05                        | 0.434                | 107.87              | 2132.76                        | 0.440                | 108.09              | 2172.22                       | 0.438                | 106.57              |   |   |   |   |   |   |   |   |
| 5,000             | 2,350.31          | 0.488                | 111.56              | 2,347.22          | 0.483                | 112.96              | 2405.63            | 0.432                | 118.65              | 2410.64           | 0.428                | 118.83              | 2444.19                         | 0.432                | 117.4               | 2401.61                       | 0.433                | 111.67              | 2386.52                       | 0.432                | 111.90              | 2394.23                        | 0.436                | 114.57              | 2376.31                        | 0.436                | 113.38              | 2389.32                        | 0.433                | 114.16              | 2362.18                        | 0.434                | 112.93              | 2352.28                        | 0.439                | 113.17              | 2391.24                       | 0.438                | 111.15              |   |   |   |   |   |   |   |   |
| 5,238             | -                 | -                    | -                   | -                 | -                    | -                   | -                  | -                    | -                   | -                 | -                    | -                   | -                               | -                    | -                   | -                             | -                    | -                   | -                             | -                    | -                   | -                              | -                    | -                   | -                              | -                    | -                   | -                              | -                    | -                   | -                              | -                    | -                   | -                              | -                    | -                   | -                             | -                    | -                   | - | - | - |   |   |   |   |   |
| 5,340             | -                 | -                    | -                   | -                 | -                    | -                   | -                  | -                    | -                   | -                 | -                    | -                   | -                               | -                    | -                   | -                             | -                    | -                   | -                             | -                    | -                   | -                              | -                    | -                   | -                              | -                    | -                   | -                              | -                    | -                   | -                              | -                    | -                   | -                              | -                    | -                   | -                             | -                    | -                   | - | - | - | - |   |   |   |   |
| 5,436             | -                 | -                    | -                   | -                 | -                    | -                   | -                  | -                    | -                   | -                 | -                    | -                   | -                               | -                    | -                   | -                             | -                    | -                   | -                             | -                    | -                   | -                              | -                    | -                   | -                              | -                    | -                   | -                              | -                    | -                   | -                              | -                    | -                   | -                              | -                    | -                   | -                             | -                    | -                   | - | - | - | - |   |   |   |   |
| 5,500             | 2,593.77          | 0.487                | 117.08              | 2,589.17          | 0.484                | 119.39              | 2626.64            | 0.442                | 117.63              | 2619.99           | 0.419                | 120.05              | 2664.05                         | 0.440                | 115.32              | 2624.50                       | 0.446                | 95.99               | 2603.37                       | 0.434                | 91.75               | 2612.30                        | 0.436                | 92.58               | -                              | -                    | -                   | -                              | -                    | -                   | -                              | -                    | -                   | -                              | -                    | -                   | -                             | -                    | -                   | - | - | - | - |   |   |   |   |
| 5,764             | -                 | -                    | -                   | -                 | -                    | -                   | -                  | -                    | -                   | -                 | -                    | -                   | -                               | -                    | -                   | -                             | -                    | -                   | -                             | -                    | -                   | -                              | -                    | -                   | -                              | -                    | -                   | -                              | -                    | -                   | -                              | -                    | -                   | -                              | -                    | -                   | -                             | -                    | -                   | - | - | - | - | - |   |   |   |
| 5,800             | -                 | -                    | -                   | -                 | -                    | -                   | -                  | -                    | -                   | -                 | -                    | -                   | -                               | -                    | -                   | -                             | -                    | -                   | -                             | -                    | -                   | -                              | -                    | -                   | -                              | -                    | -                   | -                              | -                    | -                   | -                              | -                    | -                   | -                              | -                    | -                   | -                             | -                    | -                   | - | - | - | - | - |   |   |   |
| 6,000             | 2,836.94          | 0.486                | 120.92              | 2,833.29          | 0.488                | 123.84              | 2865.67            | 0.478                | 126.66              | 2861.98           | 0.484                | 121.54              | 2885.22                         | 0.442                | 119.23              | 2844.73                       | 0.440                | 113.39              | -                             | -                    | -                   | -                              | -                    | -                   | -                              | -                    | -                   | -                              | -                    | -                   | -                              | -                    | -                   | -                              | -                    | -                   | -                             | -                    | -                   | - | - | - | - | - |   |   |   |
| 6,500             | 3,080.06          | 0.486                | 124.05              | 3,077.85          | 0.489                | 125.62              | 3106.93            | 0.483                | 128.91              | 3091.20           | 0.458                | 121.04              | 3109.54                         | 0.449                | 118.45              | 3066.29                       | 0.443                | 117.71              | -                             | -                    | -                   | -                              | -                    | -                   | -                              | -                    | -                   | -                              | -                    | -                   | -                              | -                    | -                   | -                              | -                    | -                   | -                             | -                    | -                   | - | - | - | - | - | - |   |   |
| 6,797             | -                 | -                    | -                   | -                 | -                    | -                   | -                  | -                    | -                   | -                 | -                    | -                   | -                               | -                    | -                   | -                             | -                    | -                   | -                             | -                    | -                   | -                              | -                    | -                   | -                              | -                    | -                   | -                              | -                    | -                   | -                              | -                    | -                   | -                              | -                    | -                   | -                             | -                    | -                   | - | - | - | - | - | - | - |   |
| 6,800             | -                 | -                    | -                   | -                 | -                    | -                   | -                  | -                    | -                   | -                 | -                    | -                   | -                               | -                    | -                   | -                             | -                    | -                   | -                             | -                    | -                   | -                              | -                    | -                   | -                              | -                    | -                   | -                              | -                    | -                   | -                              | -                    | -                   | -                              | -                    | -                   | -                             | -                    | -                   | - | - | - | - | - | - | - | - |
| 7,000             | 3,222.81          | 0.486                | 132.8               | 3,219.61          | 0.484                | 130.8               | 3325.44            | 0.481                | 134.13              | 3325.40           | 0.468                | 135.18              | -                               | -                    | -                   | -                             | -                    | -                   | -                             | -                    | -                   | -                              | -                    | -                   | -                              | -                    | -                   | -                              | -                    | -                   | -                              | -                    | -                   | -                              | -                    | -                   | -                             | -                    | -                   | - | - | - | - | - | - | - | - |

\*Static surface pressure and temperature obtained from facility operating record  
<sup>1</sup> Total depth to top of cement plug = 6,797 feet below ground surface  
<sup>2</sup> Total depth to top of cement plug = 6,804 feet below ground surface  
<sup>3</sup> Total depth to bridge = 5,764 feet below ground surface  
<sup>4</sup> Gauge temporarily stuck at depth = 5,238 feet below ground surface

# Digital Subsurface Solutions Analysis & Interpretation Services



## Pressure Transient Analysis (PTA)

Company : A & M Engineering and Environmental Services, Inc.  
Reservoir : Arbuckle Formation  
Well : MES#1  
JOB : Pressure Transient Analysis Fall Off Test  
Job dates : 15<sup>th</sup> October to 20<sup>th</sup> October 2025  
Report date : 12<sup>th</sup> November 2025  
PTEs : Velerian Lopes, Ashraf Hussein  
Job reference : DS-2025-17021





Company: A&M Engineering and Environmental Services, Inc.

County, State: Lincoln, Oklahoma

Reservoir: Arbuckle Formation

Well: MES#1- Water Injector

## **A & M Engineering and Environmental Services, Inc.**

### **MES#1**

#### **Arbuckle Formation**

(Open Hole Interval: 5,173 ft. – 6,804 ft)

Open Hole

#### **Pressure Transient Analysis**

#### **Fall Off Test**

Surface and Bottomhole Pressure Monitoring

Interpreters:

Velerian Lopes: Analysis & Interpretation Hub, Reservoir Lead,

Vlopes@slb.com,

Ashraf Hussein: Analysis & Interpretation Reservoir Lead

AHussein18@slb.com, +1 405 249 7676



## Contents

|  |    |
|--|----|
| A01 • Main results.....  | 4  |
| B01 • Interpretation with downhole pressure gauge data (Gauge 50592) .....                           | 9  |
| B02 • Comparison of Log-Log plot with downhole pressure gauge data for Jun 2025 & Oct 2025 .....     | 12 |
| C01 • Summary of PTA Inputs - Pressure Fall Off on Oct 2025 .....                                    | 13 |
| C02 • Comparison of PTA Results - Pressure Fall Off on Oct 2025, Jun 2025, Nov 2024 and Nov 2023.... | 14 |
| Appendix 1: Static Pressure and Temperature Gradients .....  | 16 |
| Appendix 2: MES # 1 Well Construction Revision Diagram (9-23-2020) .....                             | 19 |



**DISCLAIMER**

SAVE FOR THAT EXPRESSLY STATED IN THE AGREEMENT, SLB MAKES NO WARRANTIES, EITHER EXPRESS OR IMPLIED, STATUTORY OR OTHERWISE IN CONNECTION WITH ITS PERFORMANCE OF THE SERVICES OR ANY DELIVERABLES HEREUNDER, OR THE USE OF THE SERVICES OR DELIVERABLES BY CUSTOMER. SLB DOES NOT GUARANTEE ANY RESULTS. CUSTOMER HAS FULL RESPONSIBILITY FOR ITS USE OF THE DELIVERABLES AND ANY INTERPRETATIONS, RECOMMENDATIONS AND/OR DESCRIPTIONS PROVIDED BY SLB HEREUNDER. ALL INTERPRETATIONS, RECOMMENDATIONS AND/OR RESERVOIR DESCRIPTIONS ARE OPINIONS BASED ON INFERENCES FROM MEASUREMENTS AND EMPIRICAL RELATIONSHIPS AND ON ASSUMPTIONS, WHICH INFERENCES AND ASSUMPTIONS ARE NOT INFALLIBLE, AND WITH RESPECT TO WHICH COMPETENT SPECIALISTS MAY DIFFER. IN ADDITION, SUCH INTERPRETATIONS, RECOMMENDATIONS AND/OR RESERVOIR DESCRIPTIONS MAY INVOLVE THE OPINION AND JUDGMENT OF CUSTOMER AND/OR INFORMATION AND DATA FURNISHED BY CUSTOMER. SLB CANNOT AND DOES NOT WARRANT THE ACCURACY, CORRECTNESS OR COMPLETENESS OF ANY INTERPRETATION, RECOMMENDATION AND/OR RESERVOIR DESCRIPTION. UNDER NO CIRCUMSTANCES SHOULD ANY INTERPRETATION, RECOMMENDATION AND/OR RESERVOIR DESCRIPTION BE RELIED UPON AS THE SOLE BASIS FOR ANY DRILLING, COMPLETION, WELL TREATMENT, PRODUCTION OR OTHER FINANCIAL DECISION, OR ANY PROCEDURE INVOLVING ANY RISK TO THE SAFETY OF ANY DRILLING VENTURE, DRILLING RIG OR ITS CREW OR ANY OTHER INDIVIDUAL. CUSTOMER HAS FULL RESPONSIBILITY FOR ALL SUCH DECISIONS AND FOR ALL DECISIONS CONCERNING OTHER PROCEDURES RELATING TO THE DRILLING OR PRODUCTION



Company: A & M Engineering and Environmental Services, Inc.  
 County, State: Lincoln, Oklahoma  
 Reservoir: Arbuckle Formation      Well: MES#1- Water Injector

**A01 • Main results**

The pressure recorders were located at the surface to record the Well Head (Tubing) Pressure and at the bottom of the well at 5,228 ft to assess the near wellbore conditions and obtain reservoir parameters for the Arbuckle formation over the open hole interval 5,173 ft.-6,804 ft. Downhole pressure gauge data was used to evaluate the formation permeability, skin factor and formation pressure.

Bottomhole pressure transient data provided reasonable match, as radial flow regime was observed. Spherical flow regime was clearly observed, indicating flow into wellbore exhibits limited entry behaviour. Vertical well model was presented here as part of appendix.

The testing procedure consisted of two main events:

\* Water Injection: Recorded for ~48 hours. Average surface injection flowrate: 200.32 gal/min (~9,157 STB/D). The recorded injection pressure prior to shut-in was BHP= 2,985.93 Psig and WHP= 736.03 psig.

\* Pressure Fall Off: Recorded for ~ 72 hours. The recorded pressure at the end of shut-in was BHP= 2,491.56 psig and WHP= ~202.76 psig.

The injection and pressure fall off test procedure consisted of the following events:

*Table 1: Events Summary at Bottom Hole and Surface*

| Real Date<br>MM/DD/YY | Real Time<br>HH:MM:SS | Elapsed Time<br>Minutes | Pressure<br>psiG | Temperature<br>deg. F | Tag<br>Number | Comment                           |
|-----------------------|-----------------------|-------------------------|------------------|-----------------------|---------------|-----------------------------------|
| 10/15/25              | 12:14:03              | 32.03330                | 210.923          | 74.20                 | 14            | RIH - 0 -                         |
| 10/15/25              | 12:38:53              | 56.86670                | 2527.289         | 102.79                | 15            | 5228' GAUGE SET                   |
| 10/15/25              | 12:50:33              | 68.53330                | 2525.211         | 100.83                | 16            | BEGIN INJECTION                   |
| 10/17/25              | 13:07:43              | 2965.70000              | 2985.931         | 78.32                 | 17            | SHUT-IN BEGIN FALL-OFF            |
| 10/20/25              | 13:05:23              | 7283.36700              | 2491.563         | 97.56                 | 1             | POOH static stop @ 5228 feet TVD. |
| 10/20/25              | 13:12:23              | 7290.36700              | 2391.241         | 111.15                | 2             | POOH static stop @ 5000 feet TVD. |
| 10/20/25              | 13:17:53              | 7295.86700              | 2172.224         | 106.57                | 3             | POOH static stop @ 4500 feet TVD. |
| 10/20/25              | 13:24:33              | 7302.53300              | 1953.018         | 100.67                | 4             | POOH static stop @ 4000 feet TVD. |
| 10/20/25              | 13:30:13              | 7308.20000              | 1733.975         | 94.92                 | 5             | POOH static stop @ 3500 feet TVD. |
| 10/20/25              | 13:36:53              | 7314.86700              | 1514.849         | 88.38                 | 6             | POOH static stop @ 3000 feet TVD. |
| 10/20/25              | 13:43:33              | 7321.53300              | 1295.930         | 83.88                 | 7             | POOH static stop @ 2500 feet TVD. |
| 10/20/25              | 13:48:03              | 7326.03300              | 1076.160         | 79.31                 | 8             | POOH static stop @ 2000 feet TVD. |
| 10/20/25              | 13:55:13              | 7333.20000              | 857.026          | 75.27                 | 9             | POOH static stop @ 1500 feet TVD. |
| 10/20/25              | 14:00:13              | 7338.20000              | 636.255          | 71.95                 | 10            | POOH static stop @ 1000 feet TVD. |
| 10/20/25              | 14:05:53              | 7343.86700              | 418.576          | 69.47                 | 11            | POOH static stop @ 500 feet TVD.  |
| 10/20/25              | 14:11:23              | 7349.36700              | 243.799          | 67.07                 | 12            | POOH static stop @ 100 feet TVD.  |
| 10/20/25              | 14:18:23              | 7356.36700              | 187.748          | 78.19                 | 13            | POOH static stop @ 0 feet TVD.    |

*Table 2 Injection and pressure fall off test events. Upper Table: Downhole event, and Lower Table: Surface Events*

| Real Date<br>MM/DD/YY | Real Time<br>HH:MM:SS | Elapsed Time<br>Minutes | Pressure<br>psiG | Temperature<br>deg. F | Tag<br>Number | Comment                      |
|-----------------------|-----------------------|-------------------------|------------------|-----------------------|---------------|------------------------------|
| 10/15/25              | 12:07:52              | 21.86670                | 65.852           | 0.00                  | 1             | OPEN WELLHEAD SURFACE GAUGES |
| 10/15/25              | 12:50:22              | 64.36670                | 217.446          | 0.00                  | 2             | INJECTION PUMP START         |
| 10/17/25              | 13:07:32              | 2961.53300              | 736.027          | 0.00                  | 3             | INJECTION STOP BEGIN SHUT-IN |
| 10/20/25              | 13:05:02              | 7279.03300              | 202.757          | 0.00                  | 4             | END FALL-OFF TEST            |



- 1. F50592: Bottom hole pressure Top - gauge 50592
- 2. F50133: Bottom hole pressure Bottom - gauge 50133
- 3. F50766: Surface pressure WHP – gauge 50766
- 4. F50794: Surface pressure WHP – gauge 50794

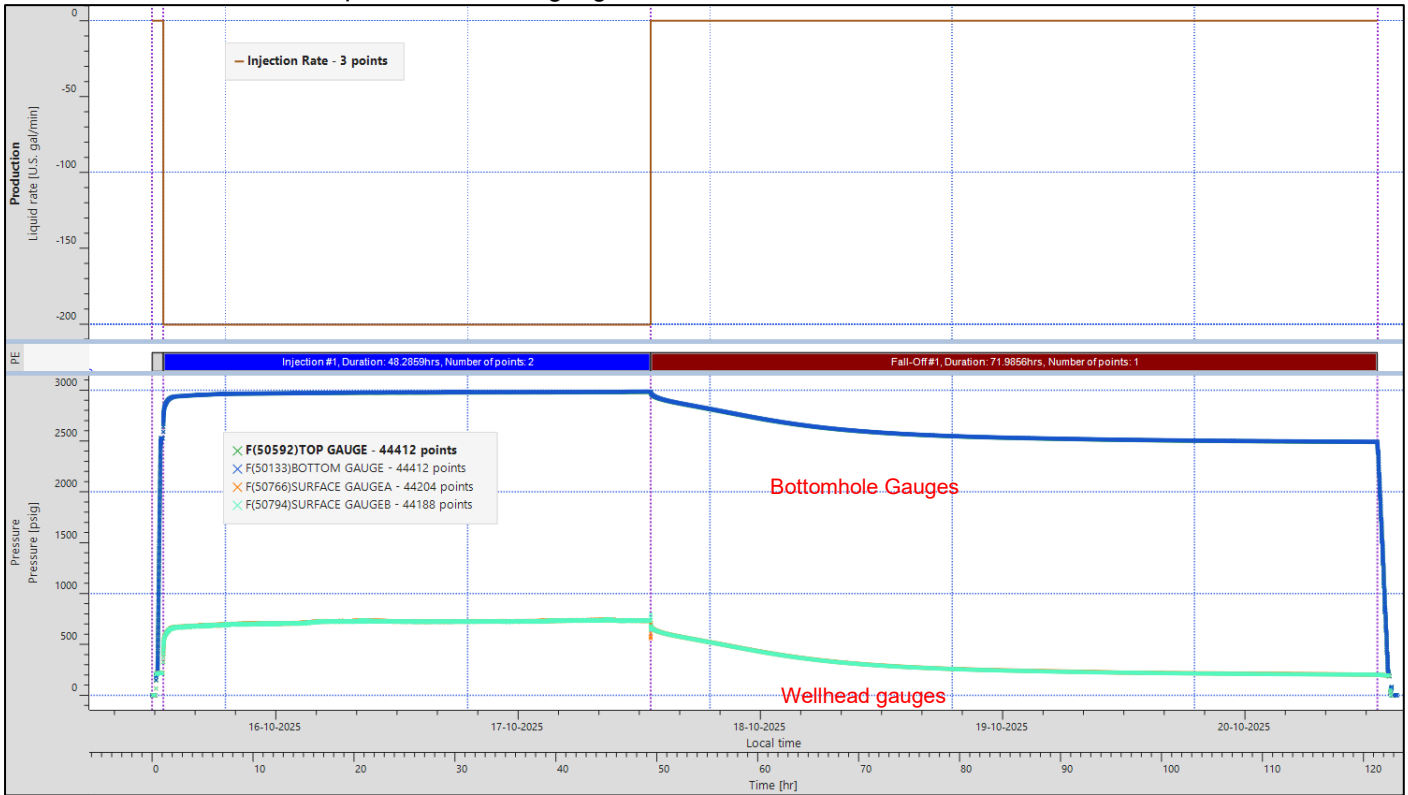


Figure 1: Cartesian Plot for Injection flow rate and Pressure Falloff for gauges #50592 and #50133 @ 5,228 ft and wellhead gauges #50766 and #50794

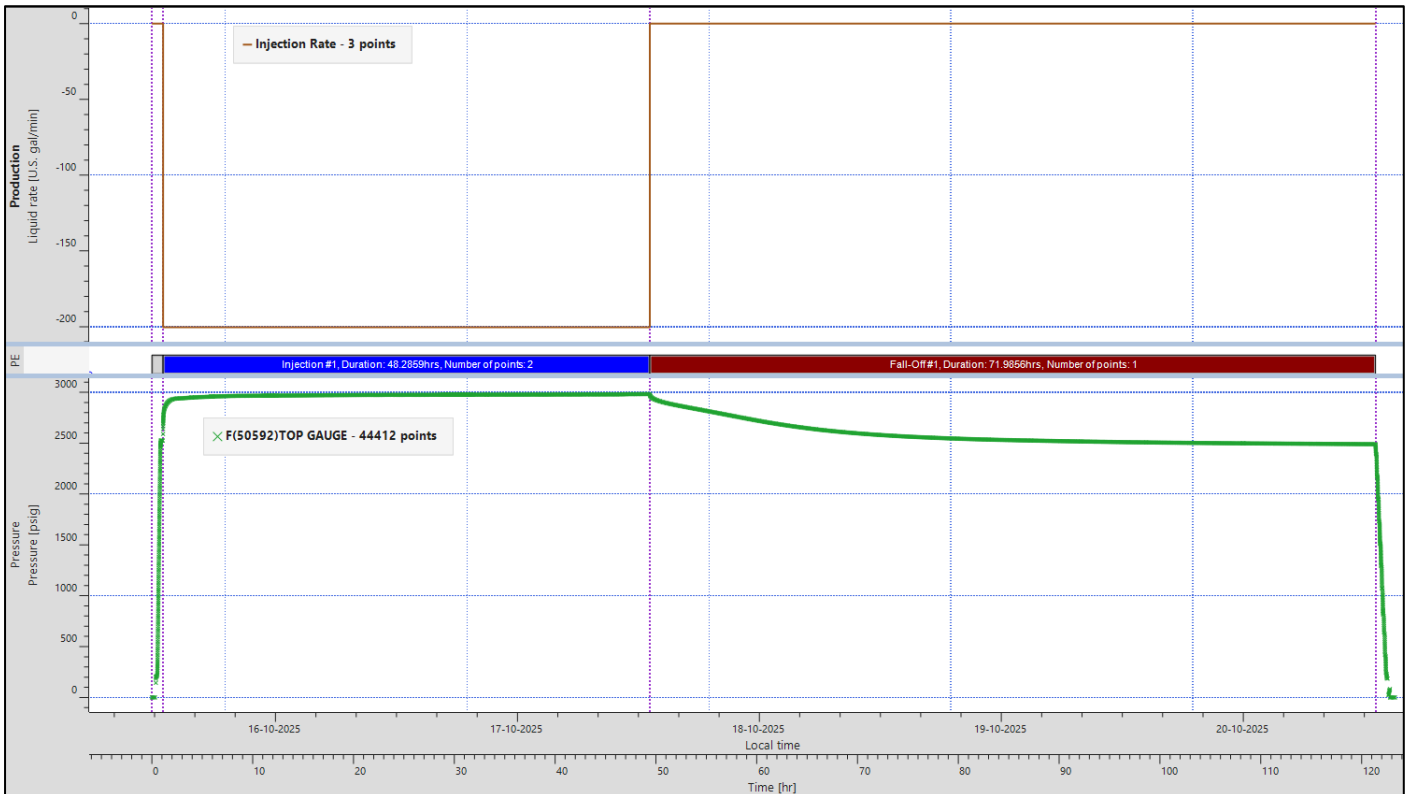


Figure 2: Pressure data for gauges considered for PTA analysis. Gauge #50592 @ 5,228 ft

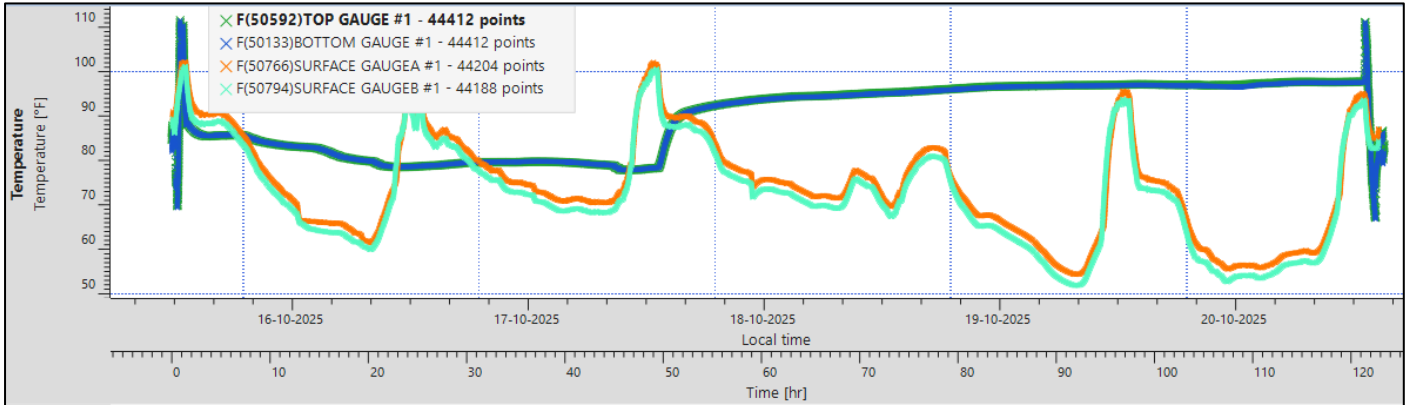


Figure 3: Temperature readings for gauge wellhead (50766-orange, 50794-aqua) and bottom (50592 and 50133 in green and blue colour).

The water fluid properties were estimated based on the reported field water sp. gravity (~1.008 g/cc) and down hole pressure & temperature conditions. The bottomhole and surface pressure data quality is compared in Figure 4, indicating noisy surface pressure data, which reflects in the fall off pressure derivatives presented in Figure 5.

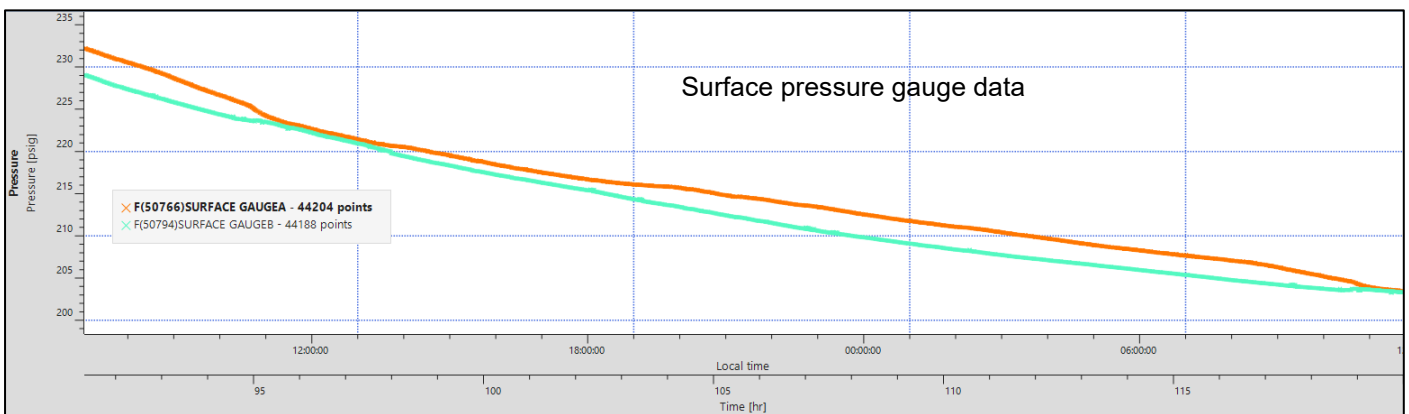
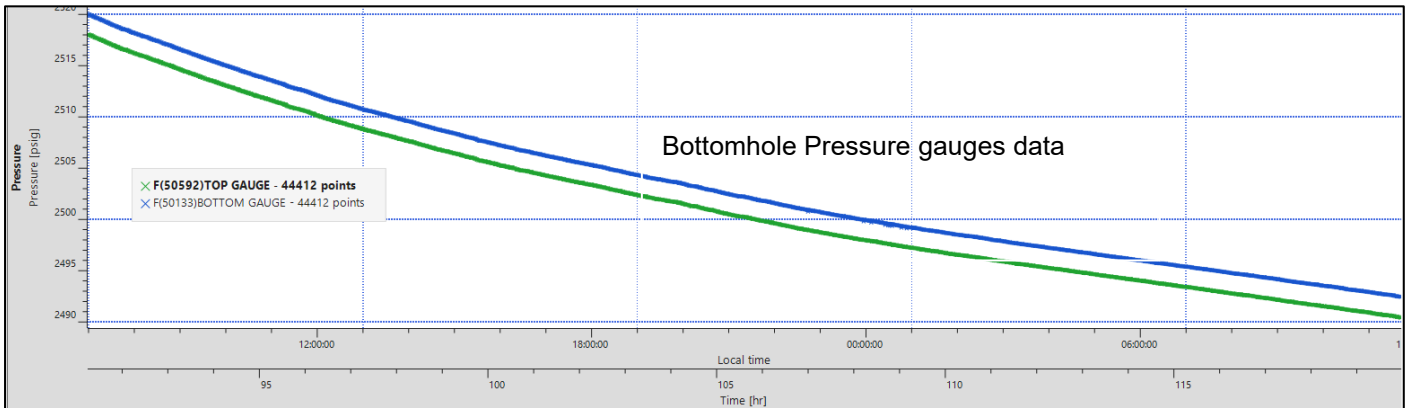


Figure 4: Bottom hole and surface pressure gauges data quality

Along with bad data quality of surface pressure gauge, fall off analysis of this gauge present two wellbore dynamics effects:

- small noise at early times in the surface pressure gauge. However, it does not have an important impact in the analysis.
- spikes in the derivative late times which look associated to temperature variations. This phenomenon is mainly affecting the surface pressure gauges as presented in Figure 5.

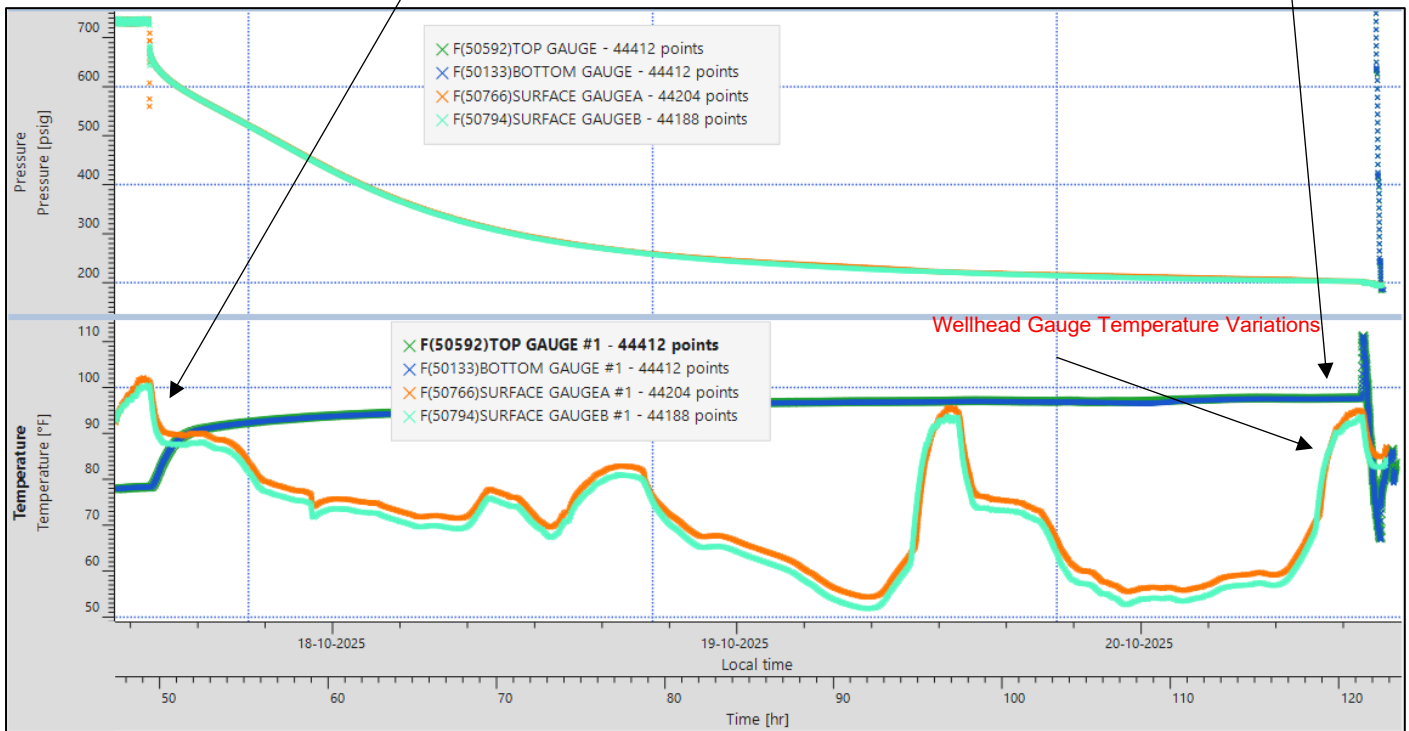
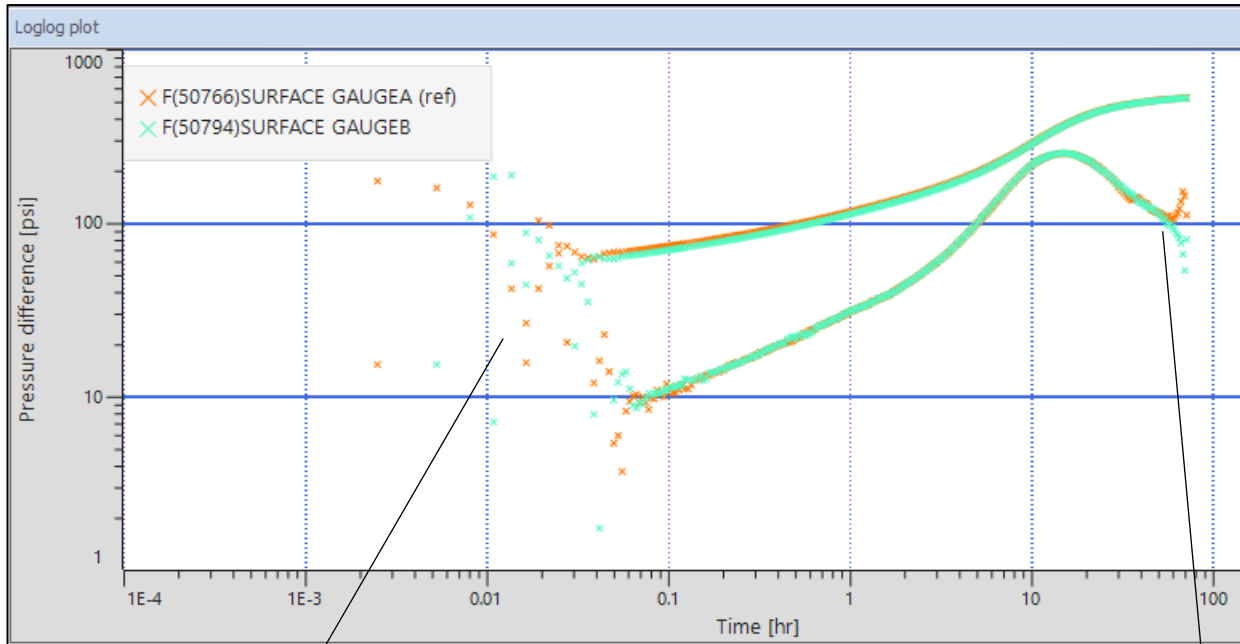


Figure 5: Early and late time pressure transient wellbore dynamics effect

The results described below show the estimation of **kh** and **skin** by the log-log, Semilog and test history match. The complete injection flow rate history was considered as per Table 1 (flow rate of 200.32 PM or ~9,157 STB/D). The main PTA results are summarized below:

Pressure Fall Off: Recorded for ~72 hours. The recorded pressure at the end of shut-in was BHP= 2,491.56 psig and WHP= ~202.76 psig.

The pressure and temperature gradients performed after the fall off period from 5,228 ft to well head are presented in Appendix 1 and the respective mean gradient values are presented in the Table 3, below.



Company: A &amp; M Engineering and Environmental Services, Inc.

County, State: Lincoln, Oklahoma

Reservoir: Arbuckle Formation

Well: MES#1- Water Injector

Table 3: PTA model result table

|  | <b>PTA Reservoir Model Results Downhole Gauges</b> |
|--|--|
| Fall Off test duration, hrs                            | 72   |
| Estimated BHP Injection Pressure before shut-in, psig  | 2,985.93   |
| Estimated BHP Pressure after 72 hours of shut-in, psig | 2,491.56   |
| Permeability- Thickness, k*h                           | 65,198 md-ft                                       |
| Permeability, k (assuming net pay of 300 ft)           | 217.33 md  |
| Total Skin, S  | -4.47  |
| Investigation Radius, Rinv                             | 3,743 ft   |
| Reservoir Pressure, P* [Horner Plot] @ 5,228 ft.       | 2,460.00 psig                                      |
| Injectivity Index (II)                                 | 12.89 STB/D/psi                                    |
| Storage, C, bbl/psi                                    | 0.519695   |
| Pressure gradient between 0 and 5,228 ft               | 0.438 psi/ft                                       |
| Temperature gradient between 0 and 5,228 ft            | 0.010 °F / ft                                      |

\*\* BHC: Bottom hole conditions



### B01 • Interpretation with downhole pressure gauge data (Gauge 50592)

The diagnostic Log-Log plot for the Falloff pressure transient test recorded with downhole gauges is presented in Figure 6. The pressure falloff derivative plot was used for early and middle times flow regime identification, the log-log scale shows three main flow regimes:

- At early times, Wellbore Storage (WBS) effects were observed until about 0.02 hr. Changing wellbore storage was applied. The obtained wellbore storage from the time match was 0.52 bbl/psi with delta t of 0.02 hr. The wellbore-dominated time is considered small for this type of test for a well which has been shut-in at the bottomhole.
- Pressure drop caused by near-wellbore damage was observed to be very short interval. The estimated total skin value was  $S = -4.47$ . This negative skin could be due to acid treatment or presence of possible linear flow.
- Possible Infinite Acting Radial Flow (IARF) was observed between 59 and 68 hrs. The formation properties, such as average drainage area pressure and permeability were estimated from this flow regime. Permeability-Thickness,  $k^*h = 65,198.00$  md-ft. Considering an effective injection thickness of 300 ft (from previous report dated on Nov 2023, Nov 2024 and Jun 2025) an effective horizontal permeability is estimated in the order of 217 md. Average drainage area pressure is estimated as 2,460psig and the fall off test investigation radius is 3,743 ft.
- The water injectivity Index is computed as 12.89 STB/D/psi.

Graphical analyses are presented in Figures 6, 7 and 8, including field data and history match analytical model.

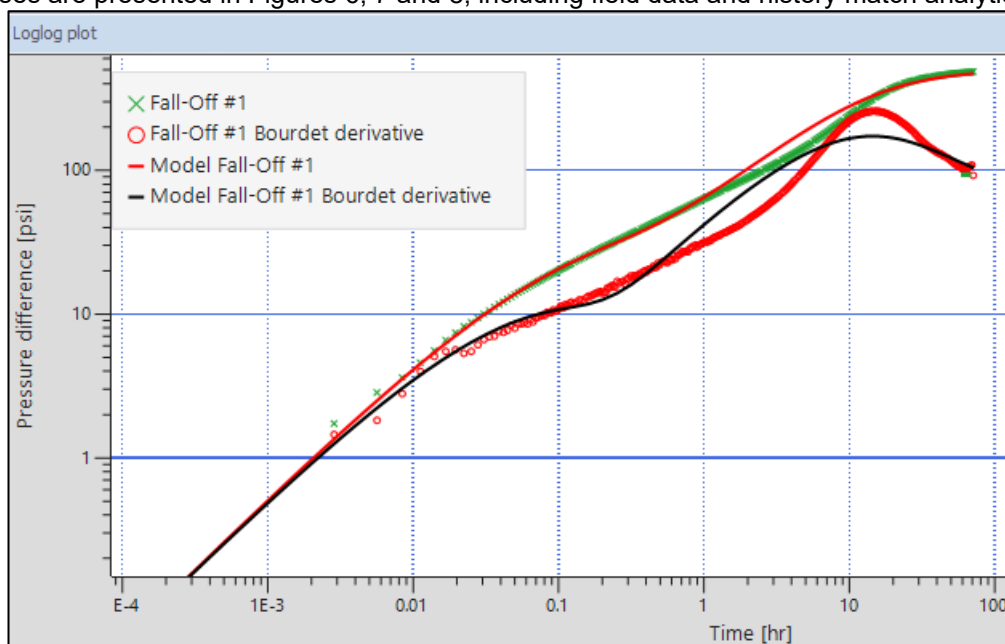


Figure 6: Log-Log Plot and PTA Model for pressure falloff with downhole gauge 50592 (Vertical, Radial Composite, Infinite)

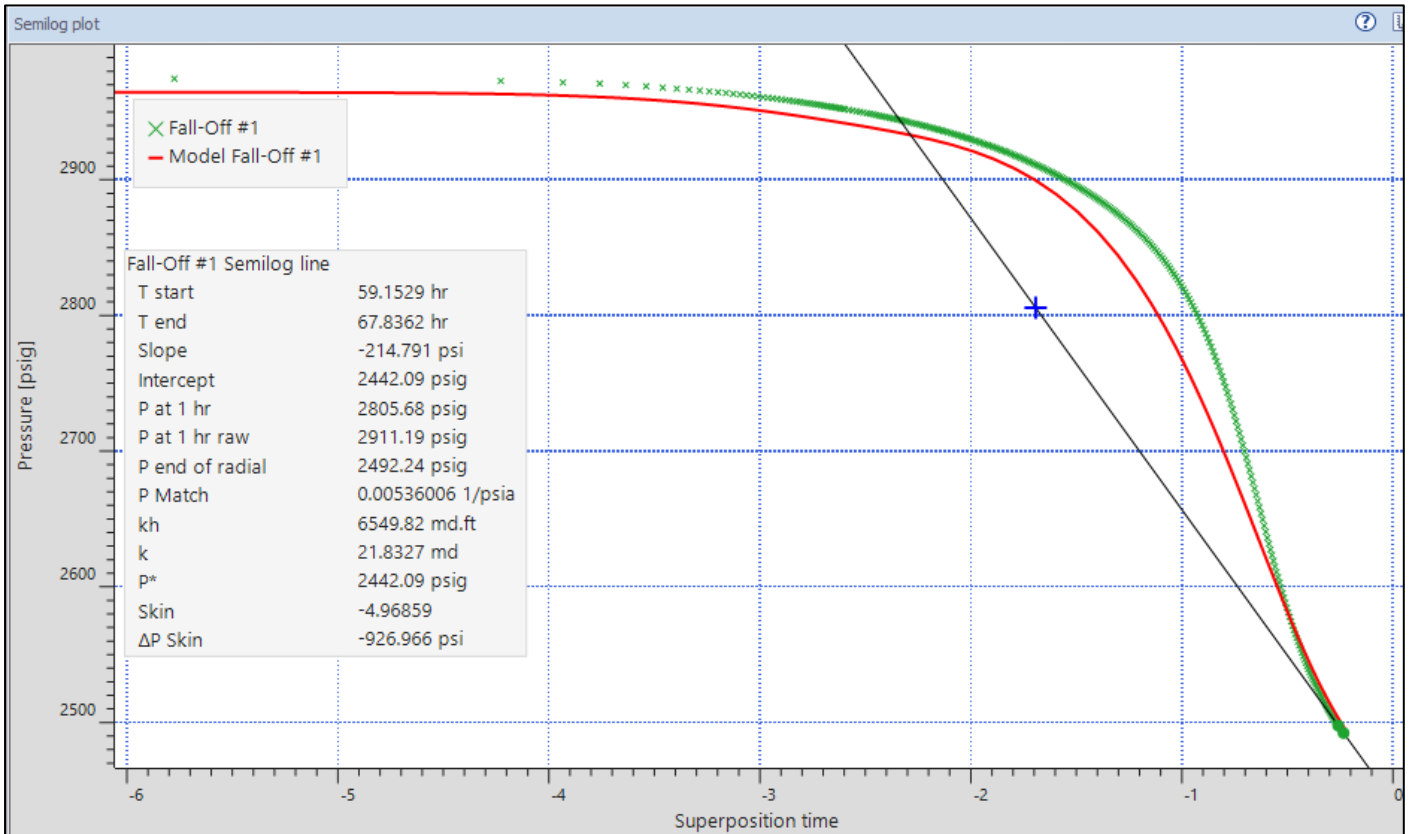


Figure 7: Semi log Diagnostic Plot and model for Pressure Falloff with downhole gauge 50592

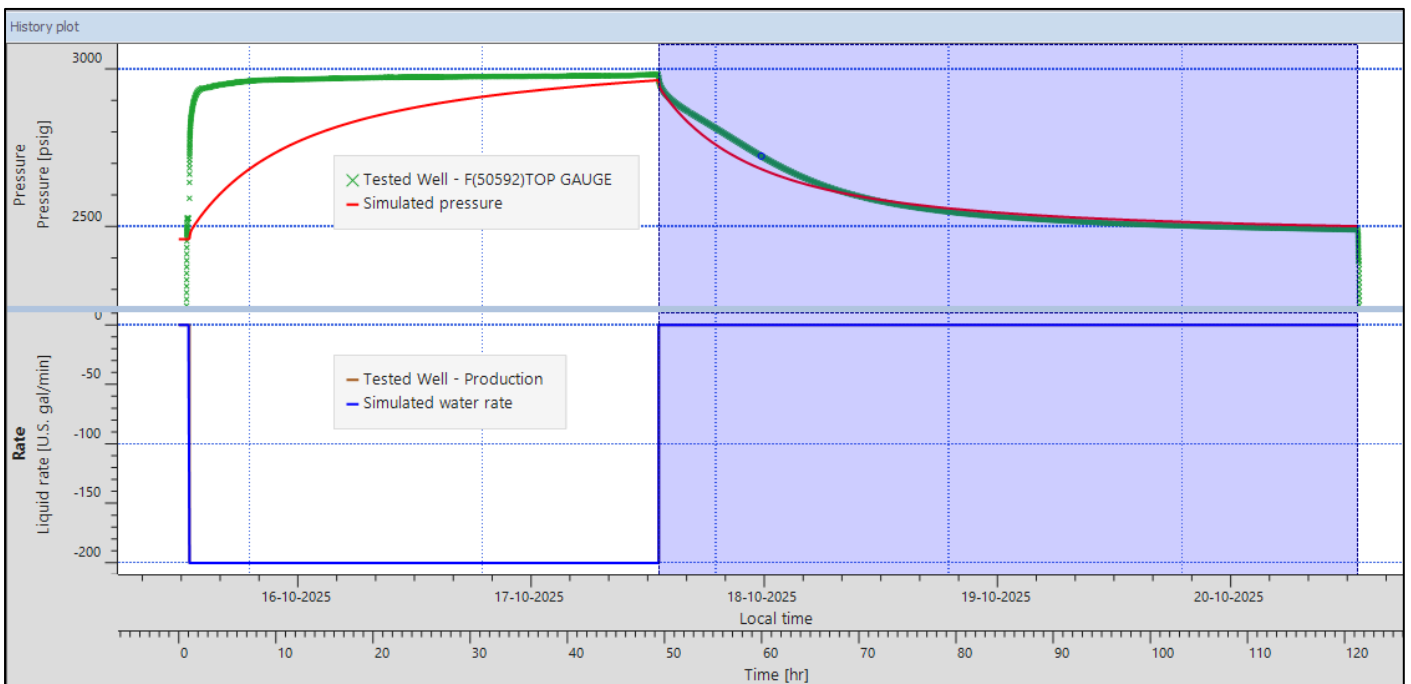


Figure 8: Top plot: Test bottomhole pressure data (green colour) and history match model (red colour), gauge 50592. Bottom plot: injection rate (gal/min).

Radial composite model is used for this fall off analysis: It is used to represent a reservoir with distinct zones of varying properties, often separated by a discontinuity. This model is particularly useful for simulating reservoirs where there have been changes in fluid properties, formation characteristics, or where stimulation or flooding operations have occurred.

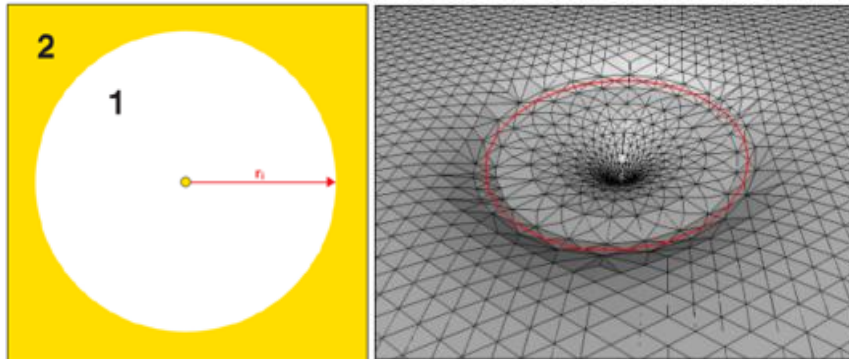


Figure 9. Radial Composite inner & outer compartments (left) with pressure profile (right)

Below table shows description of different parameters for Radial composite model.

| Permeability      | Fissure permeability   |
|-------------------|--|
| Composite radius  | Distance from the well to the interface  |
| Mobility ratio    | Ratio of inner zone to outer zone mobility: $M = \frac{(k/\mu)_{inner}}{(k/\mu)_{outer}}$                    |
| Diffusivity ratio | Ratio of inner zone to outer zone diffusivity: $D = \frac{(k/\phi\mu c_t)_{inner}}{(k/\phi\mu c_t)_{outer}}$ |

With the radial composite reservoir, the apparent mobility and diffusivity will move from the inner values (compartment 1) to the outer values (compartment 2), the final mobility will be that of compartment 2.



**B02 • Comparison of Log-Log plot with downhole pressure gauge data for Jun 2025 & Oct 2025**

As seen in figure below, IARF flow regime stabilization levels are quite different than Jun 2025 data. Some changes in radial composite model is observed.

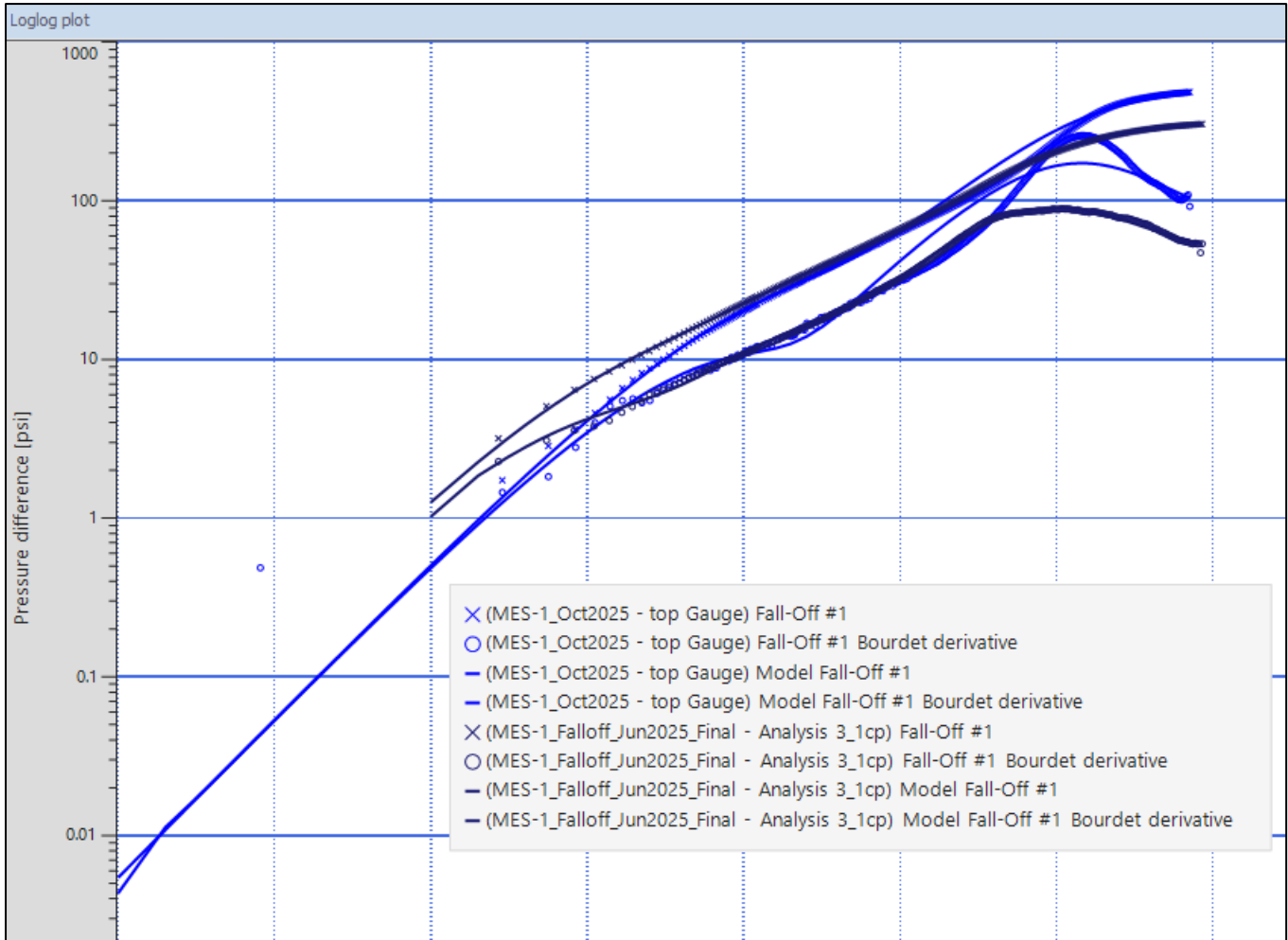


Figure 10: Comparison of Log-Log plot with downhole pressure gauge data for Jun 2025(black colour) & Oct 2025 (blue colour)



**C01 • Summary of PTA Inputs - Pressure Fall Off on Oct 2025**

| <b>Analysis summary</b>  |                              |
|--------------------------|------------------------------|
| Name                     | Falloff                      |
| Reference well           | MES#1                        |
| PVT ref. phase           | Water                        |
| PVT phases               | Water                        |
| Active prod.             | Injection                    |
| Open Hole Interval       | 5,173 – 6,804 ft             |
| Active press. datum      | BHP @ 5,228 ft               |
| Analysis type            | Standard                     |
| <b>Model description</b> |                              |
| Active model             | Analytical                   |
| Wellbore                 | Constant                     |
| Well                     | Vertical                     |
| Reservoir                | Radial Composite             |
| Boundary                 | Infinite                     |
| Other wells incl.?       | No                           |
| Rate dep. skin?          | No Data                      |
| Time dep. skin?          | No Data (no SRT)             |
| <b>Test parameters</b>   |                              |
| rw                       | 3.948 in                     |
| h                        | 300 ft                       |
| Rock compressibility     | 3.00E-06 psi <sup>-1</sup>   |
| Φ                        | 0.14                         |
| Top reservoir depth      | 5,173 ft                     |
| <b>Fluid Model</b>       |                              |
| Phase                    | Water                        |
| B                        | 1.0 B/STB                    |
| μ                        | 1.26 cp                      |
| ct                       | 5.24500E-6 psi <sup>-1</sup> |
| Sw                       | 1                            |
| Cw                       | 2.88162E-6 psi <sup>-1</sup> |
| co                       | 0 psi <sup>-1</sup>          |
| cg                       | 0 psi <sup>-1</sup>          |
| PVT model                | Water                        |
| Tref                     | 98 °F                        |
| Pref                     | 2,492 psig                   |
| Water gravity            | 1.008 sp. gr.                |
| Salinity                 | 10,000 ppm                   |
| Bw                       | Spivey                       |
| ρw                       | Internal                     |
| μw                       | Constant                     |



Pressure Transient Analysis      Pressure Fall Off Test, October 2025  
 Company: A & M Engineering and Environmental Services, Inc.  
 County, State: Lincoln, Oklahoma  
 Reservoir: Arbuckle Formation      Well: MES#1- Water Injector

**C02 • Comparison of PTA Results - Pressure Fall Off on Oct 2025, Jun 2025, Nov 2024 and Nov 2023**

| <b>Main Results</b>                     |                          |                       |                    |                    |
|---|--------------------------|-----------------------|--------------------|--------------------|
|   | <b>Oct-25</b>            | <b>Jun-25</b>         | <b>2024</b>        | <b>2023</b>        |
| Transmissibility, kh/μ                  | 51,744.5 md.ft/cp        | 69,000.00 md.ft/cp    | 76,210.30 md.ft/cp | 79,330.10 md.ft/cp |
| Permeability, k                         | 217.33                   | 230                   | 254.03 md          | 264.43 md          |
| Mobility, k/μ                           | 172.482                  | 230                   | 254.03 md/cp       | 264.43 md/cp       |
| Total skin                              | -4.47                    | -3.37                 | 19.76              | 16.59              |
| Initial Pressure, Pi                    | 2460                     | 2500                  | 2,518.63 psia      | 2,529.72 psia      |
| Wellbore Storage, C                     | 0.519695 bbl/psi         | 0.178278 bbl/psi      | 0.220537 bbl/psi   | 0.256143 bbl/psi   |
| <b>Model - Well &amp; wellbore</b>      |                          |                       |                    |                    |
| Wellbore model                          | Constant                 | Changing fair         | Changing fair      | Changing hegegan   |
| Final wellbore storage                  | 0.519695 bbl/psi         | 0.0776277 bbl/psi     | 1.26061 bbl/psi    | 0.61368 bbl/psi    |
| C[initial]/C[final]                     | NA                       | 2.29657               | 0.174945           | 0.417389           |
| Dt changing storage                     | NA                       | 0.601702 hr           | 0.0856841 hr       | 0.0822642 hr       |
| Well type                               | Vertical                 | Vertical              | Vertical           | Vertical           |
| Skin                                    | -4.47                    | -3.37                 | 19.76              | 16.59              |
| <b>Diagnostic</b>                       |                          |                       |                    |                    |
| Wellbore storage                        | Constant                 | Constant              | Constant           | Constant           |
| Well                                    | Finite radius            | Finite radius         | Finite radius      | Finite radius      |
| Reservoir                               | Radial composite         | Radial composite      | Homogeneous        | Homogeneous        |
| Boundary                                | Infinite                 | Infinite              | Infinite           | Infinite           |
| Reference rate                          | 200.32 gpm (9,157 STB/D) | 268 gpm (9,189 STB/D) | 6,548.57 STB/D     | 6,000.00 STB/D     |
| Extraction start time                   | 0 hr                     | 0 hr                  | 0 hr               | 0 hr               |
| P @ dt=0                                | 2974.59 psig             | 2,935.28 psig         | 2,873.09 psia      | 2,808.31 psia      |
| <b>Model - Reservoir &amp; boundary</b> |                          |                       |                    |                    |
| Reservoir type                          | Radial Composite         | Radial Composite      | Homogeneous        | Homogeneous        |
| Boundary type                           | Infinite                 | Infinite              | Infinite           | Infinite           |
| Initial pressure                        | 2,460.00 psig            | 2,500.00 psig         | 2,518.63 psia      | 2,529.72 psia      |
| Transmissivity                          | 65,198.0 md.ft/cp        | 69,000.0 md.ft/cp     | 76,210.30 md.ft    | 79,330.10 md.ft    |
| Permeability                            | 217.33 md                | 230 md                | 254.03 md          | 264.43 md          |
| Thickness                               | 300 ft                   | 300 ft                | 300 ft             | 300 ft             |
| Porosity                                | 0.14                     | 0.14                  | 0.14               | 0.14               |
| Composite Radius                        | 205.104 ft               | 232.502 ft            |                    |                    |
| Mobility Ratio                          | 6.61                     | 5.8                   |                    |                    |
| Diffusivity Ratio                       | 0.047                    | 0.12                  |                    |                    |
| Outer Permeability                      | 32.86 md                 | 39.65 md              |                    |                    |

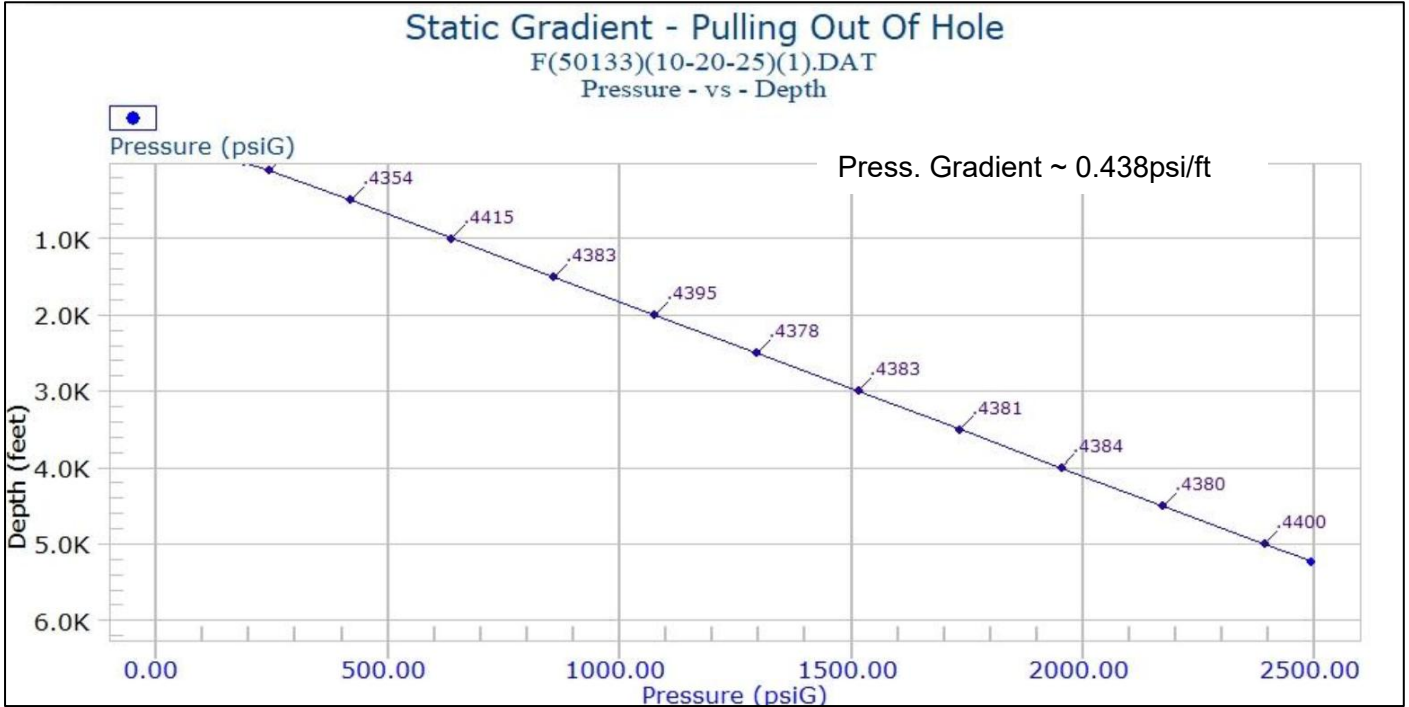


**Appendix 1:  
Static Pressure and Temperature  
Gradients**



**Appendix 1: Static Pressure and Temperature Gradients**

**Static Pressure Gradient – Pulling Out of Hole\***



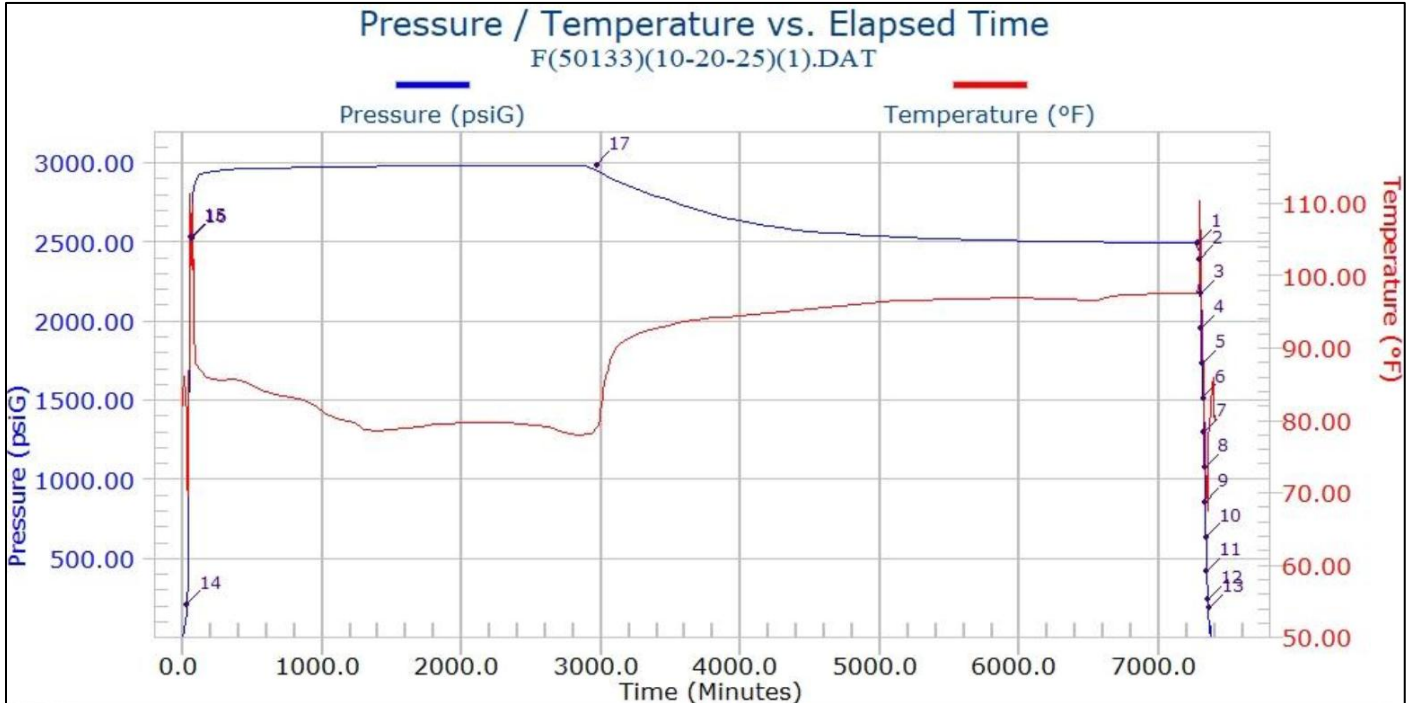
**Pressure & Temperature Gradient Table**

| Static Survey - Pulling Out Of The Hole |           |              |      |      |          |             |             |               |
|---|-----------|--------------|------|------|----------|-------------|-------------|---------------|
| Real Date                               | Real Time | Elapsed Time | WLM  | TVD  | Pressure | Gradient    | Temperature | Gradient      |
| MM/DD/YY                                | HH:MM:SS  | Minutes      | feet | feet | (psiG)   | (psiG/feet) | (deg. F)    | (deg. F/feet) |
| 10/20/25                                | 14:18:23  | 7356.36667   | 0    | 0    | 187.748  | .5605       | 78.185      | -.1112        |
| 10/20/25                                | 14:11:23  | 7349.36667   | 0    | 100  | 243.799  | .4369       | 67.066      | .0060         |
| 10/20/25                                | 14:05:53  | 7343.86667   | 0    | 500  | 418.576  | .4354       | 69.472      | .0050         |
| 10/20/25                                | 14:00:13  | 7338.20000   | 0    | 1000 | 636.255  | .4415       | 71.948      | .0066         |
| 10/20/25                                | 13:55:13  | 7333.20000   | 0    | 1500 | 857.026  | .4383       | 75.269      | .0081         |
| 10/20/25                                | 13:48:03  | 7326.03333   | 0    | 2000 | 1076.160 | .4395       | 79.308      | .0092         |
| 10/20/25                                | 13:43:33  | 7321.53333   | 0    | 2500 | 1295.930 | .4378       | 83.884      | .0090         |
| 10/20/25                                | 13:36:53  | 7314.86667   | 0    | 3000 | 1514.849 | .4383       | 88.375      | .0131         |
| 10/20/25                                | 13:30:13  | 7308.20000   | 0    | 3500 | 1733.975 | .4381       | 94.915      | .0115         |
| 10/20/25                                | 13:24:33  | 7302.53333   | 0    | 4000 | 1953.018 | .4384       | 100.668     | .0118         |
| 10/20/25                                | 13:17:53  | 7295.86667   | 0    | 4500 | 2172.224 | .4380       | 106.572     | .0091         |
| 10/20/25                                | 13:12:23  | 7290.36667   | 0    | 5000 | 2391.241 | .4400       | 111.146     | -.0596        |
| 10/20/25                                | 13:05:23  | 7283.36667   | 0    | 5228 | 2491.563 |             | 97.559      |               |

\* After LQC data acquired from Precision Wireline



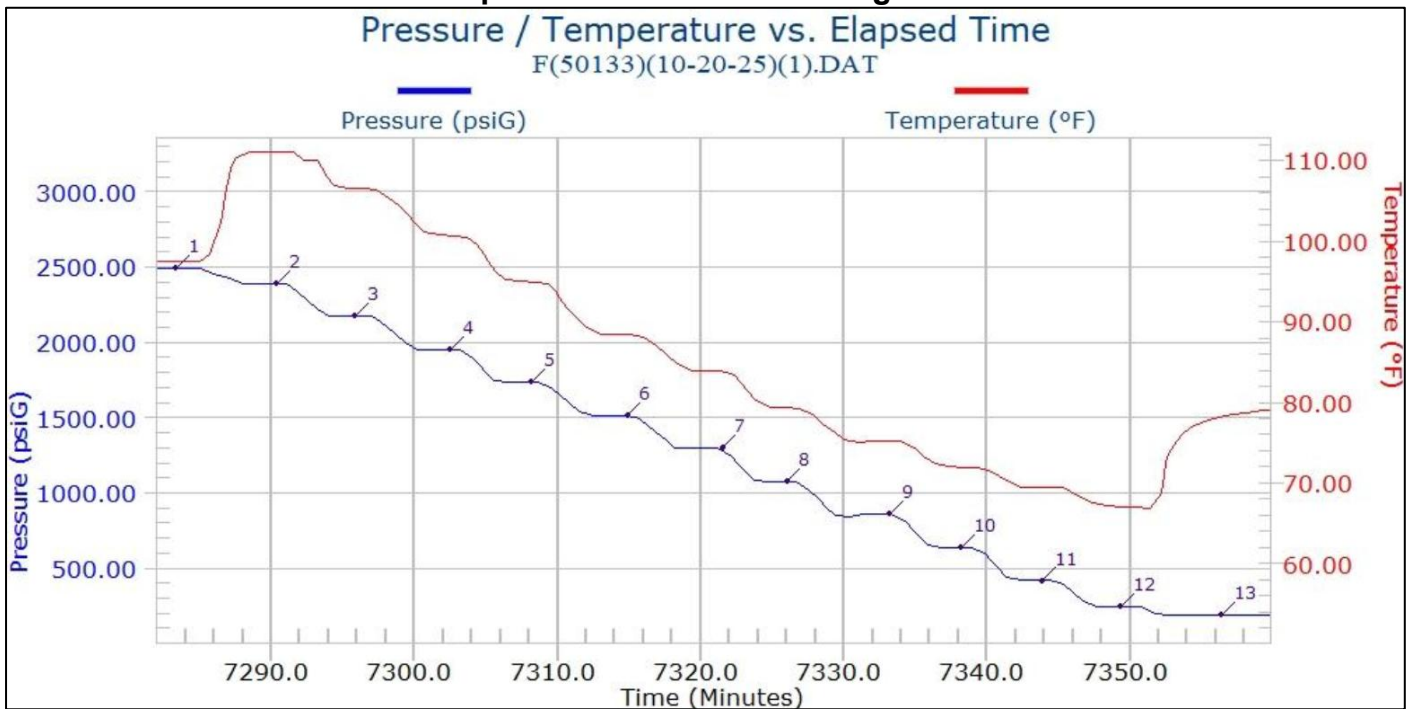
### Pressure / Temperature Records for Gradient Analysis\* (Gauge 50133 on 15/10/2025)



Pressure & Temperature records from bottom hole gauges 50133. Pressure: blue color and Temperature: red color.

\* After LQC data acquired from Precision Wireline

### Static Temperature Gradient – Pulling Out of Hole\*



\* After LQC data acquired from Precision Wireline

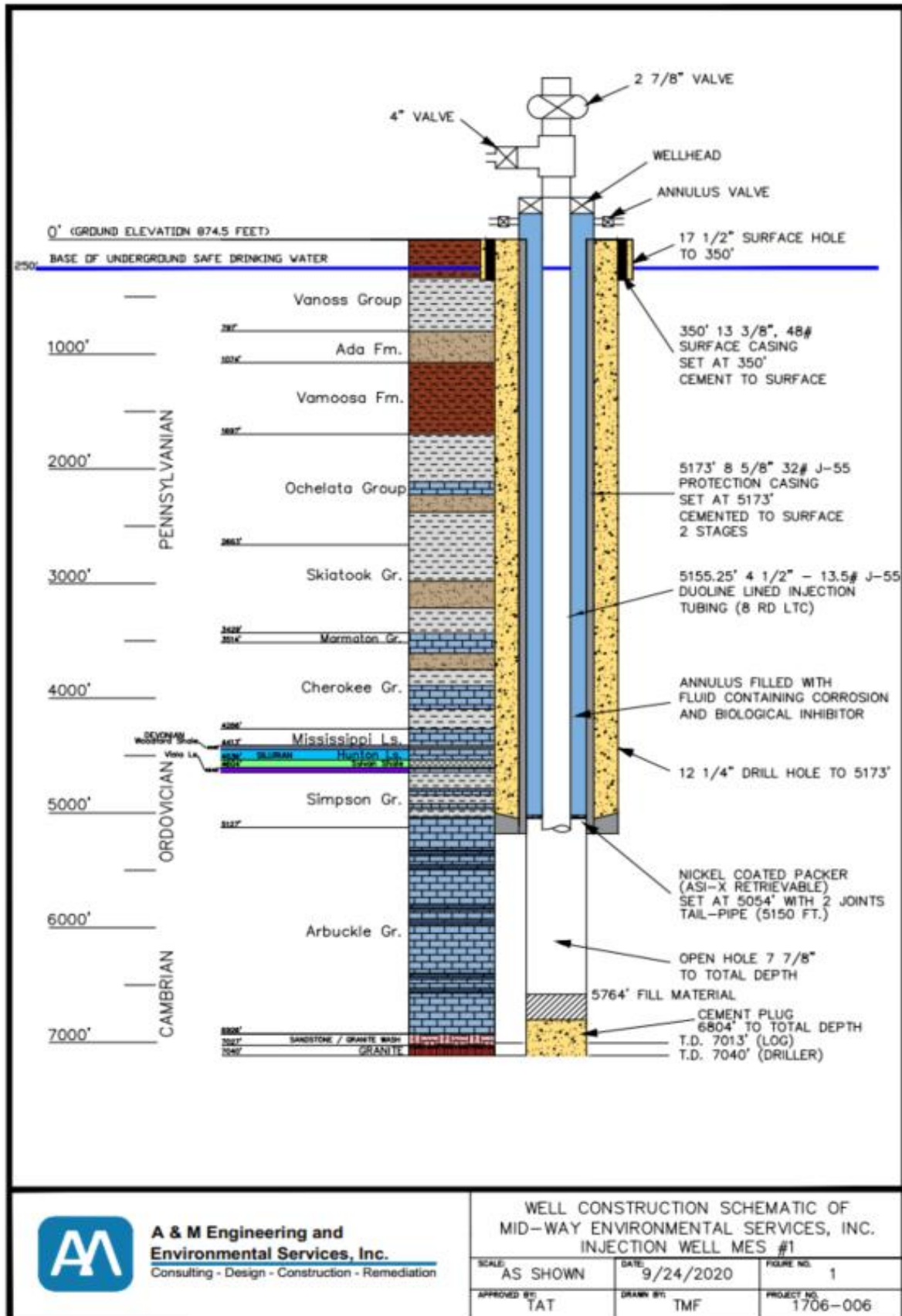


**Appendix 2**

**MES #1 Well Construction  
Revision 9-23-2020**



Appendix 2: MES # 1 Well Construction Revision Diagram (9-23-2020)



A & M Engineering and Environmental Services, Inc. Consulting - Design - Construction - Remediation

WELL CONSTRUCTION SCHEMATIC OF MID-WAY ENVIRONMENTAL SERVICES, INC. INJECTION WELL MES #1

|                  |                 |                      |
|------------------|-----------------|----------------------|
| SCALE: AS SHOWN  | DATE: 9/24/2020 | FIGURE NO. 1         |
| APPROVED BY: TAT | DRAWN BY: TMF   | PROJECT NO. 1706-006 |

\* Collar locator logs in June and November 2020 show the top of packer to be at 5138' and the EOT at 5234'. Note from Precision Wireline report on Nov 11, 2021.

**PRECISION WIRELINE**  
**Data Summary**



**MID-WAY ENVIRONMENTAL SERVICES INC.**

**BOTTOM HOLE PRESSURE**

**MES #1**

**10/15/2025 TO 10/20/2025**

**PRECISION WIRELINE**



PRECISION WIRELINE  
2402 S MONROE  
ENID OK 73701  
Phone: 580-233-0033 Fax:

### **Company Information**

Company Name: MID-WAY ENVIRONMENTAL SERVICES INC.  
Division:  
Representative: ORPHIUS MOHAMMAD  
Address: 10010 E. 16TH ST  
Address:  
Address:  
City: TULSA State: OK Zip: 74128-4813 Country: United States  
Phone Number: 918-665-6575  
Fax Number:  
E-mail Address: <mailto:omohammad@aandmengineering.com>

Note 1:  
Note 2:  
Note 3:

### **Well Information**

Well Name: MES #1  
Well Location:  
Field and Pool:  
Status (Oil, Water, Gas, Injection): INJECTION  
Perforation Intervals: 5173-6804' OPEN-HOLE  
MPP Intervals:  
Casing Size: 8-5/8" 32  
Tubing Size: 4-1/2" 13.5# J-55  
Plug Back Total Depth: 6804'  
Total Depth: 7013'

### **Test Information**

Type Of Test: BOTTOM HOLE PRESSURE  
Date Of Test: 10/15/2025  
Start Date / Time: Begin: 10/15/2025 / 09:00AM  
End: 10/20/2025 / 03:00PM  
Duration: 120 HOURS  
Gauge Depth: 5228'  
Gauge Position: BOTTOM  
Surface Casing Pressure:  
Surface Tubing Pressure:  
Maximum Downhole Pressure:  
Maximum Downhole Temperature:  
Data Filename: F(50133)(10-20-25)(1).DAT  
Job Number:  
Reported By: RICK PORRAS



**Gauge Information**

Serial Number: 50133  
Model Number: HT-1250  
Gauge Manufacturer: Micro-Smart Systems, Inc.  
Pressure Range:  
Battery Type Used: 4251560400  
Calibration Filename: G(50133)(10-13-25).CAL

**Gauge Setup Parameters**

Gauge Power-up Date / Time: 10/15/25 11:42:01  
Test Type Setting: 10 SEC SAMPLE  
Test Duration Setting: MAX

**Service Company Information**

Company Name: PRECISION WIRELINE  
Division:  
Representative: RICK PORRAS  
Address: 2402 S MONROE  
Address:  
Address:  
City: ENID State: OK Zip Code: 73701 Country: United States  
Phone Number: 580-233-0033  
Fax Number:  
E-mail Address: pwllc@swbell.net  
Note 1: WL TAG DEPTH= 5238' TEMPORARILY STUCK  
Note 2:  
Note 3: CORRELATED TO GL



## BOTTOM HOLE PRESSURE DATA SECTION



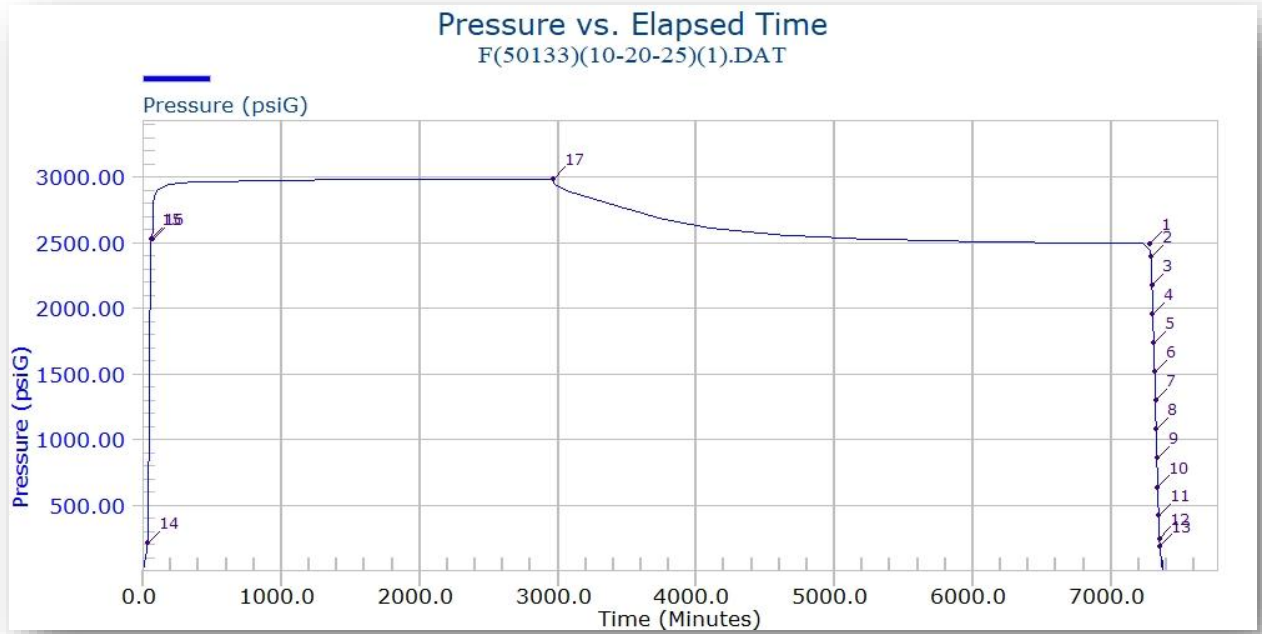
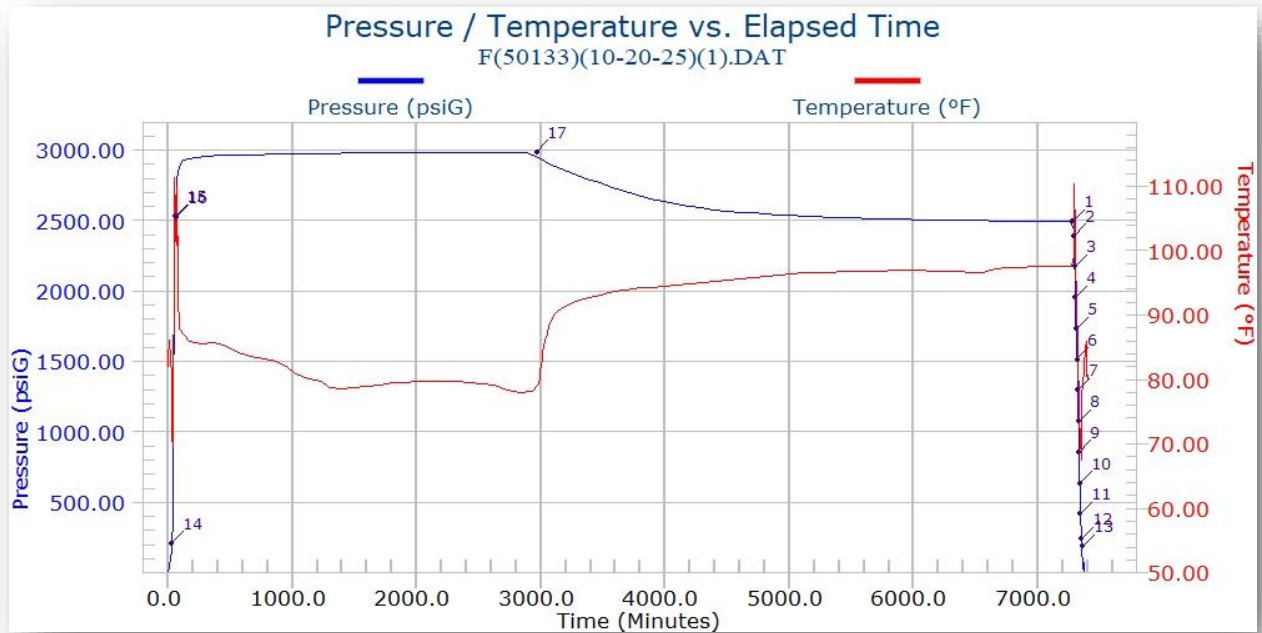
Filename: F(50133)(10-20-25)(1).DAT  
Power Up Date: 10/15/25  
Power Up Time: 11:42:01

## Event Summary

| Real Date<br>MM/DD/YY | Real Time<br>HH:MM:SS | Elapsed Time<br>Minutes | Pressure<br>psiG | Temperature<br>deg. F | Tag<br>Number | Comment                           |
|-----------------------|-----------------------|-------------------------|------------------|-----------------------|---------------|-----------------------------------|
| 10/15/25              | 12:14:03              | 32.03330                | 210.923          | 74.20                 | 14            | RIH - 0 -                         |
| 10/15/25              | 12:38:53              | 56.86670                | 2527.289         | 102.79                | 15            | 5228' GAUGE SET                   |
| 10/15/25              | 12:50:33              | 68.53330                | 2525.211         | 100.83                | 16            | BEGIN INJECTION                   |
| 10/17/25              | 13:07:43              | 2965.70000              | 2985.931         | 78.32                 | 17            | SHUT-IN BEGIN FALL-OFF            |
| 10/20/25              | 13:05:23              | 7283.36700              | 2491.563         | 97.56                 | 1             | POOH static stop @ 5228 feet TVD. |
| 10/20/25              | 13:12:23              | 7290.36700              | 2391.241         | 111.15                | 2             | POOH static stop @ 5000 feet TVD. |
| 10/20/25              | 13:17:53              | 7295.86700              | 2172.224         | 106.57                | 3             | POOH static stop @ 4500 feet TVD. |
| 10/20/25              | 13:24:33              | 7302.53300              | 1953.018         | 100.67                | 4             | POOH static stop @ 4000 feet TVD. |
| 10/20/25              | 13:30:13              | 7308.20000              | 1733.975         | 94.92                 | 5             | POOH static stop @ 3500 feet TVD. |
| 10/20/25              | 13:36:53              | 7314.86700              | 1514.849         | 88.38                 | 6             | POOH static stop @ 3000 feet TVD. |
| 10/20/25              | 13:43:33              | 7321.53300              | 1295.930         | 83.88                 | 7             | POOH static stop @ 2500 feet TVD. |
| 10/20/25              | 13:48:03              | 7326.03300              | 1076.160         | 79.31                 | 8             | POOH static stop @ 2000 feet TVD. |
| 10/20/25              | 13:55:13              | 7333.20000              | 857.026          | 75.27                 | 9             | POOH static stop @ 1500 feet TVD. |
| 10/20/25              | 14:00:13              | 7338.20000              | 636.255          | 71.95                 | 10            | POOH static stop @ 1000 feet TVD. |
| 10/20/25              | 14:05:53              | 7343.86700              | 418.576          | 69.47                 | 11            | POOH static stop @ 500 feet TVD.  |
| 10/20/25              | 14:11:23              | 7349.36700              | 243.799          | 67.07                 | 12            | POOH static stop @ 100 feet TVD.  |
| 10/20/25              | 14:18:23              | 7356.36700              | 187.748          | 78.19                 | 13            | POOH static stop @ 0 feet TVD.    |



# BOTTOM HOLE PLOTS (Gauge #50133) Start=10/15/2025 11:42:01





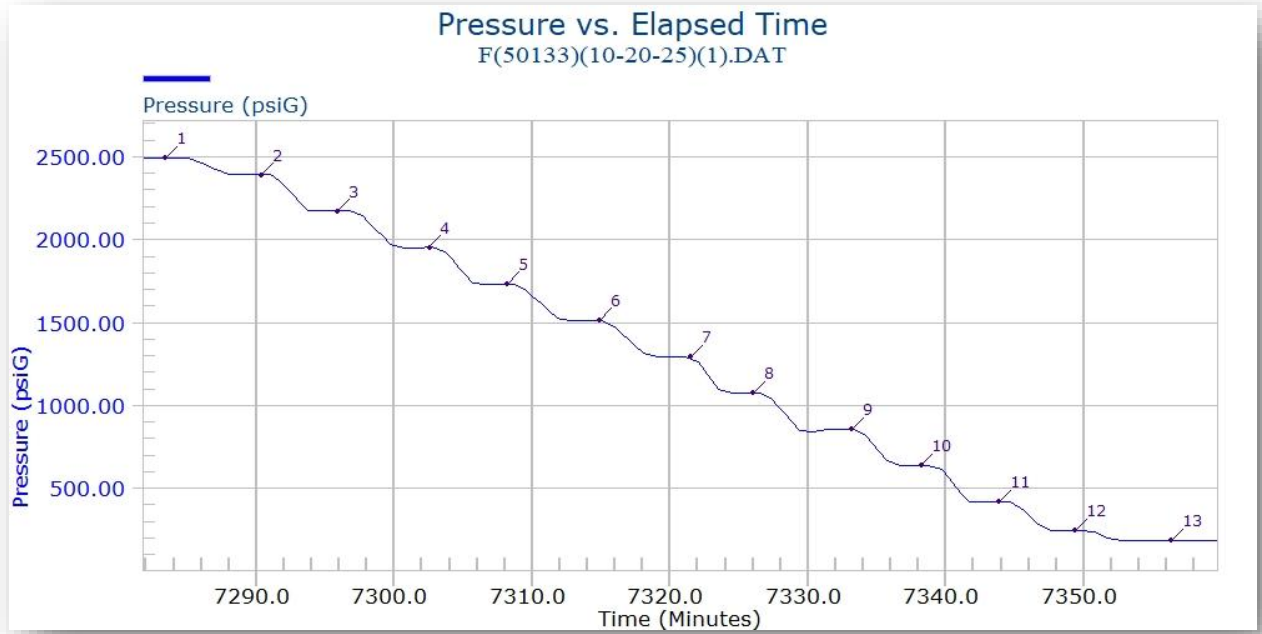
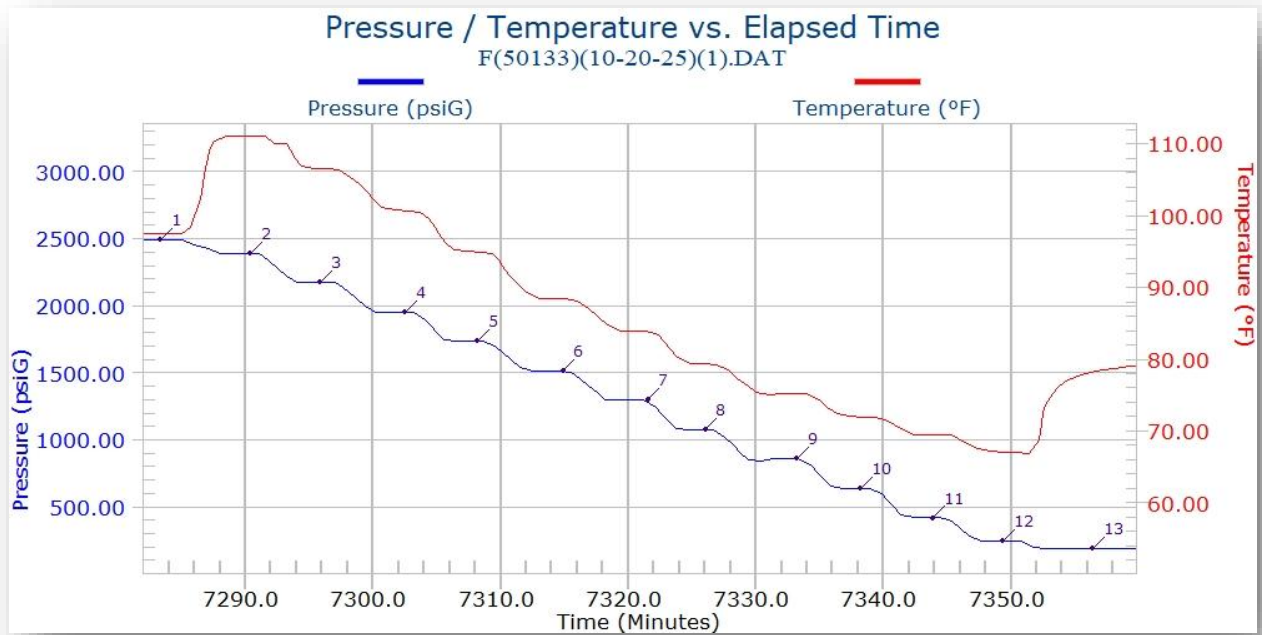
File Name: F(50133)(10-20-25)(1).DAT

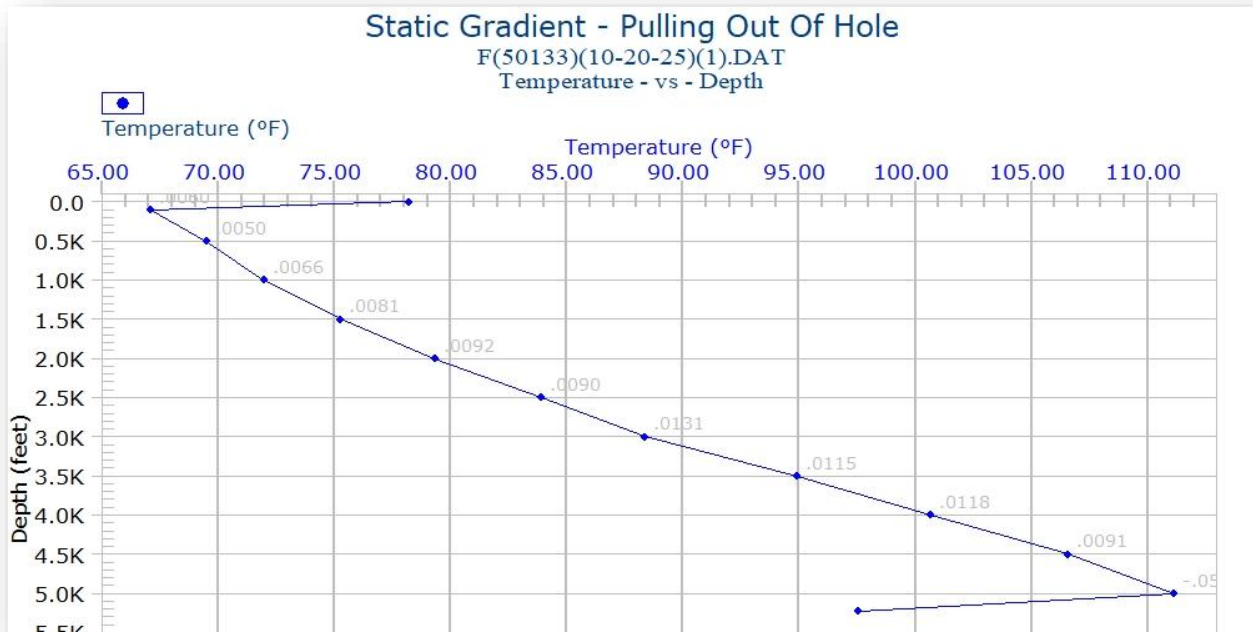
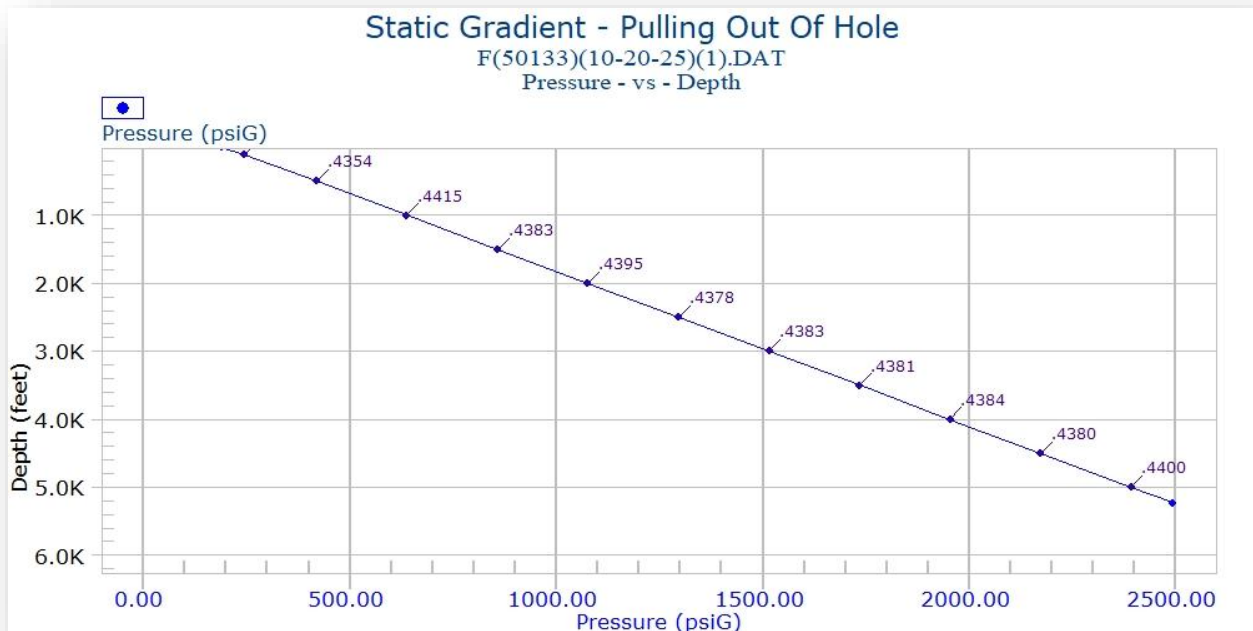
### Static Survey - Pulling Out Of The Hole

| Real Date<br>MM/DD/YY | Real Time<br>HH:MM:SS | Elapsed Time<br>Minutes | WLM<br>feet | TVD<br>feet | Pressure<br>(psiG) | Gradient<br>(psiG/feet) | Temperature<br>(deg. F) | Gradient<br>(deg. F/feet) |
|-----------------------|-----------------------|-------------------------|-------------|-------------|--------------------|-------------------------|-------------------------|---------------------------|
| 10/20/25              | 14:18:23              | 7356.36667              | 0           | 0           | 187.748            | .5605                   | 78.185                  | -.1112                    |
| 10/20/25              | 14:11:23              | 7349.36667              | 0           | 100         | 243.799            | .4369                   | 67.066                  | .0060                     |
| 10/20/25              | 14:05:53              | 7343.86667              | 0           | 500         | 418.576            | .4354                   | 69.472                  | .0050                     |
| 10/20/25              | 14:00:13              | 7338.20000              | 0           | 1000        | 636.255            | .4415                   | 71.948                  | .0066                     |
| 10/20/25              | 13:55:13              | 7333.20000              | 0           | 1500        | 857.026            | .4383                   | 75.269                  | .0081                     |
| 10/20/25              | 13:48:03              | 7326.03333              | 0           | 2000        | 1076.160           | .4395                   | 79.308                  | .0092                     |
| 10/20/25              | 13:43:33              | 7321.53333              | 0           | 2500        | 1295.930           | .4378                   | 83.884                  | .0090                     |
| 10/20/25              | 13:36:53              | 7314.86667              | 0           | 3000        | 1514.849           | .4383                   | 88.375                  | .0131                     |
| 10/20/25              | 13:30:13              | 7308.20000              | 0           | 3500        | 1733.975           | .4381                   | 94.915                  | .0115                     |
| 10/20/25              | 13:24:33              | 7302.53333              | 0           | 4000        | 1953.018           | .4384                   | 100.668                 | .0118                     |
| 10/20/25              | 13:17:53              | 7295.86667              | 0           | 4500        | 2172.224           | .4380                   | 106.572                 | .0091                     |
| 10/20/25              | 13:12:23              | 7290.36667              | 0           | 5000        | 2391.241           | .4400                   | 111.146                 | -.0596                    |
| 10/20/25              | 13:05:23              | 7283.36667              | 0           | 5228        | 2491.563           |                         | 97.559                  |                           |



# GRADIENT PLOTS (Bottom Gauge #50133)







# SURFACE DATA SECTION



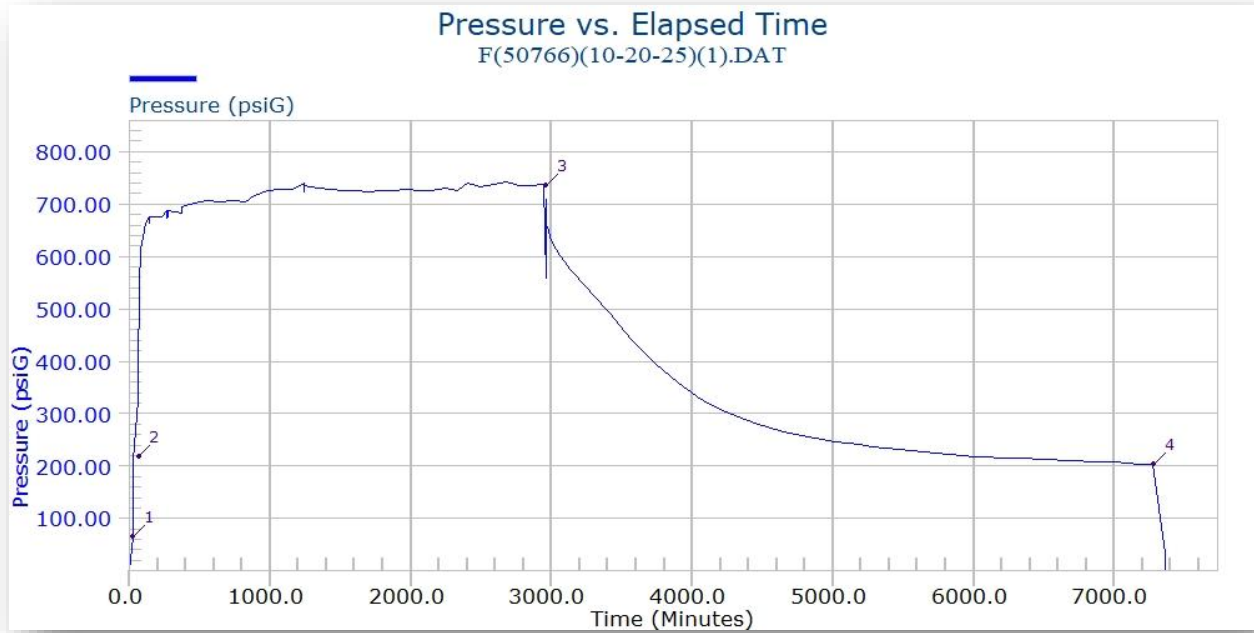
Filename: F(50766)(10-20-25)(1).DAT  
Power Up Date: 10/15/25  
Power Up Time: 11:46:00

## Event Summary

| Real Date<br>MM/DD/YY | Real Time<br>HH:MM:SS | Elapsed Time<br>Minutes | Pressure<br>psiG | Temperature<br>deg. F | Tag<br>Number | Comment                      |
|-----------------------|-----------------------|-------------------------|------------------|-----------------------|---------------|------------------------------|
| 10/15/25              | 12:07:52              | 21.86670                | 65.852           | 0.00                  | 1             | OPEN WELLHEAD SURFACE GAUGES |
| 10/15/25              | 12:50:22              | 64.36670                | 217.446          | 0.00                  | 2             | INJECTION PUMP START         |
| 10/17/25              | 13:07:32              | 2961.53300              | 736.027          | 0.00                  | 3             | INJECTION STOP BEGIN SHUT-IN |
| 10/20/25              | 13:05:02              | 7279.03300              | 202.757          | 0.00                  | 4             | END FALL-OFF TEST            |



SURFACE DATA (Gauge #50766) Start=10/15/2025 11:46:00



## **MES-1 2024 PFT REPORT**

Raw Data is not included in this appendix. Raw data is provided to DEQ with the stand alone PFT Report Submission





**A & M Engineering and  
Environmental Services, Inc.**  
Consulting - Design - Construction - Remediation

February 17, 2025

Ms. Hillary Young, P.E.  
Chief Engineer  
Land Protection Division  
Oklahoma Department of Environmental Quality  
P.O. Box 1677  
Oklahoma City, Oklahoma 73101

**RE: Annual (2024) Pressure Fall-off Test  
Mid-Way Environmental Services, Inc.  
Davenport, Oklahoma  
Permit Number IW-NH-41001-OP**

Dear Ms. Young:

Enclosed please find the results of the 2024 Pressure Fall-off Test (PFT) conducted at the above reference Mid-Way Environmental Services, Inc. (Mid-Way) commercial Class I Non-Hazardous injection well. The 2024 PFT was conducted during the period of November 13, 2024, through November 18, 2024. The PFT was conducted in accordance with the PFT Plan submitted to the Oklahoma Department of Environmental Quality (DEQ) in November 2024. The PFT Plan outlined the procedures to be followed in conducting the test and for procedures to be followed in gathering static temperature and pressure data to generate and compare the current pressure gradients with historic data.

The 2024 PFT utilized four (4) 5 kpsi rated gauges; two (2) for surface measurement recording and two (2) for bottom hole measurement recording. As DEQ suggested in the October 12, 2020 meeting, Mid-Way chose to use both surface and bottom hole gauge for 2024 PFT so that a comparison can be done between surface and bottom hole gauge for the PFT at Mid-Way. Pressure transient data interpretation and curve matching was performed by a Senior Reservoir Engineer with Schlumberger. A copy of the Schlumberger Pressure Transient Test Interpretation Report (Report) is included for review. The bottom hole gauge Pressure Transient Analysis can be found in Table 3 and Section B of the Report. The static temperature and pressure readings and gradient calculations are also included in Appendix 2 of the Report. Attached Table 2 presents a comparison of the historical formation temperature, pressure, and gradient information.

To allow the well to stabilize and reach equilibrium, the injection well had not been operated for period of approximately 5 days (120 hours) prior to initiating the PFT. Personnel from Precision Wireline, LLC of Enid, Oklahoma calibrated and connected the surface recording gauges directly to a port on the injection well and set the bottom hole gauges at a depth of 5,340 feet. The facility's horizontally mounted centrifugal pump was used as the primary pump for injection and the average pumping rate calculated for the injection period was 191 gallons per minute. A total quantity of 562,120 gallons of water was injected during the test. For the PFT conducted on November 13<sup>th</sup> through 18<sup>th</sup> of 2024, the injection (pumping) period was 49 hours 3 minutes, and the monitored recovery (fall-off) period was 72 hours.

After the 72-hour recovery portion of the test, the bottom hole gauges were used to record static temperature and pressure readings at every 500 feet interval as the tool was retrieved; with a final reading at a depth of 100 feet and 0 feet from the surface.

At the completion of the test, the surface and bottom hole gauges were retrieved by Precision Wireline, LLC personnel and the data recorded during the test was forwarded to a Senior Reservoir Engineer with Schlumberger for pressure transient data interpretation and curve matching.

Parameters utilized by Schlumberger in the pressure transient analysis included:

Formation thickness (h) = 300'

Porosity ( $\Phi$ ) = 14.0%

Water Viscosity ( $\mu_w$ ) = 1 cp

Radius of the well (r) = 0.329'

Q = 6,549 Bbl/Day

Compressibility (Ct) = 3E-6

Type curve matching was utilized by Schlumberger in analysis of the pressure transient data. Based on "best fit" to type curves, the data recorded during the 2024 PFT best fits a Radial Composite Reservoir Model, indicating different flow regimes over time. The model (chosen based on the type curves) is the same as the one used during the 2023 test interpretation.

In the Radial Composite Model, the well is at the center of a circular homogeneous zone, communicating with an infinite homogeneous reservoir. The radius of investigation based on the 2023 results is calculated to be 4,269 feet.

Calculated formation parameters based on the Radial Composite Model indicate a permeability (k) of 254.03 millidarcys (md) with a 19.76 skin factor. The skin value is similar to last year's test result (In 2023, the skin value was 16.59).

The bottom hole pressure at the end of the fall off period was 2,507.588 psi, which is similar to historic pressures estimated for the well. A Cartesian plot of recorded data (pressure vs. time) is presented in Figure 1 and 2 of the attached Schlumberger Pressure Transient Test Interpretation Report. A summary of the bottom hole pressures estimated over the last several years is presented in the table below:

**Table 1:** Estimated Bottom Hole Pressure from the Measured Surface Pressure

| Calendar Year | Estimated Bottom Hole Pressure (psi) |
|---------------|--------------------------------------|
| 2010          | 2,495                                |
| 2015          | 2,537                                |
| 2016          | 2,649                                |
| 2017          | 2,574                                |
| 2018          | 2,509                                |
| 2019          | 1,869                                |
| 2020          | 2,672                                |
| 2021          | 2,529                                |
| 2022          | 2,536.7*                             |
| 2023          | 2,529.27*                            |
| 2024          | 2507.59*                             |

\*Bottom hole pressure estimated at depth of 5,340 below ground surface

In Figure 5 of the attached Report, spikes in the derivative late times are associated with temperature variations.

Attached Table 2 presents a comparison of the historical formation pressure, temperature, and gradient information. The data indicates no apparent changes to bottom-hole pressure or temperature because of the injection activities. Please note that the pressure reading recorded near the top of the well head was comparable to the well head pressure observed on the facility's continuous recording equipment prior to initiating the static survey.

If you have any questions on this matter, or if you need additional information, please do not hesitate to contact me at 918-665-6575.

Ms. Hillary Young, P.E.

February 17, 2025

Page -4-

Sincerely,

A & M Engineering and Environmental Services, Inc.



Orphius Mohammad, PhD, P.E.

Senior Environmental Engineer

- Enclosures:
- (i) Table 2: Historical Static formation Pressure, Temperature, and Gradient information
  - (ii) Schlumberger Pressure Transient Analysis Report
  - (iii) Precision Wireline Data Summary
  - (iv) Raw Pressure Data [Bottom Hole Gauge]
  - (v) Raw Pressure Data [Surface Gauge]

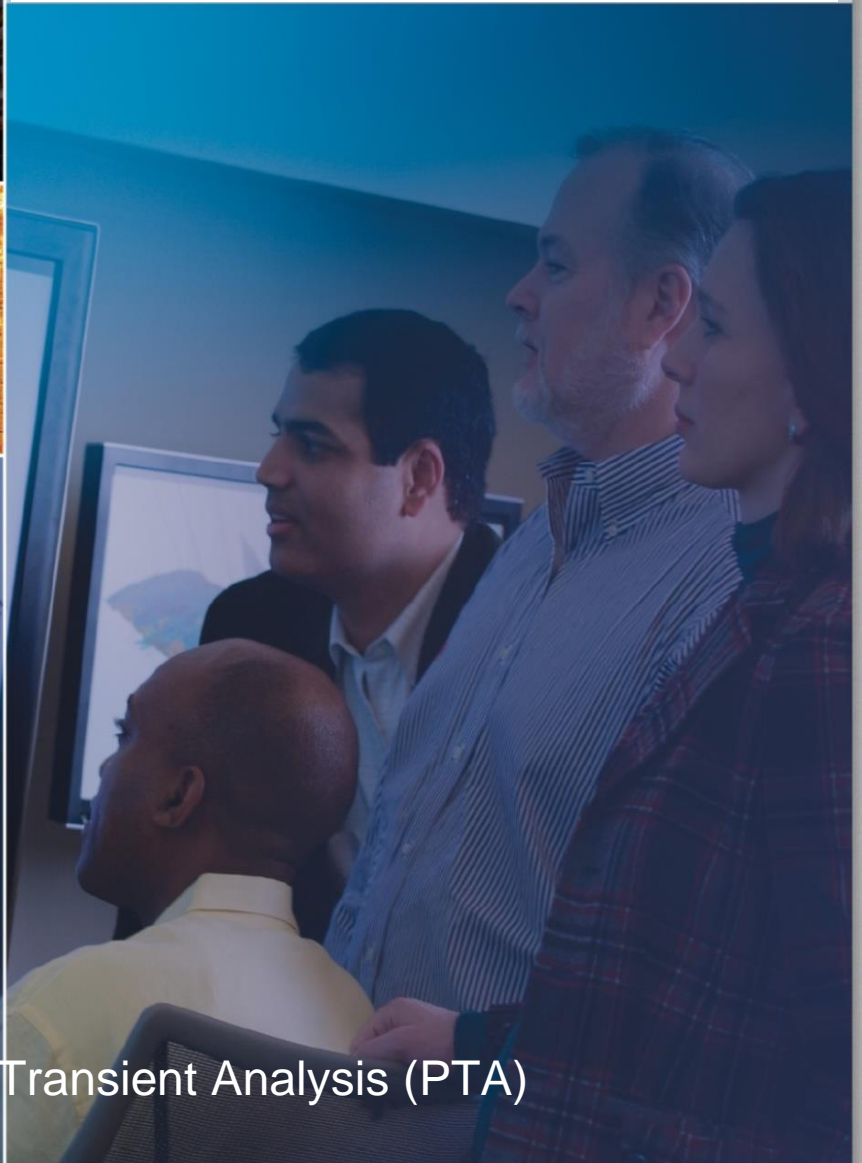
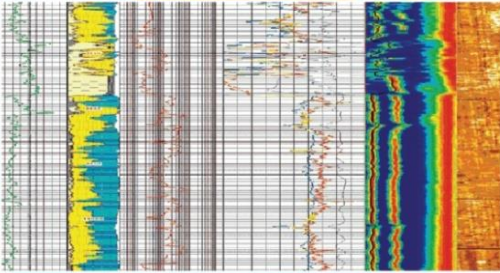
Cc: Mr. John Mitsdarfer, DEQ  
Ms. Brigette Haley, DEQ  
Mr. Tolga Ertugrul, P.E., President, Mid-Way

**Table 2:**  
**Historical Static formation Pressure, Temperature, and Gradient information**



# **SCHLUMBERGER PRESSURE TRANSIENT ANALYSIS REPORT**

# Digital Subsurface Solutions Analysis & Interpretation Services



## Pressure Transient Analysis (PTA)

Company : A & M Engineering and Environmental Services, Inc.  
Reservoir : Arbuckle Formation  
Well : MES#1  
JOB : Pressure Transient Analysis Fall Off Test  
Job date : 13<sup>th</sup> to 18<sup>th</sup> November 2024  
Report date : 4<sup>th</sup> February 2025  
PTE : Saunil Rajput, Ramy Ahmed  
Job reference : DS-2024-26423





Company: A & M Engineering and Environmental Services, Inc.

County, State: Lincoln, Oklahoma

Reservoir: Arbuckle Formation

Well: MES#1

## **A & M Engineering and Environmental Services, Inc.**

### **MES#1**

#### **Arbuckle Formation**

(Open Hole Interval: 5,173 ft. – 6,804 ft)

Open Hole

#### **Pressure Transient Analysis**

#### **Fall Off Test**

Surface and Bottomhole Pressure Monitoring

Interpreters:

Ramy Ahmed: Reservoir Engineering Team Leader

Saunil Rajput: Senior Reservoir Engineer

rahmed7@slb.com

+1 713 689 1219



## Contents

|  |    |
|--|----|
| A01 • Main results.....  | 4  |
| B01 • Interpretation with downhole pressure gauge data (Gauge 50766) .....                               | 8  |
| B02 • Spherical flow identification on Log-Log plot with downhole pressure gauge data (Gauge 50766) .... | 10 |
| B03 • Comparison of Log-Log plot with downhole pressure gauge data for 2023 & 2024 .....                 | 10 |
| C01 • Summary of PTA Inputs - Pressure Fall Off on Nov. 2024 .....                                       | 11 |
| C02 • Comparison of PTA Results - Pressure Fall Off on Nov. 2024 and Nov. 2023 .....                     | 12 |
| Appendix 1: Wellhead pressure Transform Fall-off Analysis. ....  | 14 |
| Appendix 2: Static Pressure and Temperature Gradients .....  | 17 |
| Appendix 3: MES # 1 Well Construction Revision Diagram (9-23-2020) .....                                 | 20 |



**DISCLAIMER**

SAVE FOR THAT EXPRESSLY STATED IN THE AGREEMENT, SLB MAKES NO WARRANTIES, EITHER EXPRESS OR IMPLIED, STATUTORY OR OTHERWISE IN CONNECTION WITH ITS PERFORMANCE OF THE SERVICES OR ANY DELIVERABLES HEREUNDER, OR THE USE OF THE SERVICES OR DELIVERABLES BY CUSTOMER. SLB DOES NOT GUARANTEE ANY RESULTS. CUSTOMER HAS FULL RESPONSIBILITY FOR ITS USE OF THE DELIVERABLES AND ANY INTERPRETATIONS, RECOMMENDATIONS AND/OR DESCRIPTIONS PROVIDED BY SLB HEREUNDER. ALL INTERPRETATIONS, RECOMMENDATIONS AND/OR RESERVOIR DESCRIPTIONS ARE OPINIONS BASED ON INFERENCES FROM MEASUREMENTS AND EMPIRICAL RELATIONSHIPS AND ON ASSUMPTIONS, WHICH INFERENCES AND ASSUMPTIONS ARE NOT INFALLIBLE, AND WITH RESPECT TO WHICH COMPETENT SPECIALISTS MAY DIFFER. IN ADDITION, SUCH INTERPRETATIONS, RECOMMENDATIONS AND/OR RESERVOIR DESCRIPTIONS MAY INVOLVE THE OPINION AND JUDGMENT OF CUSTOMER AND/OR INFORMATION AND DATA FURNISHED BY CUSTOMER. SLB CANNOT AND DOES NOT WARRANT THE ACCURACY, CORRECTNESS OR COMPLETENESS OF ANY INTERPRETATION, RECOMMENDATION AND/OR RESERVOIR DESCRIPTION. UNDER NO CIRCUMSTANCES SHOULD ANY INTERPRETATION, RECOMMENDATION AND/OR RESERVOIR DESCRIPTION BE RELIED UPON AS THE SOLE BASIS FOR ANY DRILLING, COMPLETION, WELL TREATMENT, PRODUCTION OR OTHER FINANCIAL DECISION, OR ANY PROCEDURE INVOLVING ANY RISK TO THE SAFETY OF ANY DRILLING VENTURE, DRILLING RIG OR ITS CREW OR ANY OTHER INDIVIDUAL. CUSTOMER HAS FULL RESPONSIBILITY FOR ALL SUCH DECISIONS AND FOR ALL DECISIONS CONCERNING OTHER PROCEDURES RELATING TO THE DRILLING OR PRODUCTION

**A01 • Main results**

The pressure recorders were located at the surface to record the Well Head (Tubing) Pressure and at the bottom of the well at 5,340 ft to assess the near wellbore conditions and obtain reservoir parameters for the Arbuckle formation over the open hole interval 5,173 ft.-6,804 ft. These two pressure records were used to evaluate the formation permeability, skin factor and formation pressure.

It is also part of this analysis to compare the formation evaluation results from each pressure record, surface, and bottom hole. It is well known that surface pressure records are affected by wellbore friction during the injection phase and storage during the shut-in phase. Surface pressure gauges data was observed to be noisy. Wellhead pressures were transformed to bottomhole conditions for pressure transient analysis. It is observed that due to noise, radial flow regime is not clearly observed for WHP transform data. Due to this, a perfect match is not obtained with the data, it seems to be the best possible outcome with the current data. Bottomhole pressure transient data provided more reasonable match, as radial flow regime was observed. Also, spherical flow regime was clearly observed, indicating flow into wellbore exhibits limited entry behaviour. Vertical well limited entry model was presented here as part of appendix.

The testing procedure consisted of two main events:

\* Water Injection: Recorded for ~48 hours (Average surface injection flowrate: 191 gal/min.

(~6,549 bbl/d). The recorded injection pressure prior to shut-in was BHP= 2,873.09 Psia and WHP= 587.5 psia.

\* Pressure Fall Off: Recorded for ~ 71 hours. The recorded injection pressure at the end of shut-in was BHP= 2,522.28 psia and WHP= ~165.1 psia.

The injection and pressure fall off test procedure consisted of the following events:

*Table 1: Events Summary at Bottom Hole and Surface*

| Real Date<br>MM/DD/YY | Real Time<br>HH:MM:SS | Elapsed Time<br>Minutes | Pressure<br>psiG | Temperature<br>deg. F | Tag<br>Number | Comment                           |
|-----------------------|-----------------------|-------------------------|------------------|-----------------------|---------------|-----------------------------------|
| 11/13/24              | 10:54:02              | 26.86670                | 157.724          | 70.43                 | 14            | RIH -0-                           |
| 11/13/24              | 11:17:02              | 49.86670                | 2512.254         | 86.35                 | 15            | 5340' GAUGE SET                   |
| 11/13/24              | 11:30:12              | 63.03330                | 2511.677         | 86.22                 | 16            | BEGIN INJECTION                   |
| 11/15/24              | 11:30:12              | 2943.03300              | 2858.412         | 71.01                 | 17            | SHUT-IN BEGIN FALL-OFF            |
| 11/18/24              | 10:19:32              | 7192.36700              | 2507.588         | 87.57                 | 1             | POOH static stop @ 5340 feet TVD. |
| 11/18/24              | 10:28:32              | 7201.36700              | 2352.281         | 113.17                | 2             | POOH static stop @ 5000 feet TVD. |
| 11/18/24              | 10:37:42              | 7210.53300              | 2132.756         | 108.09                | 3             | POOH static stop @ 4500 feet TVD. |
| 11/18/24              | 10:44:22              | 7217.20000              | 1912.913         | 101.61                | 4             | POOH static stop @ 4000 feet TVD. |
| 11/18/24              | 10:52:22              | 7225.20000              | 1692.948         | 95.75                 | 5             | POOH static stop @ 3500 feet TVD. |
| 11/18/24              | 10:58:12              | 7231.03300              | 1472.809         | 88.99                 | 6             | POOH static stop @ 3000 feet TVD. |
| 11/18/24              | 11:04:02              | 7236.86700              | 1252.629         | 84.40                 | 7             | POOH static stop @ 2500 feet TVD. |
| 11/18/24              | 11:10:02              | 7242.86700              | 1032.575         | 79.68                 | 8             | POOH static stop @ 2000 feet TVD. |
| 11/18/24              | 11:15:42              | 7248.53300              | 812.332          | 75.87                 | 9             | POOH static stop @ 1500 feet TVD. |
| 11/18/24              | 11:21:42              | 7254.53300              | 592.465          | 72.40                 | 10            | POOH static stop @ 1000 feet TVD. |
| 11/18/24              | 11:28:52              | 7261.70000              | 372.225          | 69.38                 | 11            | POOH static stop @ 500 feet TVD.  |
| 11/18/24              | 11:35:52              | 7268.70000              | 195.581          | 67.08                 | 12            | POOH static stop @ 100 feet TVD.  |
| 11/18/24              | 11:41:22              | 7274.20000              | 147.270          | 65.36                 | 13            | POOH static stop @ 0 feet TVD.    |

*Table 2 Injection and pressure fall off test events. Upper Table: Downhole event, and Lower Table: Surface Events*

| Real Date<br>MM/DD/YY | Real Time<br>HH:MM:SS | Elapsed Time<br>Minutes | Pressure<br>psiG | Temperature<br>deg. F | Tag<br>Number | Comment                      |
|-----------------------|-----------------------|-------------------------|------------------|-----------------------|---------------|------------------------------|
| 11/13/24              | 10:47:42              | 25.53330                | 151.644          | 68.65                 | 1             | OPEN WELLHEAD SURFACE GAUGE  |
| 11/13/24              | 11:30:12              | 68.03330                | 157.686          | 67.73                 | 2             | INJECTION PUMP START         |
| 11/15/24              | 11:29:15              | 2947.08300              | 572.824          | 75.84                 | 3             | INJECTION STOP BEGIN SHUT-IN |
| 11/18/24              | 10:03:55              | 7181.75000              | 150.460          | 62.58                 | 4             | END FALL-OFF TEST            |



- 1. F50766: Bottom hole pressure Top - gauge 50766
- 2. F50781: Bottom hole pressure Bottom - gauge 50781
- 3. F50794: Surface pressure WHP – gauge 50794

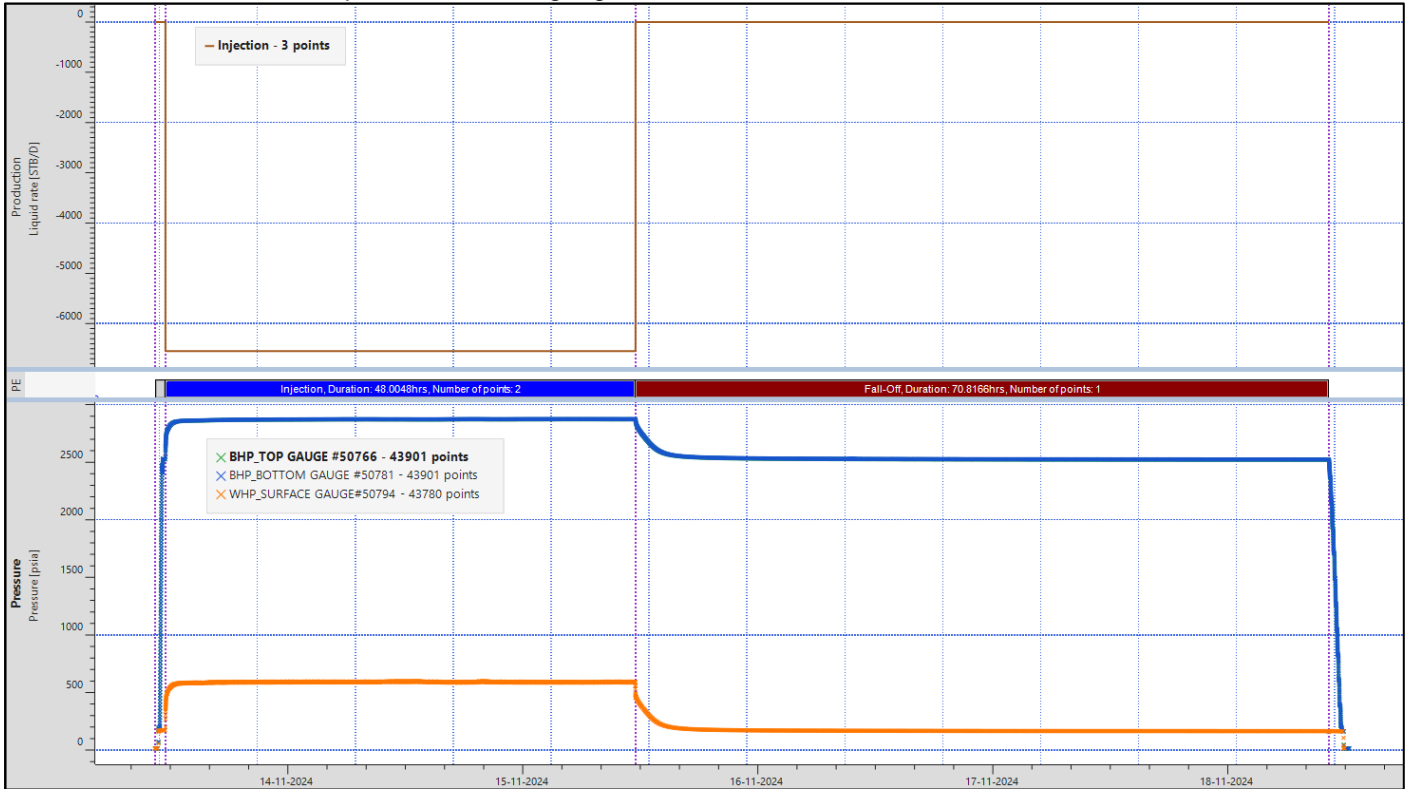


Figure 1: Cartesian Plot for Injection flow rate and Pressure Falloff for gauges #50766 and 50781 @ 5,340 ft and well head gauge #50794 (WHP: orange color, BHP: blue color, Injection rate: Brown color)

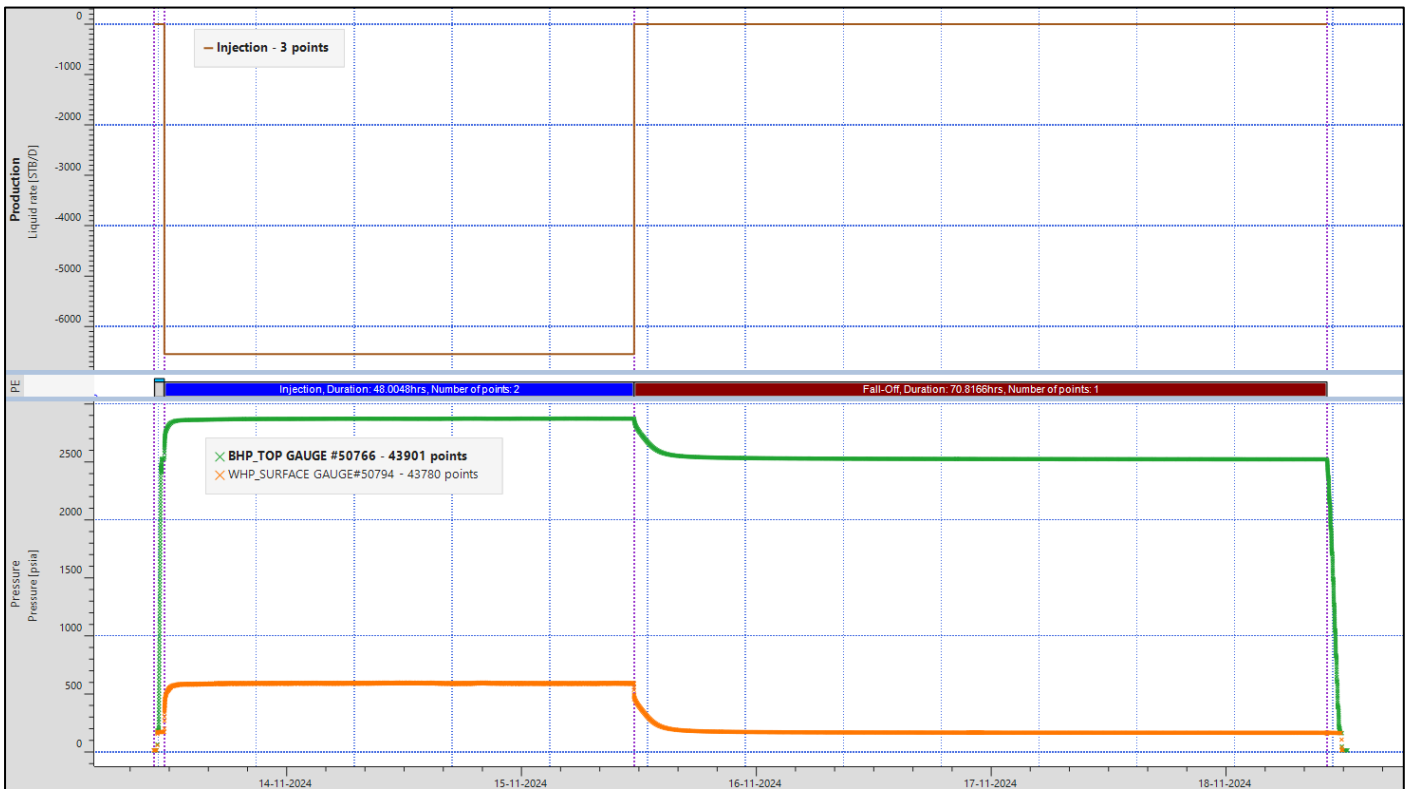


Figure 2: Pressure data for gauges considered for PTA analysis. Gauges #50766(bottom @ 5,340 ft in green color and 50794 at well head in orange color)

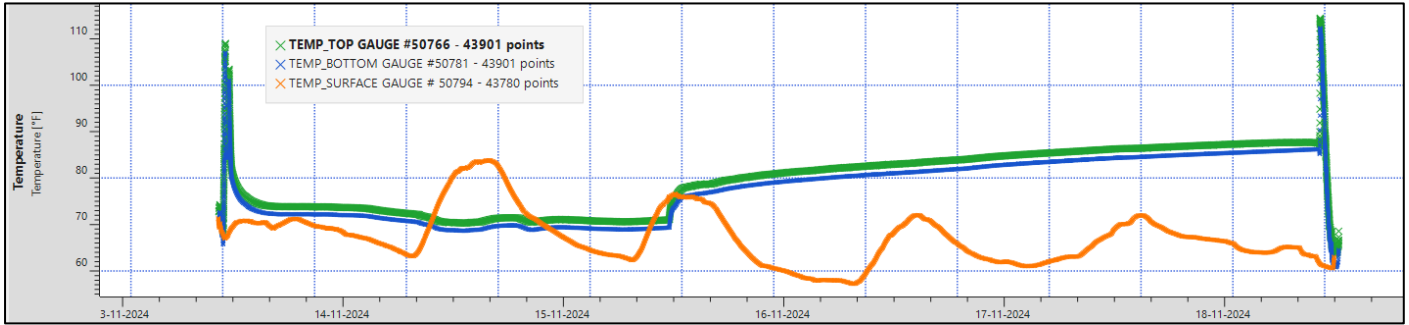


Figure 3: Temperature readings for gauge wellhead (50794 in orange color) and bottom (50766 and 50781 in green and blue color).

The water fluid properties were estimated based on the reported field water sp. gravity (~1.005 g/cc) and down hole pressure & temperature conditions. The bottomhole and surface pressure data quality is compared in Figure 4, indicating noisy surface pressure data, which reflects in the fall off pressure derivatives presented in Figure 5.

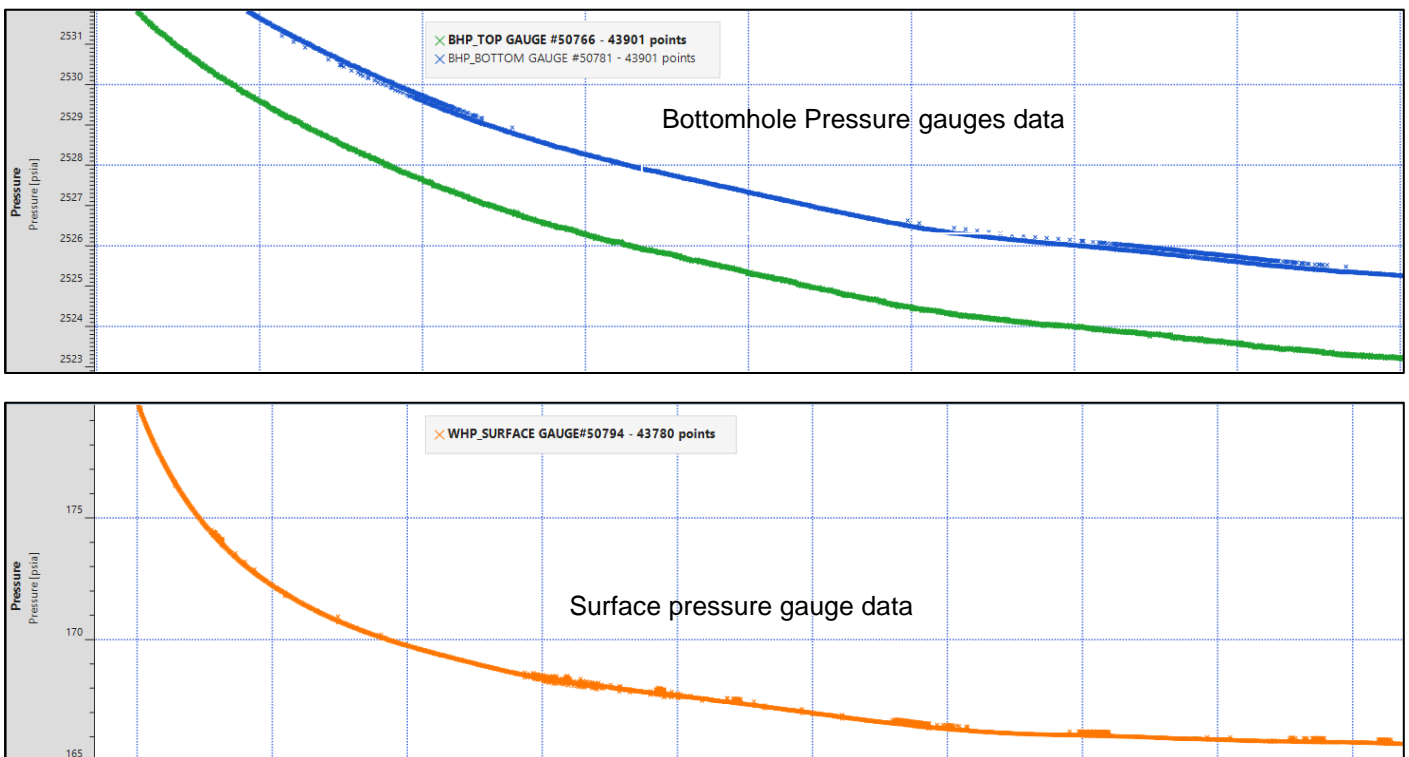


Figure 4: Bottom hole and surface pressure gauges data quality

Along with bad data quality of surface pressure gauge, fall off analysis of this gauge present two wellbore dynamics effects:

- small noise at early times in the surface pressure gauge. However, it does not have an important impact in the analysis.
- spikes in the derivative late times which look associated to temperature variations. This phenomenon is mainly affecting the surface pressure gauges as presented in Figure 5. Yet an attempt is made to transform wellhead pressures to bottomhole and interpret the data, which should be considered low confidence (Appendix 1).

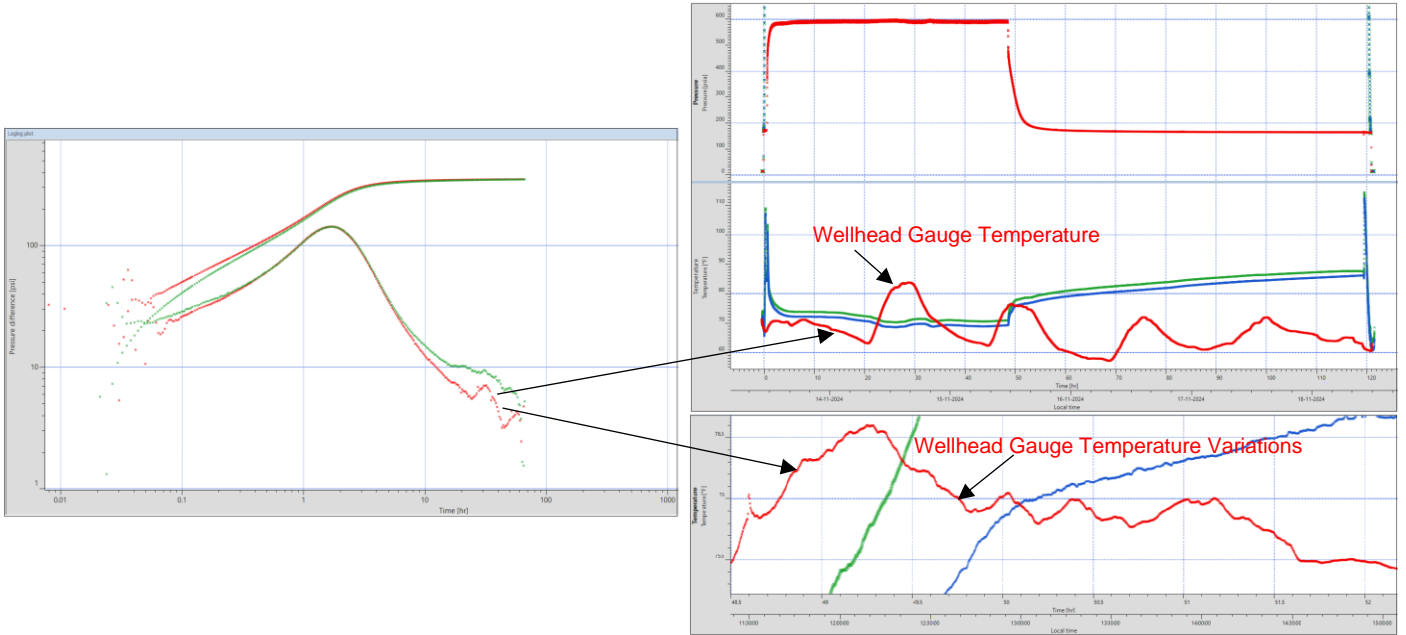


Figure 5: Early and late time pressure transient wellbore dynamics effect

The results described below show the estimation of **kh** and **skin** by the log-log, Semilog and test history match. The complete injection flow rate history was considered as per Table 1 (flow rate of 191GPM or 6,549 STB/D). The main PTA results are summarized below:

Pressure Fall Off: Recorded for ~71 hours. The recorded pressure at the end of shut-in was BHP= 2,522.28 psia and WHP= ~165.1 psia, Figure 2.

The pressure and temperature gradients performed after the fall off period from 5,340 ft to well head are presented in Appendix 2 and the respective mean gradient values are presented in the Table 3, below.

Table 3: PTA model result table

|   | PTA Reservoir Model Results Downhole Gauges |
|---|---|
| Fall Off test duration, hrs                           | 71  |
| Estimated BHP Injection Pressure before shut-in, Psia | 2,873.09                                    |
| Estimated BHP Pressure after 71 hours of shut-in, Psi | 2,522.28                                    |
| Permeability- Thickness, k*h                          | 76,210.3 md-ft                              |
| Permeability, k (assuming net pay of 300 ft)          | 254.03 md                                   |
| Total Skin, S   | 19.8  |
| Investigation Radius, Rinv                            | 4,269 ft                                    |
| Reservoir Pressure, P* [Horner Plot] @ 5,340 ft.      | 2518.63 psia                                |
| Injectivity Index (II)                                | 18.5 STB/D/psi                              |
| Changing Storage, Cf, bbl/psi                         | 1.26061                                     |
| Pressure gradient between 0 and 5,340 ft              | 0.442 psi/ft                                |
| Temperature gradient between 0 and 5,340 ft           | 0.010 °F / ft                               |

\* BHC: Bottom hole conditions



### B01 • Interpretation with downhole pressure gauge data (Gauge 50766)

The diagnostic Log-Log plot for the Falloff pressure transient test recorded with downhole gauges is presented in Figure 6. The pressure falloff derivative plot was used for early and middle times flow regime identification, the log-log scale shows three main flow regimes:

- At early times, Wellbore Storage (WBS) effects were observed until about 0.45 hr. Changing wellbore storage was applied. The obtained WBS coefficient C from the time match was 1.261 bbl/psi with delta t of 0.08568 hr. The wellbore-dominated time is considered small for this type of test for a well which has been shut-in at the bottomhole.
- Pressure drop caused by near-wellbore damage was observed between 0.45 and 4 hrs. The estimated total skin value was  $S = 19.8$ . High skin value signifies poor connection between the well and reservoir, which could be due to insufficient or plugged perforations, some mud invasion, partial penetration etc.
- Possible Infinite Acting Radial Flow (IARF) was observed between 46.0 and 57.6 hrs. The formation properties, such as average drainage area pressure and permeability were estimated from this flow regime. Permeability-Thickness,  $k^*h = 76,210.30$  md-ft. Considering an effective injection thickness of 300 ft (from previous report dated on Nov 2023) an effective horizontal permeability is estimated in the order of 254.03 md. Average drainage area pressure is estimated as 2,518.63 psi and the fall off test investigation radius is 4,269 ft.
- The water injectivity Index is computed as 18.5 STB/D/psi.

Graphical analyses are presented in Figures 7, 8 and 9, including field data and history match analytical model.

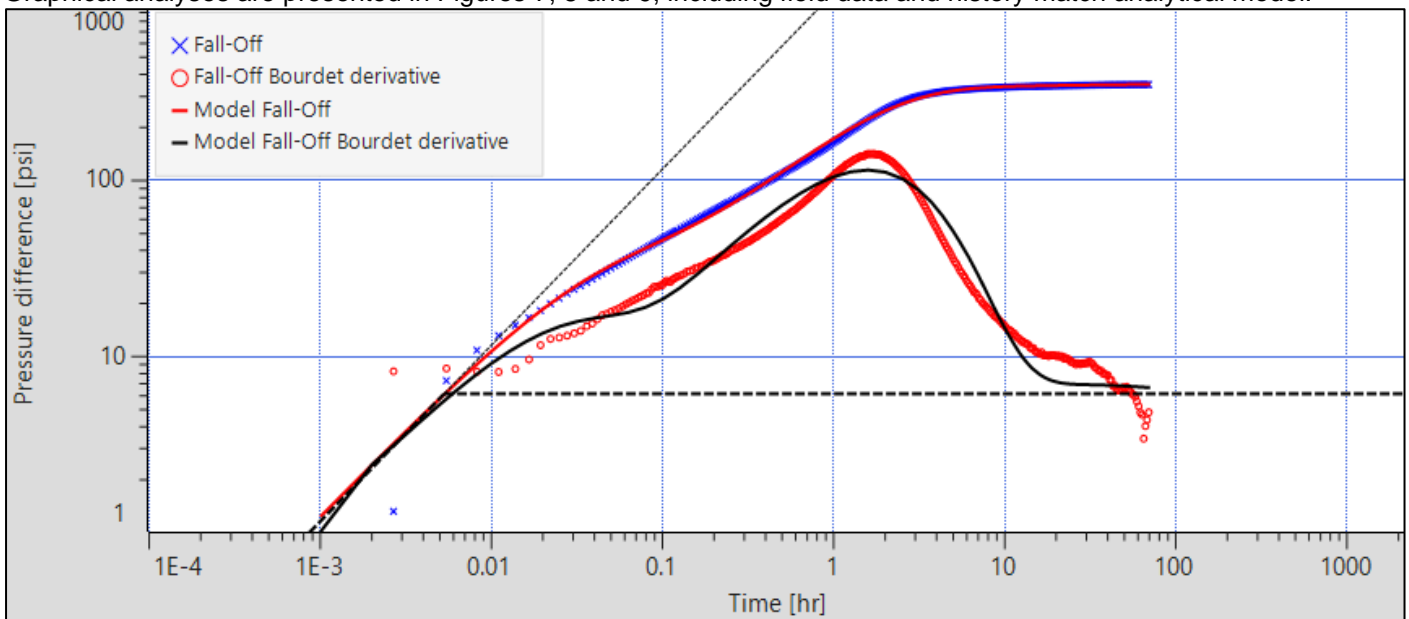


Figure 6: Log-Log Plot and PTA Model for pressure falloff with downhole gauge 50766 (Vertical Homogeneous Infinite)

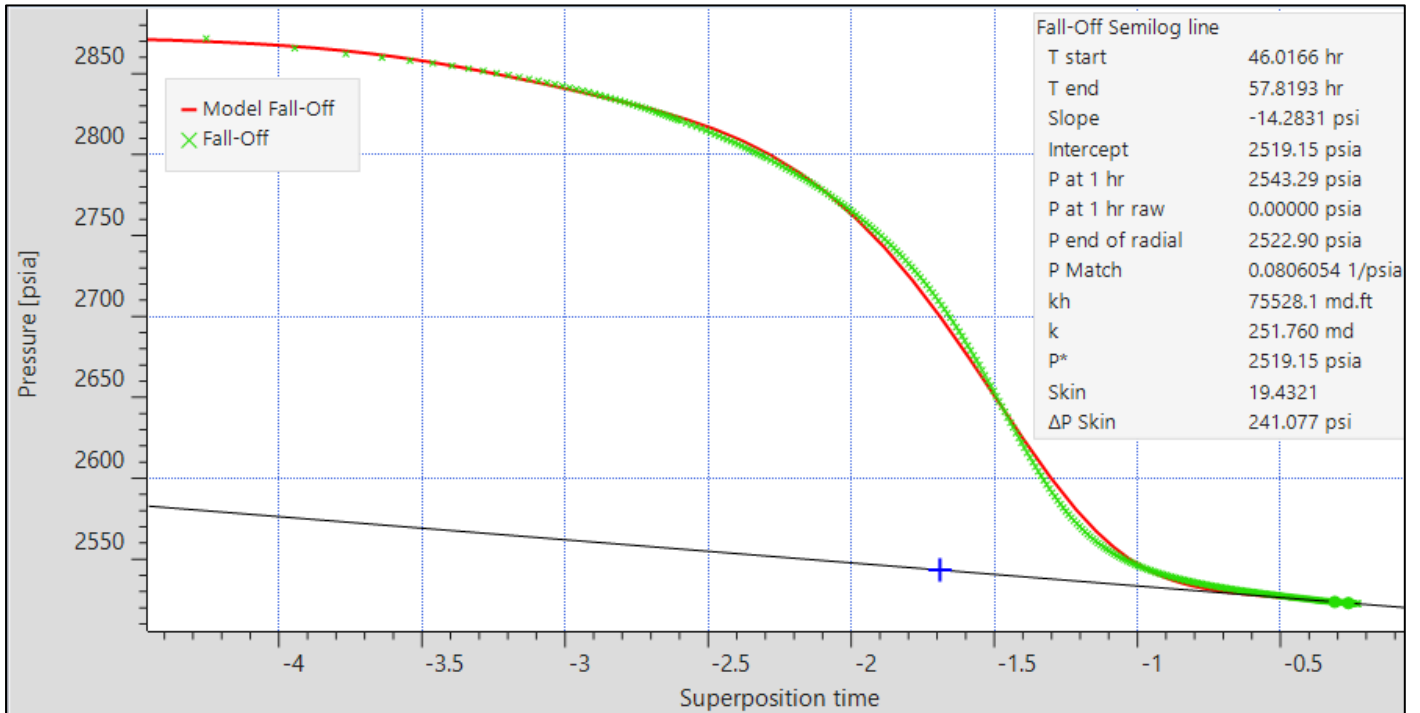


Figure 7: Semi log Diagnostic Plot and model for Pressure Falloff with downhole gauge 50766

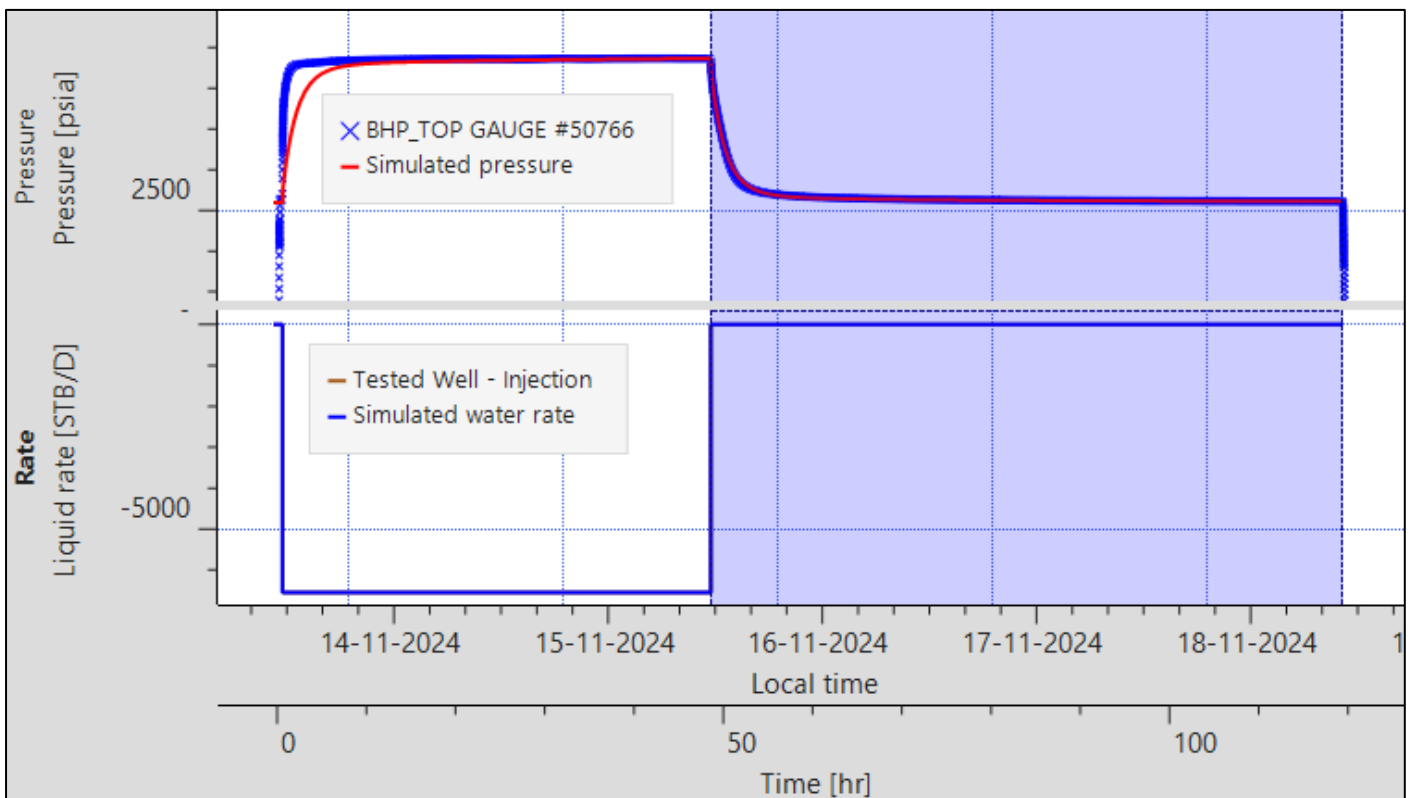


Figure 8: Top plot: Test bottomhole pressure data (blue color) and history match model (red), gauge 50766. Bottom plot: injection rate (STB/D).



### B02 • Spherical flow identification on Log-Log plot with downhole pressure gauge data (Gauge 50766)

As seen in figure below, Spherical flow regime was identified clearly on the log-log derivative curve. This indicating that there might be limited entry flow into the wellbore compared to formation thickness. This may be due to plugged (or partially) perforations.

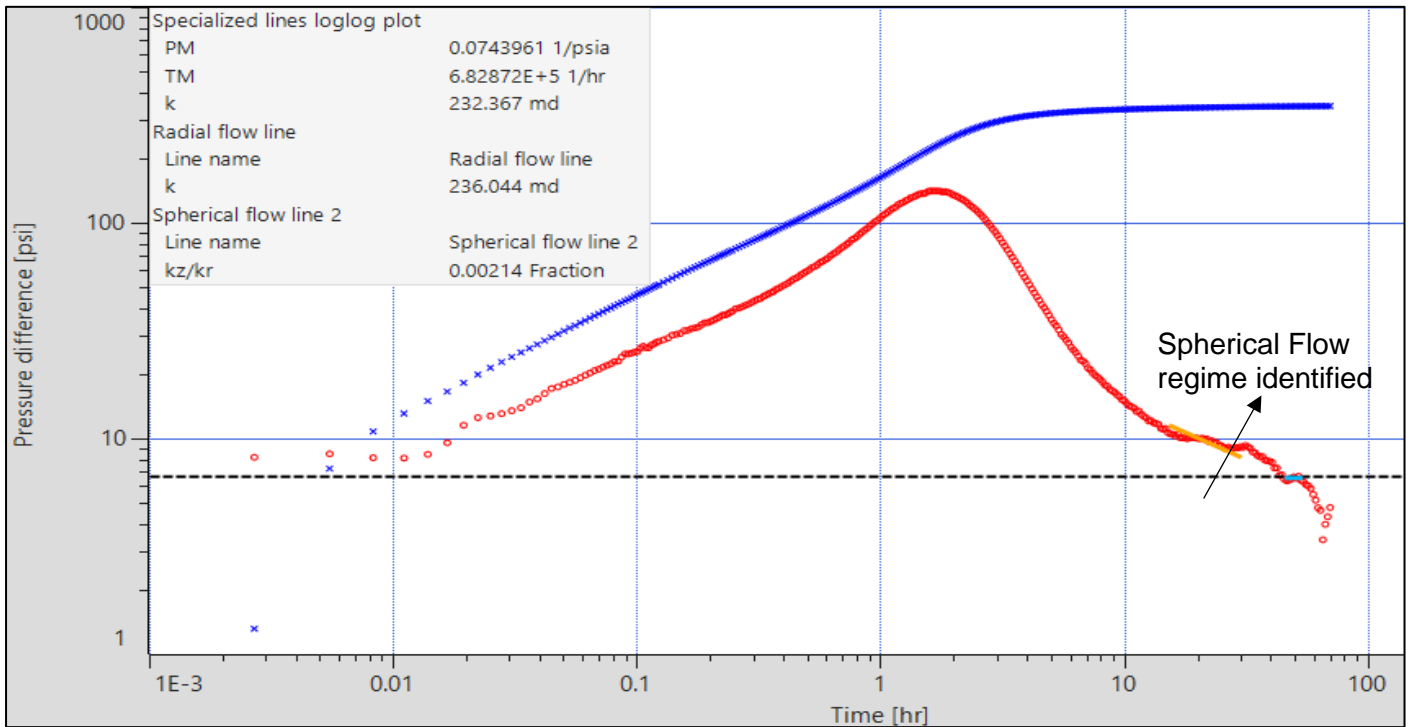


Figure 9: Flow regimes identification on Log-Log plot with downhole pressure gauge data (Gauge 50766)

### B03 • Comparison of Log-Log plot with downhole pressure gauge data for 2023 & 2024

As seen in figure below, IARF flow regime stabilization levels are closer to 2023 data. Permeability-thickness derived from IARF stabilization levels. Slightly higher skin values were observed which could be due to plugged perforations or partial penetration or incompatibility between injected fluid and formation causing extra pressure drop near wellbore.

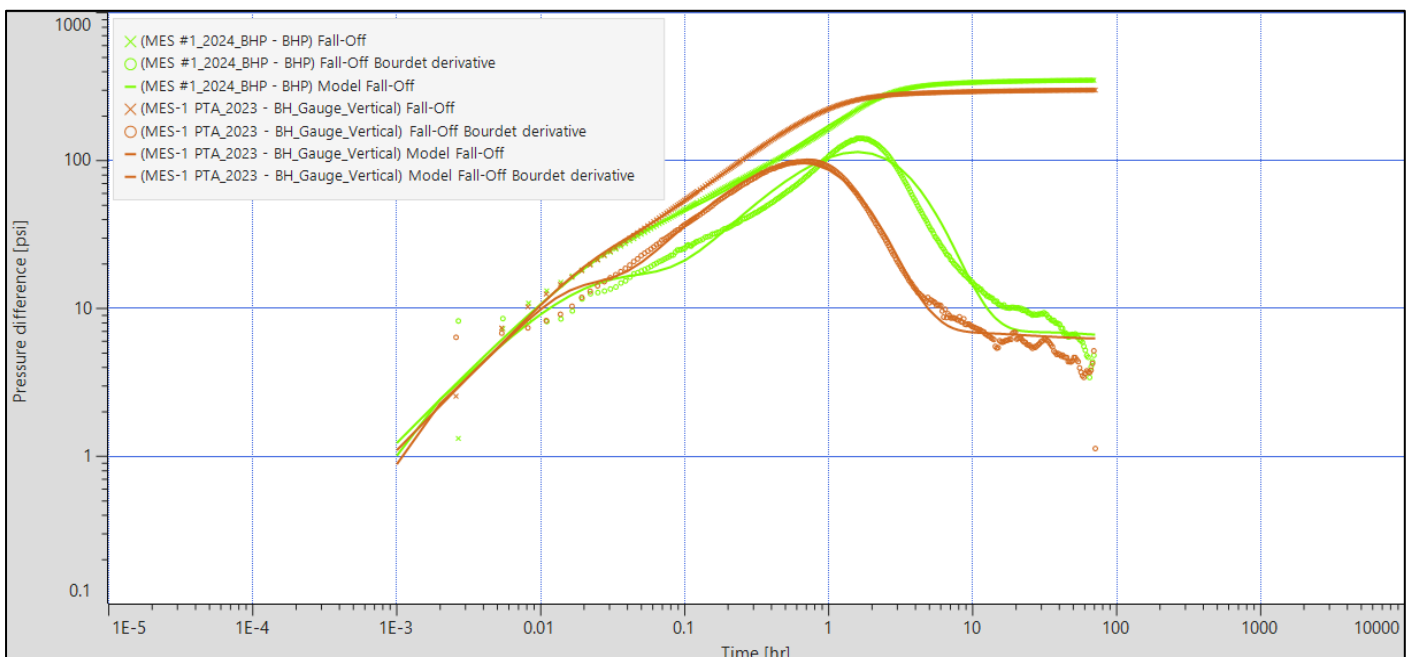


Figure 10: Comparison of Log-Log plot with downhole pressure gauge data for 2023 (orange colour) & 2024 (lime colour)



Company: A&M Engineering and Environmental Services, Inc.

County, State: Lincoln, Oklahoma

Reservoir: Arbuckle Formation

Well: MES#1- Water Injector

**C01 • Summary of PTA Inputs - Pressure Fall Off on Nov. 2024**

| Analysis summary     |                              |
|----------------------|------------------------------|
| Name                 | Falloff                      |
| Reference well       | MES#1                        |
| PVT ref. phase       | Water                        |
| PVT phases           | Water                        |
| Active prod.         | Injection                    |
| Open Hole Interval   | 5,173 – 6,804 ft             |
| Active press. datum  | BHP @ 5,340 ft               |
| Analysis type        | Standard                     |
| Model description    |                              |
| Active model         | Analytical                   |
| Wellbore             | Changing fair                |
| Well                 | Vertical                     |
| Reservoir            | Homogeneous                  |
| Boundary             | Infinite                     |
| Other wells incl.?   | No                           |
| Rate dep. skin?      | No Data                      |
| Time dep. skin?      | No Data (no SRT)             |
| Test parameters      |                              |
| rw                   | 3.948 in                     |
| h                    | 300 ft                       |
| Rock compressibility | 3.00E-06 psi <sup>-1</sup>   |
| Φ                    | 0.14                         |
| Top reservoir depth  | 5,173 ft                     |
| Fluid Model          |                              |
| Phase                | Water                        |
| B                    | 1.01332 B/STB                |
| μ                    | 1 cp                         |
| ct                   | 5.92092E-6 psi <sup>-1</sup> |
| Sw                   | 1                            |
| Cw                   | 1.19E-5 psi <sup>-1</sup>    |
| co                   | 0 psi <sup>-1</sup>          |
| cg                   | 0 psi <sup>-1</sup>          |
| PVT model            | Water                        |
| Tref                 | 110 °F                       |
| Pref                 | 1,800 psia                   |
| Water gravity        | 1.005 sp. gr.                |
| Salinity             | 6,394 ppm                    |
| Bw                   | Spivey                       |
| ρw                   | Internal                     |
| μw                   | Constant                     |



Company: A&M Engineering and Environmental Services, Inc.

County, State: Lincoln, Oklahoma

Reservoir: Arbuckle Formation

Well: MES#1- Water Injector

**C02 • Comparison of PTA Results - Pressure Fall Off on Nov. 2024 and Nov. 2023**

| Main Results                 |                    |                    |
|------------------------------|--------------------|--------------------|
|                              | 2024               | 2023               |
| Transmissibility, kh/μ       | 76,210.30 md.ft/cp | 79,330.10 md.ft/cp |
| Permeability, k              | 254.03 md          | 264.43 md          |
| Mobility, k/μ                | 254.03 md/cp       | 264.43 md/cp       |
| Total skin                   | 19.76              | 16.59              |
| Initial Pressure, Pi         | 2,518.63 psia      | 2,529.72 psia      |
| Wellbore Storage, C          | 0.220537 bbl/psi   | 0.256143 bbl/psi   |
| Model - Well & wellbore      |                    |                    |
| Wellbore model               | Changing fair      | Changing hegeman   |
| Final wellbore storage       | 1.26061 bbl/psi    | 0.61368 bbl/psi    |
| C[initial]/C[final]          | 0.174945           | 0.417389           |
| Dt changing storage          | 0.0856841 hr       | 0.0822642 hr       |
| Well type                    | Vertical           | Vertical           |
| Skin                         | 19.76              | 16.59              |
| Diagnostic                   |                    |                    |
| Wellbore storage             | Constant           | Constant           |
| Well                         | Finite radius      | Finite radius      |
| Reservoir                    | Homogeneous        | Homogeneous        |
| Boundary                     | Infinite           | Infinite           |
| Reference rate               | 6,548.57 STB/D     | 6,000.00 STB/D     |
| Extraction start time        | 0 hr               | 0                  |
| P @ dt=0                     | 2,873.09 psia      | 2,808.31 psia      |
| Model - Reservoir & boundary |                    |                    |
| Reservoir type               | Homogeneous        | Homogeneous        |
| Boundary type                | Infinite           | Infinite           |
| Initial pressure             | 2,518.63 psia      | 2,529.72 psia      |
| Transmissivity               | 76,210.30 md.ft    | 79,330.10 md.ft    |
| Permeability                 | 254.03 md          | 264.43 md          |
| Thickness                    | 300 ft             | 300 ft             |
| Porosity                     | 0.14               | 0.14               |
| Falloff Semi log line        |                    |                    |
| Time start                   | 46.0166 hr         | 16.4583 hr         |
| Time end                     | 57.8193 hr         | 29.1416 hr         |
| Slope                        | -14.2831 psi       | -13.0820 psi       |
| Intercept                    | 2,519.15 psia      | 2,529.47 psia      |
| P at 1 hour                  | 2,543.29 psia      | 2,551.38 psia      |
| P at 1 hour raw              | 2,708.49 psia      | 2,602.95 psia      |
| P end of radial              | 2,522.90 psia      | 2,534.87 psia      |
| Pressure Match               | 0.0806054 1/psia   | 0.0880057 1/psia   |
| Transmissivity               | 75,528.10 md.ft    | 75,554.50 md.ft    |
| Permeability                 | 251.76 md          | 251.85 md          |
| P star                       | 2,519.15 psia      | 2,529.47 psia      |
| Skin                         | 19.43              | 15.39              |
| ΔP Skin                      | 241.08 psi         | 174.98             |
| Radius of investigation      | 4,269 ft           | 3,000 ft           |



Company: A&M Engineering and Environmental Services, Inc.

County, State: Lincoln, Oklahoma

Reservoir: Arbuckle Formation

Well: MES#1- Water Injector

**Appendix 1:  
Wellhead pressure Transform Fall-  
off Analysis.**



Appendix 1: Wellhead pressure Transform Fall-off Analysis.

Interpretation with wellhead pressure gauge converted to bottomhole gauge data (Gauge 50794)

The diagnostic Log-Log plot for the Falloff pressure transient test recorded with downhole gauges is presented in Figure 11. The pressure falloff derivative plot was used for early and middle times flow regime identification, the log-log scale shows three main flow regimes:

At early times, Wellbore Storage (WBS) effects were observed until about 0.52 hr. Changing wellbore storage was applied. The obtained WBS coefficient C from the time match was 1.1976 bbl/psi with delta t of 0.0056 hr.

Pressure drop caused by near-wellbore damage was observed between 0.52 and 4.5 hrs. The estimated total skin value was S= 20.

Infinite Acting Radial Flow (IARF) was not clearly observed for the fall off data. The best possible match was still attempted with the data and results were presented below in figure 11.

Graphical analyses are presented in Figures 12 and 13, including field data and history match analytical model.

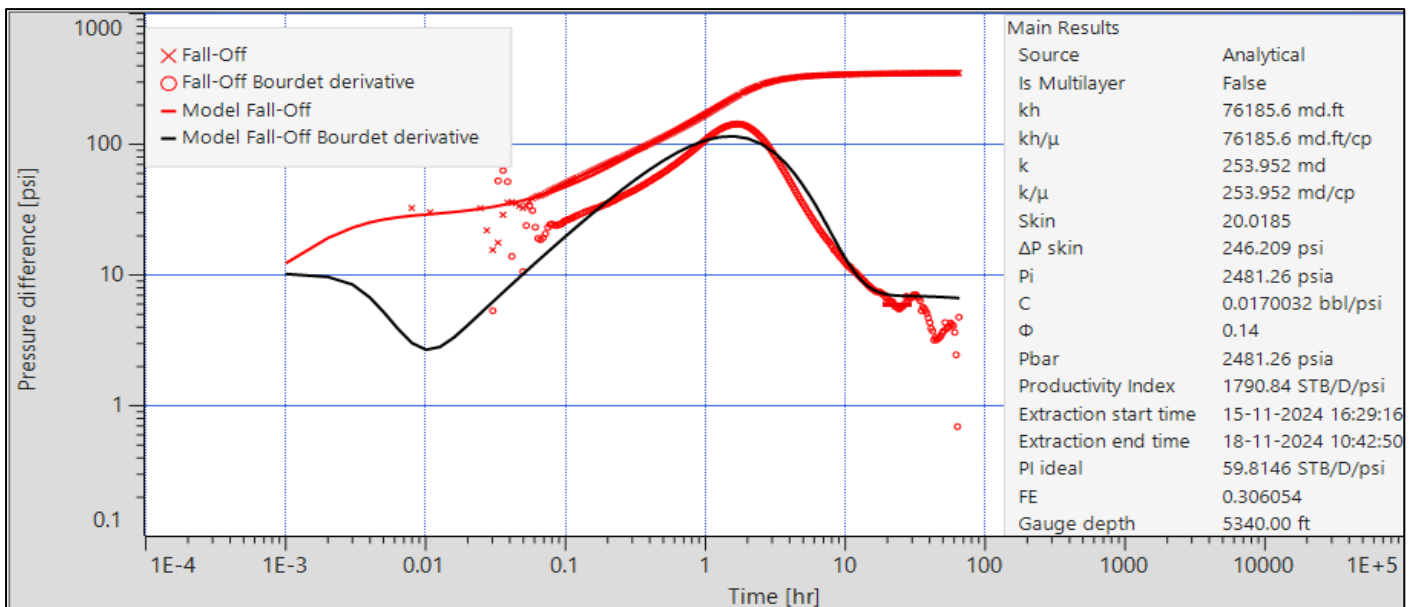


Figure 11: Log-Log Plot and PTA Model for pressure falloff with wellhead pressure gauge 50794 Transform (Vertical Homogeneous Infinite)

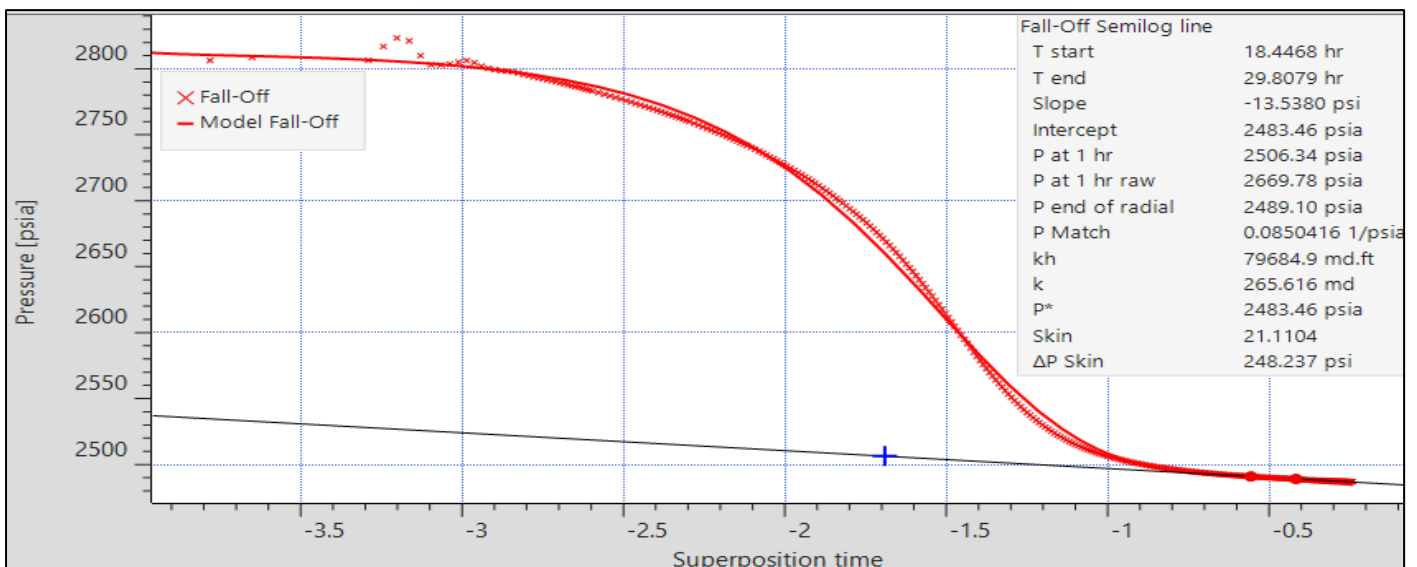


Figure 12. Semi-log Diagnostic Plot and model for Pressure Falloff with downhole gauge 50794.

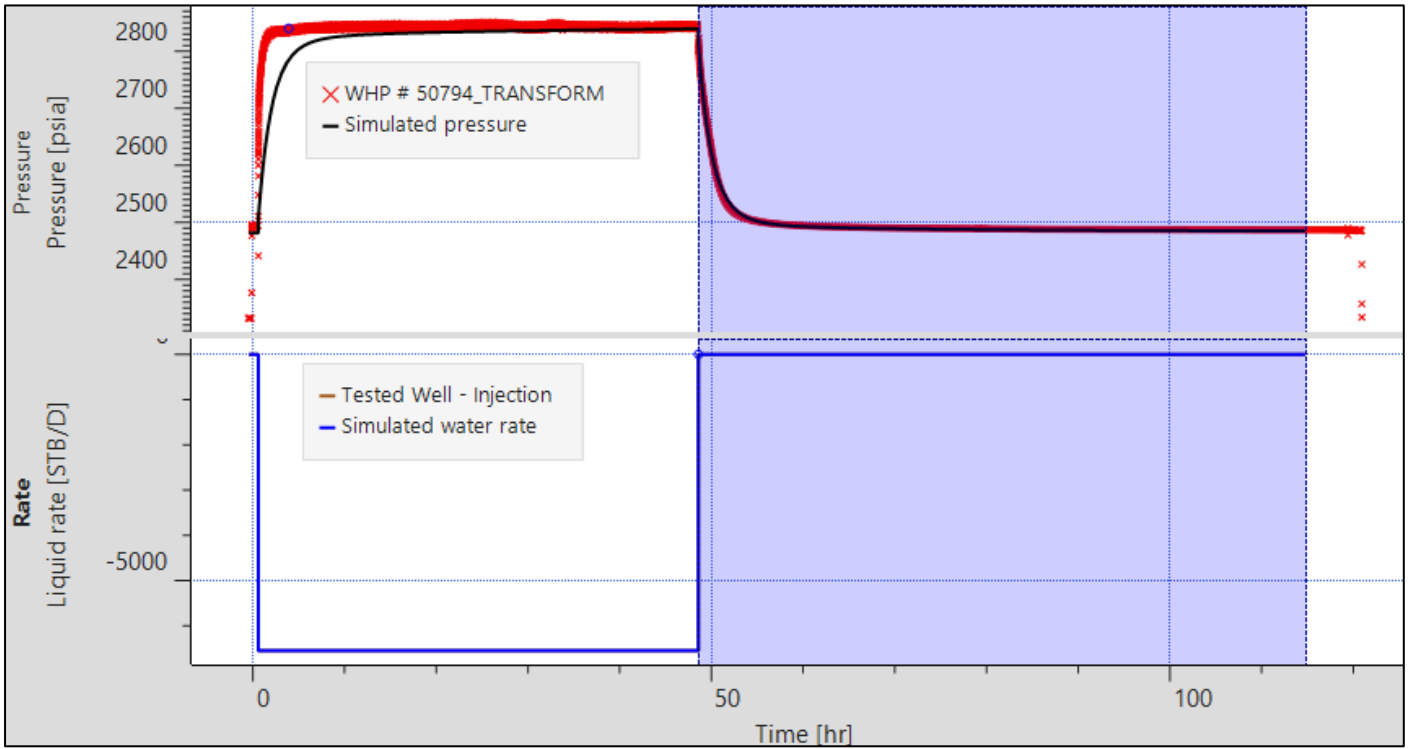


Figure 13. Test bottomhole pressure data (red color) and history match model (black), gauge 50794 (Wellhead gauge data Transform). Bottom plot: injection rate (STB/D).



Company: A&M Engineering and Environmental Services, Inc.

County, State: Lincoln, Oklahoma

Reservoir: Arbuckle Formation

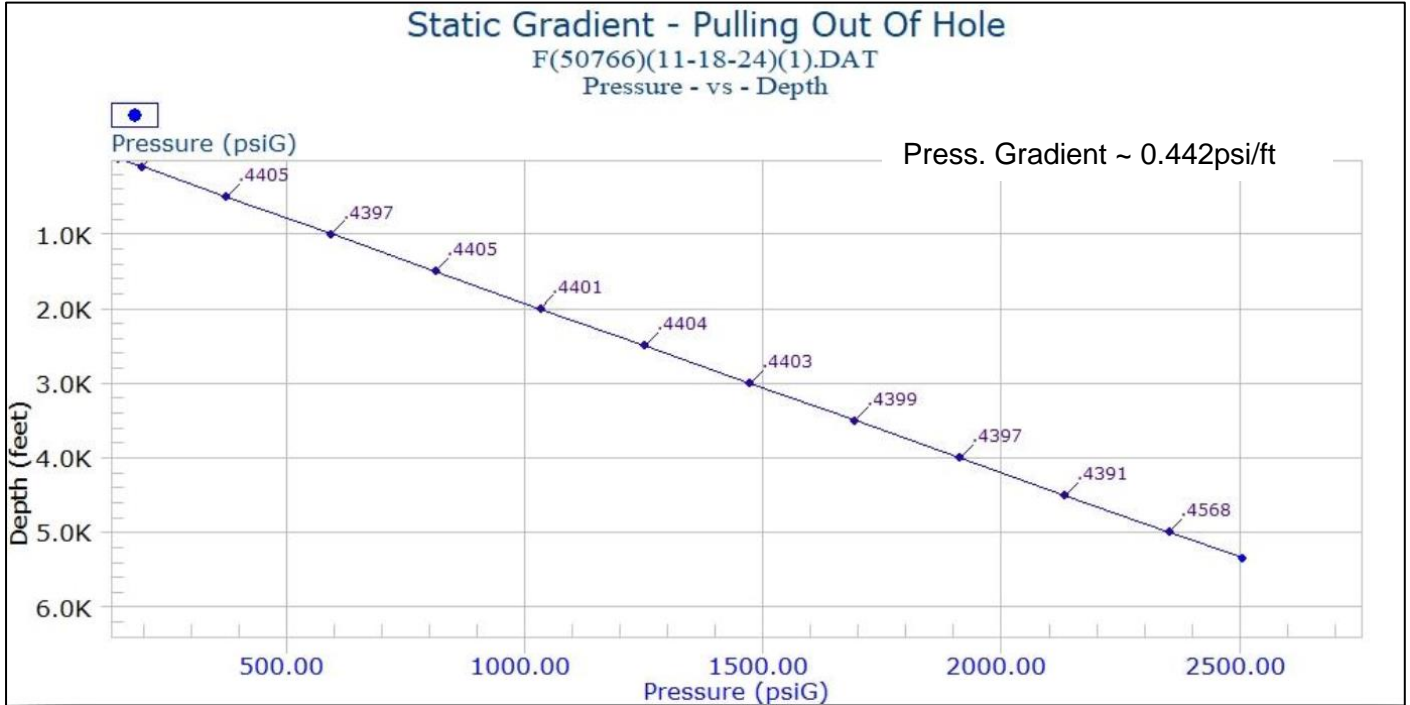
Well: MES#1- Water Injector

**Appendix 2:  
Static Pressure and Temperature  
Gradients**



**Appendix 2: Static Pressure and Temperature Gradients**

**Static Pressure Gradient – Pulling Out of Hole\***



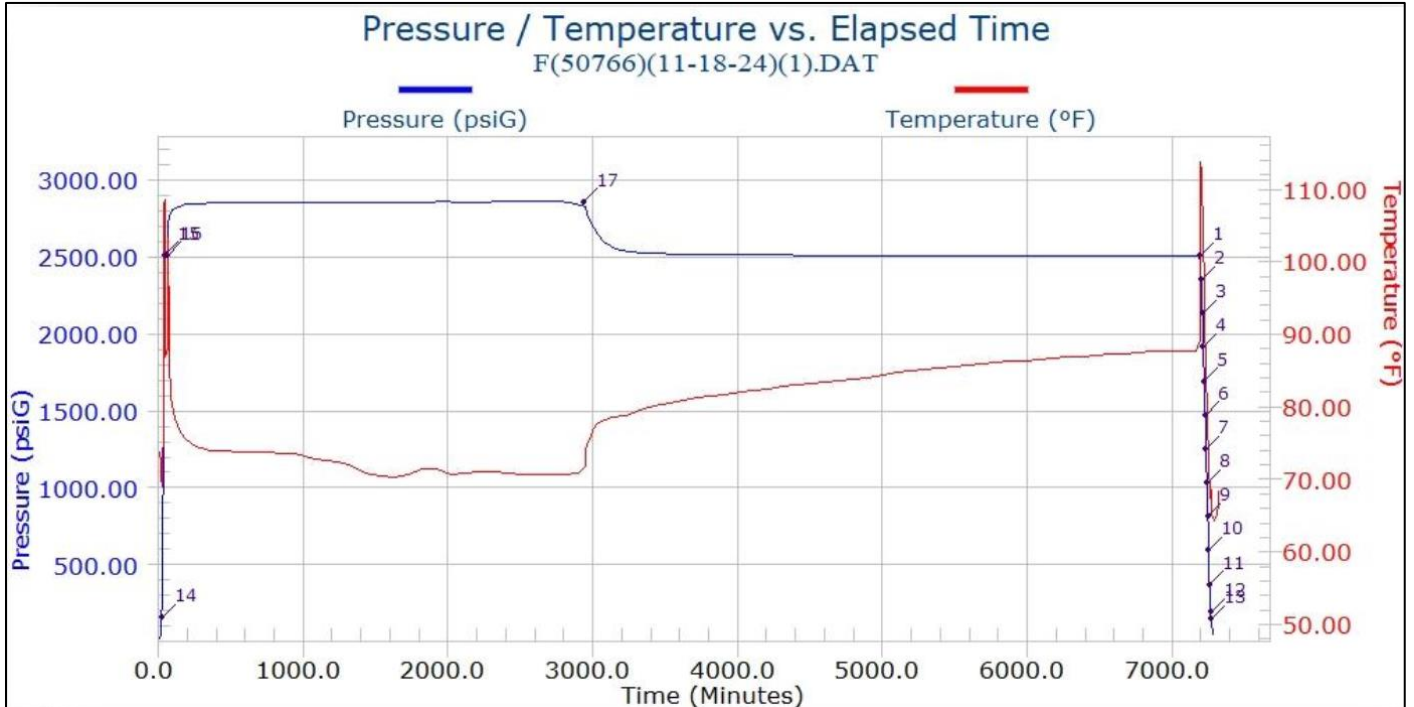
**Pressure & Temperature Gradient Table**

| Real Date<br>MM/DD/YY | Real Time<br>HH:MM:SS | Elapsed Time<br>Minutes | WLM<br>feet | TVD<br>feet | Pressure<br>(psiG) | Gradient<br>(psiG/feet) | Temperature<br>(deg. F) | Gradient<br>(deg. F/feet) |
|-----------------------|-----------------------|-------------------------|-------------|-------------|--------------------|-------------------------|-------------------------|---------------------------|
| 11/18/24              | 11:41:22              | 7274.20000              | 0           | 0           | 147.270            | .4831                   | 65.356                  | .0173                     |
| 11/18/24              | 11:35:52              | 7268.70000              | 0           | 100         | 195.581            | .4416                   | 67.081                  | .0057                     |
| 11/18/24              | 11:28:52              | 7261.70000              | 0           | 500         | 372.225            | .4405                   | 69.376                  | .0060                     |
| 11/18/24              | 11:21:42              | 7254.53333              | 0           | 1000        | 592.465            | .4397                   | 72.401                  | .0069                     |
| 11/18/24              | 11:15:42              | 7248.53333              | 0           | 1500        | 812.332            | .4405                   | 75.872                  | .0076                     |
| 11/18/24              | 11:10:02              | 7242.86667              | 0           | 2000        | 1032.575           | .4401                   | 79.676                  | .0095                     |
| 11/18/24              | 11:04:02              | 7236.86667              | 0           | 2500        | 1252.629           | .4404                   | 84.404                  | .0092                     |
| 11/18/24              | 10:58:12              | 7231.03333              | 0           | 3000        | 1472.809           | .4403                   | 88.991                  | .0135                     |
| 11/18/24              | 10:52:22              | 7225.20000              | 0           | 3500        | 1692.948           | .4399                   | 95.748                  | .0117                     |
| 11/18/24              | 10:44:22              | 7217.20000              | 0           | 4000        | 1912.913           | .4397                   | 101.613                 | .0130                     |
| 11/18/24              | 10:37:42              | 7210.53333              | 0           | 4500        | 2132.756           | .4391                   | 108.093                 | .0101                     |
| 11/18/24              | 10:28:32              | 7201.36667              | 0           | 5000        | 2352.281           | .4568                   | 113.165                 | -.0753                    |
| 11/18/24              | 10:19:32              | 7192.36667              | 0           | 5340        | 2507.588           |                         | 87.573                  |                           |

\* After LQC data acquired from Precision Wireline



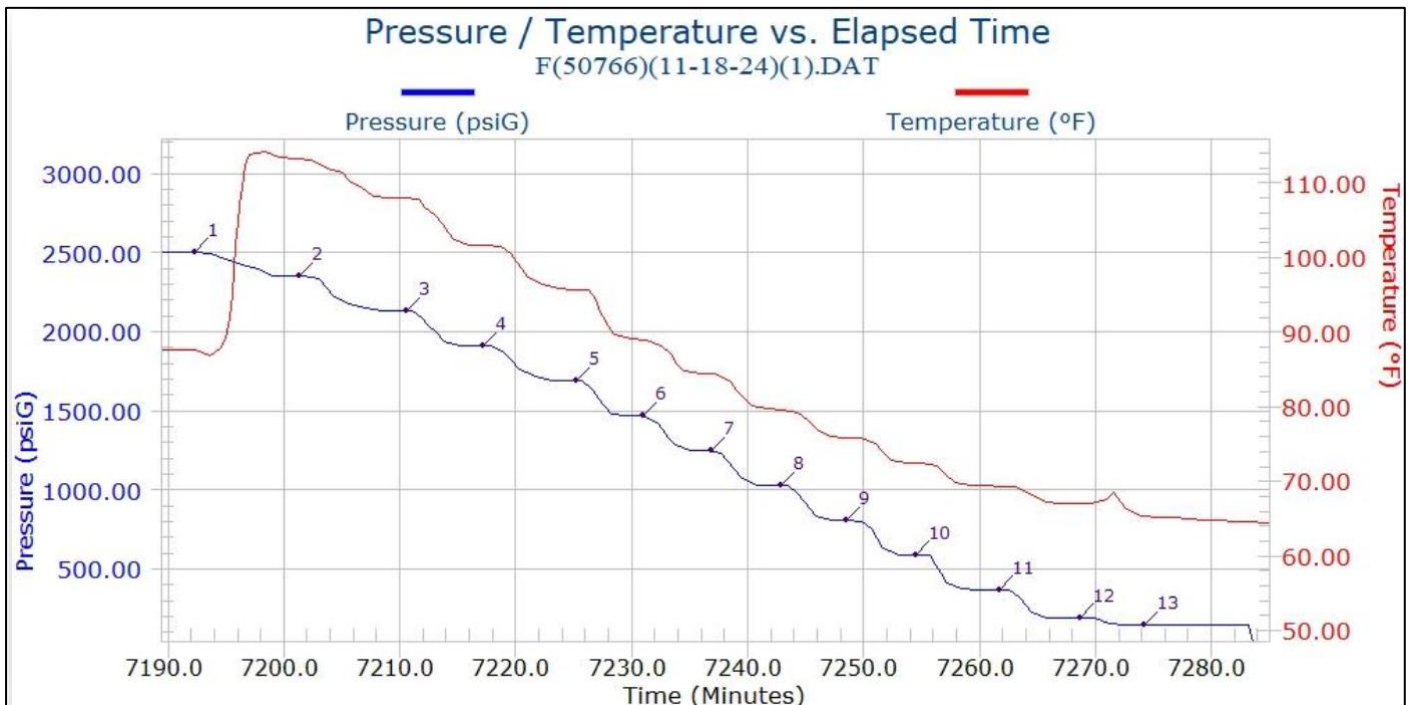
### Pressure / Temperature Records for Gradient Analysis\* (Gauge 50766 on 11/08/2024)



Pressure & Temperature records from bottom hole gauges 50766. Pressure: blue color and Temperature: red color.

\* After LQC data acquired from Precision Wireline

### Static Temperature Gradient – Pulling Out of Hole\*



\* After LQC data acquired from Precision Wireline



Company: A&M Engineering and Environmental Services, Inc.

County, State: Lincoln, Oklahoma

Reservoir: Arbuckle Formation

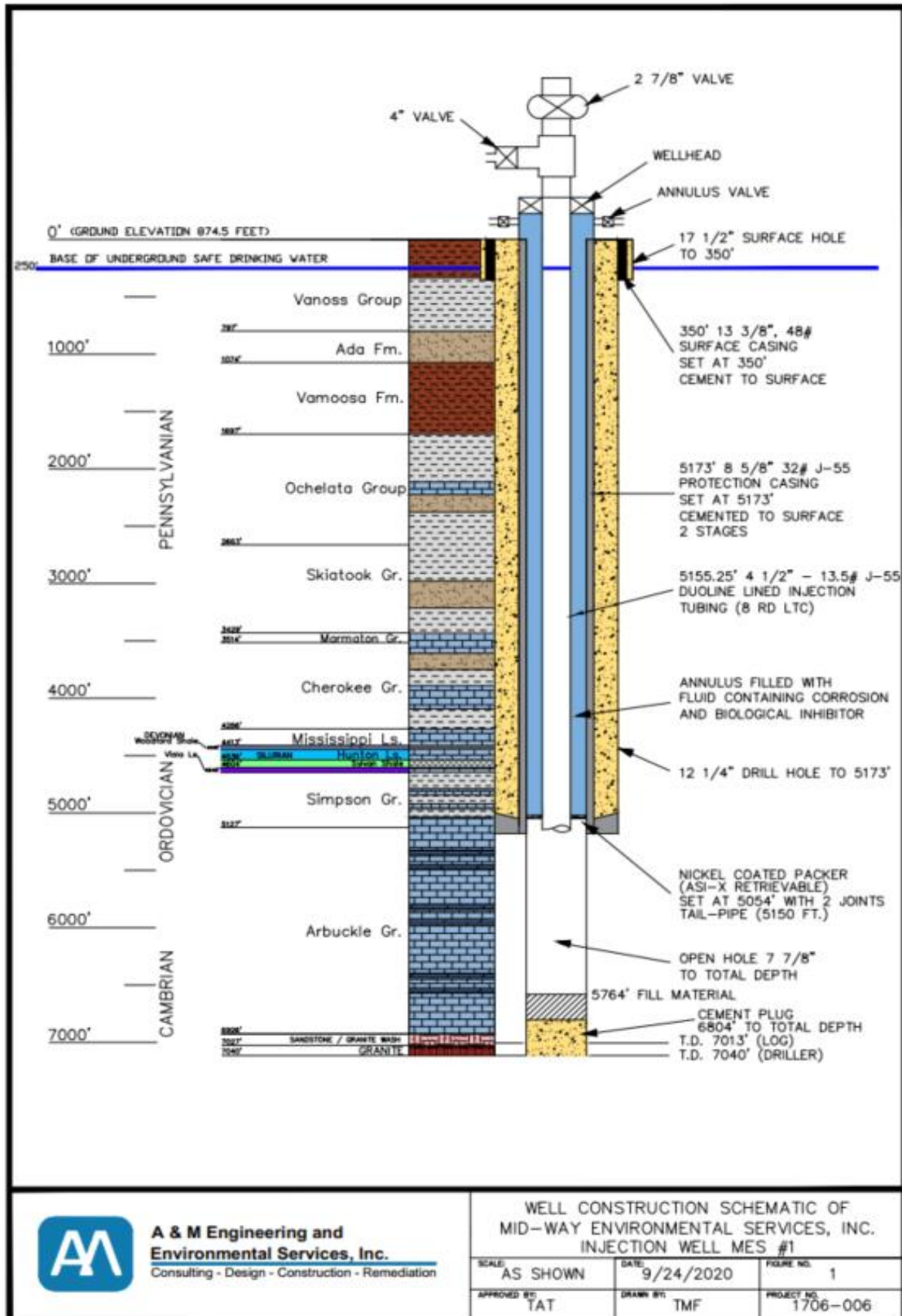
Well: MES#1- Water Injector

**Appendix 3**

**MES #1 Well Construction  
Revision 9-23-2020**



Appendix 3: MES # 1 Well Construction Revision Diagram (9-23-2020)



\* Collar locator logs in June and November 2020 show the top of packer to be at 5138' and the EOT at 5234'. Note from Precision Wireline report on Nov 11, 2021.

**PRECISION WIRELINE**  
**Data Summary**



**MID-WAY ENVIRONMENTAL SERVICES INC.**

**BOTTOM HOLE PRESSURE**

**MES #1**

**11/13/2024 to 11/18/2024**

**PRECISION WIRELINE**



PRECISION WIRELINE  
2402 S MONROE  
ENID OK 73701  
Phone: 580-233-0033 Fax:

**Company Information**

Company Name: MID-WAY ENVIRONMENTAL SERVICES INC.  
Division:  
Representative: ORPHIUS MOHAMMAD  
Address: 10010 E. 16TH ST  
Address:  
City: TULSA State: OK Zip: 74128-4813 Country: United States  
Phone Number: 918-665-6575  
Fax Number:  
E-mail Address: <mailto:omohammad@aandmengineering.com>  
Note 1:  
Note 2:  
Note 3:

**Well Information**

Well Name: MES #1  
Well Location:  
Field and Pool:  
Status (Oil, Water, Gas, Injection): INJECTION  
Perforation Intervals: 5173-6804'  
MPP Intervals:  
Casing Size: 8-5/8" 32  
Tubing Size: 4-1/2" 13.5# J-55  
Plug Back Total Depth: 6804'  
Total Depth: 7013'

**Test Information**

Type Of Test: BOTTOM HOLE PRESSURE  
Date Of Test: 11/13/2024  
Start Date / Time: Begin: 11/13/2024 / 09:00AM  
End: 11/18/2024 / 01:00PM  
Duration: 120 HOURS  
Gauge Depth: 5340'  
Gauge Position: TOP  
Surface Casing Pressure:  
Surface Tubing Pressure:  
Maximum Downhole Pressure:  
Maximum Downhole Temperature:  
Data Filename: F(50766)(11-18-24)(1).DAT  
Job Number:  
Reported By: RICK PORRAS



**Gauge Information**

Serial Number: 50766  
Model Number: HT-1250  
Gauge Manufacturer: Micro-Smart Systems, Inc.  
Pressure Range:  
Battery Type Used: 4241570306  
Calibration Filename: G(50766)(03-15-24).CAL

**Gauge Setup Parameters**

Gauge Power-up Date / Time: 11/13/24 10:27:10  
Test Type Setting: 10 SEC SAMPLE  
Test Duration Setting: MAX

**Service Company Information**

Company Name: PRECISION WIRELINE  
Division:  
Representative: RICK PORRAS  
Address: 2402 S MONROE  
Address:  
Address:  
City: ENID State: OK Zip Code: 73701 Country: United States  
Phone Number: 580-233-0033  
Fax Number:  
E-mail Address: pwillc@swbell.net  
Note 1: WL TAG DEPTH= 5360'  
Note 2: ENCOUNTERED BRIDGE @ 5334'  
Note 3: CORRELATED TO GL



## BOTTOM HOLE PRESSURE DATA SECTION



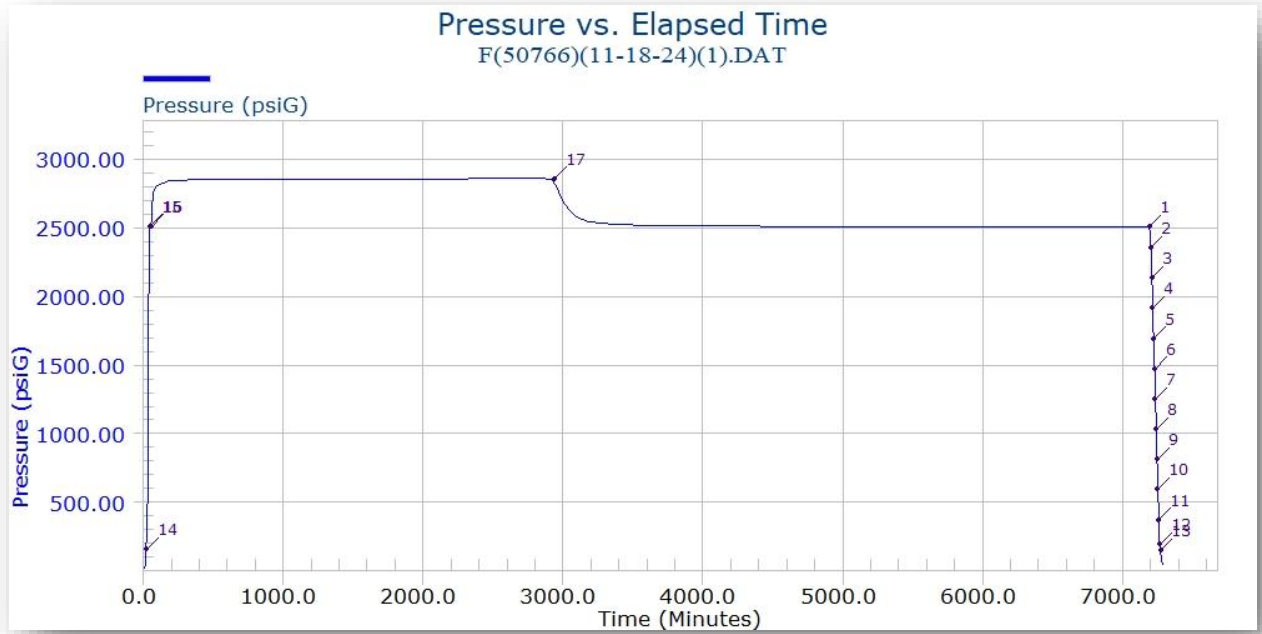
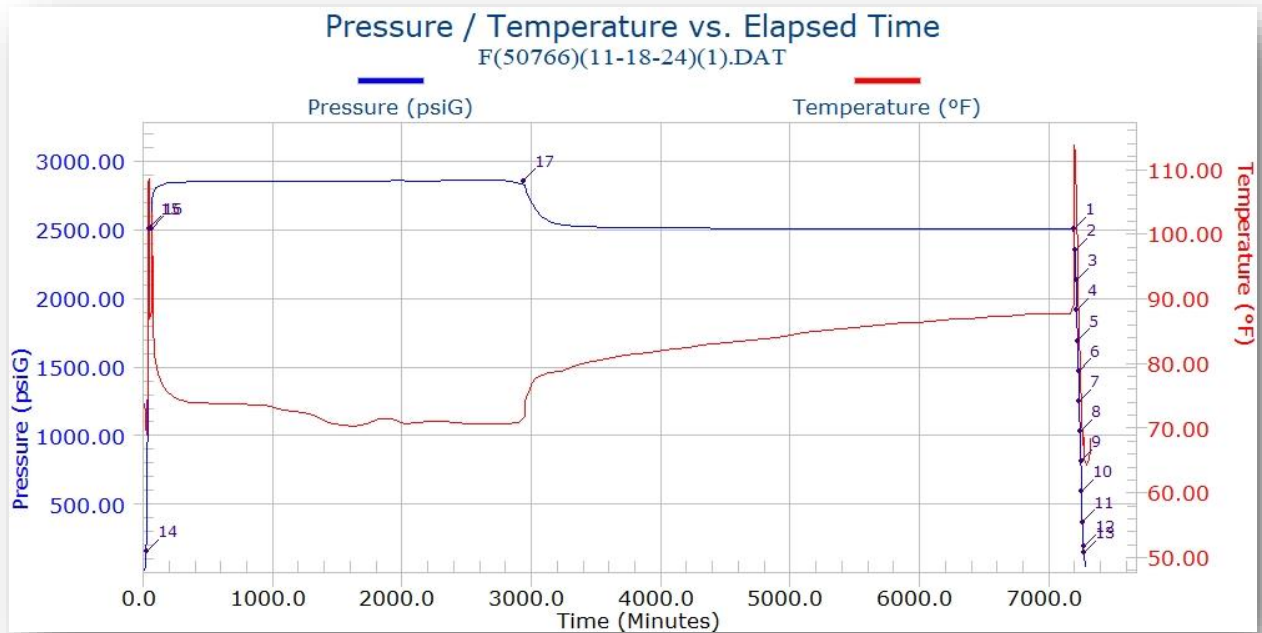
**Filename:** F(50766)(11-18-24)(1).DAT  
**Power Up Date:** 11/13/24  
**Power Up Time:** 10:27:10

## Event Summary

| Real Date<br>MM/DD/YY | Real Time<br>HH:MM:SS | Elapsed Time<br>Minutes | Pressure<br>psiG | Temperature<br>deg. F | Tag<br>Number | Comment                           |
|-----------------------|-----------------------|-------------------------|------------------|-----------------------|---------------|-----------------------------------|
| 11/13/24              | 10:54:02              | 26.86670                | 157.724          | 70.43                 | 14            | RIH -0-                           |
| 11/13/24              | 11:17:02              | 49.86670                | 2512.254         | 86.35                 | 15            | 5340' GAUGE SET                   |
| 11/13/24              | 11:30:12              | 63.03330                | 2511.677         | 86.22                 | 16            | BEGIN INJECTION                   |
| 11/15/24              | 11:30:12              | 2943.03300              | 2858.412         | 71.01                 | 17            | SHUT-IN BEGIN FALL-OFF            |
| 11/18/24              | 10:19:32              | 7192.36700              | 2507.588         | 87.57                 | 1             | POOH static stop @ 5340 feet TVD. |
| 11/18/24              | 10:28:32              | 7201.36700              | 2352.281         | 113.17                | 2             | POOH static stop @ 5000 feet TVD. |
| 11/18/24              | 10:37:42              | 7210.53300              | 2132.756         | 108.09                | 3             | POOH static stop @ 4500 feet TVD. |
| 11/18/24              | 10:44:22              | 7217.20000              | 1912.913         | 101.61                | 4             | POOH static stop @ 4000 feet TVD. |
| 11/18/24              | 10:52:22              | 7225.20000              | 1692.948         | 95.75                 | 5             | POOH static stop @ 3500 feet TVD. |
| 11/18/24              | 10:58:12              | 7231.03300              | 1472.809         | 88.99                 | 6             | POOH static stop @ 3000 feet TVD. |
| 11/18/24              | 11:04:02              | 7236.86700              | 1252.629         | 84.40                 | 7             | POOH static stop @ 2500 feet TVD. |
| 11/18/24              | 11:10:02              | 7242.86700              | 1032.575         | 79.68                 | 8             | POOH static stop @ 2000 feet TVD. |
| 11/18/24              | 11:15:42              | 7248.53300              | 812.332          | 75.87                 | 9             | POOH static stop @ 1500 feet TVD. |
| 11/18/24              | 11:21:42              | 7254.53300              | 592.465          | 72.40                 | 10            | POOH static stop @ 1000 feet TVD. |
| 11/18/24              | 11:28:52              | 7261.70000              | 372.225          | 69.38                 | 11            | POOH static stop @ 500 feet TVD.  |
| 11/18/24              | 11:35:52              | 7268.70000              | 195.581          | 67.08                 | 12            | POOH static stop @ 100 feet TVD.  |
| 11/18/24              | 11:41:22              | 7274.20000              | 147.270          | 65.36                 | 13            | POOH static stop @ 0 feet TVD.    |



# BOTTOM HOLE PLOTS (Gauge #50766) Start=11/13/2024 10:27:10





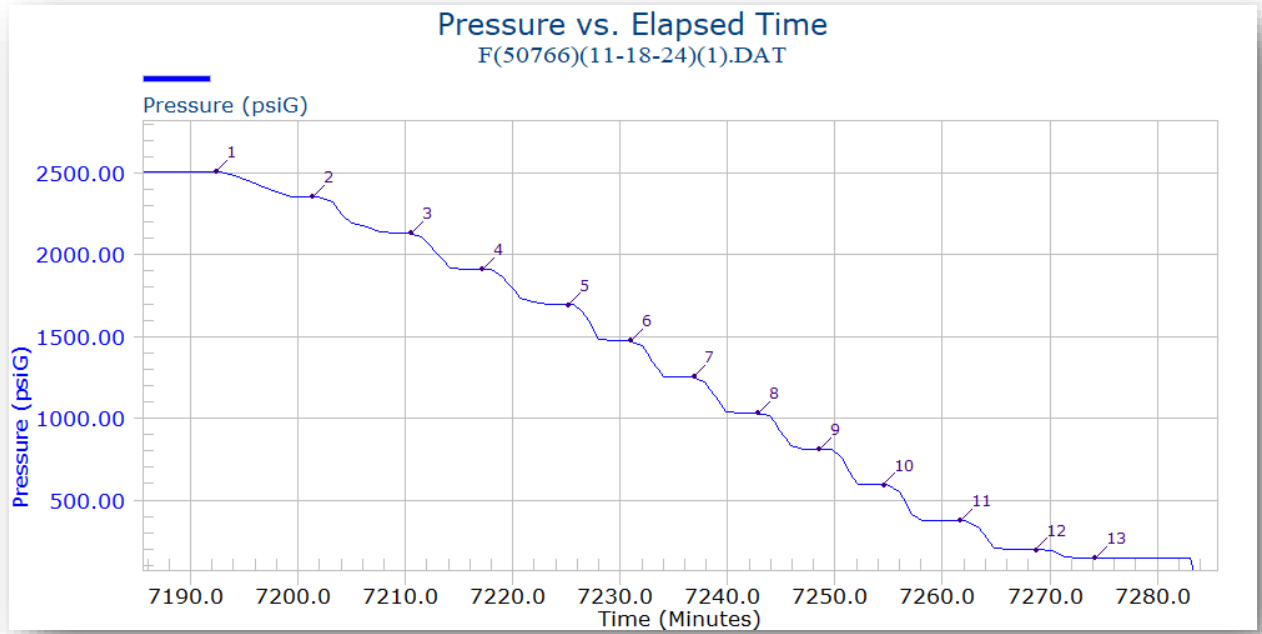
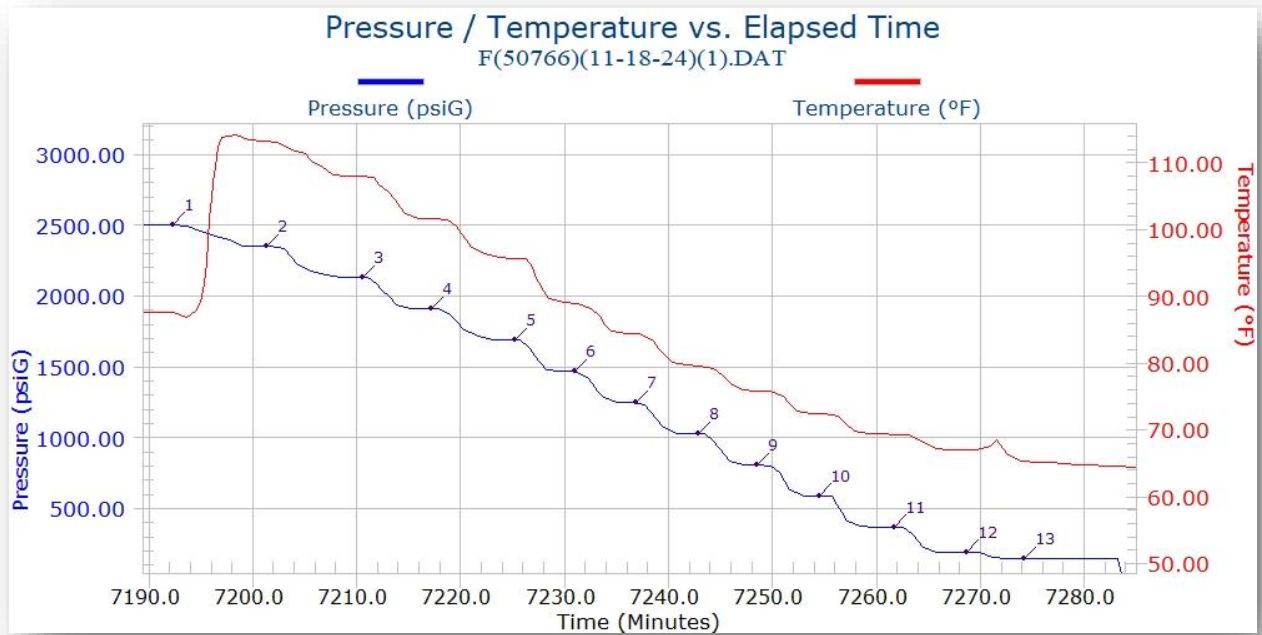
File Name: F(50766)(11-18-24)(1).DAT

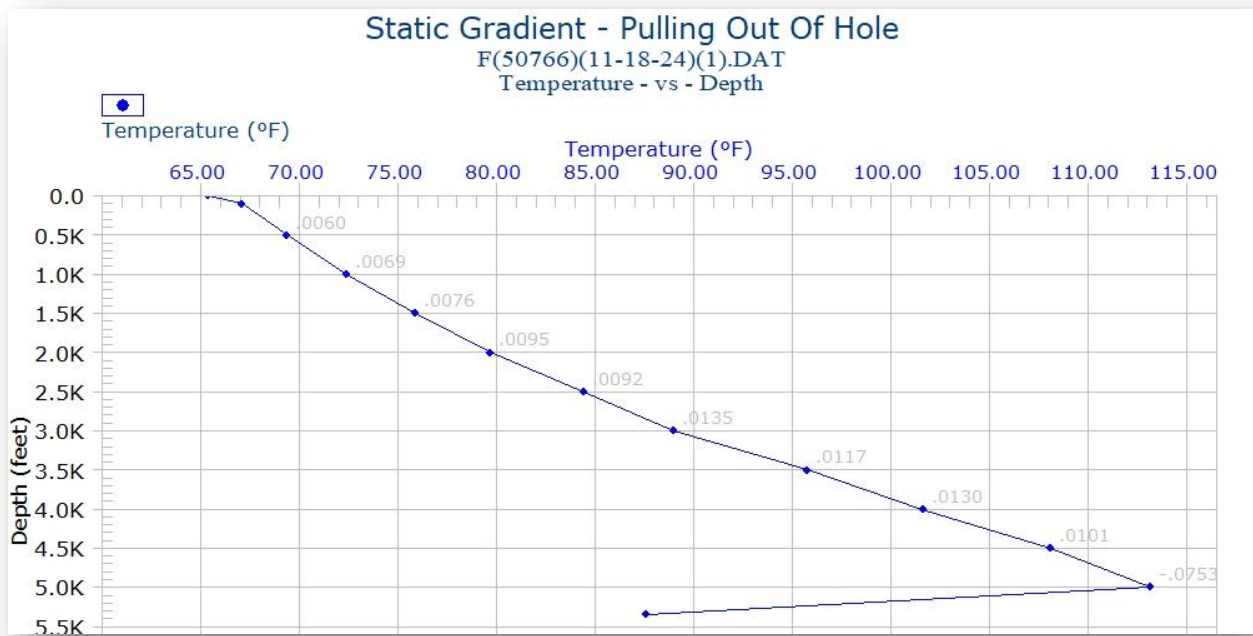
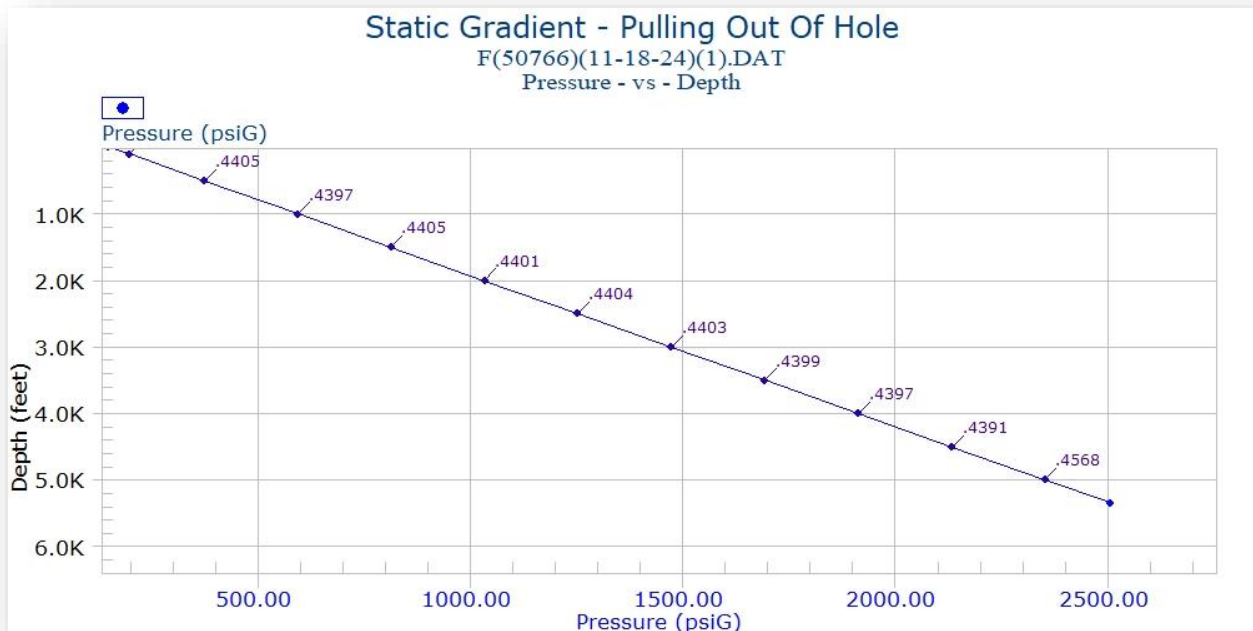
### Static Survey - Pulling Out of the Hole

| Real Date<br>MM/DD/YY | Real Time<br>HH:MM:SS | Elapsed Time<br>Minutes | WLM<br>feet | TVD<br>feet | Pressure<br>(psiG) | Gradient<br>(psiG/feet) | Temperature<br>(deg. F) | Gradient<br>(deg. F/feet) |
|-----------------------|-----------------------|-------------------------|-------------|-------------|--------------------|-------------------------|-------------------------|---------------------------|
| 11/18/24              | 11:41:22              | 7274.20000              | 0           | 0           | 147.270            | .4831                   | 65.356                  | .0173                     |
| 11/18/24              | 11:35:52              | 7268.70000              | 0           | 100         | 195.581            | .4416                   | 67.081                  | .0057                     |
| 11/18/24              | 11:28:52              | 7261.70000              | 0           | 500         | 372.225            | .4405                   | 69.376                  | .0060                     |
| 11/18/24              | 11:21:42              | 7254.53333              | 0           | 1000        | 592.465            | .4397                   | 72.401                  | .0069                     |
| 11/18/24              | 11:15:42              | 7248.53333              | 0           | 1500        | 812.332            | .4405                   | 75.872                  | .0076                     |
| 11/18/24              | 11:10:02              | 7242.86667              | 0           | 2000        | 1032.575           | .4401                   | 79.676                  | .0095                     |
| 11/18/24              | 11:04:02              | 7236.86667              | 0           | 2500        | 1252.629           | .4404                   | 84.404                  | .0092                     |
| 11/18/24              | 10:58:12              | 7231.03333              | 0           | 3000        | 1472.809           | .4403                   | 88.991                  | .0135                     |
| 11/18/24              | 10:52:22              | 7225.20000              | 0           | 3500        | 1692.948           | .4399                   | 95.748                  | .0117                     |
| 11/18/24              | 10:44:22              | 7217.20000              | 0           | 4000        | 1912.913           | .4397                   | 101.613                 | .0130                     |
| 11/18/24              | 10:37:42              | 7210.53333              | 0           | 4500        | 2132.756           | .4391                   | 108.093                 | .0101                     |
| 11/18/24              | 10:28:32              | 7201.36667              | 0           | 5000        | 2352.281           | .4568                   | 113.165                 | -.0753                    |
| 11/18/24              | 10:19:32              | 7192.36667              | 0           | 5340        | 2507.588           |                         | 87.573                  |                           |



# GRADIENT PLOTS (Top Gauge #50766)







# SURFACE DATA SECTION



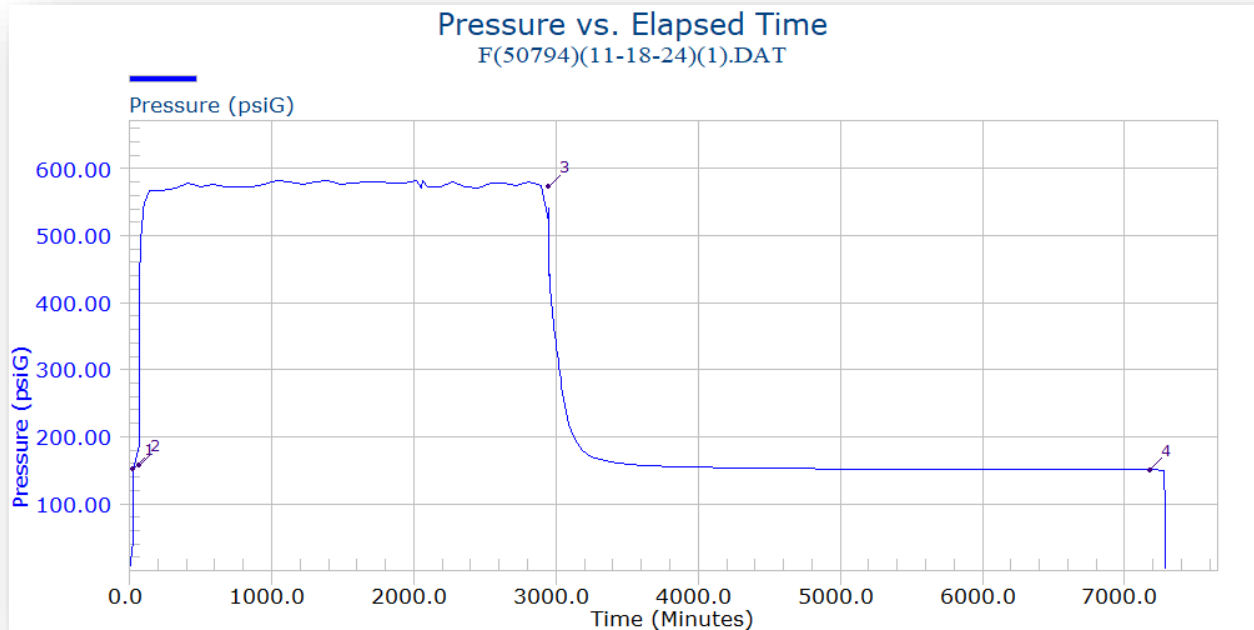
Filename: F(50794)(11-18-24)(1).DAT  
Power Up Date: 11/13/24  
Power Up Time: 10:22:10

## Event Summary

| Real Date<br>MM/DD/YY | Real Time<br>HH:MM:SS | Elapsed Time<br>Minutes | Pressure<br>psiG | Temperature<br>deg. F | Tag<br>Number | Comment                      |
|-----------------------|-----------------------|-------------------------|------------------|-----------------------|---------------|------------------------------|
| 11/13/24              | 10:47:42              | 25.53330                | 151.644          | 68.65                 | 1             | OPEN WELLHEAD SURFACE GAUGE  |
| 11/13/24              | 11:30:12              | 68.03330                | 157.686          | 67.73                 | 2             | INJECTION PUMP START         |
| 11/15/24              | 11:29:15              | 2947.08300              | 572.824          | 75.84                 | 3             | INJECTION STOP BEGIN SHUT-IN |
| 11/18/24              | 10:03:55              | 7181.75000              | 150.460          | 62.58                 | 4             | END FALL-OFF TEST            |



SURFACE DATA (Gauge #50794) Start=11/13/2024 10:22:10



## **APPENDIX F**

### **RESPONSE TO NOTICE OF DEFICIENCY LETTER DATED OCTOBER 9, 2013 - RESPONSE TO DEFICIENCY NUMBER 7**



## DEFICIENCY NUMBER 7

The projected pressure increase from the Mid – Way injection well in the report document was based on a homogenous infinite acting model calculation. The calculation does not address any possible reservoir geologic boundaries such as faults or other active injection wells that may be present. The second fall – off test had a response at late test times indicating more than a single boundary, which may represent nearby faulting impacts, was present and that area well data indicated at least two other active injectors are present with one of them confirmed as disposing into the same formation as the proposed Mid – Way well. Pressure buildup projections in the permit application should address both the fault concerns identified on the fall – off test and the impact of other area injectors, as well as any producers in the same injection zone. Also, please comment on the sufficiency of the detailed deep reservoir characteristics given the presence of large faults in the regional area and the evidence of nearby faults in the fall – off tests.

### **Response:**

In order to properly address Deficiency Number 7, this response will provide for a re-assessment of the second fall-off test; assessment of possible reservoir geologic boundaries; re-analysis of pressure buildup projections based on possible boundaries; and a discussion regarding the sufficiency of deep reservoir characteristics.

In this response, Mid-Way has primarily focused on the results of the second pressure fall-off test conducted in October 2010. Due to placement of the pressure gauges at a depth well below the injection zone, the first test, conducted in May 2010, did not result in significant pressure increases/fall-off records to effectively analyze the test as explained in Section 8 of the *MES Construction Completion Report and Application for Operating Permit*. Additionally, well stimulation activities were conducted after the May 2010 test.

In responding to Deficiency Number 7, Mid-Way engaged Dr. Evren Ozbayoglu, an associate professor at the University of Tulsa - McDougall School of Petroleum Engineering, to provide an independent third party review of the deficiency comments and also to perform the necessary modeling and projection calculations based on information collected by A&M Engineering and other subcontractors such as Schlumberger. It is important to note that all test data utilized in responding to this deficiency has been provided to the DEQ through previous submittals. Dr. Ozbayoglu's analysis is provided as **Attachment 2**.

In addition, Mid-Way also requested the services of Schlumberger to perform a re-evaluation of their previous dual porosity, infinite acting model based Transient Analysis Report. Schlumberger's re-evaluation report is provided as **Attachment 4**.

### **Dr. Ozbayoglu's Review**

In light of DEQ's deficiency comments, Dr. Ozbayoglu performed a re-assessment of the second fall-off test for MES #1 utilizing test data that was previously submitted to DEQ in **Appendix Q** of the *MES Construction Completion Report and Application for Operating Permit*. Dr. Ozbayoglu's assessment of the second fall-off test data was consistent with EPA's analysis showing a response at late test times that matched a homogenous reservoir type curve having two perpendicular no-flow boundaries. Dr. Ozbayoglu's analysis concurs with the possible presence of two perpendicular no-flow boundaries and he calculates both boundaries to be approximately 1200 feet from MES #1. Dr. Ozbayoglu's analysis indicated a high reservoir permeability of approximately 2000 md, which is also consistent with EPA's assessment. As a result, and for purposes of reservoir evaluation and modeling, Dr. Ozbayoglu considered the reservoir at MES #1 to be a homogeneous system with the presence of two perpendicular no-flow boundaries when making his hydraulic calculations.

Dr. Ozbayoglu does caution in his report that DEQ's reference to faulting impacts identified on the fall-off test requires a clarification. The term "fault" in transient analysis refers to a no-flow boundary, which may or may not be due to a geologic fault. While faulting is known to occur regionally throughout Lincoln County, results of evaluation conducted and previously provided in the *MES Construction Completion Report and Application for Operating Permit* (and in response to the Notice of Deficiency Letter dated February 8, 2013), did not identify any known faults that penetrated the Arbuckle Group in the immediate area of MES #1. There is no geologic evidence to suggest that the nearby no-flow boundaries indicated by the testing analysis are due to a geological fault(s). However, because geology is an important factor that must be considered during the interpretation of pressure fall-off test data, Mid-Way has again examined the geology and known faulting conditions in the regional area of the MES #1 injection well. The results of the geologic re-examination are included in **Attachment 5**.

In addition to the perpendicular no-flow boundaries, Dr. Ozbayoglu also considered the possible impact of nearby injectors as identified in DEQ's comments. The Twin Cities injector is situated approximately 0.82 miles from MES #1. Well logs have identified that the Twin Cities injector also targets the Arbuckle Group for saltwater disposal. The Twin Cities injector has been in operation for approximately 10 years, injecting up to a maximum average of 13 bbl/min. According to Oklahoma Corporation Commission records, the average injection rate for the well during a six year period of record was 7.55 bbl/min; with a maximum average rate

of 12.97 bbl/min injected in 2009. For evaluation purposes, Dr. Ozbayoglu utilized the maximum injection rate of 13 bbl/min.

To date, no increase in pressure has been observed at MES #1 since 2010 thereby indicating that either the injector is located on the other side of a possible no-flow boundary and therefore not impacting MES #1, or that the effect of the injector is very limited due to the high permeability of the reservoir. Despite the possibility that the Twin Cities injector may not be hydraulically connected to MES #1, Dr. Ozbayoglu does consider the possible interference of the injector in his hydraulic calculations.

The second injector identified by DEQ, Wm. T. Tipton #2, is located approximately 0.76 miles from MES #1; targets the Prue Sand formation at a depth of 3505 to 3517 feet; and is approximately 1600 feet shallower than the top of the Arbuckle. Oklahoma Corporation Commission records indicate that, historically, injection into the Wm. T. Tipton #2 was limited to approximately 200 bbl/year. Injection rates over the last few years have increased to 1825 bbls/year. However, injection into the Prue Sand is not anticipated to have an effect on the Arbuckle Group. Several shale layers including those of the lower Pennsylvanian strata and the confining Woodford and Sylvan Shales, isolate the Prue from the top of the Arbuckle.

Dr. Ozbayoglu’s initial hydraulic calculations examined the reservoir fracture pressure and local pressure buildup scenarios at MES #1. Dr. Ozbayoglu used the following input data in performing his hydraulic calculations:

|   |       |
|---|-------|
| Formation pressure gradient (psi/ft)                    | 0.472 |
| Fracture pressure gradient (psi/ft)                     | 0.639 |
| Tubing inner diameter (in)                              | 3.958 |
| Tubing length (ft)                                      | 5080  |
| Relative roughness                                      | 0     |
| Injected fluid specific gravity                         | 1.2   |
| Plastic viscosity of injected fluid (cp)                | 1.1   |
| Yield point of injected fluid (lb/100 ft <sup>2</sup> ) | 0     |
| Average formation permeability (md)                     | 2000  |
| Average formation porosity (%)                          | 13.5  |
| Effective formation thickness (ft)                      | 180   |
| Well openhole diameter (in)                             | 7.875 |
| Depth of top of the injection zone (ft)                 | 5080  |

Dr. Ozbayoglu calculated the theoretical maximum allowable injection rate for MES #1 which over a 50 year injection period, would not induce fracturing of the reservoir formation. The theoretical maximum allowable injection rate was calculated to be 35 bbl/min which

corresponds to a surface injection pressure of 2660 psi and a bottom hole pressure slightly less than the calculated formation fracture pressure of 3245.8 psi. Mid-Way has requested a maximum surface injection pressure of 1350 psi, approximately 50% less than the pressure required to initiate formation fracture. A surface injection pressure of 1350 psi correlates to an injection rate of 23.4 bbl/min. To illustrate the formation response to injection, Dr. Ozbayoglu provides pressure calculations for flow rates of 10, 15, 20 and 24 bbl/min at continuous injection periods of 1 day, 1 month, 1 year, 5 years, 10 years, 25 years and 50 years in Table 3 of his report.

To assess the radial impact of injection at MES #1, Dr. Ozbayoglu performed reservoir pressure buildup projection calculations at a distance from MES #1 based on a continuous injection rate of 23.4 bbl/min, which corresponds to the maximum surface injection pressure of 1350 psi requested by Mid-Way; a homogeneous reservoir model with the presence of two perpendicular no-flow boundaries; and the nearby Twin Cities injector. The pressure buildup projections are performed for continuous injection intervals of 10 years, 25 years and 50 years, as provided in Dr. Ozbayoglu's report as Figures 4, 5 and 6 respectively. These figures show the total pressure buildup at MES #1 over 50 years to be approximately 500 psi. It is important to note that Mid-Way does not anticipate continuous injection at 23.4 bpm. Mid-Way's Solid Waste Facility Permit restricts the facility from accepting more than 450 gpm (10.7 bbl/min) of waste on an annual operating basis and it is anticipated that the average annual injection rate will likewise approximate 450 gpm.

In addition to pressure buildup projections, Dr. Ozbayoglu performed wastewater front migration projections based on a homogeneous reservoir model with the presence of two perpendicular no-flow boundaries and considering the nearby Twin Cities injector. Since wastewater front migration is directly related to the volume of injectate injected over a period of time, Dr. Ozbayoglu considered a continuous injection rate of 11 bbl/min (462 gallons per minute) to be the maximum operating injection rate for the facility if it were to operate 24-hours per day and 7 days per week. Also, in this analysis Dr. Ozbayoglu used an effective injection zone of 300 feet rather than 180 feet indicating that the well stimulation previously performed resulted in an improvement of the effective injection interval. These input parameters were adjusted as such to provide a more realistic analysis of wastewater migration rather than examining worst case and unrealistic scenarios.

Dr. Ozbayoglu's model output for wastewater front migration is provided in Figures A.1 – A.5 of his report and show the wastewater front after 10, 20, 30, 40, and 50 years of continuous injection at 11 bbl/min. The furthest wastewater migration after 50 years of injection is projected to be approximately one mile from MES #1. Again, it is important to note that this is still a conservative projection because Mid-Way's maximum acceptance limit and anticipated

continuous injection rate of 450 gallons per minute is less than the 11 bbl/min injection rate that Dr. Ozbayoglu is using in his calculations.

### **Schlumberger's Review**

At the request of Mid-Way Environmental Services, Inc., Schlumberger performed a re-evaluation of the data collected during the October 15, 2010 pressure-fall-off test. Personnel conducting the re-evaluation were reminded of the use of large quantities of fresh water during the injection portion of the test; the use of acid to stimulate the Arbuckle Group after the May 2010 pressure fall-off testing; the geology of the site including the hydraulic connection between the Arbuckle Group and the lowermost sands of the Simpson Group; and a general description of the dolomites and sands of the Arbuckle Group. In addition, transient analysis performed by EPA and provided to Mid-Way by DEQ and EPA was provided to Schlumberger for review and consideration.

In the re-evaluation, Schlumberger again supports the dual porosity model, but does not consider the reservoir to be infinite. Schlumberger states that the pressure derivative in the later time region (after ~35 hours) could be the result of the short injection period or may indicate reservoir boundaries. However, the dual porosity model is again supported because of the radial flow periods observed.

Discussion with Schlumberger indicated that similar plots to that observed in MES #1 (two periods of radial flow with a half-slope transition) have been observed in other reservoir systems containing fluids with distinct viscosities and densities.

Schlumberger's re-evaluation report is included in **Attachment 4**.

### **Conclusions**

In assessing the second pressure fall-off test, Dr. Ozbayoglu used a homogeneous reservoir model with the possible presence of two no-flow boundaries (consistent with EPA's assessment) and conducted reservoir evaluation and modeling considering this model. Schlumberger supported a dual porosity reservoir model with a transition between two radial flow regimes. As evident by EPA, Dr. Ozbayoglu, and Schlumberger, interpretations are not always consistent. Different models can be supported and projections can be calculated accordingly. For example, the observed half-slope observed could be consistent with the homogeneous reservoir with two no-flow boundaries or, it could be a transition zone in a composite system which explains the two radial flow regimes observed by Schlumberger. However, for reservoir calculations and analysis, it is believed that "worst case" scenarios were utilized and under the proposed operating conditions, anticipated formation pressure buildup and water front projections are within acceptable limits.

Mid-Way believes other factors associated with the pressure fall-off test may affect the interpretation of results. They include the use of large amounts of fresh water in the tests, which due to density and viscosity differences between the formation fluids and fresh water may have impacted the overall test results and interpretation.

Injection of fresh water into a salt-water bearing fractured dolomite formation (similar to the Arbuckle) has been shown to result in convection currents being established within the formation (Hickey, 1989 included in **Attachment 6**). Circulation occurs as a result of density gradients related to salinity variations. The effect of possible convection currents on the results of the MES #1 short term pressure fall-off test is unknown.

Dr. Ozbayoglu concurred with EPA's interpretation of a finite homogeneous system model having two possible perpendicular no-flow boundaries. Since the nearby Twin Cities injector has been identified as the only injector within the 1-mile well review area to be targeting the Arbuckle Group for saltwater disposal, Dr. Ozbayoglu also assumed that the Twin Cities injector impacted MES #1 despite reports that no impact has been observed at MES #1 since drilling of the MES #1 well in 2010. Based on this model, Dr. Ozbayoglu examined formation response to injection; assessed formation fracture pressures; and projected reservoir pressure buildup and wastewater front migration from MES #1.

Dr. Ozbayoglu determined that a surface injection pressure greater than 2660 psi, applied for 50 years on a continuous basis, would be required to initiate fracture of the reservoir formation. This surface injection pressure correlates to an injection rate of 35 bbl/min and a bottom hole pressure just below the formation fracture pressure of 3245.8 psi after 50 years. Based on this assessment, Mid-Way's requested surface injection pressure of 1350 psi provides a Safety Factor of 1.97 (based on the pressure ratio of 2660/1350 psi) if the well was to operate at this maximum pressure on a continuous basis. Pressure buildup projections were based on the requested maximum surface injection pressure of 1350 psi. The associated continuous flow rate of 23.4 bbl/min was utilized by Dr. Ozbayoglu to develop pressure buildup projections at 10, 25 and 50 years showing that pressure buildup would not exceed the formation fracture pressure.

However, despite performing the pressure buildup calculations at 23.4 bbl/min, Mid-Way is unable to inject at that rate on a continuous basis due to restrictions in the facilities acceptance capacity. When considering that the total allowable injection volume is limited to the facility's total allowable acceptance volume of 450 gallons per minute (10.7 bbl/min), disposal on a continuous basis results in a safety factor of 2.18 (based on the injection rate ratio of 23.4/10.7 bbl/min) with regard to Dr. Ozbayoglu's calculations.

In projecting wastewater front migration, Dr. Ozbayoglu adjusted the effective injection zone thickness to provide a more realistic analysis. A thickness of 180 ft was initially established as a *minimum* effective injection zone thickness based on initial testing of the well in May 2010. Temperature survey logs indicated a larger interval that was initially accepting injected fresh water. An improvement to wellbore conditions was identified in the second fall-off test and was the result of acid stimulation of the well. As a result, Dr. Ozbayoglu justifies the use of a 300 ft effective injection zone thickness and utilizes this value in calculating the wastewater front migration front. Additionally, since wastewater front calculations are driven by injection volumes, Dr. Ozbayoglu uses a continuous injection rate of 11 bbl/min to be more consistent with the facility's permit limitations. Based on these input values, a homogeneous reservoir model with two perpendicular no-flow boundaries and the nearby Twin Cities injector, it is determined that the wastewater front will be approximately one mile away from MES #1 after 50 years of continuous injection.

Schlumberger's interpretation supported a dual porosity reservoir model with a transition between two radial flow regimes. The source of this heterogeneity could possibly be the difference in the viscosity and density of the reservoir fluid and the fresh water which was injected into the reservoir or the change in the permeability. This scenario better explains the two radial flow regimes.

### **Summary of Conclusions**

Although there are differing professional opinions on the exact reservoir model which can be applied to MES #1, modeling of anticipated formation pressures increase, pressure distribution within the formation, and advancement of the injected fluid front under extreme (worst case) operating conditions indicates the formation is suitable and able to safely accept injected liquids, without concern for exceedances of formation fracture pressure and the initiation of fractures. In fact, the Arbuckle Group has historically been used for the safe injection of waste water generated from oil exploration and production activities.

Considering Mid-Way's permit limitation based on facility acceptance volume (i.e., 450 gpm (10.7 bbl/min)) it is anticipated that the average operating injection rate at MES #1 will be similar. The surface injection pressure corresponding to an injection rate of 450 gpm at MES #1 will be far below the requested maximum surface injection pressure of 1350 psi. As provided in Table 9-1 of the *MES Construction Completion Report and Application for Operating Permit*, Schlumberger's Injection Rate and Pressure Simulation, based on injection data from the October 2010 Injection and Pressure Fall-Off Test, indicates that the surface injection pressure corresponding to an injection rate of 450 gpm (for 24 hours of steady pumping) is anticipated to be less than 750 psi.

However, in order to provide for the anticipated short term need to inject at a greater rate (due to facility down time, well maintenance activities, etc.) Mid-Way requested a maximum surface injection pressure of 1350 psi. Evaluation indicates that for injection at this maximum pressure for a 50 year period, the associated rate of injection (23.4 bbl/min) still provides a suitable margin of safety to ensure formation fracture propagation does not occur.

Analysis has also indicated that there are no nearby surface or deep seated faults in the area that will be affected by the projected injection operations at MES #1. Based on anticipated operating conditions, calculated pressure increases and distribution, Mid-Way believes there is no need to increase the Area of Review beyond the regulatory limits.

# **APPENDIX G**

## **ANALYSIS ON HYDRAULICS DURING INJECTION PROCESS AND PRESSURE DISTRIBUTION WITHIN THE FORMATION**

**BY  
EVREN M. OZBAYOGLU  
DECEMBER 2013**



**- Report -**

# **Mid-Way MES #1**

**Analysis on  
Hydraulics during Injection Process, and  
Pressure Distribution within the Formation**

**Prepared by**

**Evren M. Ozbayoglu, PhD**

**December, 2013**

## Table of Content

|  |    |
|--|----|
| Objective .....  | 4  |
| Short Biography .....  | 5  |
| 1. Summary .....   | 6  |
| 2. Pressure Distribution during Injection Process.....                                   | 6  |
| 2.1 <i>Injection Process</i> .....   | 6  |
| 2.2 <i>Hydraulic Calculations Inside Tubing and Formation</i> .....                      | 8  |
| 2.3 <i>Pressure Distribution within the Formation</i> .....                              | 12 |
| 2.4 <i>Permeability and Skin Factor Analysis</i> .....                                   | 16 |
| 2.5 Advancement of the Front End of the Injected Fluid .....                             | 19 |
| APPENDIX – A.....  | 24 |
| Answers to “Notice of Deficiency” .....  | 24 |
| Deficiency No: 2 .....   | 24 |
| Deficiency No: 5 .....   | 24 |
| Deficiency No: 6 .....   | 24 |
| Deficiency No: 7 .....   | 25 |
| Deficiency No: 8 .....   | 26 |
| APPENDIX – B .....   | 28 |
| Theory for Hydraulics of Injection Process .....   | 28 |
| B.1 Flow in Circular Pipes .....   | 28 |
| B.1.1 <i>Fluid Rheology</i> .....  | 28 |
| B.1.2 <i>Flow Regime</i> .....   | 29 |
| B.1.3 <i>Determination of the Laminar/Turbulent Boundary for a Newtonian Fluid</i> ..... | 30 |
| B.1.4 <i>Critical Reynolds Number for Bingham Plastic Fluids</i> .....                   | 31 |
| B.1.5 <i>Friction Factor</i> .....   | 32 |
| B.1.6 <i>Hydrostatic Pressure</i> .....  | 34 |
| B.2 Flow in Reservoir.....   | 34 |
| B.2.1 <i>Permeability and Skin Factor Analysis</i> .....                                 | 35 |
| B.3 <i>Approximate Estimation of the Front End of the Injected Fluid</i> .....           | 40 |
| B. References .....  | 41 |
| APPENDIX – C.....  | 42 |
| CURRICULUM VITAE.....  | 42 |

## Figures

|              |  |    |
|--------------|--|----|
| Figure – 1   | Mid-Way MES-#1 – Schematic View .....  | 7  |
| Figure – 2   | Injection free body diagram.....   | 8  |
| Figure – 4   | Pressure distribution within the formation after 10 years of injection of Mid-Way MES #1 for 23.4 bbl/min injection rate ..... | 13 |
| Figure – 5   | Pressure distribution within the formation after 25 years of injection of Mid-Way MES-#1 for 23.4 bbl/min injection rate.....  | 14 |
| Figure – 6   | Pressure distribution within the formation after 50 years of injection of Mid-Way MES-#1 for 23.4 bbl/min injection rate.....  | 15 |
| Figure – 7   | The diagnostic plot corresponding to the fall off period of the October 2010 test. ....  | 17 |
| Figure – 8   | Bottomhole pressure fall off versus Horner time during fall off test corresponding to the radial flow region .....             | 18 |
| Figure – A.1 | Injection fluid saturation after 10 years of injection with a flow rate of 11 bbl/min. ....                                    | 20 |
| Figure – A.2 | Injection fluid saturation after 20 years of injection with a flow rate of 11 bbl/min. ....                                    | 21 |
| Figure – A.3 | Injection fluid saturation after 30 years of injection with a flow rate of 11 bbl/min. ....                                    | 21 |
| Figure – A.4 | Injection fluid saturation after 40 years of injection with a flow rate of 11 bbl/min. ....                                    | 22 |
| Figure – A.5 | Injection fluid saturation after 50 years of injection with a flow rate of 11 bbl/min. ....                                    | 22 |
| Figure – B.1 | Rheogram for Bingham Plastic fluids (HWU, 2007) .....  | 29 |
| Figure – B.2 | Flow regimes (HWU, 2007) .....   | 30 |
| Figure – B.3 | Hedstrom number versus critical Reynolds number (Bourgoyne et al, 1998).....   | 32 |
| Figure – B4  | No-flow boundary systems (Stewart, 2011) .....   | 38 |
| Figure – B5  | Pressure derivative response for different fault systems (Stewart, 2011) .....   | 40 |

## Tables

|           |   |    |
|-----------|---|----|
| Table – 1 | Input data used for the hydraulic calculations .....                                    | 9  |
| Table – 2 | Frictional pressure losses and hydrostatic pressure calculations inside the tubing..... | 10 |
| Table – 3 | Estimation of bottomhole pressure and injection pressure at the surface.....            | 11 |

## **Objective**

This report is prepared as a third party opinion on the performance and behavior of the Mid-Way Environmental Services, Inc. (Mid-Way) injection well (MES #1) based on a 50 year injection period into an interval of approximately 5080ft – 5260 ft in the Arbuckle Formation. Based on the pressure fall-off test considered, formation in consideration fits to a homogeneous formation with the presence of perpendicular no-flow boundaries.

This report includes surface and bottomhole pressure calculations considering the hydraulics inside the tubing string as well as flow within the formation; and pressure distribution within the formation considering the no-flow boundaries as well as the interference of another nearby injection well, Twin Cities.

## Short Biography

Evren M. Ozbayoglu is currently an Associate Professor of The University of Tulsa, McDougall School of Petroleum Engineering. He has earned his B.Sc and M.Sc. from Middle East Technical University (METU), Petroleum & Natural Gas Engineering Department, Ankara – Turkey, and his PhD degree from The University of Tulsa. He worked as a faculty at METU, Petroleum & Natural Gas Engineering Department till 2009, and he is working for TU since then. His work is mostly focused on drilling engineering related topics, such as non-Newtonian fluid behavior and hydraulics, multiphase flow, foams, cuttings transport and hole cleaning, tubular mechanics, directional and horizontal drilling, etc. He has numerous publications, papers and book chapters, and participated in several industrial projects related with these topics. He has been teaching drilling engineering oriented courses in undergraduate and graduate level for more than 10 years. He was awarded for “Allen Chapman Distinguished PhD Student” in 2002, and “Prof.Dr Mustafa Parlar – METU Educator of the Year” in 2003, 2005 and 2006. He is an SPE member since 1994.

### Contact Information:

Evren M. Ozbayoglu, PhD  
Associate Professor Dr.  
The University of Tulsa  
McDougall School of Petroleum Engineering Department  
800 S Tucker Dr. Tulsa OK 74104  
Tel: 918-631 2972  
e-mail: [evren-ozbayoglu@utulsa.edu](mailto:evren-ozbayoglu@utulsa.edu)

**Report  
Mid-Way MES #1**

**Analysis on  
Formation / Fracture Pressures,  
Hydraulics during Injection Process, and  
Tubular Stability**

**1. Summary**

Mid-Way MES #1 is located within Section 9-14N-5E in Lincoln County, Oklahoma. Based on the information obtained from the pressure distribution in this field, maximum injection rates, maximum injection pressures at the surface and corresponding bottomhole pressures are estimated. Also, considering a “transition” period, pressure distribution in the formation was calculated as a function of time assuming continuous injection at the maximum injection rate.

Formation is considered to be a homogeneous system with the presence of two perpendicular no-flow boundaries. Also, there exists an interfering nearby injection well, Twin Cities, which is about 0.8 miles away from Mid-Way MES #1, continuously injecting with a flow rate of 13 bbl/min for 10 years.

**2. Pressure Distribution during Injection Process**

Estimation of the required injection pressures at the surface, bottomhole pressures, and the pressure distribution in the formations due to the injection process require estimation of hydrostatic pressure distribution and frictional pressure losses inside the tubing during the injection process, and the pressure drop occurring as the injection fluid flows through the porous media in the horizontal plane.

***2.1 Injection Process***

A schematic of Mid-Way MES #1 is presented below (Fig.1). The well is vertical with a total depth of 7040 ft. The open hole size is 7<sup>7/8</sup> in. A 8<sup>5/8</sup> in. J-55 32 lb/ft casing is set at 5173 ft, and cemented up to the surface. An injection tubing of 4<sup>1/2</sup> in. J-55 12.75 lb/ft LTC is installed to a depth of 5203 ft, with a packer at 5115.5 ft.

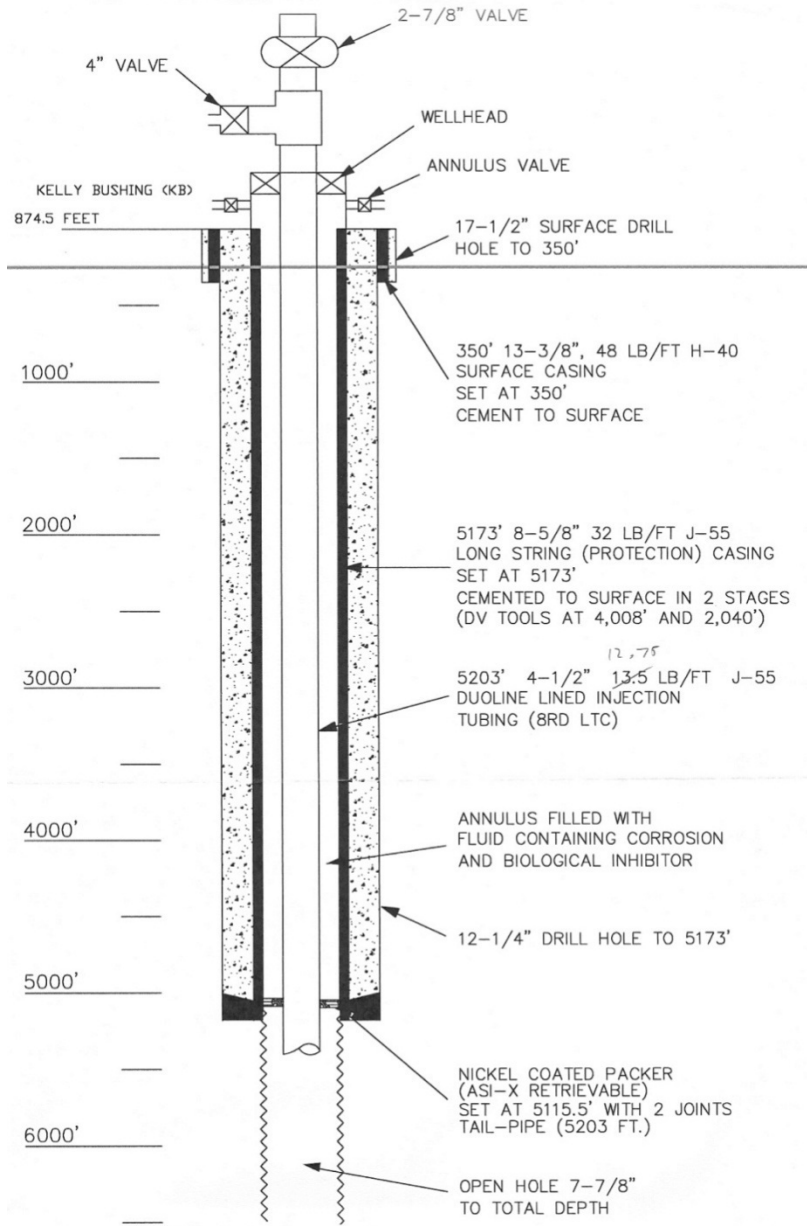


Figure – 1 Mid-Way MES-#1 – Schematic View

A 10.0 ppg (sp.gr.=1.2) fluid with an average plastic viscosity of 1.1cp (kinematic viscosity = 1.17E-5 ft<sup>2</sup>/s) with no yield stress is assumed to be injected from the surface into the Arbuckle formation starting at depth of 5,080 ft. Previous injection tests conducted in Mid-Way MES #1 indicated that the injected fluid goes into the formations at approximate depths of 5080 – 5260 ft, therefore the effective injection interval is assumed to be approximately 180 ft.

A schematic of the injection process and the calculation methodology of the pressure distribution, considering hydrostatic pressure, frictional losses, and flow in porous media are presented below (Fig.2).

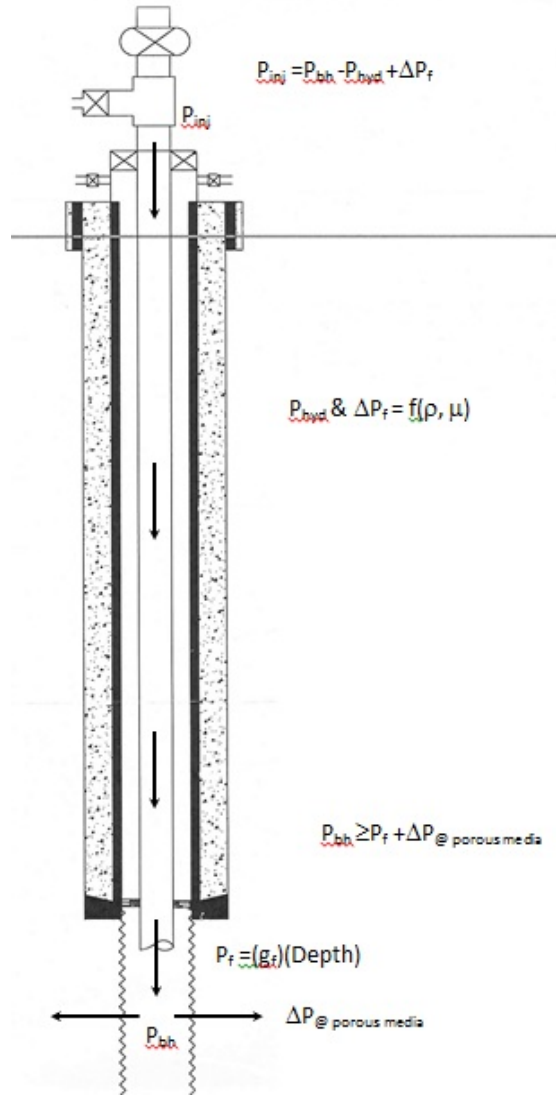


Figure – 2 Injection free body diagram

## 2.2 Hydraulic Calculations Inside Tubing and Formation

Calculation procedure is as follows:

1. Formation pressure is determined using the formation pressure gradient and depth.
2. Frictional pressure losses and hydrostatic pressure inside the tubing are calculated.
3. Pressure change in porous media is determined using the transient radial flow equation with the help of superposition approach considering no-flow boundaries as well as interfering nearby injection well.
4. Bottomhole pressure is estimated using formation pressure and pressure change in porous media (upper limit is the fracture pressure).

5. Injection pressure is determined using bottomhole pressure, hydrostatic pressure inside the tubing, and frictional pressure losses inside the tubing.

During the injection process, the formation is not allowed to be fractured. Therefore, there exists a maximum injection rate that generates a bottomhole pressure theoretically equal to the fracture resistance of the formation. Using this constraint, the maximum injection rate can be determined. Calculations are conducted using the following input data (Table-1):

Table – 1 Input data used for the hydraulic calculations

|   |       |
|---|-------|
| Formation pressure gradient (psi/ft)                    | 0.472 |
| Fracture pressure gradient (psi/ft)                     | 0.639 |
| Tubing inner diameter (in)                              | 3.958 |
| Tubing length (ft)                                      | 5080  |
| Relative roughness                                      | 0     |
| Injected fluid specific gravity                         | 1.2   |
| Plastic viscosity of injected fluid (cp)                | 1.1   |
| Yield point of injected fluid (lb/100 ft <sup>2</sup> ) | 0     |
| Average formation permeability (md)                     | 2000  |
| Average formation porosity (%)                          | 13.5  |
| Effective formation thickness (ft)                      | 180   |
| Well openhole diameter (in)                             | 7.875 |
| Depth of top of the injection zone (ft)                 | 5080  |

Using the equations provided in Appendix-B for hydrostatic pressure (Equation-B.16), frictional pressure loss (Equation-B.11), pressure behavior using the superposition principle in time (Equation-B.38), bottomhole pressures and required surface pressures for the injection process for different injection rates are calculated.

Table-2 provides the information about the frictional pressure losses and hydrostatic pressures for a specific injection flow rate.

Table-3 presents the results for the pressure change expected in the formation due to the injection process as a function of time, injection pressure at the surface and related bottomhole pressure, and the comparison of this pressure with the maximum allowable bottomhole pressure (which is equal to the fracture pressure).

Table – 2 Frictional pressure losses and hydrostatic pressure calculations inside the tubing

| injection rate (bbl/min) | velocity inside tubing (ft/s) | effective viscosity (cp) | Reynolds number | Hedstrom number | critical Reynolds number | Flow Regime | friction factor | frictional pressure loss gradient (psi/ft) | frictional pressure loss (psi) | hydrostatic pressure (psi) |
|--------------------------|-------------------------------|--------------------------|-----------------|-----------------|--------------------------|-------------|-----------------|--|--------------------------------|----------------------------|
| 2                        | 2.2                           | 1.1                      | 73197.2         | 0               | 2100                     | Turbulent   | 0.00476         | 0.002                                      | 11.8                           | 2707.7                     |
| 4                        | 4.4                           | 1.1                      | 146394.5        | 0               | 2100                     | Turbulent   | 0.00412         | 0.008                                      | 40.8                           | 2707.7                     |
| 6                        | 6.6                           | 1.1                      | 219591.7        | 0               | 2100                     | Turbulent   | 0.00381         | 0.016                                      | 84.8                           | 2707.7                     |
| 8                        | 8.8                           | 1.1                      | 292788.9        | 0               | 2100                     | Turbulent   | 0.00360         | 0.027                                      | 142.7                          | 2707.7                     |
| 10                       | 11.0                          | 1.1                      | 365986.2        | 0               | 2100                     | Turbulent   | 0.00346         | 0.041                                      | 213.9                          | 2707.7                     |
| 12                       | 13.1                          | 1.1                      | 439183.4        | 0               | 2100                     | Turbulent   | 0.00334         | 0.057                                      | 298.0                          | 2707.7                     |
| 14                       | 15.3                          | 1.1                      | 512380.6        | 0               | 2100                     | Turbulent   | 0.00325         | 0.076                                      | 394.5                          | 2707.7                     |
| 16                       | 17.5                          | 1.1                      | 585577.9        | 0               | 2100                     | Turbulent   | 0.00318         | 0.097                                      | 503.2                          | 2707.7                     |
| 18                       | 19.7                          | 1.1                      | 658775.1        | 0               | 2100                     | Turbulent   | 0.00311         | 0.120                                      | 623.8                          | 2707.7                     |
| 20                       | 21.9                          | 1.1                      | 731972.3        | 0               | 2100                     | Turbulent   | 0.00306         | 0.145                                      | 756.2                          | 2707.7                     |
| 22                       | 24.1                          | 1.1                      | 805169.6        | 0               | 2100                     | Turbulent   | 0.00301         | 0.173                                      | 900.1                          | 2707.7                     |
| 24                       | 26.3                          | 1.1                      | 878366.8        | 0               | 2100                     | Turbulent   | 0.00296         | 0.203                                      | 1055.4                         | 2707.7                     |
| 26                       | 28.5                          | 1.1                      | 951564.0        | 0               | 2100                     | Turbulent   | 0.00292         | 0.235                                      | 1221.9                         | 2707.7                     |
| 28                       | 30.7                          | 1.1                      | 1024761.3       | 0               | 2100                     | Turbulent   | 0.00288         | 0.269                                      | 1399.6                         | 2707.7                     |
| 30                       | 32.9                          | 1.1                      | 1097958.5       | 0               | 2100                     | Turbulent   | 0.00285         | 0.305                                      | 1588.2                         | 2707.7                     |

Table – 3 Estimation of bottomhole pressure and injection pressure at the surface

| injection rate (bbl/min) | injection duration (hr) | increase in the formation pressure (psi) | expected bottomhole pressure (psi) | estimated surface injection pressure (psi) | maximum allowable bottomhole pressure (psi) | maximum possible injection pressure (psi) | Inj.P. design factor | Bot.P. design factor |
|--------------------------|-------------------------|--|------------------------------------|--|---|---|----------------------|----------------------|
| 10                       | 24                      | 193.6                                    | 2592.0                             | 98.2                                       | 3245.8                                      | 945.6                                     | 9.63                 | 1.25                 |
| 10                       | 720                     | 233.4                                    | 2689.9                             | 196.1                                      | 3245.8                                      | 985.4                                     | 5.03                 | 1.21                 |
| 10                       | 8760                    | 265.0                                    | 2721.5                             | 227.7                                      | 3245.8                                      | 1017.0                                    | 4.47                 | 1.19                 |
| 10                       | 43800                   | 289.4                                    | 2745.9                             | 252.1                                      | 3245.8                                      | 1041.4                                    | 4.13                 | 1.18                 |
| 10                       | 87600                   | 302.4                                    | 2758.9                             | 265.0                                      | 3245.8                                      | 1054.4                                    | 3.98                 | 1.18                 |
| 10                       | 219000                  | 322.3                                    | 2778.8                             | 285.0                                      | 3245.8                                      | 1074.3                                    | 3.77                 | 1.17                 |
| 10                       | 438000                  | 339.2                                    | 2795.7                             | 301.9                                      | 3245.8                                      | 1091.2                                    | 3.61                 | 1.16                 |
| 15                       | 24                      | 229.1                                    | 2627.5                             | 367.1                                      | 3245.8                                      | 1214.5                                    | 3.31                 | 1.24                 |
| 15                       | 720                     | 288.8                                    | 2745.3                             | 484.9                                      | 3245.8                                      | 1274.2                                    | 2.63                 | 1.18                 |
| 15                       | 8760                    | 335.5                                    | 2792.0                             | 531.6                                      | 3245.8                                      | 1320.9                                    | 2.48                 | 1.16                 |
| 15                       | 43800                   | 369.7                                    | 2826.2                             | 565.7                                      | 3245.8                                      | 1355.1                                    | 2.40                 | 1.15                 |
| 15                       | 87600                   | 386.8                                    | 2843.3                             | 582.9                                      | 3245.8                                      | 1372.2                                    | 2.35                 | 1.14                 |
| 15                       | 219000                  | 412.3                                    | 2868.8                             | 608.4                                      | 3245.8                                      | 1397.7                                    | 2.30                 | 1.13                 |
| 15                       | 438000                  | 433.4                                    | 2889.9                             | 629.5                                      | 3245.8                                      | 1418.8                                    | 2.25                 | 1.12                 |
| 20                       | 24                      | 264.6                                    | 2663.0                             | 711.5                                      | 3245.8                                      | 1558.9                                    | 2.19                 | 1.22                 |
| 20                       | 720                     | 344.1                                    | 2800.6                             | 849.1                                      | 3245.8                                      | 1638.4                                    | 1.93                 | 1.16                 |
| 20                       | 8760                    | 406.0                                    | 2862.5                             | 910.9                                      | 3245.8                                      | 1700.3                                    | 1.87                 | 1.13                 |
| 20                       | 43800                   | 449.9                                    | 2906.4                             | 954.8                                      | 3245.8                                      | 1744.2                                    | 1.83                 | 1.12                 |
| 20                       | 87600                   | 471.2                                    | 2927.7                             | 976.2                                      | 3245.8                                      | 1765.5                                    | 1.81                 | 1.11                 |
| 20                       | 219000                  | 502.3                                    | 2958.8                             | 1007.2                                     | 3245.8                                      | 1796.5                                    | 1.78                 | 1.10                 |
| 20                       | 438000                  | 527.6                                    | 2984.1                             | 1032.5                                     | 3245.8                                      | 1821.8                                    | 1.76                 | 1.09                 |
| 24                       | 24                      | 293.0                                    | 2691.4                             | 1039.1                                     | 3245.8                                      | 1886.5                                    | 1.82                 | 1.21                 |
| 24                       | 720                     | 388.4                                    | 2844.9                             | 1192.6                                     | 3245.8                                      | 1981.9                                    | 1.66                 | 1.14                 |
| 24                       | 8760                    | 462.4                                    | 2918.9                             | 1266.5                                     | 3245.8                                      | 2055.9                                    | 1.62                 | 1.11                 |
| 24                       | 43800                   | 514.1                                    | 2970.6                             | 1318.2                                     | 3245.8                                      | 2107.6                                    | 1.60                 | 1.09                 |
| 24                       | 87600                   | 538.8                                    | 2995.3                             | 1342.9                                     | 3245.8                                      | 2132.3                                    | 1.59                 | 1.08                 |
| 24                       | 219000                  | 574.2                                    | 3030.7                             | 1378.4                                     | 3245.8                                      | 2167.7                                    | 1.57                 | 1.07                 |
| 24                       | 438000                  | 602.9                                    | 3059.4                             | 1407.1                                     | 3245.8                                      | 2196.4                                    | 1.56                 | 1.06                 |

In Table-3, calculations have been conducted for an injection period of 1 day, 1 week, 1 month, 1 year, 5 years, 10 years, 25 years, and 50 years. The “maximum possible injection pressure” is the maximum surface pressure that will be observed as a limitation considering the fracture pressure of the formation, including the hydraulics within the tubing as well as the pressure required to achieve flow within the formation. It is equal to the maximum allowable bottomhole pressure minus the hydrostatic pressure plus friction losses plus the anticipated increase in the formation pressure. “Increase in the formation

pressure” is calculated by applying the superposition principle considering the no flow boundaries at the formation as well as the potential interfering well injecting into the same formation, as an open form of Eq. B.41. “Injection pressure tolerance” is the difference between the maximum possible injection pressure for the given conditions and calculated injection pressure. The last two columns are the design factors for injection pressure and bottomhole pressure. They are calculated as the maximum possible injection pressure divided by the calculated injection pressure, and fracture pressure divided by calculated bottomhole pressure, respectively. In both columns, values greater than 1.0 indicate safe operation conditions. All the calculations related with the pressure in the formation consider no-flow boundaries as well as the potential interference of the nearby injection well.

As observed from Table-3, for an injection flow rate of 20 bbl/min, it is observed that there is no fracture initiation at the vicinity of the wellbore, even after 50 years of continuous injection. For an injection rate of 20 bbl/min, the expected surface injection pressure is 1033 psi and the expected bottomhole pressure is 2984 psi after 50-years of continuous injection period.

Additionally, the maximum, allowable theoretical injection rate has been calculated for an injection period of 50 years and is 35 bbl/min. This injection rate is the maximum possible injection rate that will not cause any fractures after 50 years of injection. The corresponding surface injection pressure for this injection rate is 2660 psi, which is almost two times greater than Mid-Way’s requested allowable surface injection pressure of 1350 psi. If 1350 psi of surface injection pressure is considered as the limitation, the maximum injection rate is about 23.4 bbl/min, which satisfies this condition, even for an injection period of 50 years. For this injection rate, after 50 years, the fracture pressure at the bottomhole is not reached.

### **2.3 Pressure Distribution within the Formation**

Analysis of the fall-off test conducted in October 2010 (details are presented in section 2.4) indicates that the reservoir is likely a high permeable homogeneous reservoir with the presence of two perpendicular no-flow boundaries. Both of the boundaries appear to be approximately 1200 ft from MES #1 which is consistent with the injection fall-off analysis conducted by EPA Region 6. Also, there exists a nearby injection well which is actively injecting into the same formation for 10 years with an injection rate of 13 bbl/min. Based on the data, the permeability is around 2000 md, which is the value used during the analysis.

The pressure distribution within the formation considering the no-flow boundaries and the nearby injection well is determined up to 8000 ft from each no-flow boundary for an injection rate of 23.4 bbl/min of Mid-Way MES #1 after 10 years, 25 years and 50 years, as presented in figures 4 to 6.

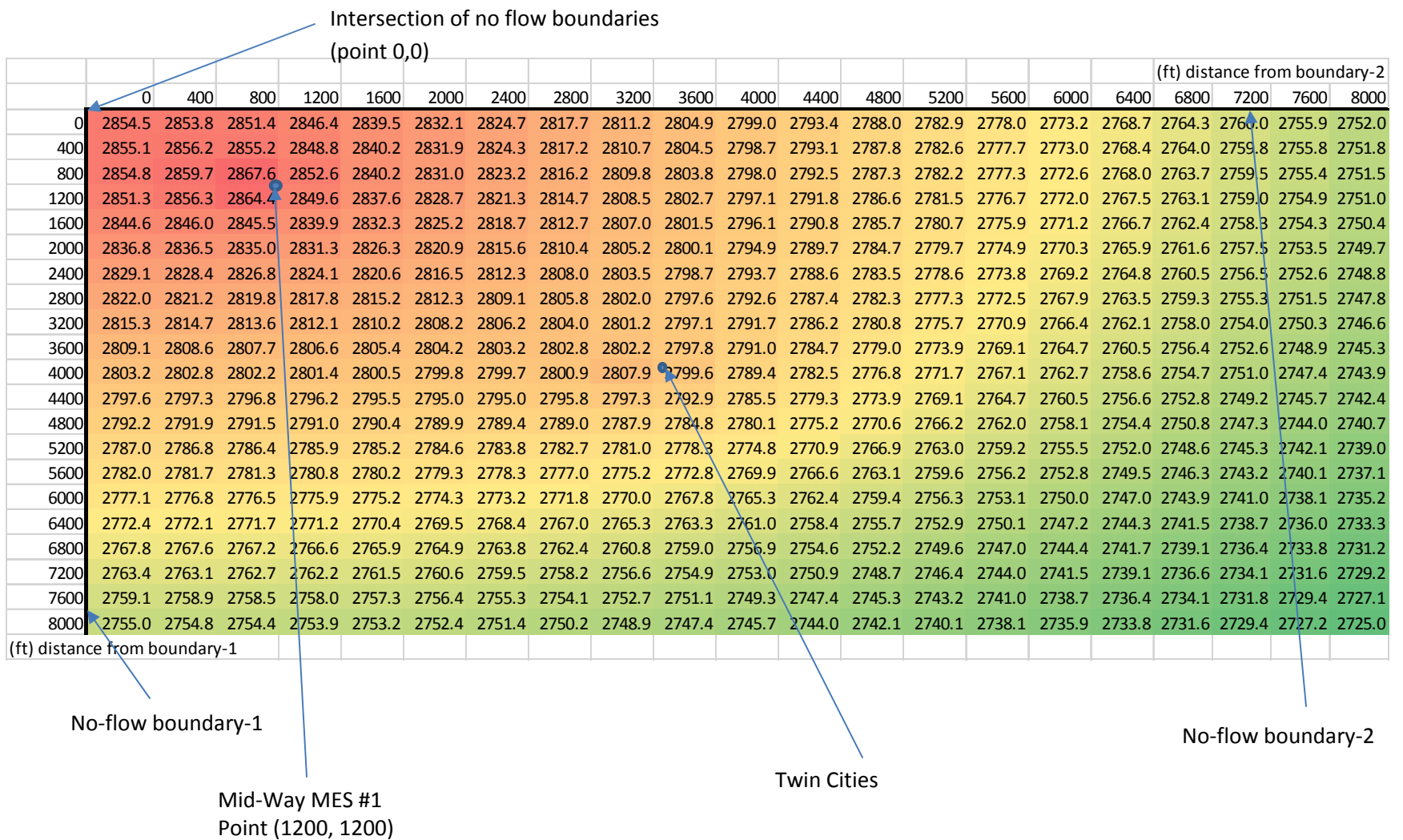


Figure – 4 Pressure distribution within the formation after 10 years of injection of Mid-Way MES #1 for 23.4 bbl/min injection rate

|                               | (ft) distance from boundary-2 |        |        |        |        |        |        |        |        |        |        |        |        |        |        |        |        |        |        |        |        |
|-------------------------------|-------------------------------|--------|--------|--------|--------|--------|--------|--------|--------|--------|--------|--------|--------|--------|--------|--------|--------|--------|--------|--------|--------|
|                               | 0                             | 400    | 800    | 1200   | 1600   | 2000   | 2400   | 2800   | 3200   | 3600   | 4000   | 4400   | 4800   | 5200   | 5600   | 6000   | 6400   | 6800   | 7200   | 7600   | 8000   |
| 0                             | 2876.7                        | 2876.1 | 2873.7 | 2868.7 | 2861.8 | 2854.4 | 2847.0 | 2840.0 | 2833.4 | 2827.2 | 2821.3 | 2815.7 | 2810.3 | 2805.2 | 2800.2 | 2795.5 | 2790.9 | 2786.5 | 2782.3 | 2778.2 | 2774.3 |
| 400                           | 2877.3                        | 2878.5 | 2877.5 | 2871.1 | 2862.5 | 2854.2 | 2846.5 | 2839.5 | 2832.9 | 2826.8 | 2820.9 | 2815.4 | 2810.0 | 2804.9 | 2800.0 | 2795.2 | 2790.7 | 2786.3 | 2782.1 | 2778.0 | 2774.1 |
| 800                           | 2877.0                        | 2882.0 | 2889.8 | 2874.8 | 2862.5 | 2853.2 | 2845.4 | 2838.5 | 2832.1 | 2826.0 | 2820.3 | 2814.8 | 2809.5 | 2804.4 | 2799.5 | 2794.8 | 2790.3 | 2785.9 | 2781.7 | 2777.7 | 2773.8 |
| 1200                          | 2873.5                        | 2878.6 | 2886.6 | 2871.9 | 2859.9 | 2851.0 | 2843.6 | 2836.9 | 2830.8 | 2825.0 | 2819.4 | 2814.0 | 2808.8 | 2803.8 | 2798.9 | 2794.3 | 2789.7 | 2785.4 | 2781.2 | 2777.2 | 2773.3 |
| 1600                          | 2866.8                        | 2868.2 | 2867.8 | 2862.2 | 2854.6 | 2847.4 | 2840.9 | 2834.9 | 2829.2 | 2823.7 | 2818.3 | 2813.1 | 2808.0 | 2803.0 | 2798.1 | 2793.5 | 2789.0 | 2784.7 | 2780.5 | 2776.6 | 2772.7 |
| 2000                          | 2859.0                        | 2858.8 | 2857.2 | 2853.6 | 2848.6 | 2843.2 | 2837.8 | 2832.6 | 2827.5 | 2822.3 | 2817.2 | 2812.0 | 2806.9 | 2802.0 | 2797.2 | 2792.6 | 2788.1 | 2783.8 | 2779.7 | 2775.8 | 2772.0 |
| 2400                          | 2851.4                        | 2850.7 | 2849.1 | 2846.4 | 2842.8 | 2838.8 | 2834.6 | 2830.2 | 2825.7 | 2821.0 | 2816.0 | 2810.9 | 2805.8 | 2800.8 | 2796.1 | 2791.5 | 2787.0 | 2782.8 | 2778.7 | 2774.8 | 2771.1 |
| 2800                          | 2844.2                        | 2843.5 | 2842.1 | 2840.1 | 2837.5 | 2834.5 | 2831.4 | 2828.1 | 2824.3 | 2819.8 | 2814.9 | 2809.7 | 2804.5 | 2799.5 | 2794.7 | 2790.2 | 2785.8 | 2781.6 | 2777.6 | 2773.8 | 2770.1 |
| 3200                          | 2837.6                        | 2836.9 | 2835.8 | 2834.3 | 2832.5 | 2830.5 | 2828.4 | 2826.3 | 2823.5 | 2819.3 | 2814.0 | 2808.4 | 2803.1 | 2798.0 | 2793.2 | 2788.7 | 2784.4 | 2780.2 | 2776.3 | 2772.5 | 2768.9 |
| 3600                          | 2831.4                        | 2830.8 | 2830.0 | 2828.9 | 2827.6 | 2826.4 | 2825.5 | 2825.0 | 2824.4 | 2820.0 | 2813.3 | 2806.9 | 2801.3 | 2796.2 | 2791.4 | 2786.9 | 2782.7 | 2778.7 | 2774.8 | 2771.2 | 2767.6 |
| 4000                          | 2825.5                        | 2825.1 | 2824.4 | 2823.6 | 2822.8 | 2822.1 | 2821.9 | 2823.2 | 2830.1 | 2821.9 | 2811.7 | 2804.8 | 2799.0 | 2794.0 | 2789.3 | 2785.0 | 2780.9 | 2777.0 | 2773.2 | 2769.6 | 2766.2 |
| 4400                          | 2819.9                        | 2819.5 | 2819.0 | 2818.4 | 2817.8 | 2817.3 | 2817.2 | 2818.0 | 2819.6 | 2815.2 | 2807.7 | 2801.5 | 2796.2 | 2791.4 | 2787.0 | 2782.8 | 2778.8 | 2775.1 | 2771.5 | 2768.0 | 2764.7 |
| 4800                          | 2814.5                        | 2814.2 | 2813.8 | 2813.2 | 2812.7 | 2812.1 | 2811.7 | 2811.3 | 2810.2 | 2807.1 | 2802.4 | 2797.5 | 2792.8 | 2788.4 | 2784.3 | 2780.4 | 2776.6 | 2773.0 | 2769.6 | 2766.2 | 2763.0 |
| 5200                          | 2809.3                        | 2809.0 | 2808.6 | 2808.1 | 2807.5 | 2806.8 | 2806.0 | 2805.0 | 2803.3 | 2800.6 | 2797.1 | 2793.1 | 2789.2 | 2785.2 | 2781.5 | 2777.8 | 2774.3 | 2770.9 | 2767.6 | 2764.4 | 2761.2 |
| 5600                          | 2804.2                        | 2804.0 | 2803.6 | 2803.1 | 2802.4 | 2801.6 | 2800.6 | 2799.3 | 2797.5 | 2795.1 | 2792.1 | 2788.8 | 2785.4 | 2781.9 | 2778.5 | 2775.1 | 2771.8 | 2768.6 | 2765.4 | 2762.4 | 2759.4 |
| 6000                          | 2799.3                        | 2799.1 | 2798.7 | 2798.2 | 2797.5 | 2796.6 | 2795.5 | 2794.1 | 2792.3 | 2790.1 | 2787.5 | 2784.7 | 2781.6 | 2778.5 | 2775.4 | 2772.3 | 2769.2 | 2766.2 | 2763.2 | 2760.3 | 2757.5 |
| 6400                          | 2794.6                        | 2794.4 | 2794.0 | 2793.4 | 2792.7 | 2791.8 | 2790.6 | 2789.2 | 2787.5 | 2785.5 | 2783.2 | 2780.7 | 2778.0 | 2775.2 | 2772.3 | 2769.5 | 2766.6 | 2763.8 | 2761.0 | 2758.2 | 2755.5 |
| 6800                          | 2790.0                        | 2789.8 | 2789.4 | 2788.9 | 2788.1 | 2787.2 | 2786.1 | 2784.7 | 2783.1 | 2781.2 | 2779.1 | 2776.9 | 2774.4 | 2771.9 | 2769.3 | 2766.6 | 2764.0 | 2761.3 | 2758.7 | 2756.1 | 2753.5 |
| 7200                          | 2785.6                        | 2785.4 | 2785.0 | 2784.5 | 2783.7 | 2782.8 | 2781.7 | 2780.4 | 2778.9 | 2777.2 | 2775.3 | 2773.2 | 2771.0 | 2768.6 | 2766.2 | 2763.8 | 2761.3 | 2758.8 | 2756.4 | 2753.9 | 2751.4 |
| 7600                          | 2781.4                        | 2781.2 | 2780.8 | 2780.2 | 2779.5 | 2778.6 | 2777.6 | 2776.3 | 2774.9 | 2773.3 | 2771.6 | 2769.6 | 2767.6 | 2765.5 | 2763.2 | 2761.0 | 2758.7 | 2756.3 | 2754.0 | 2751.7 | 2749.4 |
| 8000                          | 2777.3                        | 2777.1 | 2776.7 | 2776.2 | 2775.5 | 2774.6 | 2773.6 | 2772.5 | 2771.1 | 2769.6 | 2768.0 | 2766.2 | 2764.4 | 2762.4 | 2760.3 | 2758.2 | 2756.0 | 2753.9 | 2751.7 | 2749.5 | 2747.3 |
| (ft) distance from boundary-1 |                               |        |        |        |        |        |        |        |        |        |        |        |        |        |        |        |        |        |        |        |        |

Figure – 5 Pressure distribution within the formation after 25 years of injection of Mid-Way MES-#1 for 23.4 bbl/min injection rate

|                               | (ft) distance from boundary-2 |        |        |        |        |        |        |        |        |        |        |        |        |        |        |        |        |        |        |        |        |
|-------------------------------|-------------------------------|--------|--------|--------|--------|--------|--------|--------|--------|--------|--------|--------|--------|--------|--------|--------|--------|--------|--------|--------|--------|
|                               | 0                             | 400    | 800    | 1200   | 1600   | 2000   | 2400   | 2800   | 3200   | 3600   | 4000   | 4400   | 4800   | 5200   | 5600   | 6000   | 6400   | 6800   | 7200   | 7600   | 8000   |
| 0                             | 2899.0                        | 2898.4 | 2896.0 | 2890.9 | 2884.1 | 2876.6 | 2869.3 | 2862.3 | 2855.7 | 2849.4 | 2843.5 | 2837.9 | 2832.6 | 2827.4 | 2822.5 | 2817.7 | 2813.2 | 2808.8 | 2804.5 | 2800.5 | 2796.5 |
| 400                           | 2899.6                        | 2900.7 | 2899.7 | 2893.4 | 2884.7 | 2876.4 | 2868.8 | 2861.7 | 2855.2 | 2849.0 | 2843.2 | 2837.6 | 2832.3 | 2827.2 | 2822.2 | 2817.5 | 2812.9 | 2808.6 | 2804.3 | 2800.3 | 2796.3 |
| 800                           | 2899.3                        | 2904.2 | 2912.1 | 2897.1 | 2884.8 | 2875.5 | 2867.7 | 2860.7 | 2854.3 | 2848.3 | 2842.5 | 2837.0 | 2831.8 | 2826.7 | 2821.8 | 2817.1 | 2812.6 | 2808.2 | 2804.0 | 2799.9 | 2796.0 |
| 1200                          | 2895.8                        | 2900.9 | 2908.9 | 2894.2 | 2882.2 | 2873.3 | 2865.8 | 2859.2 | 2853.0 | 2847.2 | 2841.7 | 2836.3 | 2831.1 | 2826.0 | 2821.2 | 2816.5 | 2812.0 | 2807.6 | 2803.5 | 2799.4 | 2795.6 |
| 1600                          | 2889.1                        | 2890.5 | 2890.1 | 2884.5 | 2876.9 | 2869.7 | 2863.2 | 2857.2 | 2851.5 | 2846.0 | 2840.6 | 2835.3 | 2830.2 | 2825.2 | 2820.4 | 2815.7 | 2811.3 | 2806.9 | 2802.8 | 2798.8 | 2795.0 |
| 2000                          | 2881.3                        | 2881.0 | 2879.5 | 2875.8 | 2870.8 | 2865.4 | 2860.1 | 2854.9 | 2849.7 | 2844.6 | 2839.4 | 2834.3 | 2829.2 | 2824.2 | 2819.4 | 2814.8 | 2810.4 | 2806.1 | 2802.0 | 2798.0 | 2794.2 |
| 2400                          | 2873.6                        | 2872.9 | 2871.3 | 2868.6 | 2865.1 | 2861.0 | 2856.8 | 2852.5 | 2848.0 | 2843.2 | 2838.2 | 2833.1 | 2828.0 | 2823.1 | 2818.3 | 2813.7 | 2809.3 | 2805.1 | 2801.0 | 2797.1 | 2793.3 |
| 2800                          | 2866.5                        | 2865.7 | 2864.4 | 2862.3 | 2859.7 | 2856.8 | 2853.7 | 2850.3 | 2846.5 | 2842.1 | 2837.1 | 2831.9 | 2826.8 | 2821.8 | 2817.0 | 2812.4 | 2808.0 | 2803.9 | 2799.9 | 2796.0 | 2792.3 |
| 3200                          | 2859.8                        | 2859.2 | 2858.1 | 2856.6 | 2854.7 | 2852.7 | 2850.7 | 2848.5 | 2845.8 | 2841.6 | 2836.3 | 2830.7 | 2825.3 | 2820.2 | 2815.4 | 2810.9 | 2806.6 | 2802.5 | 2798.6 | 2794.8 | 2791.1 |
| 3600                          | 2853.6                        | 2853.1 | 2852.2 | 2851.1 | 2849.9 | 2848.7 | 2847.7 | 2847.3 | 2846.7 | 2842.3 | 2835.5 | 2829.2 | 2823.6 | 2818.4 | 2813.7 | 2809.2 | 2805.0 | 2800.9 | 2797.1 | 2793.4 | 2789.9 |
| 4000                          | 2847.7                        | 2847.3 | 2846.7 | 2845.9 | 2845.0 | 2844.3 | 2844.2 | 2845.5 | 2852.4 | 2844.1 | 2833.9 | 2827.0 | 2821.3 | 2816.2 | 2811.6 | 2807.2 | 2803.1 | 2799.2 | 2795.5 | 2791.9 | 2788.4 |
| 4400                          | 2842.1                        | 2841.8 | 2841.3 | 2840.7 | 2840.0 | 2839.6 | 2839.5 | 2840.3 | 2841.8 | 2837.4 | 2830.0 | 2823.8 | 2818.4 | 2813.6 | 2809.2 | 2805.0 | 2801.1 | 2797.3 | 2793.7 | 2790.2 | 2786.9 |
| 4800                          | 2836.7                        | 2836.5 | 2836.0 | 2835.5 | 2834.9 | 2834.4 | 2833.9 | 2833.5 | 2832.4 | 2829.3 | 2824.6 | 2819.7 | 2815.1 | 2810.7 | 2806.6 | 2802.6 | 2798.9 | 2795.3 | 2791.8 | 2788.5 | 2785.2 |
| 5200                          | 2831.5                        | 2831.3 | 2830.9 | 2830.4 | 2829.8 | 2829.1 | 2828.3 | 2827.2 | 2825.5 | 2822.9 | 2819.3 | 2815.4 | 2811.4 | 2807.5 | 2803.7 | 2800.0 | 2796.5 | 2793.1 | 2789.8 | 2786.6 | 2783.5 |
| 5600                          | 2826.5                        | 2826.2 | 2825.9 | 2825.3 | 2824.7 | 2823.9 | 2822.8 | 2821.5 | 2819.7 | 2817.3 | 2814.4 | 2811.1 | 2807.6 | 2804.2 | 2800.7 | 2797.3 | 2794.0 | 2790.8 | 2787.7 | 2784.6 | 2781.7 |
| 6000                          | 2821.6                        | 2821.4 | 2821.0 | 2820.4 | 2819.7 | 2818.8 | 2817.7 | 2816.3 | 2814.5 | 2812.3 | 2809.8 | 2806.9 | 2803.9 | 2800.8 | 2797.7 | 2794.5 | 2791.5 | 2788.5 | 2785.5 | 2782.6 | 2779.7 |
| 6400                          | 2816.9                        | 2816.6 | 2816.2 | 2815.7 | 2815.0 | 2814.0 | 2812.9 | 2811.5 | 2809.8 | 2807.8 | 2805.5 | 2802.9 | 2800.2 | 2797.4 | 2794.6 | 2791.7 | 2788.9 | 2786.0 | 2783.2 | 2780.5 | 2777.8 |
| 6800                          | 2812.3                        | 2812.1 | 2811.7 | 2811.1 | 2810.4 | 2809.4 | 2808.3 | 2807.0 | 2805.3 | 2803.5 | 2801.4 | 2799.1 | 2796.7 | 2794.1 | 2791.5 | 2788.9 | 2786.2 | 2783.6 | 2780.9 | 2778.3 | 2775.7 |
| 7200                          | 2807.9                        | 2807.7 | 2807.3 | 2806.7 | 2806.0 | 2805.1 | 2804.0 | 2802.7 | 2801.2 | 2799.4 | 2797.5 | 2795.4 | 2793.2 | 2790.9 | 2788.5 | 2786.0 | 2783.6 | 2781.1 | 2778.6 | 2776.1 | 2773.7 |
| 7600                          | 2803.6                        | 2803.4 | 2803.0 | 2802.5 | 2801.8 | 2800.9 | 2799.8 | 2798.6 | 2797.2 | 2795.6 | 2793.8 | 2791.9 | 2789.9 | 2787.7 | 2785.5 | 2783.2 | 2780.9 | 2778.6 | 2776.3 | 2773.9 | 2771.6 |
| 8000                          | 2799.5                        | 2799.3 | 2798.9 | 2798.4 | 2797.7 | 2796.9 | 2795.9 | 2794.7 | 2793.4 | 2791.9 | 2790.3 | 2788.5 | 2786.6 | 2784.6 | 2782.6 | 2780.5 | 2778.3 | 2776.1 | 2773.9 | 2771.7 | 2769.5 |
| (ft) distance from boundary-1 |                               |        |        |        |        |        |        |        |        |        |        |        |        |        |        |        |        |        |        |        |        |

Figure – 6 Pressure distribution within the formation after 50 years of injection of Mid-Way MES-#1 for 23.4 bbl/min injection rate

In figures 4 to 6, the first column represents the relative distance from the horizontal no flow boundary (named as boundary-2) in feet while the first row represents the relative distance from the vertical no flow boundary (named as boundary-1) in feet. The intersection of these boundaries (perpendicular) are assumed to be at point 0,0 which is on the left top. The numbers presented in the colored section are the pressures. The color scale indicates the relative magnitude of these pressures, such that red represents higher pressures, and green represents lower pressures. The pressure values presented in these figures are calculated by applying the superposition principle, using Eq. B.41.

From figures 4 to 6, it can be seen that the pressure increase within the reservoir never exceeds the fracture resistance of the formation for all times, such that the maximum pressure calculated after 50 years of injection for 23.4 bbl/min is 2990 psi, and the fracture pressure is estimated to be 3245 psi. Also, response of the increase in the pressure within the formation away from Mid-Way MES #1 when compared with the pressure at the bottomhole of Mid-Way MES #1 is very limited such that, the difference between the pressure at the injection well and 5000 ft away, is about 160 psi or less, and at 7000 ft away, the pressure difference is about 200 psi.

#### **2.4 Permeability and Skin Factor Analysis**

Data from the October 2010 injection fall off test was incorporated to form the diagnostic plot of the test. The bottomhole pressure fall off and its derivative versus time for the fall off period are shown in Fig.7. The injection flow rate was constant at 8.5 bbl/min for the 29.33 hours of injection period and the pressure sensor was at 5300 ft during this test. It is assumed that the injected fluid was fresh water. The total compressibility is assumed to be  $7.3E-6 \text{ psi}^{-1}$ . Reservoir thickness is considered 180 ft, porosity is considered to be 0.135 and the viscosity of water is considered to be 1 cp.

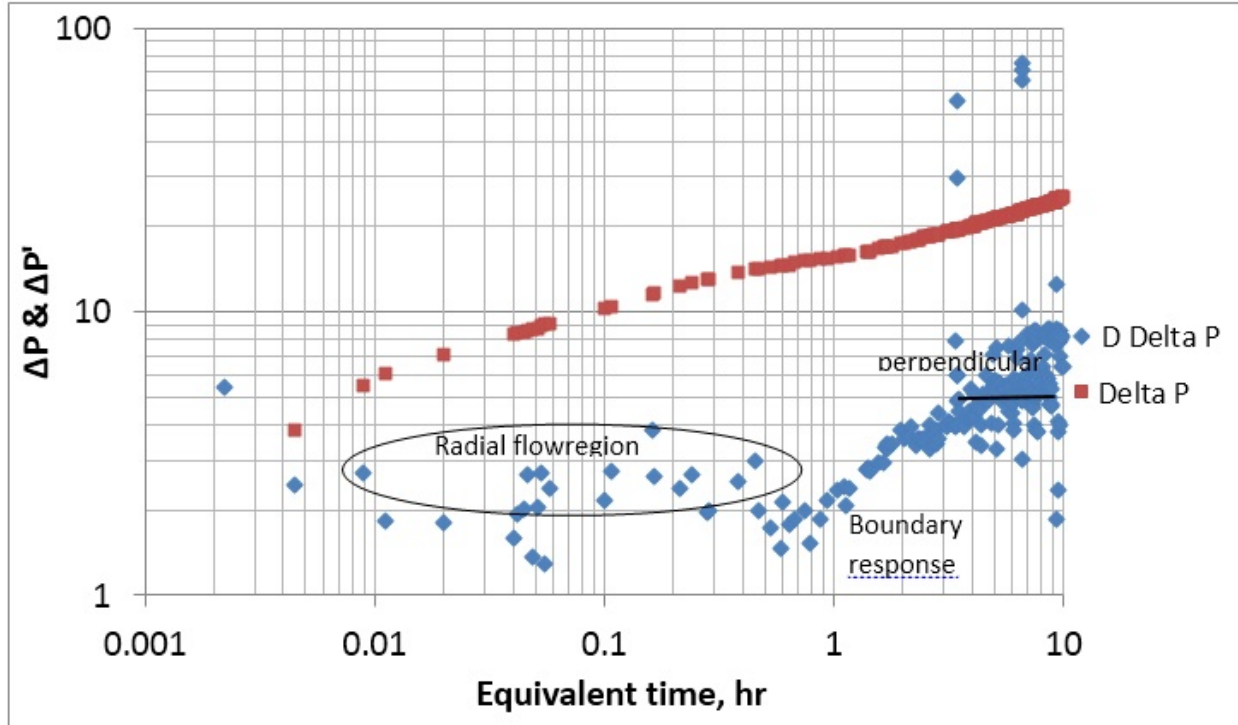


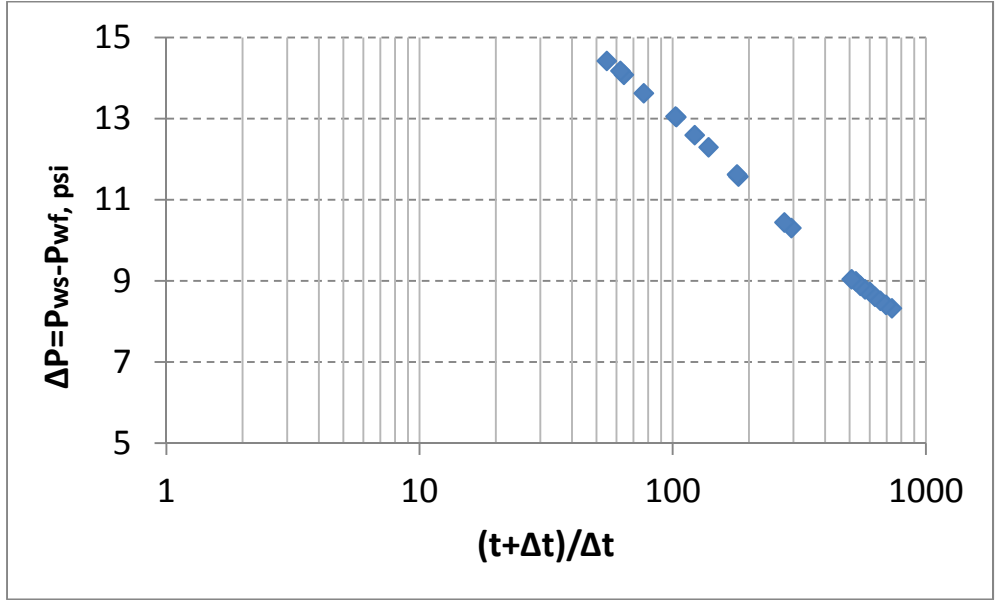
Figure – 7 The diagnostic plot corresponding to the fall off period of the October 2010 test.

From the analysis of the diagnostic plot shown in Figure 7, we conclude that the data points before one hour equivalent time to be corresponding to the radial flow region, and the analyzable data corresponding to the late time of the test show the effect of no-flow boundaries of the reservoir. Right after the radial flow region, it is clearly observed that there exists no-flow boundaries based on the analysis of the derivative of delta pressure versus equivalent time. Following the boundary response region, data is a little scattered, but the best fit is a flat line, which indicates the presence of two perpendicular no-flow boundaries.

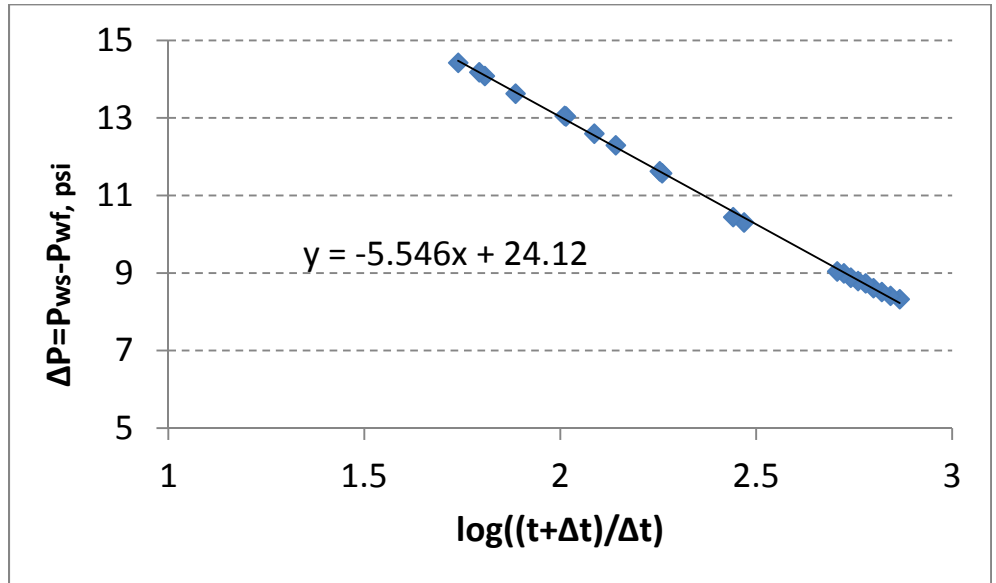
Regarding the possibility of an interfering well, Twin cities, which is about 0.8 miles away from Mid-Way MES #1, due to the apparent very high permeability within the formation (which is presented below), the pressure distribution is relatively fast, which prevents localized pressure build-ups. Since the no-flow boundaries are perpendicular, the non-bounded part of the reservoir acts like an infinite reservoir. Considering that Twin Cities is injecting into the Arbuckle formation at a similar depth as Mid-Way MES #1 is planning to inject at, and since there has not been a significant pressure change observed at Mid-Way MES #1 for the last two years, this indicates two possibilities; either Twin Cities is located on the other side of the no-flow boundary such that there is no hydraulic connection between these two wells or, if Twin Cities is an interfering well, the effect of the well is very limited due to high permeability.

Here, we use the Horner method to obtain the permeability of the reservoir. Figures 8a and 8b, respectively, show the plots of pressure fall off with respect to the Horner time and the log of Horner

time for the infinite acting radial flow region. These plots indicate the results of the diagnostic plots which show that the flow for this region is radial. Figure 8b is used to obtain the slope of the pressure fall off with respect to the Horner time and also the fall off pressure after one hour shut in time for skin factor computations.



(a)



(b)

Figure – 8 Bottomhole pressure fall off versus Horner time during fall off test corresponding to the radial flow region

From the regression analysis, we obtain that the equation of the hypothetical straight line which represents the linear relation between the bottomhole pressure fall off and log of Horner time. Considering the radial flow region data points, we obtain this equation as:

$$\Delta P = -5.546 \log((t+\Delta t)/\Delta t) + 24.12 \quad (1)$$

Therefore, slope,  $m$ , is estimated as -5.546 psi/log cycle. Using the information provided, and considering the payzone thickness as 180 ft,  $k.h$  is calculated as 358,857.6 md-ft (eqs.B.36 & B.39-Appendix-B). Thus, permeability,  $k$ , can be estimated as 1993.653md.

Using the provided information, skin analysis is also conducted, considering a porosity value of 13.5 % and  $\Delta P_{ws(1 \text{ hr})}$  of 15.9013 psi. Skin is calculated to be -4.82, which indicates a stimulation job (eq.B.40-Appendix-B). Since an acidizing process took place in the payzone, the calculation of a negative skin makes sense.

## 2.5 Advancement of the Front End of the Injected Fluid

According to the Mid-Way's "Construction Completion Report and Operating Permit Application" (Dec. 2010) Section 8 page 77, the first injection test in May 2010 which was conducted before acidizing with a rate of 6 bpm (tubing size was 2<sup>7/8</sup>in), the surface injection pressure was measured as 1500 psi. The second injection test in October 2010, which was after the acidizing and using a rate of 8.5 bpm (tubing size was 4<sup>1/2</sup>in), the surface injection pressure was measured as 510 psi. During both tests the injection fluid was fresh water. The frictional pressure losses during the first and second injection tests were calculated as 960 psi and 125 psi, respectively. Since the surface pressure showed the combination of frictional losses inside the tubings and the losses inside the formation, pressure losses in the formation for the first test and the second test were determined as 540 psi and 385 psi, respectively.

Under the assumption that the permeabilities and fluid viscosities were constant in both injection operations, considering the frictional pressure losses inside the tubings and comparing the two cases using Darcy's equation for radial flow for an infinite system,

$$Q = \frac{2 \pi k h}{\mu} \frac{\Delta P}{\ln\left(\frac{r_e}{r_w}\right)} \quad (2)$$

where  $Q$  is the flow rate,  $k$  is the permeability,  $h$  is the thickness,  $\mu$  is the viscosity,  $\Delta P$  is the pressure drop,  $r_e$  is the drainage radius, and  $r_w$  is the wellbore radius, a comparison can be made for both injection tests, such as

$$\frac{(6)}{(8.5)} = \frac{(180)(540)\zeta}{h(385)\zeta} \quad (3)$$

where  $\zeta$  is the unit conversion, it is observed that the interval thickness where the injection took place has improved from 180 ft (before acidizing) to approximately 350 ft (after acidizing). In order to be on the conservative side, improved thickness is considered to be 300 ft.

The advancement of the front of the injected fluid in the formation is investigated using an in-house numerical simulator. To do so, a simulation model of the reservoir is prepared where the MES #1 is located about 1050 ft from the two no-flow boundaries. The injection rate is set equal to 11 bbl/min and a constant pressure boundary is considered at the distance of 2300 ft from the well. The 2D simulation model has 80\*80 gridblock where each gridblock is 300\*300 ft. From the pressure transient test analysis of the well MES-#1, the injectivity of the well is calculated as  $k.h= 358,857.6$  md-ft. Injection interval thickness is considered to be 300 ft, based on the fact that acidizing improved the initial effective thickness. For a formation thickness of 300 ft, permeability is considered as 1196.2 md. The saturation profile of the injected fluid is presented in the following figures after 10, 20, 30, 40 and 50 years of injection, respectively. In these graphs, x and y axes are representing the number of 300 ft \* 300 ft blocks, and the colored scales indicate the saturation levels with 1.0 being 100% saturation. Saturation levels between 50% and 55% were considered to be the location of the injected fluid front.

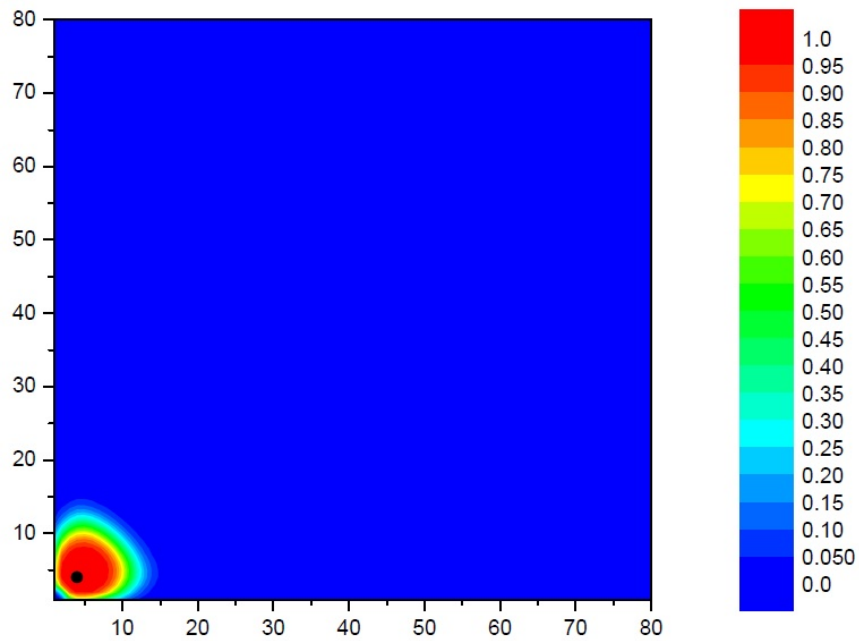


Figure – A.1 Injection fluid saturation after 10 years of injection with a flow rate of 11 bbl/min.

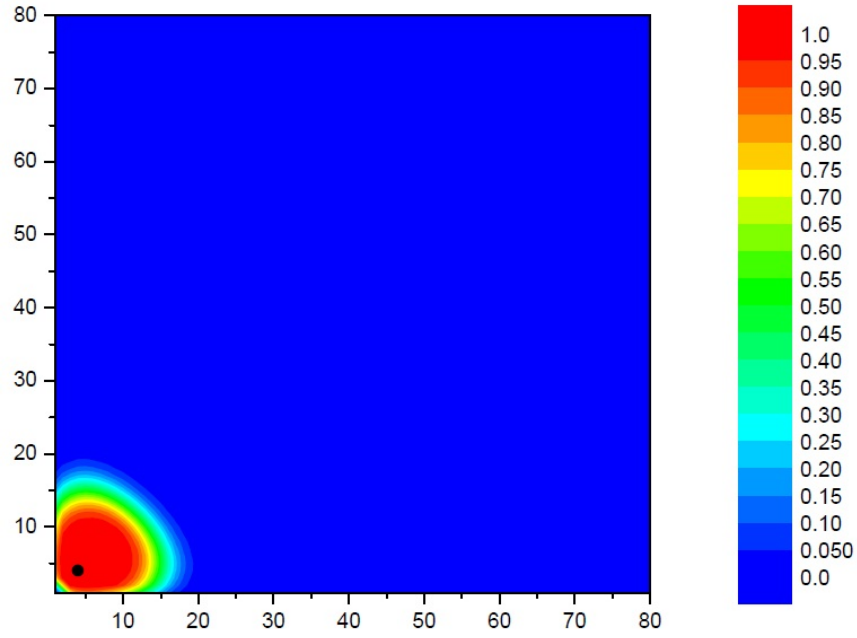


Figure – A.2 Injection fluid saturation after 20 years of injection with a flow rate of 11 bbl/min.

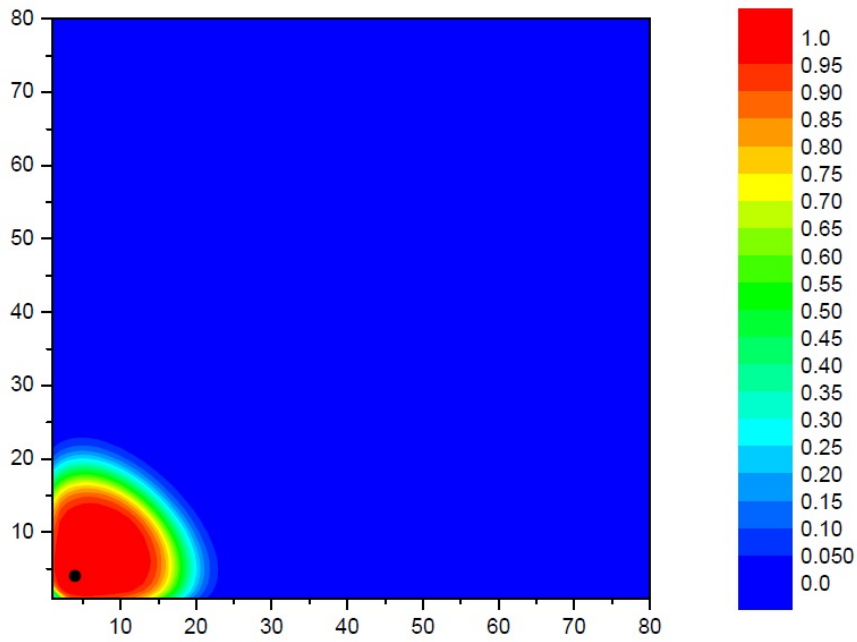


Figure – A.3 Injection fluid saturation after 30 years of injection with a flow rate of 11 bbl/min.

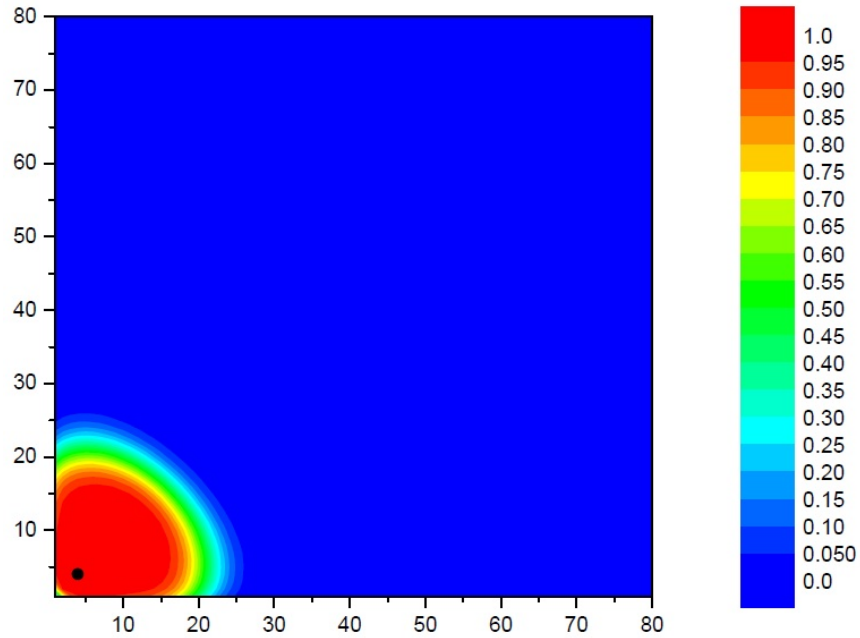


Figure – A.4 Injection fluid saturation after 40 years of injection with a flow rate of 11 bbl/min.

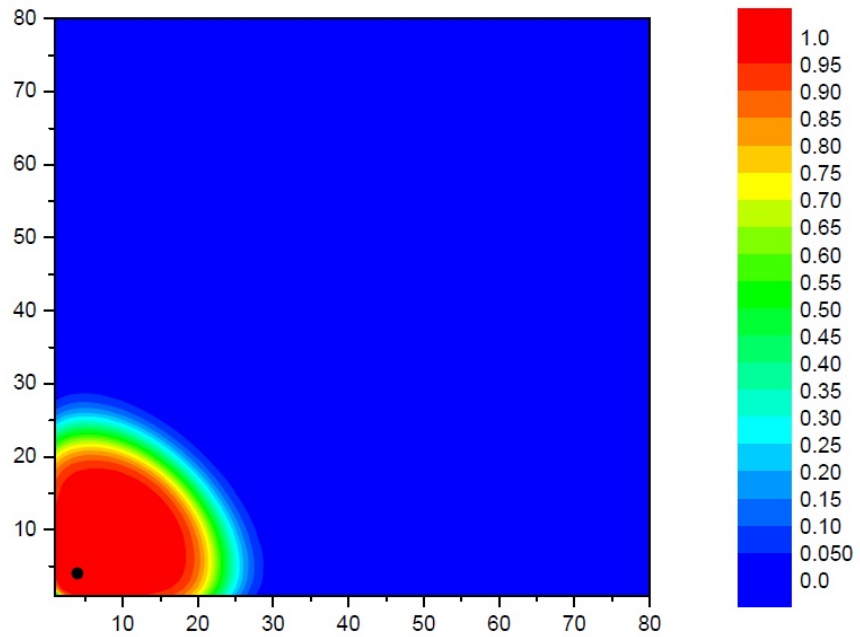


Figure – A.5 Injection fluid saturation after 50 years of injection with a flow rate of 11 bbl/min.

As seen from the figures, considering a formation thickness of 300 ft, for an injection rate of 11 bbl/min, after 10 years, the front end is estimated to be 2,100 ft away from Mid-Way MES #1, and after 50 years, the front end is estimated to be 5,400 ft away from Mid-Way MES #1. Therefore, it is estimated that a

distance of approximately 1.0 miles is reached after 50 years of continuous injection with a rate of 11 bbl/min.

**APPENDIX – A**  
**Answers to “Notice of Deficiency”**

The followings are the answers addressing to the deficiencies identified by Oklahoma Department of Environmental Quality.

**Deficiency No: 2**

*“Mid-Way anticipates that 30% of the injectate will have a specific gravity (SG) of 1.0, 50% will have an SG of 1.026 and 20% will have an SG of 1.2. Mid-Way further states that due to anticipated mixing of compatible liquids to be injected, it is expected that the maximum SG of the injectate will be 1.05. Because the exact nature the waste stream is unknown, Mid-Way should use an SG of 1.2 in its calculations. Please indicate how using the greater SG impacts fracture pressure considerations.”*

In all calculations including hydraulic calculations as well as pressure distribution estimations, a fluid density of 1.2 is assumed. Fracture pressure is not reached in all cases presented in this report, which includes Mid-Way’s requested allowable surface injection pressure of 1350 psi.

**Deficiency No: 5**

*“Mid-Way has shown that injected fluid goes into formations at approximate depths of 5080 — 5500 feet; therefore, the top of the injection interval should be taken as 5080 feet.”*

Formation top is assumed to be 5080 ft, and formation thickness is taken as 180 ft during most of the calculations. For front-end determination calculations for the injected fluid in Section 2.5, the thickness is considered to be 300 ft. It should be pointed out that a formation thickness of 180 ft is likely a worst case scenario since this thickness was determined prior to the stimulation of the injection zone (i.e. acid job) that Mid-Way conducted in July 2010.

**Deficiency No: 6**

*“Static Arbuckle reservoir pressure is identified as 200 psi at the surface in the Mid-Way report document titled "Analysis Reports for Injection Well MES #1." This data indicates that the reservoir is essentially "artesian", already capable of flowing at the surface, without considering any additional injection from the proposed Mid-Way disposal well. Additional injection into the interval would result in an increase in the "artesian" pressure conditions, providing a potential pathway through area wells not properly plugged or constructed into underground sources of drinking water (USDW). The current area of review (AOR) radius of one mile is likely sufficient to address the infinite radius of pressure influence concern. Mid-Way should reassess the appropriate size AOR needed to protect the USDW.”*

A 200 psi difference is observed due to the fluid density change inside the tubing. Originally, the formation has a fluid having a specific gravity of approximately 1.1. However, during the injection testing process, the injected fluid was pure water, i.e., specific gravity is 1.0. Since there is no flow observed at the surface even though the well is open to atmospheric pressure when the tubing is full of 1.1. sp. gr. fluid, it is clear that the well is not an “artesian” at all. When the fluid in the tubing is replaced by fresh water after an injection process and shut in, a pressure of 200 psi is observed at the surface. This

pressure is due to the change of density of the fluid in the tubing. As the well is allowed to flow, for a while, flow is observed at the surface, and the fluid flowing out of the well is observed to be fresh water, which is the fluid used during the injection testing process. Then, the flow stops, although the well is totally open to atmosphere. This is due to the formation fluid replacing the fresh water inside of the tubing causing an equilibrium condition to be reached between the hydrostatic pressure of the fluids inside the tubing and the formation pressure.

**Deficiency No: 7**

*“The projected pressure increase from the Mid-Way injection well in the report document was based on a homogeneous infinite acting model calculation. The calculation does not address any possible reservoir geologic boundaries such as faults or other active injection wells that may be present. The second fall-off test had a response at late test times indicating more than a single boundary, which may represent nearby faulting impacts, was present and that area well data indicated at least two other active injectors are present with one of them confirmed as disposing into the same formation as the proposed Mid-Way well. Pressure buildup projections in the permit application should address both the fault concerns identified on the fall-off test and the impact of other area injectors, as well as any producers in the same injection zone. Also, please comment on the sufficiency of the detailed deep reservoir characteristics given the presence of large faults in the regional area and the evidence of nearby faults in the fall-off tests.”*

After plotting the pressure derivative versus equivalent time, analysis reveals that the formation has no-flow boundaries. This is because the slope changes (based on the pressure derivative response) after the radial flow regime. The analyzable data associated with the late time response indicates that the system seems to be more like a perpendicular no-flow boundary system. Therefore, the formation is considered to be a homogeneous system with the presence of two perpendicular no-flow boundaries. Also, there exists a nearby injection well (i.e. Twin Cities) approximately 0.8 mile away from Mid-Way MES-#1 that is estimated to have been injecting less than average of 13 bbl/min for 10 years. As mentioned on page 18, considering that Twin Cities is injecting into the Arbuckle formation at a similar depth as Mid-Way MES #1 is planning to inject at, and since there has not been a significant pressure change observed at Mid-Way MES #1 for the last two years, this indicates two possibilities; either Twin Cities is located on the other side of the no-flow boundary such that there is no hydraulic connection between these two wells or, if Twin Cities is an interfering well, the effect of the well is very limited due to high permeability.. Thus, all of the formation pressure distribution calculations as well as the injection calculations presented in this report considered the described no-flow boundaries as well as the nearby injection well. While analyzing the pressure response data, different models can be considered and the analysis will be performed accordingly. Different set of data can be obtained depending on the selected model. This is where geology plays an important role. As it pertains to the portion of this question requesting Mid-Way to address the “fault concerns identified on the fall-off test”, a clarification needs to be made. When the term “fault” is used in transient analysis it means that there is a no flow boundary, which may or may not be due to a geologic fault. In the case of Mid-Way MES #1, there is not any geologic evidence to suggest that the two perpendicular no flow boundaries determined from the testing analysis are due to a geologic fault(s).

It should be noted that a formation thickness of 180 ft is likely a worst case scenario since this thickness was determined prior to the stimulation of the injection zone (i.e. acid job) that Mid-Way conducted in July 2010. As mentioned in Section 2.5, the thickness is increased to approximately 300 ft during the front-end calculations.

Based on the pressure distribution analysis, it can be concluded that the pressure increase within the reservoir never exceeds the fracture resistance of the formation for all times, such that the maximum pressure calculated after 50 years of injection for 23.4 bbl/min is 2990 psi, and the fracture pressure is estimated to be 3245 psi. Also, response of the increase in the pressure within the formation away from Mid-Way MES #1 when compared with the pressure at the bottomhole of Mid-Way MES #1 is very limited such that, the difference between the pressure at the injection well and 5000 ft away, is about 160 psi or less, and at 7000 ft away, the pressure difference is about 200 psi.

#### **Deficiency No: 8**

*“The fall-off analyses indicated an unusual reservoir combination of an ultra-high permeability zone (>1 Darcy) and stimulated completion representative of a natural fracture system. When coupled with possible local boundaries, it results in uncertainty about how far and in what direction any injection pressure build up would be distributed.”*

After considering the formation as a homogeneous formation with the presence of two perpendicular no-flow boundaries, the average permeability of the formation is determined to be approximately 2000 md. For a dolomite formation, these types of permeability values are common. The permeability value used for calculations is 2000 md. Since the permeability is very high, pressure transmission is also expected to be very fast. A formation pressure distribution analysis is conducted for Mid-Way MES #1 injection rate of 23.4 bbl/min for 10, 25 and 50 years of injection period, considering the no-flow boundaries as well as the interference due to the nearby injection well. It is observed that the fracture pressure is never reached at any location, even though the distances observed are more than 8000 ft from each boundary. The worst pressure build-up is observed at the vicinity of Mid-Way MES #1 and at the interception of the no-flow boundaries, still significantly less than the fracture pressure of the formation even after 50 years of injection process with a rate of 23.4 bbl/min. Related case study is presented in Figure 6. The highest pressure after 50 years of injection expected is at the vicinity of Mid-Way MES #1, which is 2990 psi, and the fracture pressure is estimated to be 3245 psi. This shows that there is no risk of fracturing the formation, even with injecting 23.4 bbl/min, including the consideration of no-flow boundaries as well as interfering well.

As mentioned in Section 2.5, according to the Mid-Way’s “Construction Completion Report and Operating Permit Application” (Dec. 2010) Section 8 page 77, the first injection test in May 2010 which was conducted before acidizing with a rate of 6 bpm (tubing size was 2<sup>7/8</sup>in), the surface injection pressure was measured as 1500 psi. The second injection test in October 2010, which was after the acidizing and using a rate of 8.5 bpm (tubing size was 4<sup>1/2</sup>in), the surface injection pressure was

measured as 510 psi. During both tests the injection fluid was fresh water. Under the assumption that the permeabilities and fluid viscosities were constant in both injection operations, considering the frictional pressure losses inside the tubings and comparing the two cases using Darcy's equation, it is observed that the interval thickness where the injection took place has improved from 180 ft (before acidizing) to approximately 300 ft (after acidizing). Please refer to Section 2.5 for a detailed explanation. The analysis for determining the front-end of the injected fluid shows that for an injection rate of 11 bbl/min, after 10 years, the front end is estimated to be 2,100 ft away from Mid-Way MES #1, and after 50 years, the front end is estimated to be 5,400 ft away from Mid-Way MES #1. Therefore, it is estimated that a distance of approximately 1.0 miles is reached after 50 years of continuous injection with a rate of 11 bbl/min.

## APPENDIX – B

### Theory for Hydraulics of Injection Process

This appendix includes the details about the theoretical background on the hydraulics of injection process through a tubing into a porous media.

#### **B.1 Flow in Circular Pipes**

Understanding the hydraulics of flow of a fluid through circular pipes requires a proper rheological characterization of the fluid and identification of the flow regime.

##### ***B.1.1 Fluid Rheology***

Most of the fluids are more complex than the Newtonian fluids, expected to respond to an applied shearing stress by flowing in a manner such that the velocity gradient is strictly proportional to the applied stress. The shear stress to shear rate relationship of these fluids is not linear and cannot, therefore, be characterized by a single value, such as the coefficient of viscosity. These fluids are classified as non-Newtonian fluids. The shear stress of a non-Newtonian fluid is not directly proportional to shear rate and this is why their relationship cannot be described by a single parameter. It is possible however to define an apparent viscosity which is the shear stress to shear rate relationship measured at a given shear rate. The apparent viscosity is the slope of the line between the origin and the shear stress and shear rate intercept at any given shear rate.

The Bingham fluid is to some extent a limiting or idealized case. It is a fluid for which a finite shearing stress is required to initiate motion and for which there is a linear relationship between the shearing stress in excess of the initiating stress and the resulting velocity gradient. Materials that behave like Bingham Plastics include thickened hydrocarbon greases, certain asphalts and bitumens, some emulsions and pseudo-homogeneous suspensions of ultra-fine or fine particles in liquids at intermediate concentrations, water suspensions of clay, fly ash, finely divided minerals, quartz, and paint systems. Some of the drilling muds fall in this category. The constitutive equation for a Bingham fluid is

$$\tau = \tau_y + \mu_p \gamma \tag{B.1}$$

where  $\tau_y$  is the yield stress and  $\mu_p$  is the coefficient of rigidity, so-called plastic viscosity. The yield stress is obtained by extrapolation to zero velocity gradient and the coefficient of rigidity corresponds with the slope of the line of the plot of a  $\tau$  vs  $\gamma$  graph.

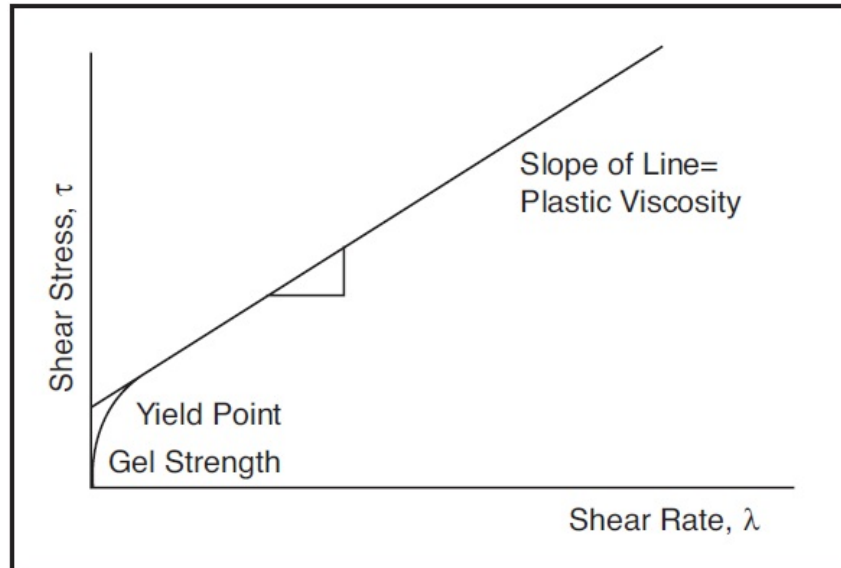
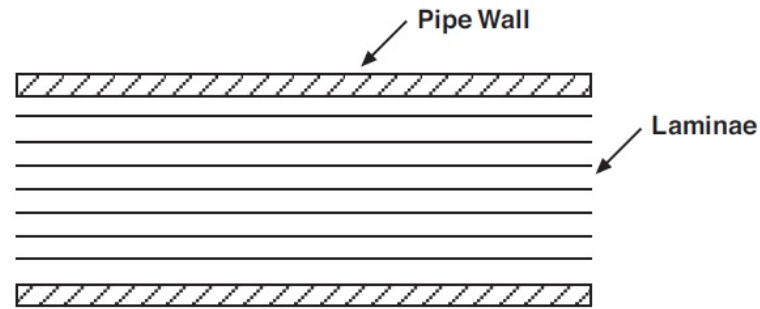


Figure – B.1 Rheogram for Bingham Plastic fluids (HWU, 2007)

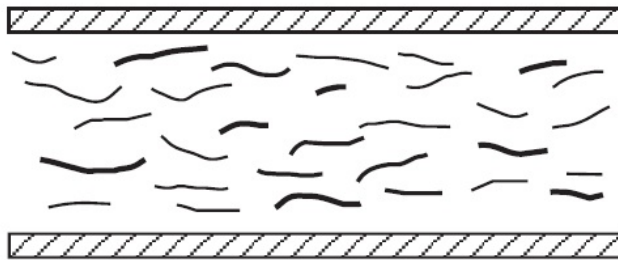
Models which behave according to the Bingham plastic model will not flow until the applied shear stress,  $\tau$ , exceeds a certain minimum shear stress value known as the yield point,  $\tau_y$ , but after the yield point has been exceeded, changes in shear stress are directly proportional to changes in shear rate, with the constant of proportionality being called the plastic viscosity,  $\mu_p$ . In reality the fluid will flow when the gel strength of the fluid has been exceeded. The yield point defined in the Bingham model is in fact an extrapolation of the linear relationship between stress and shear rate at medium to high shear rates and as such describes the dynamic yield of the fluid. The gel strength represents the shear stress to shear rate behavior of the fluid at near zero shearing conditions. This model can be used to represent a Newtonian fluid when the yield strength is equal to zero ( $\tau_y = 0$ ). In this case the plastic viscosity is equal to the Newtonian viscosity (HWU, 2007).

### **B.1.2 Flow Regime**

The first published work on fluid flow patterns in pipes and tubes was done by Osborne Reynolds. He observed the flow patterns of fluids in cylindrical tubes by injecting dye into the moving stream. On the basis of this type of work it is possible to identify two distinct types of flow pattern.



a) Laminar Flow



b) Turbulent Flow

Figure – B.2 Flow regimes (HWU, 2007)

#### **B.1.2.1 Laminar Flow:**

In this type of flow, layers of fluid move in streamlines or laminae. There is no microscopic or macroscopic intermixing of the layers. Laminar flow systems are generally represented graphically by streamlines.

#### **B.1.2.2 Turbulent Flow :**

In turbulent flow there is an irregular random movement of fluid in a transversedirection to the main flow. This irregular, fluctuating motion can be regarded assuperimposed on the mean motion of the fluid.

#### **B.1.3 Determination of the Laminar/Turbulent Boundary for a Newtonian Fluid:**

Reynolds showed that when circulating Newtonian fluids through pipes the onset of turbulence was dependent on the following variables:

- Pipe diameter,  $D$ ,
- Density of fluid,  $\rho$
- Viscosity of fluid,  $\mu$
- Average flow velocity,  $v$

He also found that the onset of turbulence occurred when the following combination of these variables exceeded a value of 2100.

This is a very significant finding since it means that the onset of turbulence can be predicted for pipes of any size, and fluids of any density or viscosity, flowing at any rate through the pipe. This grouping of variables is generally termed a dimensionless group and is known as the Reynolds number. In field units, this equation is

$$N_{Re} = \frac{928 \rho v D}{\mu} \quad (\text{B.2})$$

where  $\rho$  is the fluid density in ppg,  $v$  is the average fluid velocity in ft/s,  $D$  is the pipe inner diameter in in, and  $\mu$  is the viscosity in cp. Average fluid velocity, in field units, can be estimated as

$$v = \frac{Q}{2.448 D^2} \quad (\text{B.3})$$

where  $v$  is in ft/s,  $Q$  is the flow rate in gal/min, and  $D$  is in inches (Bourgoyne et al, 1998).

Reynolds found that as he increased the fluid velocity in the tube, the flow pattern changed from laminar to turbulent at a Reynolds number value of about 2100. However, later investigators have shown that under certain conditions, i.e., with non-Newtonian fluids and very smooth conduits, laminar flow can exist at very much higher Reynolds numbers. For Reynolds numbers of between 2,000 and 4,000 the flow is actually in a transition region between laminar flow and fully developed turbulent flow.

For practical purposes, in field units, the mean viscosity to be used in Reynolds number correlation for Bingham Plastics in pipes is presented below, as a function of plastic viscosity,  $\mu_p$ , yield stress,  $\tau_y$ , pipe diameter,  $D$ , and average fluid velocity,  $\bar{v}$ .

$$\bar{\mu} = \mu_p + \frac{6.66 \tau_y D}{\bar{v}} \quad (\text{B.4})$$

where  $\mu$  and  $\mu_p$  is in cp,  $\bar{v}$  is in ft/sec,  $D$  is in inches,  $\tau_y$  is in lb/100 ft<sup>2</sup> (Bourgoyne et al, 1998).

#### **B.1.4 Critical Reynolds Number for Bingham Plastic Fluids**

Hanks presented a laminar-turbulence criteria for Bingham Plastic fluids. A dimensionless term, called Hedstrom number is introduced.

$$N_{He} = \frac{\rho D^2 \tau_y}{\mu_p^2} \quad (\text{B.5})$$

In field units, Hedstrom number,  $N_{He}$  is expressed as

$$N_{He} = \frac{37100 \rho D^2 \tau_y}{\mu_p^2} \quad (\text{B.6})$$

Hanks pointed out that, there exists a relation between Hedstrom number and critical Reynolds number, i.e., if Reynolds number is higher, flow is turbulent. The relation in graphical form is as shown in the figure.

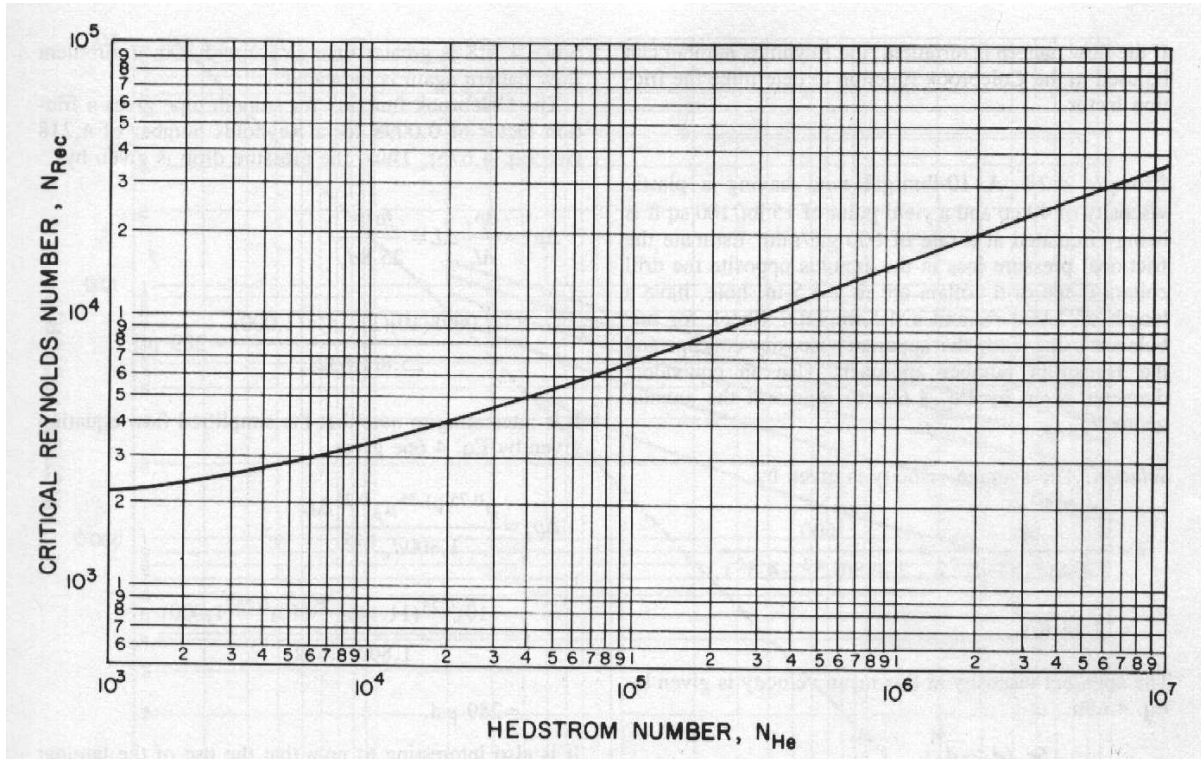


Figure – B.3 Hedstrom number versus critical Reynolds number (Bourgoyne et al, 1998)

If the calculated Reynolds number using mean viscosity is larger than critical Reynolds number, flow is turbulent.

### B.1.5 Friction Factor

The kinetic energy per volume of a fluid is known to be

$$K_E = \frac{1}{2} \rho \bar{v}^2 \quad (B.7)$$

It has been observed that, there is a relation between the ratio of the wall shear stress,  $\tau_w$ , and the kinetic energy of a fluid,  $K_E$ , which is a dimensionless quantity, called friction factor. Thus, friction factor is defined as

$$f_f = \frac{\tau_w}{K_E} = \frac{2\tau_w}{\rho \bar{v}^2} \quad (\text{B.8})$$

For a circular pipe, the relation between wall shear stress and frictional pressure loss can be derived as

$$\tau_w = \frac{\Delta P D}{\Delta L 4} \quad (\text{B.9})$$

Combining this definition with friction factor equation yields

$$\frac{\Delta P}{\Delta L} = \frac{2 f_f \rho \bar{v}^2}{D} \quad (\text{B.10})$$

This equation is a variation of Darcy-Weisbach equation (frictional pressure drop equation for Newtonian fluids), and is called Fanning equation (Whittaker, 1985). The friction factor is called the Fanning friction factor, which is commonly used in fluid mechanics. In field units, this equation is presented as

$$\frac{\Delta P}{\Delta L} = \frac{f_f \rho \bar{v}^2}{25.8 D} \quad (\text{B.11})$$

$\frac{\Delta P}{\Delta L}$  is calculated in psi/ft,  $\mu_p$  is in cp,  $\bar{v}$  is in ft/sec,  $D$  is in inches,  $\tau_w$  is in lb<sub>f</sub>/100 ft<sup>2</sup>, and  $\rho$  is in ppg (Bourgoyne et al, 1998).

For Laminar flow, relation between friction factor,  $f_f$ , and Reynolds Number,  $N_{Re}$ , is derived as

$$f_f = \frac{16}{N_{Re}} \quad (\text{B.12})$$

Colebrook equation (modified version of Nikuradze equation) is most widely used empirical correlation of friction factor for Newtonian fluids and Bingham Plastic fluids for turbulent flow regimes. Colebrook equation is given as

$$\frac{1}{\sqrt{f_f}} = 4 \log \left( N_{Re} \sqrt{f_f} \right) - 0.395 \quad (\text{B.13})$$

An iterative solution is required since  $f_f$  is present in both sides of the equation. For practical purposes, an approximation of Colebrook's equation is presented by Haaland (1983) as

$$\frac{1}{\sqrt{f}} = -3.6 \log \left( \frac{6.9}{N_{Re}} \right) \quad (\text{B.14})$$

Therefore, once the friction factor is determined properly, frictional pressure loss can be calculated.

### B.1.6 Hydrostatic Pressure

Hydrostatic pressure is defined as the pressure exerted by the weight of a static fluid column. Mathematically, it is represented as

$$P_{hyd} = \int_{h_1}^{h_2} \rho_f \bar{g} dh = \rho_f \bar{g} (h_2 - h_1) \quad (B.15)$$

Where  $h$  is the vertical fluid column length,  $\rho_f$  is the fluid density, and  $g$  is the gravitational constant. In field units, hydrostatic pressure (psi) is defined as

$$P_{hyd} = 0.052 \rho H \quad (B.16)$$

where density is in ppg, and fluid column height is in ft (Bourgoyne et al, 1998).

## B.2 Flow in Reservoir

The basic equation for the radial flow of a single phase fluid in a homogeneous porous medium is derived as

$$\frac{1}{r} \frac{\partial}{\partial r} \left( \frac{k \rho}{\mu} r \frac{\partial P}{\partial r} \right) = \phi C \rho \frac{\partial P}{\partial t} \quad (B.17)$$

Here,  $\phi$ ,  $C$ ,  $\mu$  and  $k$  are porosity, total compressibility, fluid viscosity, and permeability, respectively. This equation is non-linear since the coefficients on both sides are themselves functions of the dependent variable, the pressure. In order to obtain analytical solutions, it is first necessary to linearize the equation by expressing it in a form in which the coefficients have a negligible dependence upon the pressure and can be considered as constants (Dake, 1978).

One of the solutions for this equation is considering “transient flow”. This condition is only applicable for a relatively short period after some pressure disturbance has been created in the reservoir. In terms of the radial flow model this disturbance would be typically caused by altering the well's production / injection rate at  $r = r_w$ . In the time for which the transient condition is applicable it is assumed that the pressure response in the reservoir is not affected by the presence of the outer boundary, thus the reservoir appears infinite in extent. Unless the reservoir is extremely small, the boundary effects will not be felt and the reservoir is, mathematically, infinite. Here, both the pressure and pressure derivative, with respect to time, are themselves functions of both position and time.

After linearization, and re-arranging the terms, radial flow equation can be written as

$$\frac{1}{r} \frac{\partial}{\partial r} \left( r \frac{\partial P}{\partial r} \right) = \frac{\phi C_t \mu}{k} \frac{\partial P}{\partial t} \quad (B.18)$$

Here,  $\phi$ ,  $C$ ,  $\mu$  and  $k$  are assumed to be constant. Boundary conditions assuming a constant flow rate are:

$$P = P_f \text{ at } t = 0, \text{ for all } r \quad (\text{B.19})$$

$$P = P_f \text{ at } r = \infty, \text{ for all } t \quad (\text{B.20})$$

$$\lim_{r \rightarrow 0} r \frac{\partial P}{\partial r} = \frac{q \mu}{2 \pi k h} \text{ for } t > 0 \quad (\text{B.21})$$

If dimensionless terms for time and pressure are introduced, such that

$$t_D = \frac{k t}{\phi \mu C_t r_w^2} \quad (\text{B.22})$$

and

$$P_D(r_D, t_D) = \frac{2 \pi k h}{q \mu} (P_{r,t} - P_i) \quad (\text{B.23})$$

where

$$r_D = \frac{r}{r_w} \quad (\text{B.24})$$

Substituting these into radial diffusivity equation gives the general diffusivity equation in the dimensionless form.

$$\frac{1}{r_D} \frac{\partial}{\partial r_D} \left( r_D \frac{\partial P_D}{\partial r_D} \right) = \frac{\partial P_D}{\partial t_D} \quad (\text{B.25})$$

Where the boundary conditions in the dimensionless form are expressed as:

$$P_D(r_D, t_D = 0) = 0 \quad (\text{B.26})$$

$$P_D(r_D \rightarrow \infty, t_D) = 0 \quad (\text{B.27})$$

$$P_D(r_D = 1, t_D) = 1 \quad (\text{B.28})$$

## **B.2.1 Permeability and Skin Factor Analysis**

### **B.2.1.1 Constant Rate Flow Test**

The solution of the above equation in terms of dimensionless variables is

$$P_D(r_D, t_D) = -\frac{1}{2} Ei\left(-\frac{r_D^2}{4t_D}\right) \quad (\text{B.29})$$

Where  $Ei(x)$  is the exponential integral of  $x$ . Following the above equation, the pressure drop at any given point in the reservoir and at any given time can be computed by

$$\Delta P(r, t) = \frac{141.2 q \mu}{k h} P_D(r_D, t_D) \quad (\text{B.30})$$

Where  $\Delta P$  is in psi,  $q$  is in bbl/day,  $\mu$  is in cp,  $k$  is in md and  $h$  is in ft. For  $\frac{r_D^2}{4t_D} < 0.01$  (pressure drop at wellbore and long production/injection time), the  $Ei(-x)$  can be approximated as,

$$Ei(-x) = \ln(1.781 x) \quad (B.31)$$

Hence, for the pressure drop at the wellbore, we obtain,

$$P_{wD}(t_D) = \frac{1}{2}(\ln t_D + 0.809) \quad (B.32)$$

Substituting for the dimensionless variables in the solution equation and some rearrangements, we obtain the transient flow" solution (in field units) as

$$\Delta P = P_w - P_f = \frac{2.34 \times 10^5 q \mu}{k h} \left( \log t + \log \frac{k}{\phi \mu C_t r_w^2} - 3.23 \right) \quad (B.33)$$

$P$ 's are in psi,  $q$  is in bbl/min,  $\mu$  is in cp,  $k$  is in md,  $C$  is in  $^{-1}$ ,  $t$  is in hr,  $r_w$  is in inches (Dake, 1978).

If the well is stimulated (negative skin) or formation around the wellbore is damaged (positive skin), the pressure drop at the wellbore follows:

$$P_i - P_{bh} = \frac{141.2 q \mu}{k h} (P_D(r_{wD}, t_D) + S) \quad (B.34)$$

Similarly, the bottomhole pressure of a well for the radial flow of a single phase fluid at transient flow period in field units can be derived as

$$P_{bh} = P_i + \frac{162.6 q \mu}{k h} \left( \log t + \log \frac{k}{\phi \mu C_t r_w^2} - 3.23 + 0.87 S \right) \quad (B.35)$$

Here,  $P_{bh}$  is the bottomhole pressure (psi),  $P_i$  is the initial formation pressure (psi),  $q$  is the flow rate (bbl/day),  $\mu$  is the fluid viscosity (cp),  $k$  is the permeability (md),  $h$  is the payzone thickness (ft),  $\phi$  is the porosity (fraction),  $C$  is the compressibility ( $\text{psi}^{-1}$ ),  $r_w$  is the wellbore radius (in), and  $S$  is the skin factor (dimensionless).

When transient flow conditions prevail, a plot of  $P_{bh}$  versus  $\log t$  should be linear with slope

$$m = \frac{162.6 q \mu}{k h} \quad (B.36)$$

from which  $k.h$  and  $k$  can be determined, when the slope is determined for a log cycle. Furthermore, using the value of  $P_{bh}$  at  $1^{\text{st}}$  hour taken from the linear trend for a flowing time of one hour and solving explicitly for  $S$  gives (Dake 1978),

$$S = 1.151 \left( \frac{P_{bh(1 \text{ hr})} - P_i}{m} - \log \frac{k}{\phi \mu C_t r_w^2} + 3.23 \right) \quad (B.37)$$

### B.2.1.2 Pressure Buildup Test

Assume that a well has injected with a constant flow rate into an infinite acting reservoir for  $t$  hours, and then shut-in. The relation between the pressure behavior and time can be derived from the superposition principle (in time):

$$\Delta P(r, \Delta t) = \frac{141.2 q \mu}{k h} [P_D(r_D, t_D(tp + \Delta t)) - P_D(r_D, t_D(\Delta t))] \quad (\text{B.38})$$

Substituting for dimensionless pressure, we obtain,

$$P_{ws} = P_{wf} + \frac{162.6 q \mu}{k h} \left( \log \frac{t + \Delta t}{\Delta t} \right) \quad (\text{B.39})$$

Where  $P_{ws}$  is the shut-in pressure at the bottomhole. Therefore, if  $P_{ws}$  versus  $\log \frac{t + \Delta t}{\Delta t}$  is plotted, the slope will be equal to eq.B.36. Therefore, the permeability can be calculated (Dake, 1978).

The skin from build-up test can be computed using the following equation:

$$S = 1.151 \left( \frac{P_{ws(1 \text{ hr})} - P_{wf}}{m} - \log \frac{k}{\phi \mu C_t r_w^2} + 3.23 \right) \quad (\text{B.40})$$

### B.2.1.3 Reservoir with no-flow boundaries

To develop the transient pressure analysis for reservoirs with no-flow boundaries, the superposition principle in space is implemented. For these systems, usually the no-flow boundary is replaced with one or a set of imaginary wells which are identical to the well under consideration. In the below figure, a set of no-flow boundaries are shown. For each case, the combination of image wells is represented for modeling the system.

Case I is a well with the distance  $L$  from a no-flow boundary. In this case the no-flow boundary will be represented by 1 image well with equal distance  $2L$  from the active well. Case II shows an active well with distance  $L$  from two parallel no-flow boundaries. In this case the two no-flow boundaries will be represented with a set of image wells in both sides of the no-flow boundaries with distances  $2L, 4L, \dots$  from the active well. Case III shows the active well and a set of perpendicular no-flow boundaries. In this case three image wells are required. Case IV pertains to a U-shaped fault (no-flow boundary) system and case V shows a set of two intersecting no-flow boundaries with a 45 degrees angle between them.

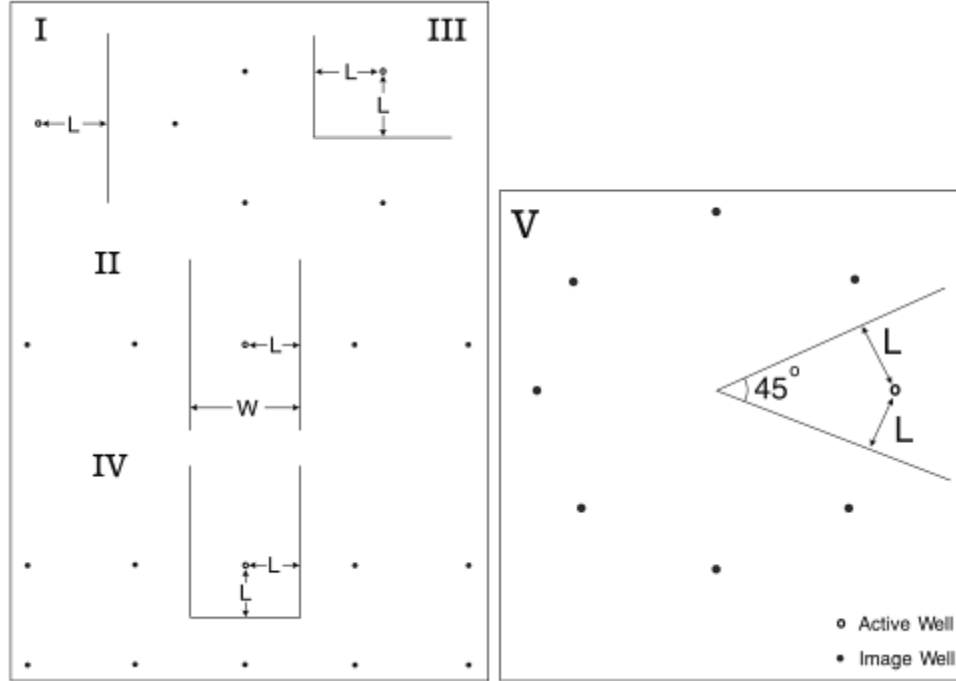


Figure – B4 No-flow boundary systems (Stewart, 2011)

According to the superposition principle, the pressure drop at each point in the reservoir at a given time is equal to the summation of pressure drops from both the active well and its corresponding image wells.

$$\Delta P(r, t) = \frac{141.2 q \mu}{k h} [P_D(r_{D0}, t_D) + \sum_{i=1}^{n_{im}} P_D(r_{Di}, t_D)] \quad (B.41)$$

Where  $P_D(r_{D0}, t_D)$  is the dimensionless pressure-drop corresponding to the active well and  $P_D(r_{Di}, t_D)$  corresponds to the dimensionless pressure drop corresponding to the image well  $i$ .  $n_{im}$  is the number of image wells. Using the above equation, one can compute the bottomhole pressure at the active well for case I (one no-flow boundary at distance  $L$  from the active well) as:

$$P_{bh} = P_i + \frac{162.6 q \mu}{k h} \left( \log t + \log \frac{k}{\phi \mu C_t r_w^2} - 3.23 + 0.87 s \right) + \frac{70.6 q \mu}{k h} Ei \left( \frac{-948 \phi \mu C_t (2L)^2}{kt} \right) \quad (B.42)$$

#### B.2.1.4 Flow region determination using diagnostic plot for pressure transient analysis

The diagnostic plot is a log-log plot of bottomhole pressure of the well and its log-derivative with respect to time versus time. The diagnostic plot is used to diagnose the type of the flow region (infant acting reservoir, boundary, etc) during a transient well test. The data corresponding to different flow regions are selected and then analyzed properly to estimate the reservoir properties as well as possible boundaries for the reservoir. The pressure derivative is defined as:

$$\Delta t \frac{d\Delta P}{d\Delta t} = \frac{d\Delta p}{d \ln \Delta t} \quad (B.43)$$

Where  $\Delta P$  and  $\Delta t$ , respectively, are the pressure drop (or build up) and the time interval of the test. Based on what we discussed before, for the transient flow region, we have,

$$\Delta P = P_w - P_f = \frac{70.6 q \mu}{k h} \left( \ln \left( \frac{kt}{948 \phi \mu C_t r_w^2} \right) + 0.809 \right) \quad (\text{B.44})$$

Therefore,

$$\frac{d\Delta P}{dt} = \frac{1}{t} \frac{70.6 q \mu}{k h} \quad (\text{B.45})$$

Or

$$t \frac{d\Delta P}{dt} = \frac{70.6 q \mu}{k h} \quad (\text{B.46})$$

This shows that the value of the derivative is constant, i.e., in the diagnostic plot of pressure derivative with respect to time, the slope of the curve corresponding to the infinite acting flow region is zero. For a well inside a reservoir, the reservoir acts as an infinite reservoir until the pressure disturbance reaches the outer boundaries of the reservoir. Diagnostic plot can also be used to determine the type of boundary of the reservoir. For example, for a semi-infinite reservoir (the no-flow boundary of case I) from Equation B.41, one can determine that once the pressure disturbance reaches the no-flow boundary, the slope of the derivative curves increases and becomes zero again while the new value of the derivative approximately is double its value corresponding to the infinite acting region. The schematic of the pressure derivative behavior for a reservoir with different type of flow boundaries are shown in below figure.

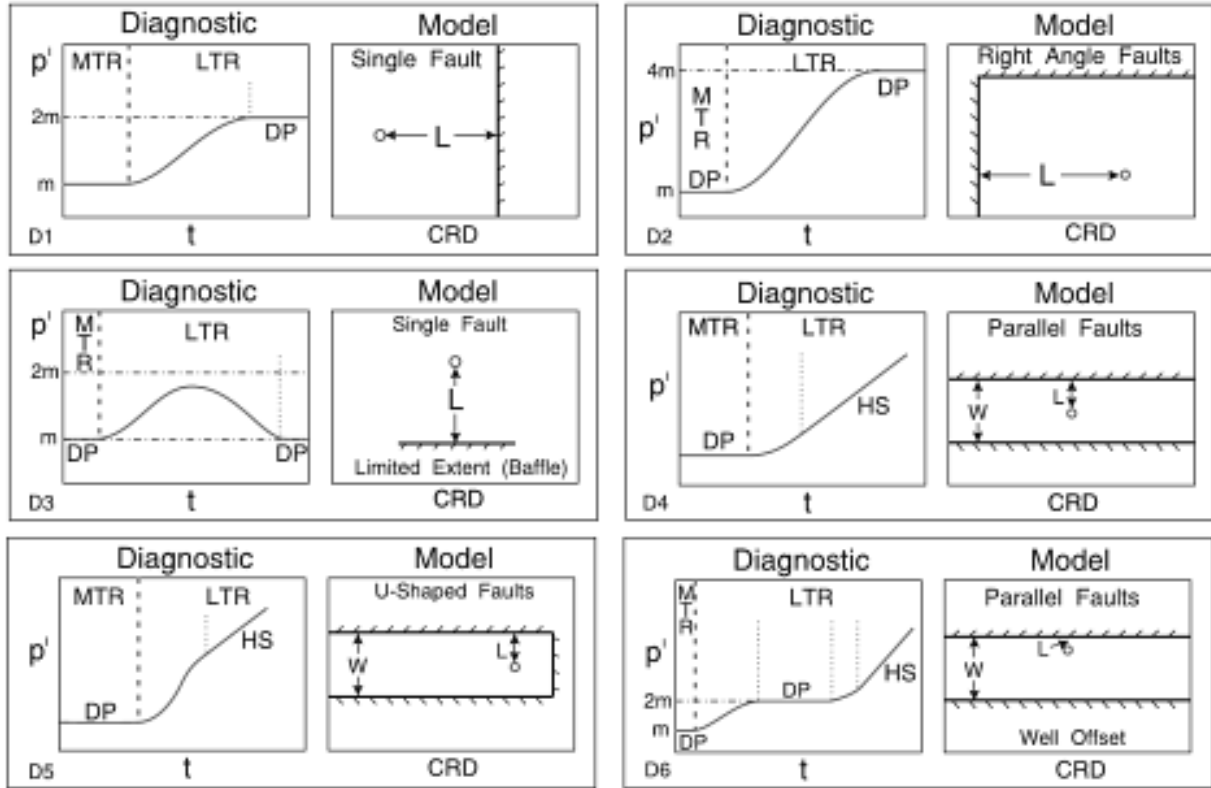


Figure – B5 Pressure derivative response for different fault systems (Stewart, 2011)

### B.3 Approximate Estimation of the Front End of the Injected Fluid

Assuming a perfect radial flow in the formations, a piston-type flow with no fingering, no flow in  $z$  or  $\theta$  direction, and ignoring any heterogeneity and anisotropy within the formations, a volume balance can be established between the injected fluid and the fluid flowing within the reservoir.

$$q t = \pi r_f^2 h \phi - \pi r_w^2 h \phi \quad (B.47)$$

Here,  $r_f$  is the front end of the injected fluid. Since  $r_w \ll r_f$ , solving the above equation yields

$$r_f = \sqrt{\frac{q t}{\pi h \phi}} \quad (B.48)$$

In field units,

$$r_f = 0.00196 \sqrt{\frac{q t}{\pi h \phi}} \quad (B.49)$$

Where  $r_f$  is in miles,  $q$  is in bbl/min,  $t$  is in hr,  $h$  is in ft.

The above equation is for a well in infinite reservoir. For a case that the active well is surrounded with two perpendicular faults, with a reasonable assumption we can modify the above equation to obtain the location of the front. To do so, we neglect the volume of the reservoir which is located between the two

no-flow boundaries and the well. Therefore, the area which the front advances through would be  $\frac{1}{4}$  of the area in the case of an infinite reservoir. From this assumption, we can estimate the location of the front by

$$q t \cong \frac{\pi}{4} r_f^2 h \phi \quad (\text{B.50})$$

Hence

$$r_f = 0.00784 \sqrt{\frac{q t}{\pi h \phi}} \quad (\text{B.51})$$

Where  $r_f$  is in miles,  $q$  is in bbl/min,  $t$  is in hr,  $h$  is in ft.

## **B. References**

1. The Institute of Petroleum Engineering, Heriot-Watt University, "Drilling Engineering", Chapter-10, 2007
2. Bourgoyne Jr. A.T., Chenevert M.E., Millheim K.K., Young Jr. F.S., "Applied Drilling Engineering", SPE Textbook Series, Chapter-4, 1998
3. Whittaker A., "Theory and Application of Drilling Fluid Hydraulics", EXLOG, Chapter-5, 1985
4. Haaland, S., "Simple and Explicit Formulas for the Friction Factor in Turbulent Flow", Trans. ASME, Journal of Fluids Engineering, vol.103, 89-90, 1983
5. Dake L.P., "Fundamentals of Reservoir Engineering", Elsevier, Chapter-7, 1978
6. Lee J, "Well Testing", SPE Textbook Series, Chapter-3, 1982
7. Stewart G., "Well Test design and Analysis", PennWell, 2011.

**APPENDIX – C**  
**CURRICULUM VITAE – EVREN M. OZBAYOGLU, Ph.D.**

**PERSONAL DATA**

**Date of Birth:** September 8, 1973  
**Place of Birth:** Ankara, Turkey  
**Marital Status:** Married  
**Home Address:** 9623 S 98<sup>th</sup> E Place, Tulsa OK 74133 – USA  
**Work Address:** The University of Tulsa, McDougall School of Petroleum Engineering, 800 S Tucker Dr. Tulsa OK 74104 – USA  
**Telephone:** Office: +1 (918) 631 2972  
Cellular: +1 (918) 607 1237  
**Fax:** +1 (918) 631 2059, +1 (918) 631 5170  
**e-mail:** [evren-ozbayoglu@utulsa.edu](mailto:evren-ozbayoglu@utulsa.edu)

**EDUCATION**

**1998-2002 The University of Tulsa, Tulsa, OK**

Doctor of Philosophy in Petroleum Engineering, Spring 2002  
Major: Drilling  
Cumulative GPA: 3.60 out of 4.0  
Ph.D. Dissertation: Cuttings Transport with Foam in Horizontal and Highly-Inclined Wellbores

**1996-1998 Middle East Technical University, Ankara, Turkey**

Master of Science in Petroleum and Natural Gas Engineering  
Major: Production  
Cumulative GPA: 3.70 out of 4.0  
M.Sc. Thesis: Wax Deposition in Horizontal Wells, 1998

**1991-1996 Middle East Technical University, Ankara, Turkey**

Bachelor of Science in Petroleum and Natural Gas Engineering  
Cumulative GPA: 3.18 out of 4.0 (Honor)

**1984-1991 Ankara Gazi Anatolian High School, Ankara, Turkey**

Major: Mathematics  
Cumulative GPA: 8.45 out of 10.0

**1979-1984 TED Ankara College-Primary School, Ankara, Turkey**

Cumulative GPA: 5.0 out of 5.0

## **WORK EXPERIENCE**

### **2009-Present University of Tulsa, Tulsa, Oklahoma, USA**

Working as an Associate Professor at TU – Petroleum Engineering Department, and conducting research at TU – Drilling Research Projects. Major interest is focused on drilling technology, multiphase flow, hole cleaning, computer applications and related topics.

### **2002-2009 Middle East Technical University, Ankara, Turkey**

Worked as an instructor (2002-2003), Assistant Professor (2003-2009), and Associate Professor (2009), and a researcher at METU Petroleum & Natural Gas Engineering Department, tenured. Also coordinated several master and doctorate level projects as well as industrial (national and international) and government supported projects.

### **1998-2002 University of Tulsa, Tulsa, Oklahoma, USA**

Worked as a graduate assistant and computer administrator at TU Petroleum Engineering, Drilling Research Projects. Major interests are; underbalanced drilling technology, cuttings transport, directional and horizontal well technology, fluid rheology, wellbore mechanics, software engineering, artificial neural networks. Participated in drilling projects sponsored by several major oil companies as well as US-DOE.

### **1996-1998 Middle East Technical University, Ankara, Turkey**

Worked as research and teaching assistant in METU Petroleum and Natural Gas Engineering Department; research assistant for METU Petroleum Research Laboratory-Drilling section; participated in several industrial projects; worked as computer administrator.

Teaching & Research Assistant Experience: Pet.E 321, Pet.E 322, Pet.E 424, Pet.E 426

### **Summer 1995 Turkish Petroleum Oil Corporation, Ankara, Turkey**

Conducted experiments on drilling fluids and cement slurries at TPAO Research Center; analyzed field data and logs; participated in “Pressure Control Simulator” workshop.

### **Summer 1994 Turkish Petroleum Oil Corporation, Luleburgaz, Turkey**

Investigated Hamitabat gas field, gas production and distribution facilities; participated in workover and acidizing operations; visited LPG plant; visited NG-electricity conversion plant.

## COMPUTER SKILLS

- Operating System MS Windows, MS DOS
- *Language* C++, Fortran, Basic
- *Software* MS Office, ANSYS, Fluent, PipePhase, Statistica, Mathematica

## PUBLICATIONS

### Conference Papers

- Osgouei R.E., Yoong W.L.S., **Ozbayoglu M.E.**, “Calculations of Equivalent Circulating Density in Underbalanced Drilling Operation”, IPTC 16601, International Petroleum Technology Conference, Beijing, China, 26–28 March 2013
- Karimi Vajargah, A., Miska, S. Z., Yu, M., **Ozbayoglu, M.E.**, “Feasibility Study of Applying Intelligent Drill Pipe in Early Detection of Gas Influx during Conventional Drilling”, SPE 163445, 2013, 2013 SPE / IADC Drilling Conference and Exhibition, March 05-07, 2013, Amsterdam, The Netherlands
- Sorgun M., Ozbayoglu A.M., **Ozbayoglu M.E.**, “Estimation of Frictional Pressure Losses in Annulus with Pipe Rotation Using Support Vector Machines and Computational Fluid Dynamics”, 10<sup>th</sup> International Congress on Advances in Civil Engineering, 17-19 October, 2012, Middle East Technical University, Ankara, Turkey
- Arslan M., **Ozbayoglu M.E.**, Miska S.Z., Yu M., Takach N., Mitchell R.F., “Buckling of Buoyancy Assisted Tubulars”, SPE 159747, SPE Annual Technical Conference and Exhibition held in San Antonio, Texas, USA, 8-10 October 2012
- Cheung E., Takach N., **Ozbayoglu M.E.**, Majidi R., Bloys B., “Improvement of Hole Cleaning Through Fiber Sweeps”, SPE Deepwater Drilling and Completions Conference, 20-21 June 2012, Galveston, Texas, USA
- **Ozbayoglu M.E.**, “Rheological Characterization of Non-Newtonian Drilling Fluids Considering Gelation Process”, Technische Universitat Bergakademie Freiberg, 63. Berg- und Hüttenmännischer Tag Freiburger Forschungsforum, June 2012
- Osgouei R.E., **Ozbayoglu M.E.**, Ozbayoglu A.M., “A Mechanistic Model to characterize the Two Phase Drilling Fluid Flow through inclined Eccentric Annular Geometry”, SPE 155147, SPE Oil and Gas India Conference and Exhibition held in Mumbai, India, 28–30 March 2012
- Rajabov V., Miska S.Z., Mortimer L., Yu M., **Ozbayoglu M.E.**, “The Effects of Back Rake and Side Rake Angles on Mechanical Specific Energy of Single PDC Cutters with Selected Rocks at Varying Depth of Cuts and Confining Pressures”, SPE 151406, IADC/SPE Drilling Conference and Exhibition, 6-8 March 2012, San Diego, California, USA
- Ozbayoglu A.M., Etehad R.O., **Ozbayoglu M.E.**, Yuksel E., “Determination of Cuttings Transport Properties of Aerated Drilling Fluids”, IPETGAS 2011 May 11th-13th 2011 Ankara – Turkey
- Gokdemir M.G., **Ozbayoglu M.E.**, Majidi R., Miska S.Z., Takach N., Yu M., “Gelation and Time Dependent Rheological Behavior of Oil / Synthetic Based Drilling Fluids”, AADE-11-NTCE-81, 2011 AADE National Technical Conference and Exhibition, Houston TX, April 12-14, 2011
- Vankadari A., Miska S.Z., Takach N., **Ozbayoglu M.E.**, Majidi R., Growcock F., Stouffer C., “Experimental Study of Torque-Reducing Additives for Extended Reach Drilling”, AADE-11-NTCE-14, 2011 AADE National Technical Conference and Exhibition, Houston TX, April 12-14, 2011
- Sorgun M., Etehad R.O., **Ozbayoglu M.E.**, Ozbayoglu M.A., “Gas-Liquid Flow through Horizontal Eccentric Annuli: CFD and Experiments compared”, ASME-ISME-KSME Joint Fluids Engineering Conference 2011, Hamamatsu, Japan, 24-29 July 2011

- **Ozbayoglu M.E.**, Ettehad R.O., Ozbayoglu A.M., Yuksel E., "Estimation of "Very-Difficult-to-Identify" Data for Hole Cleaning, Cuttings Transport and Pressure Drop Estimation in Directional and Horizontal Drilling", SPE 136304, IADC/SPE Asia Pacific Drilling Technology Conference and Exhibition, Ho Chi Minh City, Vietnam, 1-3 November 2010
- Ozbayoglu, A.M., **Ozbayoglu, M.E.** and Ozbayoglu, G., "Regression Techniques and Neural Network for the Estimation of Gross Calorific Value of Turkish Coals", Proceedings of the XIIth International Mineral Processing Symposium, pp. 1175-1180, October 6-8, 2010, Cappadocia-Nevsehir, Turkey
- Sorgun M., Aydin I., Schubert J., **Ozbayoglu M.E.**, "Modeling of Newtonian Fluids in Annular Geometries with Inner Pipe Rotation", FEDSM-ICNMM2010-31176, ASME 2010, 3<sup>rd</sup> Joint US-European Fluids Engineering Summer Meeting, Montreal, Canada, August 1-5, 2010
- Mokthari M., **Ozbayoglu M.E.**, "Laboratory Investigation on Gelation Behavior of Xanthan Crosslinked with Borate Intended To Combat Lost Circulation", SPE 136094, SPE Production and Operations Conference and Exhibition, Tunis, Tunisia, 8-10 June 2010
- **Ozbayoglu M.E.**, Ettehad R.O., Ozbayoglu A.M., Yuksel E., "Hole Cleaning Performance of Gasified Drilling Fluids in Horizontal Well Sections", SPE 131378, SPE International Oil and Gas Conference and Exhibition, Beijing, China, 8-10 June 2010
- Eren T., **Ozbayoglu M.E.**, "Real Time Optimization of Drilling Parameters During Drilling Operations", SPE 129126, SPE Oil and Gas India Conference and Exhibition, Mumbai, India, 20-22 January 2010
- **Ozbayoglu M.E.**, Ettehad R.O., Ozbayoglu A.M., Yuksel E., "Flow Pattern Identification of Gas-Liquid Flow Through Horizontal Annular Geometries", SPE 129123, SPE Oil and Gas India Conference and Exhibition, Mumbai, India, 20-22 January 2010
- **Ozbayoglu M.E.**, Sorgun M., "Frictional Pressure Loss Estimation of Water-Based Drilling Fluids at Horizontal and Inclined Drilling With Pipe Rotation and Presence of Cuttings", SPE 127300, SPE Oil and Gas India Conference and Exhibition, Mumbai, India, 20-22 January 2010
- Ercan C., **Ozbayoglu M.E.**, "'PHPA' as a Frictional Pressure Loss Reducer and its Pressure Loss Estimation", SPE 125992, SPE/IADC Middle East Drilling Technology Conference & Exhibition, Manama, Bahrain, 26-28 October 2009
- **Ozbayoglu M.E.**, "Optimization of Liquid & Gas Flow Rates for Aerated Drilling Fluids Considering Hole Cleaning For Vertical and Low Inclination Wells", Canadian International Petroleum Conference (CIPC) 2009, Calgary, Alberta, Canada, 16-18 June 2009
- **Ozbayoglu M.E.**, Sorgun M., "Frictional Pressure Loss Estimation of Non-Newtonian Fluids in Realistic Annulus with Pipe Rotation", Canadian International Petroleum Conference (CIPC) 2009, Calgary, Alberta, Canada, 16-18 June 2009
- Sorgun, M., **Ozbayoglu M.E.**, "Experimental and Numerical Study of Predicting Frictional Pressure Losses in Concentric Annulus", 17<sup>th</sup> International Petroleum & Natural Gas Congress & Exhibition of Turkey, May 13-15, Ankara, 2009
- Arpacı, E., **Ozbayoglu M.E.**, "Buckling Analysis of Drill String with FEM", 17<sup>th</sup> International Petroleum & Natural Gas Congress & Exhibition of Turkey, May 13-15, Ankara, 2009
- **Ozbayoglu M.E.**, "Dik Kuyularda Düşük Basıncılı Sondaj Operasyonları için Sıvı ve Gaz Debisi Optimizasyonu", 17<sup>th</sup> International Petroleum & Natural Gas Congress & Exhibition of Turkey, May 13-15, Ankara, 2009
- Osgouei R.E., **Ozbayoglu M.E.**, "Cuttings Transport Properties Of Gasified Drilling Fluids", 17<sup>th</sup> International Petroleum & Natural Gas Congress & Exhibition of Turkey, May 13-15, Ankara, 2009
- **Ozbayoglu M.E.**, Ozbayoglu A.M., Osgouei R.E., Yuksel H.E., "Yatay Kuyularda Kesinti Konsantrasyonunun Dijital Görüntü İşleme Teknikleri Kullanılarak Tespiti", 17<sup>th</sup> International Petroleum & Natural Gas Congress & Exhibition of Turkey, May 13-15, Ankara, 2009

- Mokhtari, M., **Ozbayoglu M.E.**, “A Laboratory investigation of Gelation Time of Xanthan Cross-linked with Borate intended to Combat Lost Circulation” , 17<sup>th</sup> International Petroleum & Natural Gas Congress & Exhibition of Turkey, May 13-15, Ankara, 2009
- **Ozbayoglu M.E.**, Ozbayoglu A.M., Osgouei R.E., Yuksel H.E., “Yatay Kuyularda İki Fazlı Akış Sırasında Meydana Gelen Akış Örüntülerinin Dijital Görüntü İşleme Teknikleriyle Tespiti” , 17<sup>th</sup> International Petroleum & Natural Gas Congress & Exhibition of Turkey, May 13-15, Ankara, 2009
- **Ozbayoglu M.E.**, Saasen A., Sorgun M., Svanes K., “Effect of Pipe Rotation on Hole Cleaning for Water-Based Drilling Fluids in Horizontal and Deviated Wells”, IADC/SPE 114965, IADC/SPE Asia Pacific Drilling Technology Conference and Exhibition held in Jakarta, Indonesia, 25-27 August 2008
- **Ozbayoglu M.E.**, Saasen A., Sorgun M., Svanes K., “Estimating Critical Velocity to Prevent Bed Development for Horizontal-Inclined Wellbores”, SPE/IADC 108005, SPE/IADC Middle East Drilling Technology Conference & Exhibition held in Cairo, Egypt, 22–24 October 2007
- **Ozbayoglu M.E.**, “Pressure Drop at the Bit During Foam Drilling”, 8th Canadian International Petroleum Conference (58th Annual Technical Meeting), Calgary, Alberta, Canada, June 2007
- **Ozbayoglu M.E.**, Ozbayoglu A.M., “Using Neural Networks for Flow Pattern and Frictional Loss Estimation for Aerated Drilling Fluids”, 8th Canadian International Petroleum Conference (58th Annual Technical Meeting), Calgary, Alberta, Canada, June 2007
- **Ozbayoglu M.E.**, Saasen A., Sorgun M., Svanes K., “Hole Cleaning Performance of Light-Weight Drilling Fluids During Horizontal Underbalanced Drilling”, 8th Canadian International Petroleum Conference (58th Annual Technical Meeting), Calgary, Alberta, Canada, June 2007
- **Ozbayoglu M.E.**, Omurlu C., “Analysis of Two-Phase Fluid Flow Through Fully Eccentric Horizontal Annuli”, 13th International Conference on Multiphase Production Technology, 2007, BHR Group Limited, Edinburgh, UK, June 2007
- **Ettehadı R.O.**, **Ozbayoglu M.E.**, “Rate of Penetration Estimation Model for Directional and Horizontal Wells”, Türkiye 16. Uluslararası Petrol ve Doğalgaz Kongre ve Sergisi, PMO, TPJD, JMO, May 2007
- **Apak E.C.**, **Ozbayoglu M.E.**, “Heat Transfer Inside the Wellbore During Drilling Operations”, Türkiye 16. Uluslararası Petrol ve Doğalgaz Kongre ve Sergisi, PMO, TPJD, JMO, May 2007
- Ozbayoglu A.M., **Ozbayoglu M.E.**, “Estimating Flow Patterns and Frictional Pressure Losses of Two-Phase Fluids in Horizontal Wellbores Using Artificial Neural Networks”, Türkiye 16. Uluslararası Petrol ve Doğalgaz Kongre ve Sergisi, PMO, TPJD, JMO, May 2007
- **Ozbayoglu M.E.**, Saasen A., Sorgun M., Svanes K., “Estimation of Critical Fluid Velocity for Preventing Cuttings Bed Development in Highly Inclined Wells”, Türkiye 16. Uluslararası Petrol ve Doğalgaz Kongre ve Sergisi, PMO, TPJD, JMO, May 2007
- **Ozbayoglu M.E.**, “Hole Cleaning: Effects of Flow Rate, Pipe Rotation, Fluid Viscosity and Inclination”, 58. Berg -und Huttenmannischer Tag, TU Bergakademie Freiberg, Germany, May 2007
- Omurlu C., **Ozbayoglu M.E.**, “Two-Phase Flow Through Fully Eccentric Horizontal Annuli: A Mechanistic Approach”, SPE 107076, SPE/ICoTA Coiled Tubing Conference and Exhibition, The Woodlands, Texas, U.S.A, April 2007
- **Ozbayoglu M.E.**, Ozbayoglu A.M., “Flow Pattern and Frictional-Pressure-Loss Estimation Using Neural Networks for UBD Operations”, SPE/IADC 108340, IADC/SPE Managed Pressure Drilling and Underbalanced Operations Conference and Exhibition held in Galveston, Texas, 28–29 March 2007
- Dogan H.A., Gucuyener İ.H., **Ozbayoglu M.E.**, “A Comprehensive Bit Hydraulics Model for Gasified Drilling Fluids”, SPE 99596, SPE/ICoTA Coiled Tubing Conference and Exhibition, The Woodlands, Texas, U.S.A, April 2006
- **Ozbayoglu M.E.**, Omurlu C., “Friction Factors for Two-Phase Fluids for Eccentric Annuli in CT Applications”, SPE 100145, SPE/ICoTA Coiled Tubing Conference and Exhibition, The Woodlands, Texas, U.S.A, April 2006

- **Ozbayoglu M.E., Omurlu C.**, “Analysis of the Eccentricity on Flow Characteristics of Annular Flow of Non-Newtonian Fluids Using Finite Element Method”, SPE 100147, SPE/ICoTA Coiled Tubing Conference and Exhibition, The Woodlands, Texas, U.S.A, April 2006
- **Ozbayoglu M.E., Omurlu C.**, “A New Mechanistic Model for Two-Phase Flow Through Eccentric Horizontal Annulus”, SPE 100300, SPE Europec/Eage Annual Conference and Exhibition, Vienna, Austria, June 2006
- **Strauss H, Ozbayoglu A.M., Ozbayoglu M.E.**, “Estimation of Foam Stability Properties Using Image Processing & Artificial Neural Networks”, 5th North American Conference on Multiphase Technology, BHR Group Limited, Banff, Canada, June 2006
- **Dogan H.A., Gucuyener I.H., Ozbayoglu M.E.**, “Investigation of bit hydraulics for gasified drilling fluids”, 12th International Conference on Multiphase, BHR Group Limited, May 2005
- **Ozbayoglu M.E., Akin S., Eren T.**, “Analysis of the influence of bubble size and texture on foam characterization”, 12th International Conference on Multiphase, BHR Group Limited, May 2005
- **Dogan H.A., Gucuyener I.H., Ozbayoglu M.E.**, “Investigation of bit pressure drop for gasified drilling fluids”, Turkiye 15. Uluslararası Petrol ve Dogalgaz Kongre ve Sergisi, PMO, TPJD, JMO, May 2005
- **Ozbayoglu M.E., Akin S., Eren T.**, “Rheological Characterization of Foam Using Image Processing Techniques”, Turkiye 15. Uluslararası Petrol ve Dogalgaz Kongre ve Sergisi, PMO, TPJD, JMO, May 2005
- **Omurlu C., Ozbayoglu M.E.**, “Flow-Rate Optimization of Aerated Fluids for Underbalanced Applications”, Turkiye 15. Uluslararası Petrol ve Dogalgaz Kongre ve Sergisi, PMO, TPJD, JMO, May 2005
- **Ozbayoglu M.E.**, “Minimization of Drilling Cost by Optimization of the Drilling Parameters”, Turkiye 15. Uluslararası Petrol ve Dogalgaz Kongre ve Sergisi, PMO, TPJD, JMO, May 2005
- **Ozbayoglu M.E., Omurlu C.**, “Flow-Rate Optimization of Aerated Fluids for Underbalanced Coiled-Tubing Applications”, SPE 94164, SPE/ICoTA Coiled Tubing Conference and Exhibition, The Woodlands, Texas, U.S.A, April 2005
- **Ozbayoglu M.E., Akin S., Eren T.**, “Foam Characterization Using Image Processing Techniques”, SPE 93860, SPE Western Regional Meeting, Irvine, CA, U.S.A, April 2005
- **Ozbayoglu M.E.**, “A Review on Cuttings Transport While Drilling”, Freiberg Forschungsforum, 55. Berg -und Huttenmannischer Tag, TU Bergakademie Freiberg, Germany, June 2004
- **Ozbayoglu M.E., Miska S.Z., Reed T., Takach N.**, “Analysis of the Effects of Major Drilling Parameters on Cuttings Transport Efficiency for High-Angle Wells in Coiled Tubing Drilling Operations”, SPE 89334, SPE/ICoTA Coiled Tubing Conference and Exhibition, U.S.A, March 2004
- **Ozbayoglu E., Gunes C., Apak E.C.**, “Determination of Filtration of Water-Clay Suspensions Without Conducting Filtration Tests, Su-Kil Suspansiyonlarının Filtrasyonunun, Filtrasyon Testi Yapılmadan Elde Edilmesi”, 14th International Petroleum & Natural Gas Congress and Exhibition of Turkey, 12-14 May, 2003, TPJD, TMMOB-PMO, TMMOB-JMO, May 2003
- **Ozbayoglu M.E.**, “Underbalanced Drilling Techniques: Aerated Muds and Foam Applications”, Sondaj 2003 Sempozyumu, 10-11 April 2003, MTA, TMMOB-MMO
- **Ozbayoglu M.E.**, “Empirical Correlations For Estimating Bed Thickness in Horizontal Wellbores”, Turkiye 14. Uluslararası Petrol ve Dogal Gaz Kongresi ve Sergisi, 12-14 May, 2003, TPJD, TMMOB-PMO, TMMOB-JMO
- **Ozbayoglu M.E., Miska Z.S., Reed T., Takach N.**, “Cuttings Transport with Foam in Horizontal & Highly-Inclined Wellbores”, SPE 79856, SPE/IADC Drilling Conference, 19-21 February, 2003, Netherlands

- **Ozbayoglu E., Miska S., Reed T., Takach N.**, “Analysis of Bed Thickness in Horizontal and Highly-Inclined Wellbores by using Artificial Neural Networks”, SPE/CIM ITOHOS-ICHWT 78939, 4-7 November, 2002, Calgary, Alberta, Canada.
- **Ozbayoglu E., Kuru E., Miska S., Takach N.**, “A Comparative Study of Hydraulic Models for Foam Drilling”, SPE 65489, SPE/Petroleum Society of CIM International Conference on Horizontal Well Technology, 6-8 November, 2000, Calgary, Alberta, Canada.
- **Kuru E., Miska S., Ozbayoglu E., Sunthakar A.**, “Overview of Foam and Aerated Muds Hydraulics for Underbalanced Drilling”, 11<sup>th</sup> International Scientific and Technical Conference, June 29-30, 2000, Krakow, Poland
- **Kok M.V., Ozbayoglu E., Batmaz T.** “Development of Drilling Fluid Program for an Oil Field in Azerbaijan”, Offshore Mediterranean Conference, 24-26 March, Ravenna, 1999, Italy.
- **Kok M.V., Ozbayoglu E.**, “Application of EOR Techniques for Turkish Oil Fields – Economic and Technical Analysis”, Offshore Mediterranean Conference, 24-26 March, Ravenna, 1999, Italy.
- **Ozbayoglu E., Demiral B., Kok M.V.**, “Modeling of Wax Deposition in Horizontal Wells”, 7<sup>th</sup> UNITAR, International Conference on Heavy Crude and Tar Sands, 27-30 October, Beijing, 1998, China.

#### Journal Papers

- **Ozbayoglu M.E., Ettehad R.O., Ozbayoglu A.M., Yuksel E.**, “Hole Cleaning Performance of Gasified Drilling Fluids in Horizontal Well Sections”, SPE 131378, SPE Journal, Volume 17, Number 3, pp. 912-923, September (2012)
- **Sorgun M., Aydin I., Ozbayoglu E., Schubert J.J.**, “Mathematical Modeling of Turbulent Flows of Newtonian Fluids in a Concentric Annulus with Pipe Rotation”, Energy Sources, Part A, 34:540–548, 2012
- **Sorgun M., Aydin I., Ozbayoglu E.**, “Friction factors for hydraulic calculations considering presence of cuttings and pipe rotation in horizontal/highly-inclined wellbores”, Journal of Petroleum Science and Engineering, 78 (2), (2011) 407–414
- **Osgouei R.E., Ozbayoglu M.E., Ozbayoglu A.M., Yuksel E.**, “A New Model to Determine the Two Phase Drilling Fluid Behavior through Horizontal Eccentric Annular Geometry, Part B: Frictional Pressure Losses Estimation”, Energy Sources Part A, UESO-2011-0015.R1, DOI 10.1080/15567036.2011.561275, in press
- **Osgouei R.E., Ozbayoglu M.E., Ozbayoglu A.M., Yuksel E.**, “A New Model to Determine the Two Phase Drilling Fluid Behavior through Horizontal Eccentric Annular Geometry, Part A: Flow Pattern Identification and Liquid Hold up Estimation”, Energy Sources Part A, UESO-2011-0084.R1, DOI 10.1080/15567036.2011.574192, in press
- **Sorgun M., Ozbayoglu M.E.**, “Predicting Frictional Pressure Loss During Horizontal Drilling for Non-Newtonian Fluids”, Energy Sources Part A, 33:7, 631-640, 2011
- **Sorgun M., Ozbayoglu M.E.**, “A Mechanistic Model for Predicting Frictional Pressure Losses for Newtonian Fluids in Concentric Annulus”, PETROLEUM SCIENCE & TECHNOLOGY, 28:16, pp:1665-1673, (2010)
- **Ozbayoglu M.E., Sorgun M.**, “Frictional Pressure Loss Estimation of Non-Newtonian Fluids in Realistic Annulus with Pipe Rotation”, Journal of Canadian Petroleum Technology, Volume 49, Number 12, pp. 57-64, December 2010
- **Ozbayoglu M.E.**, “Optimization of Liquid & Gas Flow Rates for Aerated Drilling Fluids Considering Hole Cleaning For Vertical and Low Inclination Wells”, Journal of Canadian Petroleum Technology, Volume 49, Number 10, pp. 15-24, October 2010

- Sorgun M., **Ozbayoglu M.E.**, Aydin I., “Modeling and Experimental Study of Newtonian Fluid Flow in Annulus”, *Journal of Energy Resources Technology*, Vol. 132, September 2010.
- **Ozbayoglu M.E.**, Saasen A., Sorgun M., Svanes K., “Hole Cleaning Performance of Light-Weight Drilling Fluids During Horizontal Underbalanced Drilling”, *JOURNAL OF CANADIAN PETROLEUM TECHNOLOGY (SPE)*, Vol: 4, April issue, pp:21-26, (2010)
- **Ozbayoglu M.E.**, Saasen A., Sorgun M., Svanes K., “Critical Fluid Velocities for Removing Cuttings Bed Inside Horizontal and Deviated Wells”, *PETROLEUM SCIENCE AND TECHNOLOGY*, 28:6, 594-602 (2010)
- **Ozbayoglu M.E.**, Ercan C., “PHPA as a Frictional Pressure Loss Reducer and Its Pressure Loss Estimation”, *PETROLEUM SCIENCE AND TECHNOLOGY*, 28:6, 625-631 (2010)
- Omurlu C., **Ozbayoglu M.E.**, “Friction Factor Determination for Horizontal Two-Phase Flow Through Fully Eccentric Annuli” , *PETROLEUM SCIENCE AND TECHNOLOGY*, 27:15, 1771-1782 (2009)
- Apak E.C.,**Ozbayoglu M.E.**, “Heat Distribution within the Wellbore While Drilling”,*PETROLEUM SCIENCE AND TECHNOLOGY*, 27:7, 678-686 (2009)
- Dogay S., **Ozbayoglu M.E.**, Kok M.V., “Trajectory Estimation in Directional Drilling Using Bottom Hole Assembly Analysis”, *ENERGY SOURCES PART-A*, 31:2 553-559 (2009)
- **Ozbayoglu M.E.**, “Pressure Loss at the Bit While Drilling with Foam”, *PETROLEUM SCIENCE & TECHNOLOGY*, 27:7, 687-698 (2009)
- **Ozbayoglu M.E.**, Ozbayoglu M.A., “Estimating Flow Patterns and Frictional Pressure Losses of Two-Phase Fluids in Horizontal Wellbores Using Artificial Neural Networks”, *PETROLEUM SCIENCE & TECHNOLOGY*, 27:2, 135-149 (2009)
- **Ozbayoglu M.E.**, Miska, Z.S., Takach, N., Reed, T., “Sensitivity Analysis of Major Drilling Parameters on Cuttings Transport during Drilling Highly-inclined Wells”, *PETROLEUM SCIENCE & TECHNOLOGY*, 27:1, 122-133 (2009)
- **Ozbayoglu M.E.**, “Drill Bit Pressure Drop During Foam Drilling Operations”, *JOURNAL OF CANADIAN PETROLEUM TECHNOLOGY*, Vol: 47, Issue: 6, 64-69 (2008)
- **Ozbayoglu G.**, **Ozbayoglu A.M.**, **Ozbayoglu M.E.**, “Estimation of Hardgrove Grindability Index of Turkish Coals by Neural Networks”, *INTERNATIONAL JOURNAL OF MINERAL PROCESSING*, 85, 93-100 (2008)
- **Ozbayoglu A.M.**, Aydiner, Z., Kasnakoglu, C. and **Ozbayoglu M.E.**, “Neural network and genetic programming in pressure loss estimation in eccentric pipe flow”, *Intelligent Engineering Systems Through Artificial Neural Networks*, vol 18, pp 163-170, ASME Press, New York, 2008
- **Ozbayoglu M.E.**, Akin S., and Eren T., “Image Processing Techniques in Foam Characterization”, *ENERGY SOURCES PART-A*, 29: 1175-1185, 2007
- **Ozbayoglu M.E.**, and Omurlu C., “Modelling of Two-Phase Flow Through Concentric Annuli”, *PETROLEUM SCIENCE & TECHNOLOGY*, 25:8, 1027-1040, 2007
- **Ozbayoglu M.E.**, and Omurlu C., “Comparative Study of Yield-Power Law Drilling Fluids Flowing Through Annulus”, *PETROLEUM SCIENCE & TECHNOLOGY*, 25:8, 1041-1052, 2007
- **Ozbayoglu G.**, **Ozbayoglu M.E.**, “A New Approach for the Prediction of Ash Fusion Temperatures: A Case Study Using Turkish Lignites”, *FUEL* (85), 2006, 545-552
- Apak, E.C., **Ozbayoglu M.E.**, “Heat Transfer Inside the Wellbore During Drilling Operations, Sondaj Operasyonları Sirasında Kuyu İçerisindeki Isı Transferi”, *Turkish Journal of Oil and Gas, Türk Petrol ve Doğalgaz Dergisi*, Vol: 12, No: 3, TMMOB Petrol Mühendisleri Odası (PMO), 8-19, (October 2006)
- **Ozbayoglu M.E.**, Gunes C., Apak E.C., Kok M.V., İscan A.G., “Empirical correlations for estimating filtrate volume of water based drilling fluids”, *PETROLEUM SCIENCE AND TECHNOLOGY*, Vol: 23, No: 3-4, 423-436, March 2005

- **Ozbayoglu M.E., Miska Z.S., Takach N., Reed T.,** “Using foam in horizontal well drilling: A cuttings transport modeling approach”, JOURNAL OF PETROLEUM SCIENCE AND ENGINEERING, Vol :46, No :4, 267-282, April 2005
- **Ozbayoglu M.E., Omurlu C.,** “Minimization of Drilling Cost by Optimization of the Drilling Parameters, Sondaj Parametrelerinin Optimizasyonu ile Sondaj Maliyetinin Asgariye İndirilmesi”, Turkish Journal of Oil and Gas, Turk Petrol ve Dogal Gaz Dergisi, Vol: 10, No: 3, October 2004, 28-36
- **Ozbayoglu M.E., Gunes C., Apak E.C.,** “Determination of Filtration of Water-Clay Suspensions Without Conducting Filtration Tests, Su-Kil Suspansiyonlarının Filtrasyonunun, Filtrasyon Testi Yapılmadan Elde Edilmesi”, Turkish Journal of Oil and Gas, Turk Petrol ve Dogal Gaz Dergisi, Vol :9, No :3, TMMOB Petrol Muhendisleri Odasi (PMO), 3-11, October2003
- **Ozbayoglu, E., Kuru, E., Miska, S. and Takach, N.,** “A Comparative Study of Hydraulic Models for Foam Drilling”, Journal of Canadian Petroleum Technology, Vol :41, No :6, 2002
- **Ozbayoglu E., Demiral B. and Kok M.V.,** “Comparison of Wax Deposition in Vertical and Horizontal Oil Production Wells”, IN-SITU, 24 (1), 1-19 (2000)
- **Ozbayoglu E., Demiral B. and Kok M.V.,** “Wax Deposition in Wells”, Petroleum Science and Technology, Volume 18, Numbers 1&2, 177-195, 2000

#### Book Chapter

- Mitchell R.F., Miska S.Z., *Fundamentals of Drilling Engineering*, SPE Textbook Series Vol.12, Revision of Chapter-6, “Rotary Drilling Bits”, pp.311-384, ISBN 978-1-55563-207-6, (2011)
- Jeofizik Mühendisleri Odası, *TMMOB Jeotermal Kongresi Bildiriler Kitabı*, Oda Yayın No: 4, pp:387-404, ISBN 978-9944-89-860-7, (2009)

#### PROJECTS

- *TUCoRE; CHEVRON – TU (Ozbayoglu M.E., Ram M., Gomez L., Bloys B.),* “Top Kill – Improving Predictions & Procedures”, Theoretical & Experimental Work, (still on progress) (co-PI)
- *TUCoRE; CHEVRON – TU (Ozbayoglu M.E., Takach N., Majidi R., Bloys B.),* “Cuttings Transport Efficiency of Fiber Sweeps”, Experimental Work, (still on progress) (PI)
- *STATOIL – TU (Ozbayoglu M.E., Abdollahi J.),* “Feasibility of Low Density Drilling Fluids”, Theoretical Work, 2012 (PI)
- *SHELL – TU (Ozbayoglu M.E., Hale A.),* “Barite Sagging and Gel Breaking Pressure Determination of Synthetic-Based Drilling Fluids”, Experimental Work, 2011 (PI)
- *IMPACT TECHNOLOGIES (Ozbayoglu M.E., Oglesby K.),* “Heat Transfer and Hydraulics Modeling for Abrasive Drilling Applications”, Theoretical Work, 2010 – 2011 (PI)
- *HALLIBURTON – TU (Ozbayoglu M.E., Maxley J.),* “Determination of the Time-Dependent Rheological Behavior of Oil-Based Drilling Fluids”, Experimental and Theoretical Work, 2010 (PI)
- *STATOIL ASA – Middle East Technical Univesity (Ozbayoglu E., Saasen A.),* “Hole Cleaning Performance of Water and Oil Based Muds”, Experimental and Theoretical Work, 2006, No: 4501007879 (PI)
- *Freiberg University (Ozbayoglu M.E., Strauss H., Ozbayoglu A.M.),* “Stability of Foams under Elevated Pressures and Temperatures”, Experimental and Theoretical Work, 2006 (PI)
- *Weatherford, The University of Tulsa – Drilling Research Projects (Ozbayoglu E., Smith, J.),* “Cuttings Transport Performance of the New Drillpipe in Horizontal Wells”, Experimental Work, 2001 (PI)
- **Ozbayoglu E.,** “Cuttings Transport Performance of Aerated Drilling Fluids”, TUBITAK MAG – 108M106, 2008 (PI)

- **Ozbayoglu M.E., Akin S., Kok M.**, “Dusuk Basincli Sondaj Akiskanlarinin Karakterizasyonu: Kopuklu Akiskan Uygulamalari”, TUBITAK-MISAG, Nisan:2003 – Kasim 2004 (PI)
- **Ozbayoglu M.E.**, “Hava Karisimli Sondaj Akiskanlarinin Yatay, Yonlu ve Dikey Kuyulardaki Kesik Tasima Performansi”, METU-BAP, Mayıs 2003 – Nisan 2004 (PI)
- **Kok M.V., Ozbayoglu E.**, “Rheological Behavior of Bentonite Slurries”, Karakaya Bentonite Company – TUBITAK YDABCAG 286, 1997 (researcher)
- **Ozbayoglu E., Kok M.V., Batmaz T.**, “Experimental Analysis of Drilling Fluid Additives and Cement for Kemaleddin Oil Field-Azerbaijan”, PET Corporation, May 1996 (researcher)

#### **Short Courses for Industry**

- **Ozbayoglu M.E.**, “Underbalanced Drilling Fundamentals”, TPAO (under construction)
- **Ozbayoglu M.E., Altun G.**, “Drill String Design and Casing Design”, TPAO
- **Ozbayoglu M.E.**, “Drilling Machinery and Equipment Selection Process for Geothermal Drilling Operations”, Chamber of Turkish Mining Engineers
- **Ozbayoglu M.E.**, “Well Control and Circulation Procedures”, Association of Drillers - Turkey

#### **EDUCATIONAL ACTIVITIES**

##### **Courses**

##### **TU**

- PE 3043 – Drilling Engineering – I
- PE 4043 – Drilling Engineering – II
- PE 4063 – Well Completion and Construction Design
- PE 4993 – Independent Study
- PE 7123 – Advanced Drilling Fluids
- PE 7993 – Independent Study

##### **METU**

- PETE 110 – Introduction to Petroleum Engineering
- PETE 321 – Drilling Engineering – I
- PETE 322 – Drilling Engineering – II
- PETE 422 – Well Control
- PETE 426 – Drilling Fluids Engineering
- PETE 492 – Emerging Technologies in Drilling Engineering
- PETE 497 – Multiphase Flow
- PETE 490 – Independent Study
- PETE 501 – Drilling Hydraulics
- PETE 703 – Multiphase Flow in Pipes and Annulus
- PETE 704 – Advanced Wellbore Mechanics

##### **Other**

- MAD344 – Drilling Technology and Engineering (Hacettepe University)
- TUPEP – Horizontal and Multilateral Drilling & Completions

### **Completed Ph.D. Thesis**

- “Determination of Cuttings Transport Properties of Gasified Drilling Fluids”, Reza Ettehad Osgouei, October 2010, METU
- “Real-time-optimization of drilling parameters during drilling operations”, Tuna Eren May 2010, METU

### **Completed M.Sc. Thesis**

- “Determination of Viscoelastic Properties of Drilling Fluids”, Binh Bui, April 2012, TU
- “Study of Yield Power Law Fluids Transitional Flow Regime in Pipes”, Goktug Kalayci, March 2012 (co-advisor), TU
- “Buckling and Axial Force Transfer of Buoyancy Assisted Casing”, Mehmet Arslan, January 2012 (co-advisor), TU
- “Laboratory Investigation of Gelation Behavior of Xanthan Cross-linked with Borate Intended to Combat Lost Circulation”, Mehdi Mokhtari, December 2010 (co-advisor), METU
- “Overview of solutions to prevent liquid loading problems in gas wells”, Ozmen Binli, December 2009, METU
- “Analysis of sinusoidal and helical buckling of drill string in horizontal wells using finite element”, Erdogan Arpacı, September 2009, METU
- “Hydraulics optimization of foam drilling in drilling operations”, Ceren Ozer, October 2009, METU
- “Rate of Penetration Estimation Model for Directional and Horizontal Wells”, Reza Ettehad Osgouei, September 2007, METU
- “PHPA As a Frictional Pressure Loss Reducer and its Pressure Loss Estimation”, Can Ercan, June 2007, METU
- “A Study on Heat Transfer Inside the Wellbore During Drilling Operations”, Esat Can Apak, December 2006, METU
- “Mathematical Modeling of Horizontal Two-Phase Flow Through Fully Eccentric Annuli”, Cigdem Omurlu, June 2006, METU
- “Foam Characterization: Bubble Size and Texture Effects”, Tuna Eren, September 2004, METU
- “Investigation of Bit Hydraulics for Gasified Drilling Fluids”, Huseyin Ali Dogan, April 2004, METU

## **HONORS AND ACTIVITIES**

### **Prizes and Awards**

- SPE Journal, “2012 Outstanding Technical Editor Award”, October 2012
- SPE Reservoir Application & Engineering, “2012 Outstanding Technical Editor Award”, October 2012
- Prof.Dr. Mustafa Parlar Vakfi, “2005-2006 Egitimde Ustun Basari Odulu (Excellence in Education Award)”, December 2006
- Prof.Dr. Mustafa Parlar Vakfi, “2004-2005 Yilin Egitimcisi Odulu (Educator of the Year Award)”, December 2005
- Prof.Dr. Mustafa Parlar Vakfi, “2002-2003 Yilin Egitimcisi Odulu (Educator of the Year Award)”, December 2003
- The University of Tulsa, Allen Chapman Distinguished Ph.D. Student Award, 2001.

### **Editorial Activities**

- Associate Editor, International Journal of Oil, Gas and Coal Technology
- Reviewer, ASME Journal of Energy Resources Technology, SPE Journal, SPE Drilling & Completions, Journal of Natural Gas Science & Engineering, Chemical Engineering Communications, Industrial & Engineering Chemistry Research, ASME Journal of Fluids Engineering

### **OTHER ACTIVITIES**

- Associate Director, TUDRP
- Member, Undergraduate Curriculum Committee, TU-PE
- Undergraduate Advisor, TU-PE
- Co-chairperson, May 2003 – June 2009, METU Petroleum & Natural Gas Eng. Dept.
- Board Member, February 2004 – July 2009, TMMOB-Chamber of Petroleum Engineers
- Treasurer, February 2004 – July 2006, SPE Turkey Section
- Academic Advisor, September 2002 – July 2009, SPE METU Student Chapter

### **Conference Organization**

- PMO, TPF, JMO, 16th International Petroleum & Natural Gas Congress and Exhibition, May 2007, Ankara-Turkey
- PMO, TPF, JMO, 15th International Petroleum & Natural Gas Congress and Exhibition, May 2005, Ankara-Turkey

### **Others**

- TU-TSA, Academic Advisor, 2010-Present
- TMMOB Turkish Petroleum Engineers Chamber, Board Member, 2003-2009
- SPE Turkey, METU Student Chapter, Academic Advisor, 2002-2009
- SPE Member, 1994-Present
- SPE Turkish Student Chapter, President, METU, 1996-1998
- Tulsa University, Turkish Student Association, President, 1999-2002
- Turkish-American Association-Oklahoma, Board Member, 2000-2002

## **APPENDIX H**

### **SCHLUMBERGER RE-EVALUATION OF MES OCTOBER 2010 PRESSURE FALL OFF TEST**

**BY  
YOSMAR GONZALEZ**



## Slickline Services



# A & M Engineering and Environmental Services, Inc. Well: MES#1 (October 2010) Pressure Fall Off Review

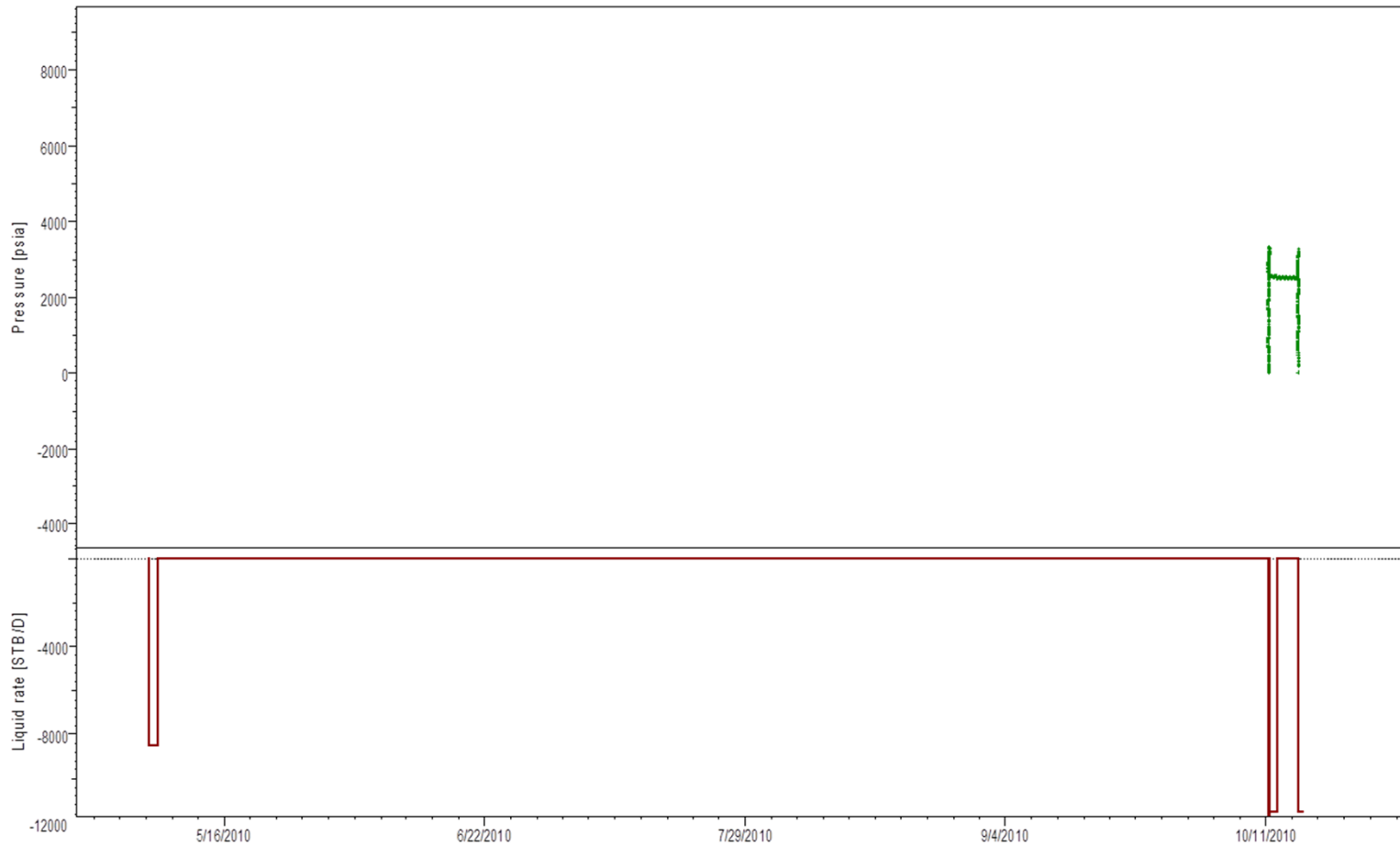
Yosmar Gonzalez

Senior Reservoir Engineer

All interpretations are opinions based on inferences from electrical or other measurements and we cannot, and do not guarantee the accuracy or correctness of any interpretation, and shall not, except in the case of gross or willful negligence on our part, be liable or responsible for any loss, costs, damages or expenses incurred or sustained by anyone resulting from any interpretations made by any of our officers, agents or employees. These interpretations are also subject to Clause 4 of our General Terms and Conditions as set out in our current Price Schedule

**Schlumberger**

# All Injection rate history and recorded Pressure vs. time



History plot (Pressure [psia], Liquid rate [STB/D] vs Time [hr])

Schlumberger Public

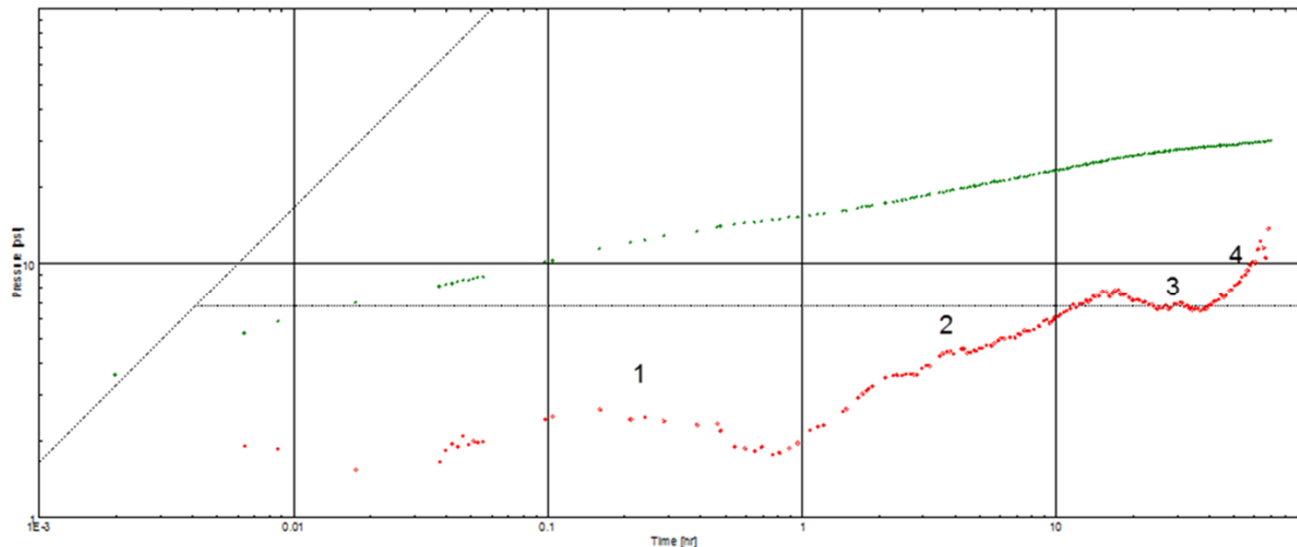


Slickline Services



Schlumberger

# Log-Log Plot (Flow Regime Identification)



Log-Log plot:  $p-p@dt=0$  and derivative [psi] vs dt [hr]

1. Possible first radial flow or initial dual porosity behavior (valley) mask by wellbore dynamics(unloading effects)
2. From 1 to 16 hours the pressure derivative shows a half unit slope
3. Radial flow regime from 23 hrs to 38 hours.
4. the pressure derivative slope increases implying boundaries effects after 38 hours and until the end of the shut-in time.

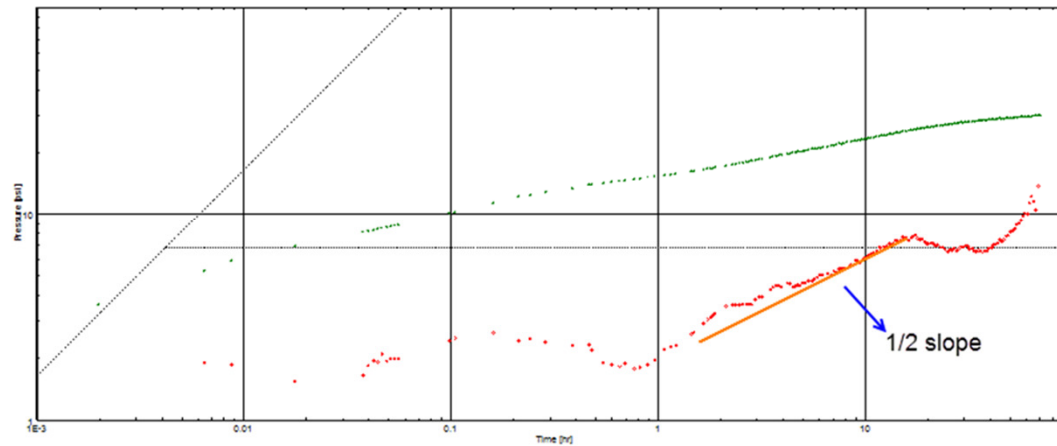


Slickline Services



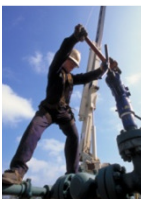
Schlumberger

# Log-Log Plot



Log-Log plot:  $p-p@dt=0$  and derivative [psi] vs dt [hr]

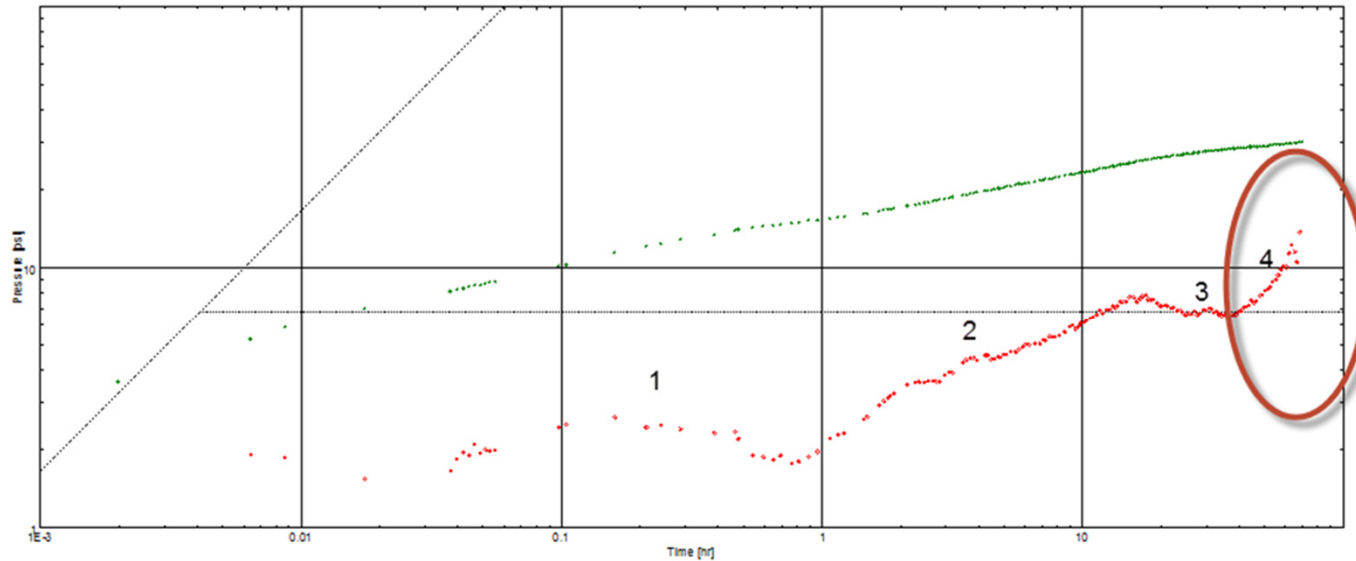
The pressure derivative shows an half slope (possible linear flow) from 1 to ~16 hours. If the well intersect a fracture- either a natural fracture or a fracture induced during well stimulation- flow will be from the fracture (s) to the well, and the fractures will be recharge from the matrix. A time period of linear flow may occur when the pressure support is primarily along a fracture or fractures connected to the well. If the fracture connected to a well are of limited extent, the flow response will progress, after a period of time to a radial flow behavior. In some Natural Fracture Reservoirs a pressure transient test may show both fracture-dominated response or a matrix-dominated response, which could be consider as a dual porosity system.



## Slickline Services



# Log-Log Plot



Log-Log plot:  $p-p@dt=0$  and derivative [psi] vs dt [hr]

The pressure derivative at the late time region (after 38 hrs. of shut-in) might be affected by the short injection time. The pressure derivative calculation corrects the pressure scale to account for the details of the well injection history. If no sufficient flow history, this will result in an “apparent” or “artificial” late-time trend in the pressure derivative that could be misinterpreted as reservoir boundaries. It is advisable to validate this pressure behavior with the geological model to validate the reservoir boundaries.



Slickline Services



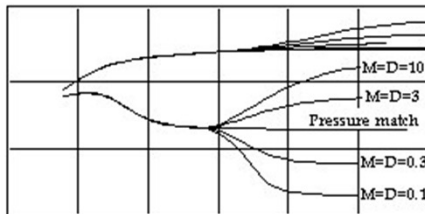
Schlumberger

# Conclusions

The flow regime between 23 and ~34 hours is assumed to be radial flow regime, under this assumption the linear flow behavior (half slope-between 0.6 and 7.8 hrs) could be related to : 1) a fracture-dominated response 2) well located in a channel or 3) a radial composite model.

The assumptions for a radial composite reservoir are: The well is at the center of a circular homogeneous zone, communicating with an infinite homogeneous reservoir. The inner and outer zones have different reservoir and/or fluid characteristics. There is no pressure loss at the interface between the two zones.

## Behavior



## Parameters

- $r_i$  - The distance from the well to the interface.
- M - Mobility ratio,  $(k/\mu \text{ inner zone}/k/\mu \text{ outer zone})$
- D - Diffusivity ratio,  $(k/\phi\mu.ct \text{ inner}/k/\phi\mu.ct \text{ outer})$

At early time a homogeneous response corresponding to the inner zone may be seen. After a transition, the reservoir shows a second homogeneous behavior, corresponding to the outer zone. The pressure derivative may show two stabilizations. The time of transition between the two homogeneous regimes is a function of  $r_i D$  and  $k/\phi\mu.ct$  for the inner zone. The ratio of the constant derivative levels is equal to the mobility ratio, the shape of the transition between the two homogeneous behaviors is governed by the ratio  $M/D$ . For this case the injected fluid was fresh water and the reservoir water being displaced has a highly saline water (120,000 to 140,000 ppm chlorides), this scenario possible caused a two zones with different mobilities within the reservoir.



Slickline Services



# Conclusions

The pressure derivative on the late time region (after the possible second radial flow) might indicate reservoir boundaries. The dual porosity model presented by Schlumberger in 2010 is supported because it has the right location for the radial flow period. The report presented by Schlumberger team in 2010 the reservoir was treated as infinite reservoir, for this review the reservoir will be treated as a faulty reservoir and no infinite considering the increase in the pressure derivative after ~35 hours.

It is not advisable to locate the radial flow regime prior to 1 hour and state the increase in the pressure derivative following the half unit slope is attributable to parallel or faulty reservoir. This scenario should be analyzed with caution. Two main flow regimens happen after 24 hours: 1) the long period of radial flow from 24 hours to 34 hours and 2) another increase in the pressure derivative after 35 hours. These flow regimes are not affected by wellbore dynamics to be ignored. In a multiple reservoir boundaries system, it is not expected to see a second radial flow period, what we expect to see is the pressure derivative increasing as is observed after 35 hours for this case.



**Slickline Services**



# APPENDIX I

MES' RESPONSE TO NOD LETTER DATED MAY 19, 2025

## TABLE 8

A SUMMARY OF THE BOTTOMHOLE PRESSURES MEASURED AT THE END OF SHUT-IN PERIOD,  
RECORDED DURING ANNUAL PFTS



## DEFICIENCY NO 8

In Section 1.6.2.1 of the Application, the well integrity tests listed include the annual PFT required by 40 C.F.R. 146.13(d) and the five-year mechanical integrity test required by 40 C.F.R. 146.13(b)(3). Please add a summary of the results and conclusions of those tests. Also, please add a section that includes the results of the most recent and previous PFTs (e.g., a table of surface and bottom hole pressures, permeability, skin, and radius of influence) to show any changes in well conditions. OAC 252:652-7-1(4).

**RESPONSE:**

**PRESSURE FALL OFF TEST (PFT)**

The results from the PFT are summarized in the following table.

**Table 8: Historical PFT Summary**

| Year | Shut -In Period | Avg. Flow Rate | Depth of Bottom Hole Measurement | Bottom Hole Pressure at End of Shut-In | Surface Wellhead Pressure During Injection | Double Porosity Reservoir      |              |       | Radial Composite Reservoir |                                |              |       |                         |
|------|-----------------|----------------|----------------------------------|--|--|--------------------------------|--------------|-------|----------------------------|--------------------------------|--------------|-------|-------------------------|
|      |                 |                |                                  |  |  | Bottom Hole Reservoir Pressure | Permeability | Skin  | Radius of Investigation    | Bottom Hole Reservoir Pressure | Permeability | Skin  | Radius of Investigation |
|      | hours           | gpm            | ft                               | psia                                   | psia                                       | psia                           | md           |       | ft                         | psia                           | md           |       | ft                      |
| 2015 | 72              | 175            | 5300                             | 2537                                   |  | 2558                           | 1140         | -4.56 | n/a                        | 2558                           | 1800         | -2.91 | n/a                     |
| 2016 | 72              | 200            | 5300                             | 2542                                   |  | 2568                           | 620          | 4.98  | 7980                       | 2571                           | 877          | 9.98  | 9490                    |
| 2017 | 72              | 185.85         | 5300                             | 2574                                   |  | 2524                           | 129          | 1.53  | n/a                        |                                |              |       |                         |
| 2018 | 72              | 355            | 5300                             | 2509                                   | 656  |                                |              |       |                            | 2505                           | 663          | 24.3  | 9640                    |
| 2019 | 82              | 204.8          | 5300                             | 2500                                   | 490  |                                |              |       |                            | 2517                           | 445          | 9.82  | 8380                    |
| 2020 | 71              | 218            | 5650                             | 2672                                   | 600.1                                      |                                |              |       |                            | 2664                           | 126          | 0.93  | 3200                    |
| 2021 | 72              | 200            | 5340                             | 2525                                   | 533.03                                     |                                |              |       |                            | 2532.7                         | 166          | 5.5   | 3400                    |
| 2022 | 72              | 202            | 5340                             | 2577.4                                 | 518.97                                     |                                |              |       |                            | 2536.7                         | 399          | 23    | 5760                    |
| 2023 | 72              | 175            | 5340                             | 2532.92                                | 540.93                                     |                                |              |       |                            | 2529.27                        | 264.43       | 16.6  | 3000                    |
| 2024 | 71              | 191            | 5340                             | 2522.28                                | 587.5                                      |                                |              |       |                            | 2518.63                        | 254.03       | 19.8  | 4269                    |
| 2025 | 71              | 200            | 5228                             | 2506.26                                | 750.73                                     |                                |              |       |                            | 2474.7                         | 217.33       | -4.47 | 3743                    |



## **APPENDIX J**

### **TABLE 5**

#### **EXISTING MES-1 UIC PERMIT - MAXIMUM ALLOWABLE INJECTION PRESSURES FOR VARIOUS SPECIFIC GRAVITIES OF INJECTATE**



**Table 5:** Existing MES-1 UIC Permit – Maximum Allowable Injection Pressures for Various Specific Gravities of Injectate

| <b>Specific Gravity</b>     | <b>Maximum Allowable Injection Pressure</b> |
|-----------------------------|---|
| Corrected to 60° Fahrenheit | (psig)                                      |
| 0.95                        | 1370  |
| 0.96                        | 1348  |
| 0.97                        | 1326  |
| 0.98                        | 1304  |
| 0.99                        | 1282  |
| 1.00                        | 1260  |
| 1.01                        | 1238  |
| 1.02                        | 1216  |
| 1.03                        | 1194  |
| 1.04                        | 1172  |
| 1.05                        | 1150  |
| 1.06                        | 1128  |
| 1.07                        | 1106  |
| 1.08                        | 1084  |
| 1.09                        | 1062  |
| 1.10                        | 1040  |
| 1.11                        | 1018  |
| 1.12                        | 996   |
| 1.13                        | 974   |
| 1.14                        | 952   |
| 1.15                        | 930   |
| 1.16                        | 908   |
| 1.17                        | 886   |
| 1.18                        | 864   |
| 1.19                        | 842   |
| 1.20                        | 820   |